GEOLOGY AND GEOCHRONOLOGY OF SILICA SANDS OF COASTAL PLAIN OF THIRUVANANTHAPURAM DISTRICT, KERALA, INDIA, WITH SPECIAL REFERENCE TO LATE QUATERNARY ENVIRONMENT

Thesis submitted to the

COCHIN UNIVERSITY OF SCIENCE AND TECHNOLOGY

in partial fulfilment of the requirements for the degree of

Doctor of Philosophy

in
Marine Geology
Under the Faculty of Marine Sciences

BY

BIJU LONGHINOS

Department of Marine Geology & Geophysics
School of Marine Sciences
Cochin University of Science & Technology
Kochi 682 016

November 2009

CERTIFICATE

*This is to certify that the thesis entitled "***GEOLOGY AND GEOCHRONOLOGY OF SILICA SANDS OF COASTAL PLAIN OF THIRUVANANTHAPURAM DISTRICT, KERALA, INDIA, WITH SPECIAL REFERENCE TO LATE QUATERNARY ENVIRONMENT***" is an authentic record of research work carried out by* **Mr. Biju Longhinos** *under my supervision and guidance in partial fulfilment of the requirements for the degree of Doctor of Philosophy in the Department of Marine Geology and Geophysics, Cochin University of Science and Technology, under the Faculty of Marine Sciences and no part thereof has been presented for the award of any degree or diploma in any other University / Institute.*

Prof. C. G. Nambiar
(Research Supervisor)
Department of Marine Geology and Geophysics
Cochin University of Science and Technology
Kochi - 682 016

Kochi
November 2009

DECLARATION

I hereby declare that the thesis entitled **"GEOLOGY AND GEOCHRONOLOGY OF SILICA SANDS OF COASTAL PLAIN OF THIRUVANANTHAPURAM DISTRICT, KERALA, INDIA, WITH SPECIAL REFERENCE TO LATE QUATERNARY ENVIRONMENT"** is an authentic record of the research work carried out by me under the supervision and guidance of Dr.C.G.Nambiar, Professor, Department of Marine Geology and Geophysics, School of Marine Sciences, Cochin University of Science and Technology, under the Faculty of Marine Sciences and no part thereof has been presented for the award of any degree in any university/institute.

Kochi
November 2009

Biju Longhinos

Acknowledgments

I would first like to take this opportunity to thank Prof. C.G.Nambiar for guiding me in carrying out this research. His insight, enthusiasm and supervision throughout the course of this work are very much appreciated. My sincere thanks also go to the Director, School of Marine Sciences for allowing me to pursue this topic and to the Head of the Department, Department of Marine Geology and Geophysics, for providing me the facilities available within the Department. I would in fact like to thank everyone in the Department for the support they rendered.

I thank the University Grants Commission, New Delhi for providing me Teacher Fellowship (FIP) for completing this work.

I also thank the Director and Dr. G. R. Ravindrakumar, Scientist (Centre for Earth Science Studies, Thiruvananthapuram) for extending help in utilizing XRD and XRF facilities for the analytical part of my work, Dr. C.M.Nautiyal (Birbal Sahani Institute of Paleobotany, Lucknow) for help in radiocarbon dating and palynological studies, Prof. Brahma Prakash (Indian Institute of Technology, Roorkee) for luminescence dating, Prof. John. A. Jaszczak (Michigan Technological University, USA) for inviting me to his laboratory and providing FE-SEM facilities, Prof. William C. Mahaney (York University, Canada) for helping me in doing quartz grain morphoscopy. Due thanks also to Prof. Paolo Cherubini (Swiss Federal Institute) and Dr. Dagmar Brandova (University of Zurich) for providing me the opportunity to be at the International Summer School on Geochronology, Arzinico, Switzerland and to present a paper related to my research.

Special thanks are due to Prof. M. RamaSarma (Former Additional Director, Department of Collegiate Education) for instilling in me the spirit to do research. He is the real force behind this achievement of mine.

I also heartily acknowledge the support rendered by my family members. Thanks also go to one and all who were part and parcel of this work at various stages.

CONTENTS

Chapter I

Introduction

1.1 Man in the Geological Time

Man is the child of the Quaternary. He evolved from the lower primates and developed into a single species of organism dominating the land on the Earth to the extent that no other species could ever reach. De Menocal (2001) and Potts (1996) have given impressive evidence in favour of the thought that the evolution of the hominid lineage was driven by the ongoing Late Cenozoic changes in the Earth's dynamics. The cultural sense in hominids developed in the Early Pleistocene and culminated into a social learning process enabling adaptation to climatic deterioration during Holocene (Boyd and Richerson, 1995; Bednarik, 2007 and Velichko et al., 2009). In short, the Pleistocene-Holocene break, though harsh with climatic vulnerabilities, provided opportunity for human to diverge from the rest primates.

What in the Holocene is responsible for initiating social learning in human being? One, the unpredicted vulnerability, in the form of heavy rains and flash floods followed by the re-emergence of monsoon systems in tropical region, melting of ice in higher latitudes and submergence of coastal lands and two, the opportunities they found from the re-greening of erstwhile savannas, tropical dry lands and higher latitude of later Pleistocene. History of human civilization reveals these climaxes. Ever since 11,600 years B.P. the Earth experienced relatively warm, wet, stable, CO_2 rich environments (Goring-Morris and Belfer-Cohen, 1998). These changes are recorded in the sedimentation process and pace at depo-centres across the world, during the Holocene.

Coastal evolution, contemporaneous with the rise and fall of sea-level, since the late Pleistocene bears the actual records of sea-level fluctuations. These records could draw out earth surface dynamics during the Late Quaternary. A great deal of work has been carried out in many parts of the world to narrow down the surface geodynamic processes that evolved social behaviour of man. The Quaternary history so far unravelled reveals that the environment varied drastically from place to place inferred by climatic and other aspects (Lamb et al, 1995; Cronin, 1999; Partridge et al., 1999; Satkunas and Stancikaite, 2009). Therefore the appearance and growth of humans in the Quaternary environment adds relevance to the study of the Quaternary and it demands for reconstructing the Quaternary environment with the finest detail.

1.2. Geological events during Late Quaternary

The Quaternary has been considered to be synonymous with the 'Ice Age', characterized by periodic wide-spread glacial activity intervened by warm environment. It has been understood that during these intervening warm environment, tropical animals like hippopotamus swam in River Thames (Walker et al., 2003). The hallmark of Quaternary, however, is not simply the occurrence of warm or cold phases of climate, but rather the high amplitude and frequency of climatic oscillations within a short geological span (Roberts and Rosen, 2009). The effects of these climatic changes were dramatic, that in mid and high latitudes ice sheets and valley glaciers waxed and waned. The area affected by the peri-glacial processes expanded and contracted. In low latitude regions the deserts and savannas shifted through several latitudes resulting in phases of aridity alternating with periods of high precipitation. Weathering rates and pedogenic processes varied with changes in temperature and precipitation. The river regime fluctuated markedly. Sea- level rose and fell, through perhaps 150 m (Roberts, 1998) and animal population was forced to migrate and adapt to these environmental changes that thrust upon them.

The pronounced oscillation in global climate during Quaternary lead to major changes in the types and rates of operation of geomorphologic processes in many parts of the world. The characteristic landforms that developed under the Quaternary climatic regimes are the hummocky moraines, trimline, friction cracks, watershed breaching,

cryoplanation benches, and thermokarst and thalassostatic terraces. The unconsolidated sediment accumulation is the characteristic lithology of Quaternary (Williams and Clerk, 1985,1995; Sinha et al., 2005). They fall under two principal types - the inorganic deposits (detritals ranging from boulders to clay) and the biogenic deposits. The biogenic sediments can be divided into organic component of humus and decayed remains of plants and animals and an inorganic compound of mollusc shells and diatoms frustules (Wenchuan, 2006). Therefore any geological scrutiny of the Quaternary largely involves study about biotic and abiotic processes accountable for the sedimentation, recorded from the terrain.

1.3. International Status of Quaternary studies along the coastlines

For more than a century, earth scientists have been accumulating evidences on sea-level fluctuation during the Quaternary period. The inter-governmental panel on climate change was in general agreement on a rise in global sea-level in the order of 0.31 to 1.10 m between 1990 and 2100 (Houghton et al., 1990). Several estimates suggested a global mean sea-level rise around 0.2 m during the last century (Pirazzoli, 1991; Gornitz and Seaber, 1990; Douglas, 1991; Peltier and Tushinghom, 1989; Yang et al., 2009; Emery and Aubrey, 1991). Based on the sea-level data from different location across the world a number of sea-level curves have been constructed, which were found to be highly useful in reconstructing global scenarios in sea-level (Kraft et al., 1987; Pirazzoli, 1991; Tushinghom and Peltier, 1993). According to Intergovernmental Panel on Climate Change (IPCC) , the global sea-level rise for this century is in the order of 18cm to 59cm (IPCC Technical Paper, 2007), while Kerr (2008) contends that it would be between 80cm and 200cm, taking into account of the retreating rate of glaciers and runoff rate of surface water into the sea. Accordingly a rise in sea-level by one meter would flood 17% of deltaic regions, reducing rice-farming land by 50 percentage. Globally, it would create more than 100 million environmental refugees (IPCC Technical Paper, 2007). Therefore the importance of understanding the geological processes during the past, especially during Holocene is highly prescribed to evade the crisis which has boosted the enthuse of scientific community in drawing out pre-historical earth environment.

The Holocene geological records are not universal or synchronous, even though the events were pan global. Fairbridge (1983) observed that the world has undergone severe geological disturbances at the advent of Holocene, manifested by transgressions and regressions. Giresse (1989) point to the fact that during the mid-Holocene, sea-level in some parts of the world was indeed higher than that of the present. This agrees with most comprehensive geophysical model of sea-level ICE-5G_VM2 (Peltier, 2004). A mid-Holocene sea-level position, at 3 m below the present MSL during 4570-5200 years B.P. was reported by Gayes et al. (1992). The sea-level continued to fall again by 3m around 3600 years B.P., before reaching the present position. According to Houghton et al. (1990) most of the mid-Holocene warming has taken place prior to 6000 years B.P. whereas corresponding higher sea-level followed at least 1000 years later.

The possibility of applying sea-level curves globally is being ruled out due to the contrasting effect of tectonic, isostatic and gravitational influences to the global variations in ice and water masses. It is a well-established fact that, changes in shape of the Earth's geoid cause regional differences in the pattern of post-glacial sea-level change. In areas such as eastern South America, West Africa and Australia, sea-level changes are largely caused by changes in water volume rather than land movement. With the discovery of geoidal deformation, it became obvious that the available database on ocean level changes differ widely over the globe and can never be expressed in terms of globally valid eustatic curves as previously believed (Fairbridge, 1966; Newman et al., 1988; Bloom, 1983; Morner, 1980b; Pirazzoli, 1991).

According to Morner (2004) Earth came into a new mode in Mid-Holocene when the glacial eustatic rise and corresponding rotational deceleration stopped. Morner (1980b; 1995) clarifies the domination of sea-level by redistribution of water masses due to interchange of angular momentum between the solid earth and main circulation system of the ocean. With respect to the late Holocene sea-level changes in the order of decades to a century, there are small to insignificant effects from glacial eustasy due to mass distribution. Similarly, the effects on the water column are seen only to be in the order of decimetres at the most (Nakiboglu and Lambeck, 1991; Morner, 1995). Instead, major effect is the dynamic redistribution of water masses via the ocean current system. It means that even if

the global sea-level has changed during the last 150 years, it can only be in the order of about 1 mm rise per year (Morner, 1992; 1995). And Prell et al. (1980) discusses the sea-level rise in Indian ocean with respect to surface circulation pattern during last glacial maxima, about 18000 years B.P. and establishes that the circulation pattern was significantly different from the modern days inferring a weaker southwest monsoon wind.

As the result of eustatic rise, large quantity of sand got accumulated in many of the coastal parts of the world. They are considered as prominent geo-scientific tool in deciphering former sea-level strands. In general, the longer the sea-level rises, the higher the possibility of its burial or drowning by marine sediments. Longer the fall in sea-level, the more probable is their preservation as depositional bodies such as beach ridges and coastal dunes. Utilizing the interplay between the marine sediments and submerged deposits, it is possible to reconstruct various episodes of high and low sea-levels, enabling to establish a sea-level curve along the coast (Fairbridge, 1983).

The studies of Schumm(1969), Goudie (1981), William and Faure (1980) and Butzer (1980) have brought out different paleogeomorphic environments from the geomorphology, palynology, micropaleontology and geoarchaeology of the Quaternary deposits in Europe, North America, Africa and Australia. However, these studies have clearly demonstrated the complexities involved in the interpretation of Quaternary continental sedimentation. They highlighted the problems encountered in establishing the cause and affect relationship due to the involvement of numerous undetectable parameters. Curray and Moore (1971) illustrated the formation of beach ridges and their importance in elucidating sea-level changes. Semenuik and Semenuik (1997) and Eronen et al. (1987) utilized the stratigraphic sequences of tidal flats and swampy environments to deduce past climatic conditions and Holocene sea-level fluctuations. Semenuik and Semenuik (1997) and Tanner (1995) also emphasized the importance of beach ridge in deciphering various stages of evolution of the coastal plain.

The incidences of rapid climate variation in the Late Pleistocene was studied by Dansgaard et al. (1993), GRIP (1993) and Ditlevsen et al. (1996). Very high-resolution climate proxy data during last 400,000 years are available from ice cores taken from the

deep ice sheets of Greenland and Antarctica. Resolution of events lasting little more than a decade is possible in Greenland ice 80,000 years old, improving to monthly resolution 3,000 years ago (GRIP, 1993). The climate fluctuations recorded in high latitude ice cores are also recorded at low latitudes. Here the sediments overlain by anoxic water inhibiting sediment mixing form the source of low- and mid-latitude climatic data with a resolution rivalling the ice core data (Bond et al., 1992; Hendy and Kennett, 1999). Schulz et al. (1996) analyzed organic matter concentrations in sediment cores at oxygen minimum depths from the Arabian Sea deposited over the past 110 thousand years. The study has brought out the strength of ocean upwelling and the strength of monsoon from the variation in organic matter deposited in Arabian Sea. Likewise, Cowling and Sykes (1999), Beerling and Woodward (1993) and Beerling et al. (2002) have brought out evidences of lower level of photosynthesis during late Pleistocene from the incidences of high stomatal density of fossil leaves. Barnola et al. (1987) has estimated the CO_2 content of the atmosphere at about 190 ppm during the last glacial compared to about 250 ppm at the beginning of the Holocene. Beerling and Woodward (1993) estimated 33% to 60% lower terrestrial carbon store on land as a result of photosynthesis during the Last Glacial Maxima.

The mass-balance calculations based on stable isotope geochemistry of $\delta\ ^{13}C$ of Holocene indicate qualitatively large drop of terrestrial carbon. Under this condition reduction of tropical forests and expansion of grass lands above 200m and falling of snowline considerably to lower heights are inferred (Flenley, 1996). Wallace (2001) has summarized the temperature fluctuations during Holocene from the incidences of iron stains.

1.4. Status of the studies on Quaternary sediment along the coastlines of India

Studies on the Quaternary deposits along the Indian coasts have received special attention in recent years from the point of view of resource utilization and human inhabitation. Tremendous growth of cities along the coast, especially harbour cities, has called in scientific focus on the nature of land-sea interfaces. This thrust has laid upon the geologists of India to establish the pace of sea-level, across time, along the coast. Past sea-levels till late Pleistocene have been fairly established at different points along the coast of

Indian sub continent.

Initial attempts to study the sea-level rise along the Indian coasts were made by Ahmed (1972) and Douglas (1991) and recent works include those of Unnikrishnan and Shankar (2007) and Raj and Yadav(2009). The east coast of India imbibed a depositional environment and hence the sea-level studies have mostly been based on its features exposed in different coastal environments, namely deltaic coasts and dune bearing coasts. Available information, however, is more qualitative. On the contrary, along the west coast, rather the northern part of the coastline, more investigation had been conducted where a great deal of information on transgressional and regressional aspects and on low stands in the continental shelf is generated. In 1972 Ahmed correlated certain land features to the global inter-glacial transgression/regression. And during the last two decades, with the generation of more data, attempts were made to integrate the knowledge globally along the coast by correlating strand line features to the glacio-eustatic sea-level changes of the Quaternary. Reddy et al., (1976) established the incidences of sea-level fluctuation along west coast during the Tertiary and early Quaternary period from ONGC oil-well data of North Eastern Arabian sea.

On the east coast, sea-level fluctuations were mostly inferred from the studies pertaining to major river deltas, coastal islands, beach ridges, rock terraces, caves and relict sediments in the continental shelves (Niyogi, 1975; Bhaskara Rao and Vaidyanathan, 1975). Studies on Holocene sea-level changes of Swatch of No Ground (in Bangladesh) in north to Kanyakumari in south have been brought out by various workers. Sen and Banerjee (1990) studied the floral and faunal assemblages and give an opinion that tidal mangrove forests flourished further north of the present extent of Sunderbans at about 6000 to 7000 years ago. Niyogi (1975) reported three levels of terrace at 6.1m, 4.7m and 3.8m above MSL in the Subarnarekha River delta and the adjoining coast of West Bengal. Chauhan et al. (1993) points at the significant variation in the intensity of monsoon, accordingly Bay of Bengal faced two dominant arid phases around Last Glacial Maxima and a monsoon phase around Pliestocene-Holocene boundary.

Sambasiva Rao (1982) grouped four strand lines in Godavari delta formed during the Holocene period. Krishna Rao et al. (1990) dated peat and wood material, shell fragments

and calcrete rich mud taken from the farthest beach ridge of the Krishna delta and reported an age of 6500 years B.P. to 2050 years B.P. Radiocarbon dating of mollusc shells from a sand bar at about 25 km from the present coastline off Nizampatnam give an age of 8200 ± 120 years B.P, suggesting a Holocene sea-level drop of about 17 m. Srinivasa Rao et al. (2005) indicate a rapid rise in the sea-level at Nizampatnam Bay during 8000 years B.P, thereby postulating the drowning of barrier island. The highest inland chenier ridges in the area are dated 6500 years B.P. and the sea remained at higher levels till 2000 years B.P.

In Pulicat lake, near Chennai, evidences of low sea stands at -49 m and -56 m in the form of pebble horizons have been identified by Nageswara Rao et al., (1988). According to Meijerink (1971) and Sambasiva Rao (1982) the Cauvery delta retains a series of three strand lines as beach ridges indicating post Wurm glacial stage transgression that inundated 11000-12000 years old Pleistocene fluvial deposits. Morphological analysis of coastal landform indicate emergence of the Rameswaram coast at about 4000 years B.P. (Rao, 1996). The terraces around Mandapam and Rameswaram coast ranging in height from 0.20 in to 0.62m above MSL, gave ages varying from 5440 ± 60 to 140 ± 45 years B.P. (Rajamanickam and Lovesan, 1990). The Tirunelveli coast of Tamilnadu, experienced a late Quaternary (Upper Pleistocene) transgression, with sea-level rise of +2 m to +8 m, clearly evident from the coastal sequences of Kudangulam and Chettikulam region. Here the Holocene transgression reached its maximum height during 6240 to 2740 years B.P., the level hardly rising 0.5 m to 1 m above the present MSL (Bruckner, 1986).

Unlike the east coast, the west coast of India is narrow and bear a few incidents of large coastal plain deposits. Among the coastal plains, along the west coast of India, Saurashtra coast is the only coast that is extensive, which is followed by the coastal region of central Kerala. Proximity to the Western Ghats and heavy run-off rivers make up the western coastal plain narrower than the eastern coastal plain. In order to establish the tentative Holocene transgression-regression history of the west coast in chronometric terms, absolute dates of beach rocks, shelf surface sediments, corals and oolitic limestone etc. from shore and coastal zone have been used by many workers. Kale and Rajaguru (1985), Nigam (1993), Hashmi et al. (1995), Rao et al. (1996), Baker and Haworth (2000) and Mathur (2005) inferred fluctuations of sea-level along the coast of Arabian sea to the tune of 1.5 m

to 2.5 m at about 6500 years B.P. and have inferred a sea-level curve from the closing phase of Pleistocene to late Holocene. Based on their work on the Neogene and Quaternary transgressional and regressional history of the west coast of India, the fluctuation of sea-level through time has been attributed to global eustatic changes in sea-level and also to the tectonic movements. From the carbonate content and the faunal composition of the coastal Arabian Sea sediments, Borole et al. (1987) provided clear-cut evidences for a major environmental change around 13,000 years B.P. in the surface ocean waters along the Saurashtra coast. The milliolitic rocks of Saurashtra coast indicating high strand line positions during Quaternary (Lele, 1973; Banerjee and Sen, 1987; Verma and Mathur, 1988; Purnachandra Rao and Veerayya, 1996; Bhatt, 2003; Mathur, 2005) is yet another evidence of Quaternary sea-level changes.

Bhatt and Bhonde (2006) who analysed the geomorphic features along the Saurashtra coast developed two major high-sea-level strand, the later being during the mid–Holocene when the sea rose 2m above the present level. Using ^{14}C ages of Cerithium and Turbo from Porbander and Mithapur areas. Mathur et al. (2004) envisaged a 2 to 3 m higher mid–Holocene sea-level with a falling trend since then.

For Maharashtra coast, Agarwal et al. (1978) and Kale and Rajaguru (1985) provided important information on a series of transgression and regression phenomena, since 35,000 B.P. based on radiocarbon dates. According to them the sea-level was considered to be very much lower than at present and it started rising since 30,000 B.P. followed by a regression and a transgression around 15,000 B.P. The sea-level attained its maximum level during the mid-Holocene. It was also observed that along the Maharashtra coast at about 6000 years B.P. the sea-level was almost the same as that at present, but in subsequent periods, i.e. between 6,000 and 2,000 years B.P. a further rise of 1 m to 6 m was indicated. This was corroborated in previous works by identifying various geomorphic features related to marine regression during Holocene and they highlighted the significance of neotectonism in shaping the shoreline.

Along the coast of Goa, Wagle et al., (1994) inferred the presence of drowned river valleys at a depth of 27 m to 35 m below the present MSL. Based on oxygen isotope and

sedimentological records of core from the south western continental margin of India, Thamban et al. (2007) studied the fluctuations in sea surface hydrography during the last deglaciation. The influence of deglacial warming and regional variation in precipitation on the hydrography of the region was noticed between Goa and Mangalore. Though significant sea surface warming occurred around 15 ka B.P. precipitation was increased significantly only after 9-8 ka B.P. Singh et al. (2001) inferred rapid rise in sea level between 15 and 10 ka B.P. Along the south west coast of India the Holocene of Arabian Sea is marked by the increase in salinity synchronous with monsoonal precipitation events on land (Thamban et al., 2007).

Agarwal and Guzdar (1974), Kale and Rajaguru (1985), Rajendran et al. (1989) Bruckner (1986), Caratini et al. (1990) and Narayana et al. (2001) have reported the abundance of peat deposits at many onshore locations adjacent to the present shoreline of the west coast. They vary in age between 7200 and 45000 yr BP. Usually the peat layers occur at 2 m, 6 m, 20 m and 40 m below the surface of the coastal alluvium(Narayana and Priju, 2002). The presence of peat suggests intense plant productivity and luxuriant growth of forests in the immediate vicinity.

One of the major developments in Quaternary studies, since 1980s, in India has been refining the resolutions of the climatic and other environmental records which sedimentary cores contain (Singh et al., 2001; Nigam, 1993). Nambiar and Rajagopalan (1995), Thamban et al. (2001) and Pandarinath et al. (2004) have brought out late Quaternary sedimentation rates along the southwest coast of India, between Cochin in central Kerala coast and Kanyakumari at the southern tip of the subcontinent. From that it can be concluded that the sedimentation rates for the topmost sediment layers are lower than those for deeper sections, suggesting that the sediment input to the southwestern continental shelf of India had been comparatively low in late Pliestocene and in Holocene compared to early and Mid Pleistocene. Church et al.(2001) and Unnikrishnan and Shankar (2007) have compared the trends in sea-level rise in both Arabian Sea and Bay of Bengal with the estimated global sea-level rise and found consistency among them. Table 1.1 lists the major Holocene events in Indian sub continent as summarized by Naidu (1999). Further Sukumar (1993), Rajagopalan et al. (1997) Mayewski et al.(2004), Saraswati et al. (2006), Sinha and

Friend (2007), Staubwasser and Weiss (2007) and Sinha and Sarkar (2009) have deduced a high fluctuating climate for India during Holocene.

Table 1.1. Important events during the Holocene in the Indian subcontinent (after Naidu, 1999)

Age	Event
1200 years B.P. to present day	Present day conditions of vegetation and climate began at 1200 years B.P. sea-level was 2m lower than the present level.
3500 to 1200 years B.P.	No pollens were preserved in Indian Lakes dried up in an oscillatory fashion
5000 to 3500 years B.P.	Moist conditions with good rainfall characterized by high values of sedges, trees and shrubs. sea-level was 6m lower than present day.
9500- 5000 years B.P.	Relatively high rainfall as indicated by the presence of Typha, Arteminia in lake sediments of Rajasthan and also greater values of upwelling indices in the Arabian Sea sediments. sea-level was 40m lower than the present day.
10,000 to 9500 years B.P.	Rainfall belts shifted west ward and precipitation was about 250mm/yr greater than the present, lake levels rose dramatically
12,000 to 10,000 years B.P.	Major deglacial event, intensification of the southwest monsoon. Younger Dryas Event. sea-level was 90m lower than the present day.

1.5. Studies on Quaternary sediments of Kerala

Different sectors of the coast of Kerala have been scrutinized by Jacob and Sastry (1952), Paulose and Narayanaswamy (1968) and Raha et al. (1983). They have brought out the stratigraphic, lithological, geochronological and paleontological aspects of the coastal geology, which directly or indirectly are linked to various aspects of sea-level changes. Recently Nair et al. (2006) has reviewd the Quaternary sedimentation along south Kerala.

The beach rocks exposed towards the west and east of Kanyakumari are studied by Thrivikramaji and Ramasarma (1981) from which they inferred a sea-level rise and fall of 4 to 5m during the Holocene. Pawar et al. (1983) and Rajendran et al. (1989) are of the opinion that the peat beds in Quaternary sequences developed from the submergence of

coastal forests and represent a series of transgression and regression Jayalakshmi et al. (2004) linked the Quaternary transgression to abnormally high intensity of Asian summer monsoons. Records of variations in rainfall based on cynobacteria from Late Quaternary sediments from the boreholes of Panavally and Ayiramthengu (Kollam district) were inferred by Limaye et al. (2009).

Rajan et al. (1992) attributed an age of 8230 to 10240 years B.P. to the decayed wood recovered from the carbonaceous clay of Ponnani and point at the Holocene transgression as the cause to the ultimate destruction of the coastal mangroves. Narayana et al (2007) reported 2-5m thick peat layers occurring at depths of 30, 40 and 50 m in the sediment fill of the Vembanad lagoon which gave radiocarbon ages of 8460 to 40000 year B.P. indicating that the environmental conditions in central part of Kerala have been very much conducive to the formation of layers of peat, during Late Quaternary.

The continental shelf of Kerala coast has been explored by many workers, leading to the discovery of submerged terraces at -92 m, -85 m, -75 m and -55 m, representing four still stands of sea-levels in the Holocene age between 9,000 and 11,000 years B.P. and according to Nair (1974, 1975) those terraces represent the sea, which was in transgressive phase. Further Nair and Hashmi (1980) and Nair et al. (2006) deduced the incidences of warmer conditions and low terrestrial run off from the occurrences of oolitic limestone in the Kerala shelf, which dates 9000 to 11000 years B.P.

The episodes of sea-level rise and fall along Kerala coastline were traced out in coastal morphological features by Samsuddin et al (1992), Suchindan et al (1996) and Haneeshkumar et al (1998). The strand plain deposits of northern Kerala are considered as morphological manifestations of marine transgression/regressions by Samsuddin et al. (1992). Suchindan et al (1996) relates the parallelism of Vembanad Lake with that of the series of inland strand lines in the Central Kerala to the repeated transgressive-regressive episodes that the coast had undergone during Holocene. Prithviraj and Prakash (1991) and Ramachandran (1992) fairly traced out the origin of a linear sand body at a depth of 20m to 30 m offshore characterized by textures of the beach deposits to a low stand of sea-level. It is also discovered that the Holocene sedimentation in outer shelf of Kerala, especially

between Mangalore and Cochin is minimal and had been unable to cover the Late Pleistocene sediments. This has been proved from the presence of thin relict terrigeneous sediments and further confirmed by the exposure of terrestrial carbonates such as calcretes and paleosols of Pleistocene age at 50 m to 60 m water depth (Rao and Thamban, 1994). Narayana et al. (2001) inferred varied temporal supply of ferrugeneous sedimens to the south east Arabian Sea during the late 20 Ka.

In a nutshell, the Quaternary studies of the coastal deposits of Kerala were based on sequences exposed either inland or laid on the shelf. Unfortunately the evidence of late Quaternary sea and land level changes and related Holocene climatic changes of the south west coastal margins of India is sparse, geographically scattered and often poorly dated.

1.6. Studies on Quaternaries of Thiruvananthapuram District

The Quaternary deposits along the coastal plains of Thiruvananthapuram District have its own entity. The deposit does not bear a physical continuum with the rest of the sedimentary basin in the north. It is separated from rest part by hills made of Tertiary sequences, abutting into sea. The plain abode silica sand of economic importance. The Kerala State Mining and Geology Department have mapped the region and estimated the quantity and quality of silica sands present over the terrain (Vasudeva, 1983). The Department estimated that the plain abode 0.4 million tonne (sub surface limit of reserve estimation being 2 to 2.5m) of 98% pure silica sand concentrated towards the north of the region centring on Menamkulam village.

Paul and Babu (2008) have undertaken a study to understand geomorphologic evolution of the terrain and deciphered four to five beach ridges and swales parallel to the present coast. They have sampled to a depth of 1 m and found that the sandy sediment belong to late Holocene to Historic times.

The above two investigations are limited in their scope to analyze the geological evolution of the Thiruvananthapuram coastal plain in detail.

1.7. Geological Perceptions about Thiruvananthapuram District

The district of Thiruvananthapuram beholds the rocks of Thiruvananthapuram Block of the Southern Granulite terrain or the Pandyan Mobile belt (Ramakrishnan and Vaidhyanathan, 2008). The Thiruvananthapuram Block, also called as Kerala Khondalite Belt (KKB) is a straight WNW-ESE belt of rocks mainly composed of garnet- sillimanite-graphite gneiss. They also bear garnet-cordierite gneisses, garnet-biotite gneisses and garnet bearing quartzo-feldspathic gneiss interlayered with charnockites. The Precambrian rocks are overlaid by Cenozoic (Figure 1.1). The Cenozoicss essentially constitute sedimentary rocks of Neogene system, which overlain Quaternary sediments.

Precambrian crystallines

The Precambrian crystalline rocks occupy a considerable area of Thiruvananthapuram district. They include khondalites, gneisses and incipient charnockites. The khondalitic rocks occupy south of Achankovil shear, defining the Kerala Khondalite Belt (KKB) and are seen associated with quartzite, calcgranulite, garnetiferous gneiss and patchy charnockites. Their age ranges between 670 and 2200 Ma (Santosh, 1986 and Chacko et al., 1987).

Though charnockite constitutes the major part of the hinterland rocks of Kerala, it is lesser in abundance than khondalite and gneiss in Thiruvananthapuram District. Charnockites are massive in appearance but on close examination yield well developed foliation or deformational banding, therefore acquires the character of gnessic granulite. Apart from this, patchy type of charnockite is also recorded. A large part of these crystalline rocks has undergone polymetamorphic and polydeformational activities. They have been cut across by younger dykes of Proterozoic age towards the northeast part of the district.

Basic intrusives

Gabbro and dolerite constitute the most common basic intrusive emplaced within the Precambrian crystalline of Southern Kerala. The NNW-SSE trending gabbroic dykes of Proterozoic age are exposed towrds the NE part of the District (Radhakrishna et al., 1999).

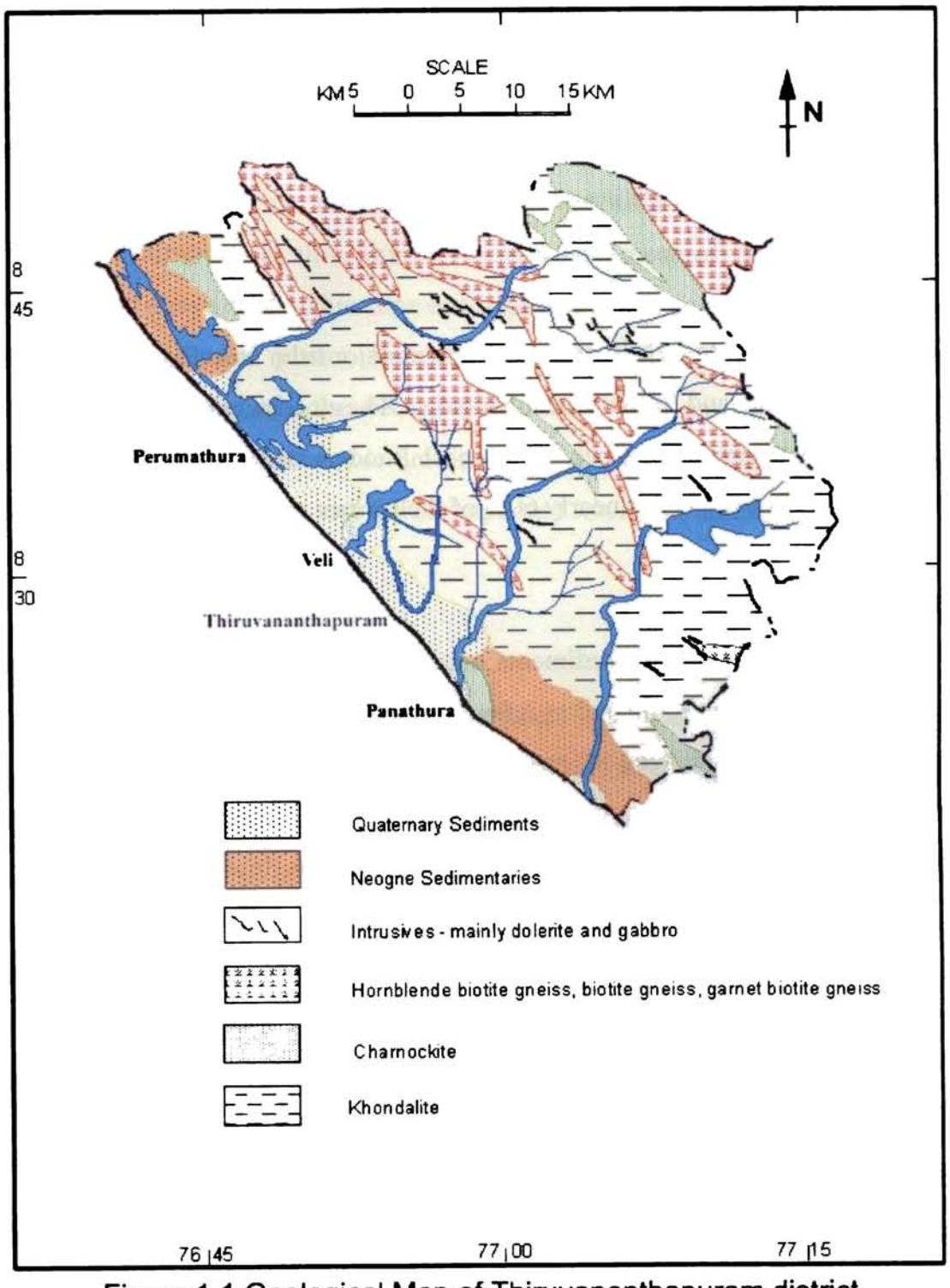

Figure 1.1 Geological Map of Thiruvananthapuram district.
(after CWRDM, 1986 and GSI, 1995)

Neogene sedimentary rocks

The Neogene sedimentary formation of Kerala unconformably overlies the Precambrians (Paulose and Narayanaswamy, 1968). In Thrivananthapuram district it is exposed towards the north and south of the district, namely along Varkala coast and

Chowara coast. They belong to two litho facies, namely the continental facies, the Warkalli beds, comprised of carbonaceous clays with lignified tissues/coal seams, china clay and friable sandstone and the marine facies, the Quilon beds, comprising sandstones and carbonaceous clays with thin bands of fossiliferous limestone depicting the transgressive episodes occurred during Burdigalian.

Laterites

Laterites of Recent to Sub-Recent age form a major litho unit and they cap over both Precambrian crystallines and Tertiary sedimentaries. They occur either as the pre-Miocene surface covering over crystalline rocks or as post Pliocene suface covering over Tertiary sedimentary rocks. Laterites cover nearly 60% of the surface area of the district.

Quaternary sediments

Unconsolidated Quaternary sediments occur along the stretch from Perumathura in the north to Panathura in the south and as a few patches near Poovar in the extreme south of the district. They include fringes of parallel sand bars, sandy flats, alluvial sands and lacustrine deposits. These are separated from the Tertiary sedimentaries by polymict pebble bed or by laterites.

In other parts of Kerala these sediments are reported to occur thicker and in the districts of Alleppey and Ernakulam, the thickness is estimated to exceed 100m. Towards northern and southern transect of the coast, the thicknesses of these sediments are in the order of a few tens of meters. Along the coast of Thiruvananthapuram district, the thicknesses of these sediments are not so far estimated.

1.8. Geomorphic features in coastal plains of Thiruvananthapuram District

Physiographically, the district of Thiruvanthapuram is divisible into three regions based on their altitude: - lowland (0-15 m), midland (20 – 75 m) and highland (> 75 m). Approximate area under each division in percentage is 10, 42 and 48 respectively.

Quaternary sediments are encountered in all geomorphic units except high lands and mountain peaks. The zone of transition between lowland and midland is next in importance with regard to the occurrence of Quaternary sediments. They form major geomorphic units in coastal plains. Coastal plains, with lagoons and vast low-lying areas fringing the coast, are an important physiographic unit and it forms the crux of economic activity and demographic concentration. In this physiographic zone, most of the areas show relief between 4 m to 6 m above MSL. This zone encompasses beach dunes, ancient beach ridges, barrier flats, coastal alluvial plains, flood plains, river terraces, marshes and lagoons. Coastal plain is wider towards the central part, while it is narrower to the south. A characteristic feature of this geomorphic unit is the series of beach ridges and swales which are roughly aligned parallel to the coast. The important lowland landforms are water bodies and wet-lands.

Water bodies

The lowland chain of water bodies in Malayalam is termed as 'Kayal' and other word in local usage is "back waters" to designate any perennial water body along the coast, means a body of brackish water along the coast. They encompass lagoons, estuaries and lakes. The coastal ones are connected with each other through a network of canals, some of which have natural origin but modified by man for navigation or agriculture or both. The key peculiarity exhibited by these water bodies is that they exhibit the combination of lagoon and estuary. Nair and Padmalal (1998) suggested that the uplifting of the coast as a factor responsible for the creation of lagoon-estuary combination.

The major water bodies in the coastal plain of Triruvananthapuram are Akkulam lagoon with closed estuary at Veli, Kadinakulam lagoon with open estuary at Perumathura and Panathura estuary at the mouth of Karamana river. These water bodies are linked seasonally through perennial wetlands, surrounding them.

Major fluvial systems are rivers Karmana and Killilar flowing in the south and Vamnapuram flowing in north, and the minor streams Amazhinjanthodu and Kulathor thodu in the central part of the coastal plain.

The river Vamanapuram is a major river in South Kerala with its network of tributaries. The trunk stream originates from the foothills of the Ponmudi hills (1074 m above msl) and the tributaries from the surrounding hills like Kallar. The river then flows onwards through Vamanpuram town and two-branch stream join at Attaramoodu where the main stream is called Kilimanurpuzha. From there the master stream flows onward and joins the Kadinamkulam kayal at the northern most extremity and by there into the Arabian Sea, in west. The major portion of the Vamanapuram River flows through midland terrain and the remaining through highlands and lowlands areas. Major lineaments are not associated with drainage basin of this river. The total length is 90 km and it drains an area of approximately 690 sq km. The main trend of the drainage basin is east west.

The river Karmana takes its origin from the Agasthyamalai and its headwater channel reaches the base of Chemmunji Mottai peak (1717 m above MSL). From this point of highest elevation the river flows in the southerly direction with frequent meanders and finally debounces into the sea through an estuary about 3 km south of Thiruvananthapuram. Out of 82 km Karmana River, 4 km run through highlands, 17.5 km through lowlands and the remaining 60.5 km through midlands. The total drainage area of the river is 464 sq km. The reservoirs at Peppara and Aruvikkara reduce the riverine strength towards its lower course.

The smaller streams Amazhinjanthodu and Killiyar run about 15km and are originated in the western parts of midlands. They have a southerly flow direction in midland and exhibit structurally controlled course. In midlands these two rivers are parallel to each other, but as it enter the coastal plain of Thiruvananthapuram the course of Killiyar river shift southeasterly and join the river Karamana at Pallathukadavu. On the other hand Amazhinjanthodu turns a U-turn, near Pattur and flows back to Kannanmoola and then turns 90 degrees west ward and drains into Aakulum- Veli lagoon, at Aakulam.

Wetlands

The most remarkable wetland form is the ridge runnel structure. It comprises a series of ridges alternated by depressions. Ridges are made of sands of various textures and are usually enriched in high silica sands. The surface sediments in runnels are sand mixed with clay and organic matter. The runnels form a conduit of water supply between major water

bodies in the region and thereby sustains with water surplus in the wetland.

The ridges and runnels are roughly parallel to the coast and show noticeable convergent and divergent trends with regional curvature and well developed convexities. The divergent convergent trends and regional curvatures cannot be possibly explained by a simplistic origin on account of a single episode of beach processes along a regressive coast line. This is further complicated by the land acclamation for city development, which has almost destroyed the very geomorphic elements in them.

Transitional plains

Transitional plains are located between the alluvium covered coastal plains and the laterite covered midland. They are of mildly undulating terrain with a slope not exceeding 5^0. The terrain has a cover of red sandy clay or clayey sand derived from the laterite upslope. These transitional plains are limited by steep sided paleoestuaries and burried river channels which get exposed in dug well sections and along stream banks.

Coastline

The coastline of Thiruvananthapuram district is nearly uniform, with a few deviations here and there. Along large segments the coastline is characterized by gently sloping beaches with sand dunes towards the hinterland immediate to it. At places, like in Vizhijam, Veli and in Varkalai lateritic and rocky cliffs are present along the shore.

Nair (1999) has divided the Kerala coast into three: submergent, emergent and stable types, and accordingly the coastline of Thiruvananthapuram is a mixed coast as it consists of elements of submergence and emergence, but largely emergent. Coastal landform of the stretch from north of the region appears to be controlled by the uplift of the Tertiaries. This coastal feature coalesces into a subdued topography further south along the coast with the appearance of mud flats, recent strands (upto 1.5 km wide) and the coast parallel estuary at the Kadinamkulam kayal. Towards Veli near Thiruvananthapuram, the gneissic rock exposures are observed close to the coast, leaving behind only a narrow recent strand. From south of Veli, coastal strands widen upto 2 km, and continue onto the north bank of Karamana river. Further south on to Kovalam promontory the subdued coastlines host

mudflats, marshes and a narrow sandbar. Geomorphology of the stretch from south of Kozhithottam Kayal is indicative of a prograded coast up to Kovalam promontory, with coast parallel water bodies.

1.9. Silica and glass sand deposits

Sand with particularly high silica levels that is used for purposes other than construction is referred to as silica sand or industrial sand. Sands and clastic sediments in general differ from the igneous and other crystalline rocks in possessing a framework of grains. The grain in sand is only in tangential contact with each other, unlike in magmatic rocks where the grains retain continuity in its contact. This retains non-cohesiveness of sandy material; its porosity gives much emphasis to its size for detailed description. A sand body is defined as a single interconnected mapable body of sand. Such accumulation occurs in many different physiographic settings.

A sand body is a natural and compelling object of study primarily because,

- It occurs in large scale
- Uniform response to some major geomorphic or sedimentological process
- Economic importance like ground water resource and mineral resource

Determination of the environment of deposition of sand body explore into the knowledge of its shape and its internal characteristics including their spatial distribution within it. It is well studied from depth profiling. Morphologically the sand bodies may be:

- Equidimensional sand bodies with length-width ratios approximately 1:1 covering thousands of square kilometres (Sheets and Blankets) ; or
- Non-equidimensional sand bodies with varying ratio between lengths versus width (Elongate sand bodies).

elements. The study area bears characteristic tropical humid climate. The area experience mild summer from March to August, having a drier period from March to May and a wetter phase from June-August (SW Monsoon) followed by a mild winter from September to January having a wetter phase (NE Monsoon) from September to November and a dry phase during early March.

Orogenic monsoon rainfall predominates in the region with average annual rainfall around 300cm with maximum during SW monsoon. The temperature ranges in between 28°C and 34°C and remains nearly constant all throughout the year showing an equatorial character. Like anywhere in Kerala the study area has high humidity of more than 80%.

1.10.3. Land Use

Human intervention in Thiruvananthapuram coastal area has started a century ago. Before that it was recorded in the history that the area contains sand dunes intervening with water bodies. By 1890's a canal was drawn out interconnecting the water bodies into sandy plane for developing water transport facilities in Travancore Kingdom. This canal still connects the water of the rivers:- Karamana, Amayizhinjhan, Kulathur and Vamanapuram at this lower extend. By the middle of 1900's an airport was built in the region by clearing off top 4-8m of sand dunes east of Shangumugham beach. In 1960's the area around Veli was donated by the villages to Government of India for building up Thumba Equitorial Rocket Launching Station and other establishments of Indian Space Research Organization. Today the whole region is used for developing scientific/military establishment in association with it. The lower region associated with sandy plains that were once used for paddy and coconut palm cultivation has given way to developing settlements associated with the above developmental projects.

1.11. Objectives of the present study

The present work aims at detailed study of Late Quaternary sediments along the Thiruvananthapuram coastal plain with the following objectives:

- to understand the surface and subsurface lithologic characters:

- to understand the age of deposition of the sediments using ^{14}C and OSL techniques;
- to understand the floral life during the period of deposition of sediments by palynological analysis of favourable sediments:
- to understand the deposits by detailed textural, mineralogical, chemical, quartz-grain morphoscopic characteristics of the sediments;
- to evaluate the Late Quaternary environment by synthesising the above data; and
- to assess the qualitative and quantitative aspects of the silica sand deposits in the area.

1.12 Methodology in brief

The present work aimed at the detailed understanding of the sediments along the Thiruvananthapuram coastal plain involved the following field/laboratory procedures:

- Reconnaissance using SRTM-DEM map and field survey covering an area of 32 sq.km collecting surface samples from 80 locations and sub surface sampling from 22 localities. (Details are given in Chapter II);
- Ages of the samples were determined by ^{14}C and OSL dating methods. (Chapter III);
- Mineralogical and textural studies by microscopy, sieve analysis, SEM-EDS and XRD (Chapter IV);
- Quartz grain morphoscopy based on SEM (Chapter V);
- Palynological study of selected samples involving standard procedure for separation and identification of spores and pollens. (Chapter VI); and
- Geochemistry of sediments by XRF. (Chapter VII)

Detailed methodologies with equipments used and procedures involved are elaborated in the concerned chapters.

Chapter II

Lithology

2.1. Introduction

Lithology is the scientific study of rock or sediment strata at point level and developing it into a record at local and regional levels. It takes into account the gross physical character of the rock column as observed in the field and categorizes rock units based on physical differences. In this chapter, the lithological data of the sample locations are encoded and their significance is arrived at. It is essentially the background to take the present work further.

2.2. Methodology

2.2.1. Reconnaissance and field surveys

In order to bring out an active form of field mapping it is necessary to perform a field reconnaissance to develop an appreciation of the topographic and geologic concerns of the area under study. The reconnaissance survey in a sandy terrain should include area assessment by toposheets, remote sensing data and by direct field visits. From toposheets and remote sensing data, it is possible to draw out the geomorphic elements at a regional level. The Shuttle Radar Topography Mission (SRTM) data is more precise in drawing out geomorphic forms, especially in highly populated area where topographic forms are marked by settlement (Farr and Kobrick, 2000). Further cores recovered from boreholes drilled on ground bring out information on lithological characters at point space.

The surface relief in the coastal plain hardly crosses the 20m contour as seen in the toposheets, hence looks like elongated flat land, bounded by hillocks to the east and sea to the west. A broad picture of the drainage and land water ratio can be derived from toposheets.

The Shuttle Radar Topography Mission (SRTM) data of National Aeronautic and Space Agency (NASA) of USA collected during 2005 was used for terrain reconnaissance. The high-resolution imaging radar system helps to generate 3-D topographic maps, digital elevation models and a 5m contour interval terrain map. This helps to picture the topography in sensible scale. From SRTM data individual characters of the terrain were brought out, as detailed below.

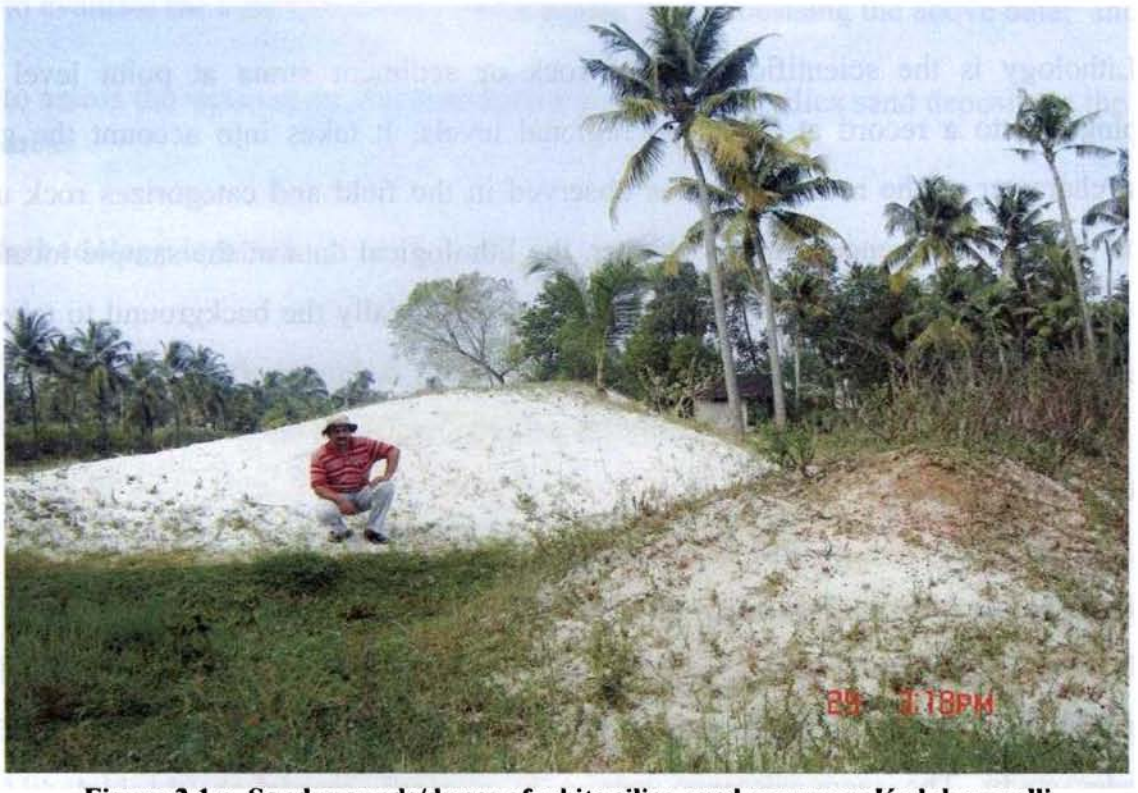

Figure 2.1.a. Sand mounds/dunes of white silica sand seen near Kadakampalli, located at the central part of the study area. The sand body is stabilized by vegetation.

The field study in the present work comprised of three components:

- A general evolution of surface features and selection of sample sites.
- Systematic sampling of surface sediments.
- Subsurface sampling for selected locations.

Small sand mounds, dunes and water-logged depressions seen all around the central portions of the study area (Figure 2.1a and 2.1b) constitute the typical landforms encountered during the field work.

Figure 2.1.b. Coalescing ridges and swales, seen across the study area. Impact of human interference now modifies this landscape.

2.2.2. Digital elevation map based on SRTM

Digital Elevation Model (DEM) is a quantitative model of part of the Earth's surface in digital form, in particular, elevation of a region. Typically, a DEM consists of an array of uniformly spaced elevation points in raster format. Terrain models are helpful for earth scientists. Graham (1974) first reported that a topographic map of the earth's surface can be prepared from phase differences recorded in the interferogram of a pair of Synthetic Aperture Radar (SAR) images. Polidori (1991) developed DEM from SAR interferometry. The Shuttle Radar Topography Mission (SRTM) has elevation data on a near-global scale that could generate high-resolution digital topographic database of Earth. SRTM-DEM has been used to study the topography of the region.

Three markedly different landforms identified from the SRTM derived map of the Thiruvananthapuram coastal plain and adjacent areas (Figure 2.2.a and 2.2.b). They are (i) Swales represented by linear areas within an altitude of 0 to 5m, consisting of coast parallel stream channels, paleo-channels, marshes and lagoons, (ii) Strand plains lying parallel to the present shoreline within an altitude of 5 to 10m. Some of these occur as isolated sub-parallel beach ridges and dunes and (iii) Lateritic hills, from 10m and above heights, which abut into

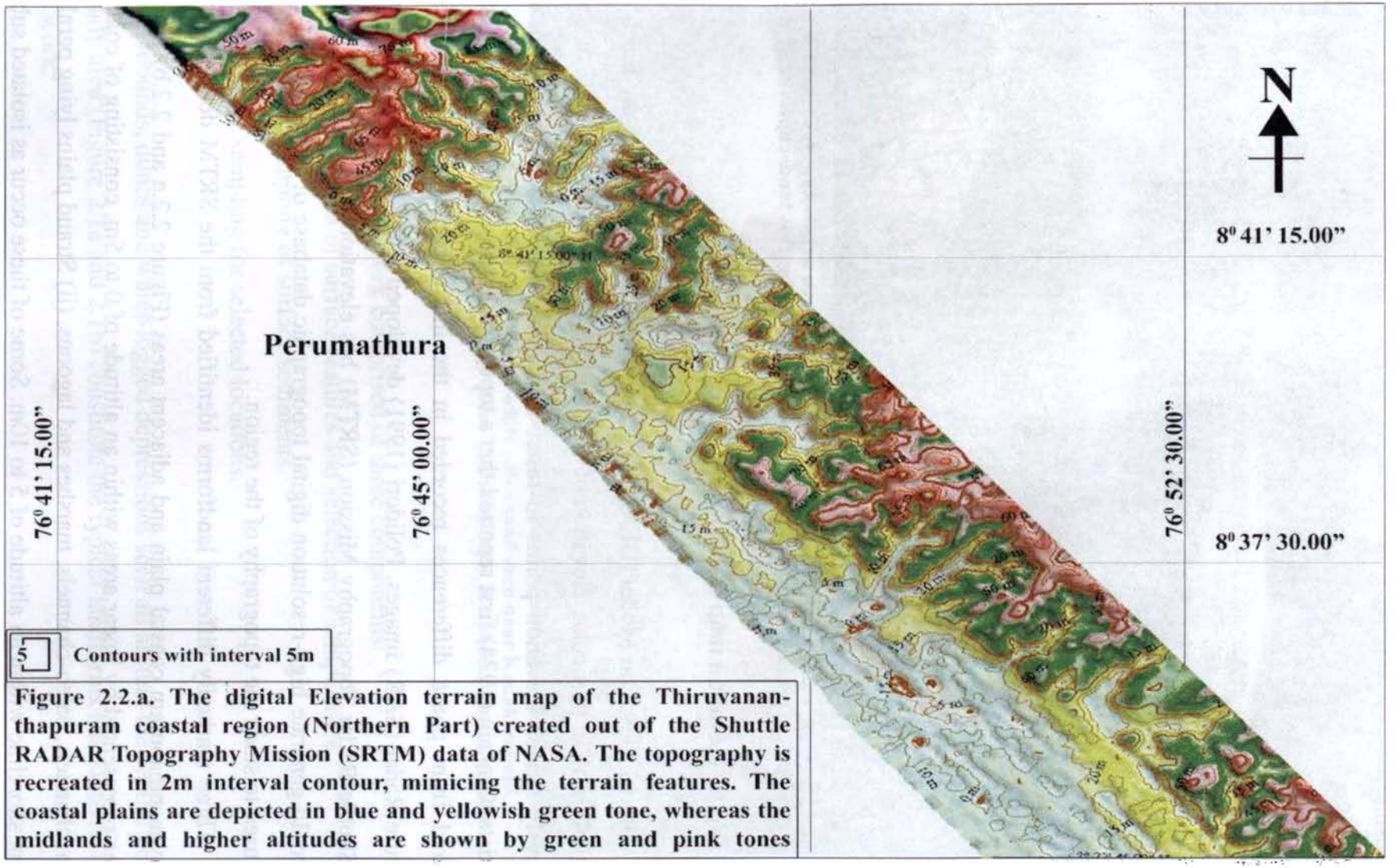

Figure 2.2.a. The digital Elevation terrain map of the Thiruvananthapuram coastal region (Northern Part) created out of the Shuttle RADAR Topography Mission (SRTM) data of NASA. The topography is recreated in 2m interval contour, mimicing the terrain features. The coastal plains are depicted in blue and yellowish green tone, whereas the midlands and higher altitudes are shown by green and pink tones

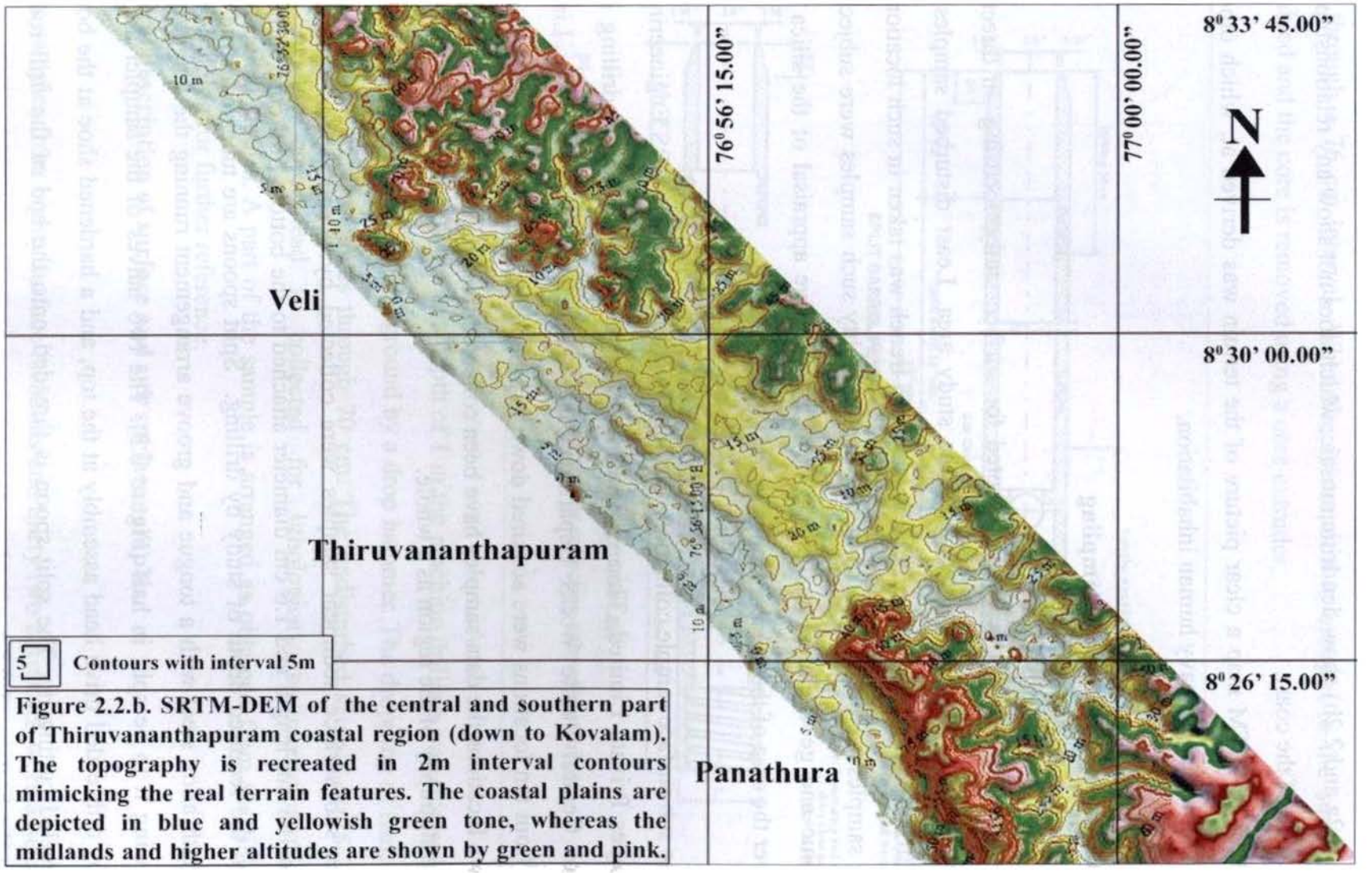

Figure 2.2.b. SRTM-DEM of the central and southern part of Thiruvananthapuram coastal region (down to Kovalam). The topography is recreated in 2m interval contours mimicking the real terrain features. The coastal plains are depicted in blue and yellowish green tone, whereas the midlands and higher altitudes are shown by green and pink.

he plain, occasionally. The swales and strand plain (seen as blue and yellowish green tone in Figure 2.2a and 2.2 b) run parallel to the coast, while the lateritic hills (seen as reddish tone in Figure 2.2a and 2.2b) show dendritic mosaic, which does not show any relationship to the configuration of the coast.

Through SRTM map a clear picture of the terrain was derived at, which otherwise was impossible due to heavy human inhabitation.

2.2.3. Surface and sub surface sampling

Normal field procedures were adopted for surface study, focusing on direct field observations at every 100 m interval of the study area. Least disturbed samples were collected from points among them. One meter deep trench was taken in such locations and sediment samples were collected from that depth. Eighty such samples were subjected to petrographic and geochemical analysis to have a qualitative appraisal of the silica sands spread over the area of the present study.

The sub surface sample collection was done in association with LBS Engineering and Technologies Private Limited, Thiruvananthapuram, who were conducting drilling in the region for Central Public Works Department and Airport Authority of India Limited. Samples from ten locations were acquired down to a depth of 30 m and from an additional twenty-two locations the data/samples have been collected from their archives to reconstruct the lithostratigraphy of the region as a whole.

The sub surface sediment samples were collected by a split spoon sampler, of dimension 108 cm length and 1.6 cm diameter attached to the bottom of a core barrel and lowered to the required depth of study by drilling. Split spoons are tubes constructed of high strength alloy steel with a tongue and groove arrangement running the length of the tube, allowing it to be split in half (Figure 2.3). The two halves of the sampler are held together by a threaded drive head assembly at the top, and a hardened shoe at the bottom, with a beveled cutting tip. The split spoon is threaded onto the end of the drill rod and lowered to the bottom of the boring by a heavy steel cable connected to the drilling mast. The sampler is forced into the soil by a drive weight that is dropped repeatedly onto the

drive head located at the top of the drill rod. The sampler is driven into the soil to a depth about six inches shorter than the length of the sampler itself. It is driven by 68 kg weight dropped through a 76 cm interval. When the split spoon is brought to the surface, it is disassembled and the core is removed using a core extruder.

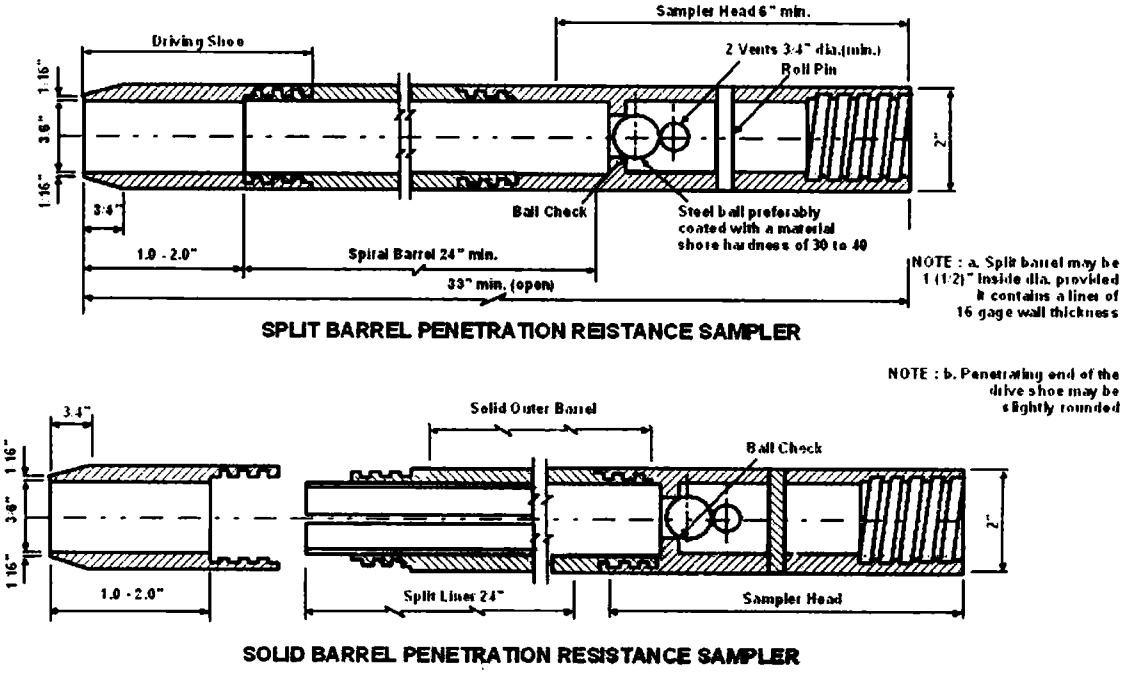

Figure 2.3. A sectional view of the sampler used for collecting subsurface samples

In order to recover samples at a depth of 1 m the machine drilling was stopped at 70 cm and the sampler is driven into the ground by a drop hammer. The dropping of hammer is continued till the corer penetrates through 70 cm. The undisturbed sample at 15-20 cm occurring at the core head is collected for lithological, sedimentological and geochronological studies. A part of the sample is arranged as obtained from the field and retained as litholog for further reference.

2.3. General description of surface and sub surface samples.

The samples from eighty surface locations and thirty two boreholes were assessed to evaluate the lithology of the study area. The surface samples were named TC1 to TC80 and subsurface sample points were marked T1 to T8 (located to eastern boarders of the northern

part of study area), P1 to P6 (located adjacent to the eastern border of the southern part of the study region) and TRV1 to TRV10 (nearly along the central region of the study area) (Figures 2.4a and 2.4b respectively).

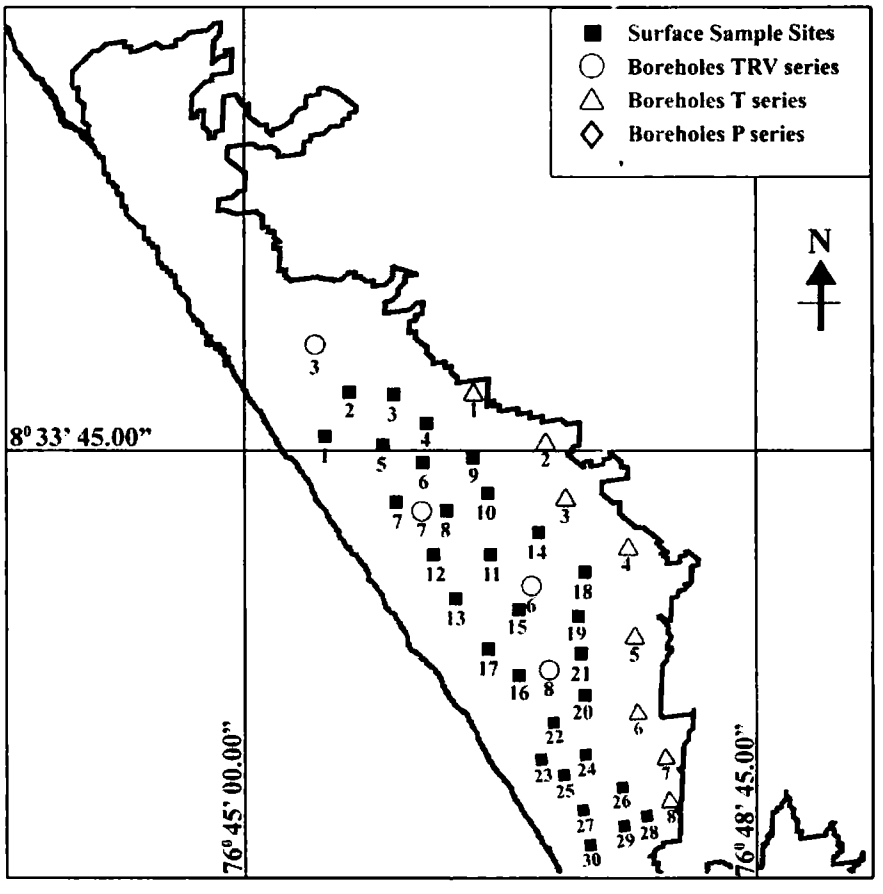

Figure 2.4.a. The map showing Sample Locations in the northern part of the study area

A brief lithological description of the sediment samples studied are furnished below. Detailed textural and mineralogical aspects are presented in Chapter IV.

2.3.1. Surface samples TC1 – TC80

Surface sample locations TC1 to TC80, fall in the white sandy flat of Thiruvananthapuram coastal plain. The samples were taken from a depth of 1 m from the surface. Natural soil formation is rare in the region, but in locations with landfills of clay waste or laterite fillings, top cover leaching effects are overprinted on sand grains. In the samples collected from TC1 to TC80 sand constitutes 100% of the sediments, of which

quartz constitutes nearly 99%, which gives it the characteristic pure white colour and a glassy appearance. There is a slight fining of sand towards the hinterland near the lake at Veli.

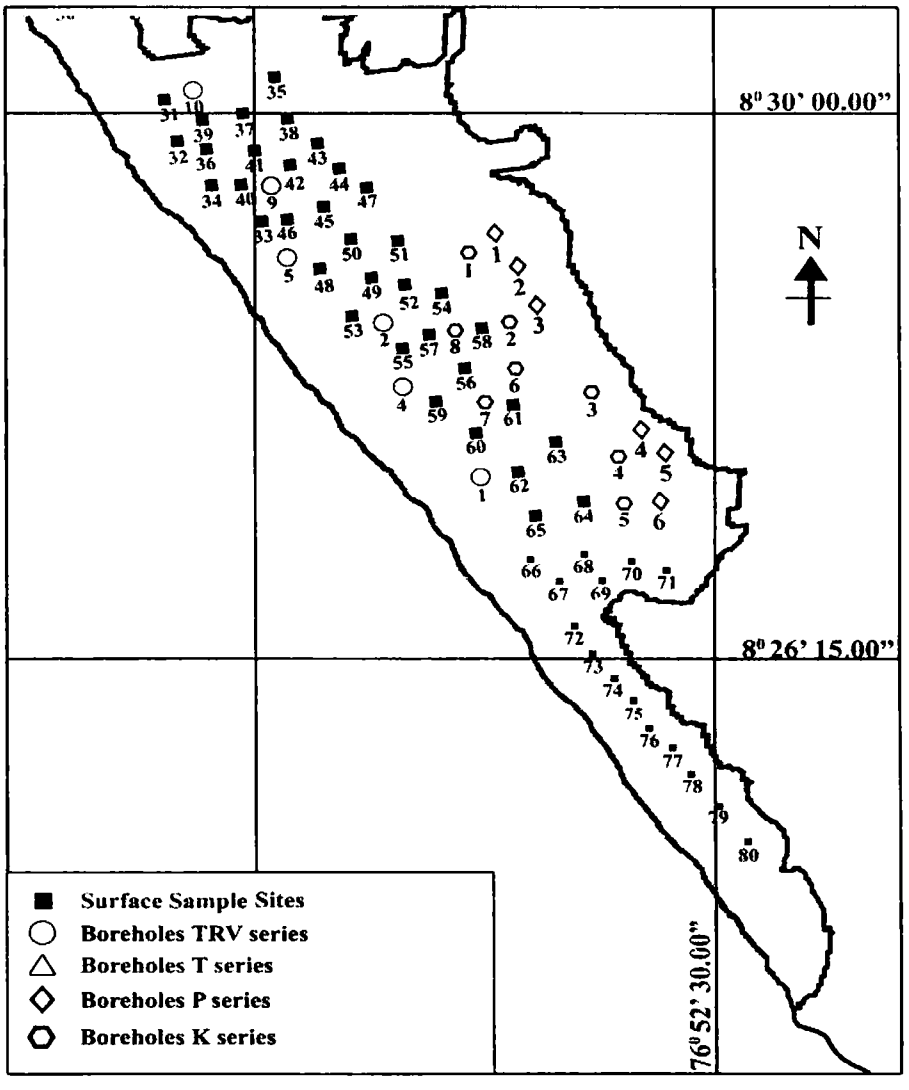

Figure 2.4.b. The map showing Sample Locations in the southern part of the study area

2.3.2. Boreholes T1- T8

The boreholes T1 to T8 fall along the eastern margin of the northern part of the study area, north of Lake Veli and in contact with lateritic hills to the east. Here the coastal plain is broader than in the south. The Litho Units of T1 to T8 are plotted in litholog (Figure 2.5a). Beneath the top soil/ land fill horizon (thickness 1m to 2.5m), is a layer of brownish black

silty clay (2.6m in T1, 1.2m in T2, 2.9m in T3, 2m in T4, 3.5m in T5, 2.7m in T6, 3m in T7 and 1.7m in T8) underlain by silty sand with slight clay (4.6m in T1, 2.6 in T2, 5m in T4, 3.5m in T5, 5.3m in T6, 2.75 in T7 and 3.3 in T8) and laterite thereafter occur. At T3 no different Litho Unit is found beneath the sandy deposit till 13m depth. Except in T3, laterite is encountered at 7-8m depth from present land surface.

2.3.3. Boreholes P1- P6

The boreholes P1 to P6 fall along the eastern margin of the southern part of the study area, south of Lake Veli, in contact with lateritic hills further east. The Litho Units of P1 to P6 are plotted in litholog (Figure 2.5b). Underlying the topsoil cover or landfill,

there exists a layer of silty sand with slight clay (6m in P1, 3.5m in P2, 0.80m in P3, 4.5 m in P4, 2.25 m in P5 and 3.5 m in P6) and it overlies a layer of brownish black silty clay (1 m in P1, 0.5 m in P3, 2 m in P4, 2.25 m in P5 and 2 m in P6; this layer is absent in P2). The brownish black clay lies unconformably over laterite. In this region lateritic basement can be found at a depth of between 4m and 7m.

2.3.4. Bore holes TRV 1 and TRV 4

In TRV 1 and TRV 4, the two deepest boreholes, which are 37 m deep, there are three noticeable sediment layers. At a depth of 8 m from the surface, the sand constitutes almost 100%, of which quartz forms nearly 99%.

At a depth of between 8 m and 10 m, the sand grains become very fine with fall in the quantity of sand to 86%, silt acquiring 8% and vegetal remains forms up to 6%, giving a fresh green color to the sediments. Characteristically they fall in the category of organic rich sand. The sand grains are very fine and composed largely of quartz followed by feldspar and heavies. Between 7 m and 8 m, the color of the sediment is slightly brown, as it is in the case at a depth of between 10 m and 11 m indicating horizons of transition.

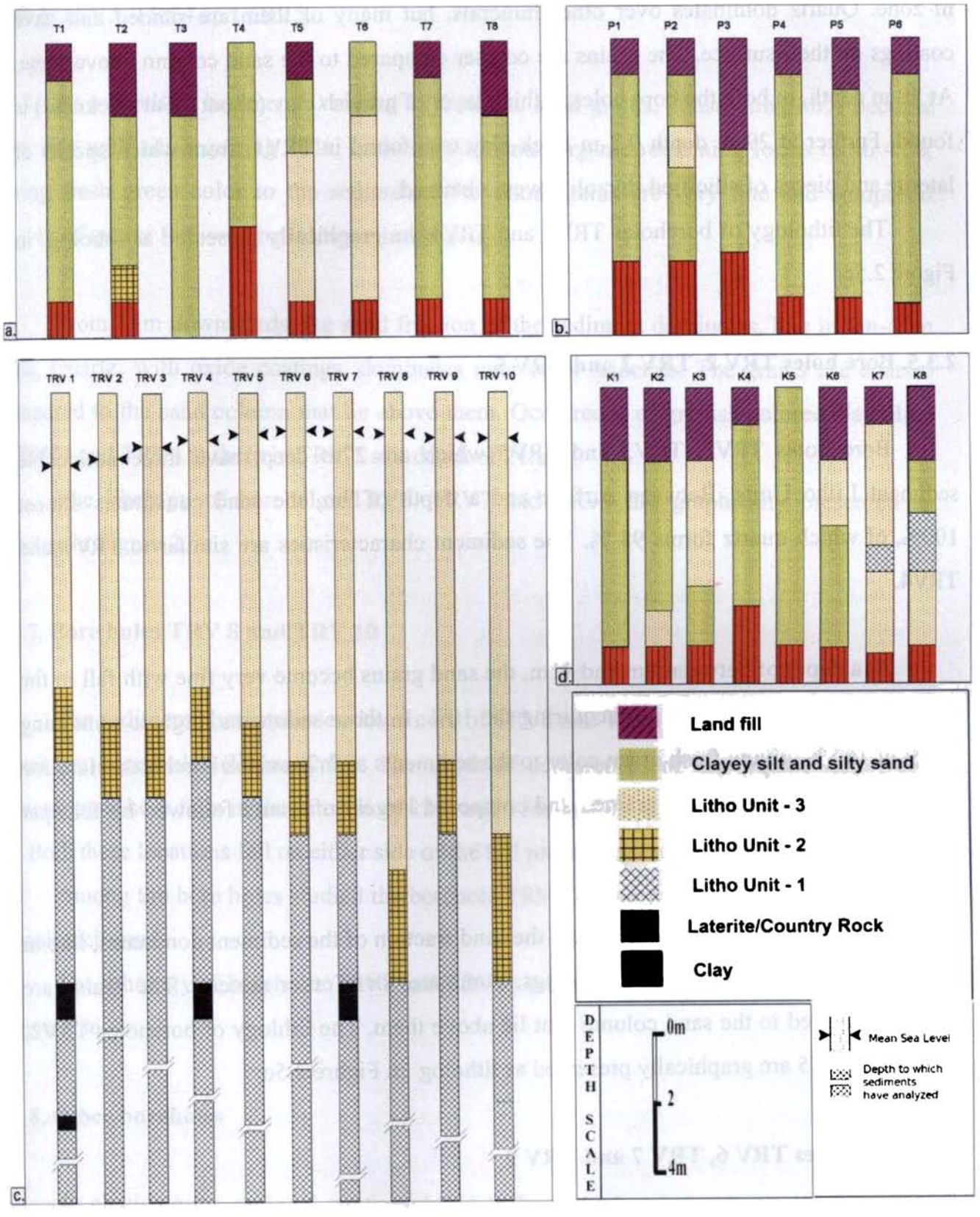

Figure 2.5. The lithologs of the study area developed from the borehole data

From 10 m downwards, the sand fraction of the sediment dominates, like in the 0-8 m zone. Quartz dominates over other minerals, but many of them are stained and have coatings on their surface. The grains are coarser compared to the sand column above them. At 20 m depth, in both the bore holes, a thick layer of greyish clay (about 0.5m thickness) is found. Further at 29 m depth 0.2 m thick clay was found in TRV1, from which specks of laterite and pieces of silicified rhyzolith were obtained.

The lithology of boreholes TRV1 and TRV4 are graphically presented as litholog in Figure 2.5c.

2.3.5. Bore holes TRV 2, TRV 3 and TRV 5

Bore holes TRV2, TRV3 and TRV5 which are 27m deep, have three noticeable sediment Litho Units. Between surface and a depth of 9m, the sand constitutes almost 100%, of which quartz forms 98 %. The sediment characteristics are similar to TRV1 and TRV4.

At a depth of between 9m and 11m, the sand grains become very fine with fall in the quantity of sand to 85% and silt acquiring the 10%. In these sediments, organic remaining forms up to 5%, giving fresh green color to the sediments as in previous boreholes. Here too the sand grains are very fine grained and composed largely of quartz followed by feldspar and heavies.

From a depth of 11m downwards, the sand fraction of the sediment dominates, like in 0m-9m zone. Quartz, with oxide coatings, dominates over other mineral. The grains are coarser compared to the sand column that lie above them. The lithlogy of boreholes TRV2, TRV3 and TRV5 are graphically presented as litholog in Figure 2.5c.

2.3.6. Bore holes TRV 6, TRV 7 and TRV 9

In bore holes TRV6, TRV7 and TRV9 which are 30 m, 26 m and 29 m deep respectively from the surface and at a depth of 10 m, sand constitutes 100% sand of the sediment, of which quartz forms 96% of the mineral population. The grains are sub angular

and the majority of them are fine grained. The sediment characteristics are similar to TRV1, TRV2, TRV3, TRV4 and TRV5.

At a depth of between 10 m and 12 5 m. the sand grains, constituting 86% become very fine with silt acquiring 10%. In these sediments, organic remaining forms up to 4 %, giving fresh green color to the sediments. The sand grains are very fine and composed largely of quartz followed by feldspar and heavies.

From 13m downwards, the sand fraction of the sediment dominates, like in 0m-10m zone. Quartz, with oxide coatings, dominates over other minerals. The grains are coarser compared to the sand column that lie above them. Occurrence of greyish colored clay alike in TRV1 and TRV4 is there in TRV 7 at a depth of 21m.

The lihology of boreholes TRV6, TRV7 and TRV9 are graphically presented as litholog in Figure 2.5c.

2.3.7. Bore holes TRV 8 and TRV 10

The sediment characteristics down core of TRV8 and TRV10 are similar to that of the remaining bore holes (Figure 2.5c). The depth of occurrences of the organic rich green colored layer here falls in the interval of 13m and 15m in TRV 8 and 12m and 16m in TRV 10. Both these locations fall on either side of the hill protruding into the coastal plain at Veli.

Among the bore holes studied the borehole TRV10 bears the deepest and the thickest organic rich sand.

The lithology of boreholes TRV8 and TRV10 are graphically presented as litholog in Figure 2.5c.

2.3.8. Other boreholes

To elucidate the regional stratigraphy, data from the boreholes located at K1, K2, K3, K4, K5, K6, K7 and K8 are used. These boreholes have a sequence different from that observed in P1-P6 and T1-T8.

At K8 there exists a brownish black silty clay (thickness 7.6m) lying over the laterite.

At K7 the top soils are underlain by a laterite cover which has a thickness of 5.5m beneath which the granulitic rock can be found, where no clastic sediments has been encountered. In location K6, The topsoil is underlaid by 5m thick fine sand underlain by highly coarse-grained sand. Here Laterite is encountered at a depth of 9m from the surface.

At location K4, 2m of fine sand is seen underlain by 14m of coarse sand, which lies over laterite.

At location K1, the stratigraphy resembles P4. In borehole K3, 3m top soil is followed by 4m of silty sand underlain by a 4m greenish organic rich sediment. Below this layer there occurs a thick column of coarse grain white sand and upto a depth of 25m.

At location K2, falling closer to eastern boarders of the study area and at the confluence of two streams, namely Amayizhanjan thodu and Chalai thodu, silty sand can be seen at a depth of 6m followed by white sand at a depth of 9m,and they are underlaid by laterite at 15m depth.

At location K5, the sediment column is full of fine white quartz sand at a depth of 12m followed by 1m thick greenish organic sediment. This layer is underlain by another layer of quartz sand, whose grain size and shape are different from the one lying above the greenish layer. This column shows much similarity to the sedimentary sequence obtained at boreholes of TRV series.

The stratigraphy of the boreholes described here are graphically presented as litholog in Figure 2.5d.

2.4. Discussion

Sand is generally distributed in riverbeds, dunes and coastal deposits on a large scale. Nearer to modern coast it is seen in close association with estuaries, flood plains and wetlands. Stratigraphical sequences of coastal sand could serve as records for reconstructing paleoenvironments for wetland coast. For the purpose of making stratigraphy, the lithological characteristics need to be accounted for with further evidences.

Based on the lithology, of surface and boreholes, of various locations in the Thiruvananthapuram coastal plain, a lithological spatial arrangement is derived at. Figure 2.6 depicts the sub surface lithostratigraphy of the study area in general from the data drawn from representative boreholes.

All eighty locations, falling in sandy plains, from where the samples are collected (See Figure 2.4a and 2.4b for sample locations) show single strata, unchangingly. The same lithological unit is encountered at a depth of between 8m and 12m depth in all the ten different bore holes sampled in the study area. Towards the eastern part of the study area, where the plain abuts into the lateritic hillocks, the same sand body thins down to a depth of 4 to 5m beneath the top soil/ land fill. In certain locations along the eastern side of the study area the top layer of silica rich sand is absent and is substituted by laterites, brownish soil and silty sand.

In short the sand that is encountered on the surface extends down to a depth of 8m (TRV1 and TRV4) to 12m (TRV10) without much change in its physical properties including constituents, colour and common appearances. This uniformity leads to the conclusion that from surface to a depth of 8 to 12m, the sand body can be considered as a single lithological unit, that is, the top most unit.

The 12 boreholes spread along the southern, central and northern region of the central part of the study area bears a sediment layer which is strikingly different from the top most layer because of its brownish green color. The lithological unit contains very fine sand and the color is attributed to the organic content, resembling present day neckron mud. One striking characteristic exhibited by these sediments at the time of collection was its 'color fading'. These sediments existing under severe reducing conditions once exposed to air, for an hour or so, fade into brown color, indicating the instances of quick oxidation.

The brownish green layer encountered spreads consistently in the study area concealed under the top-most sand layer described above. The thickness of this layer varies between 2m to 4m in different boreholes and the thickest encountered was in TRV10 located close to the lake at Veli. In the southern part of the study area, this sediment layer dips $2\text{-}3^0$ to the north while in the northern part it dips 2^0 to the south. The geographic extent and lithological uniformity with its unique physical character affix singularity to this sediment layer, therefore it can be treated as a separate unit.

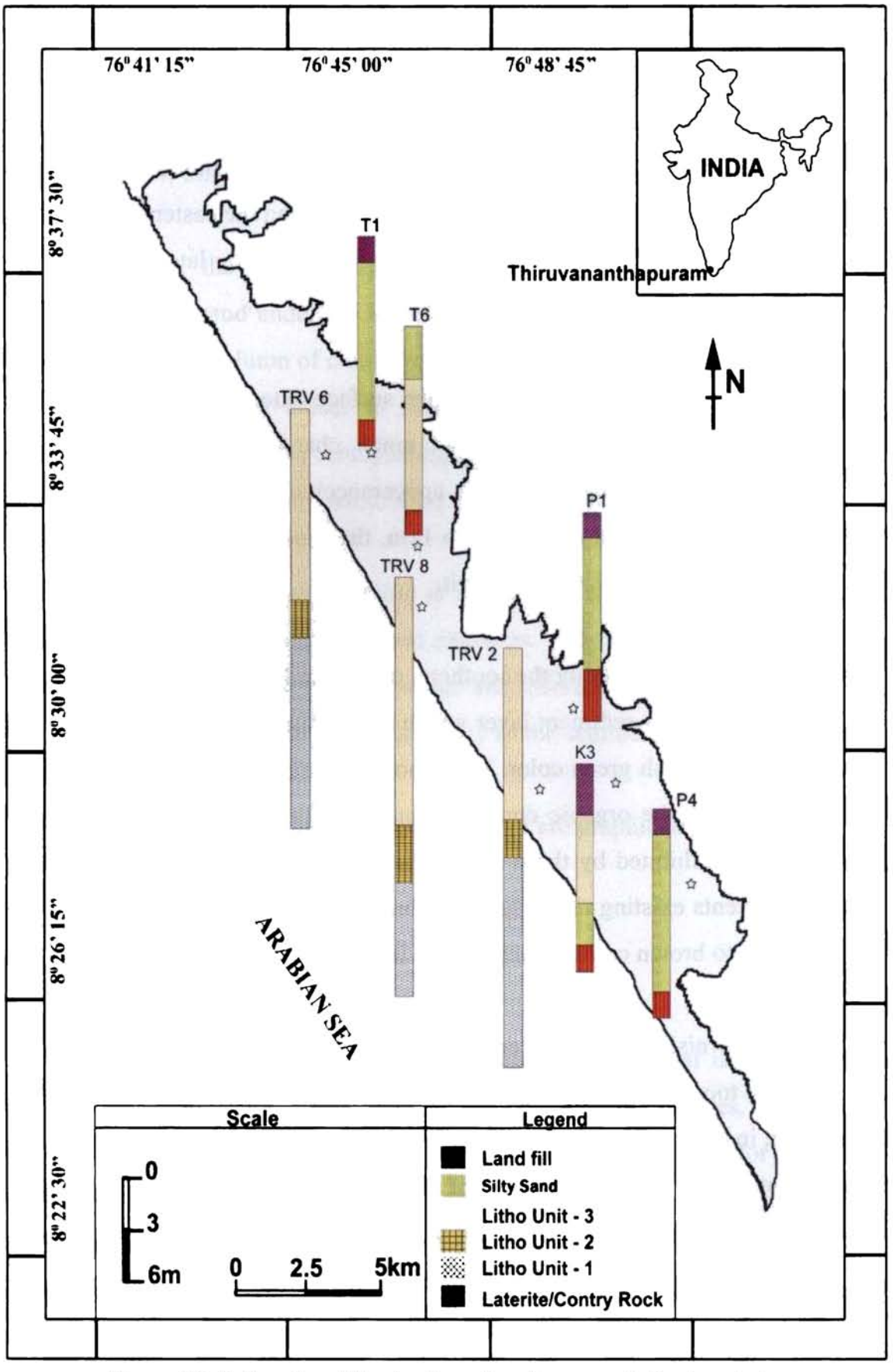

Figure 2.6. Subsurface lithostratigraphy of representative boreholes across the study area.

Underlying the above unit in the litholog, is a sequence of medium sand with slight yellow/ brown color. The color is washable and could be the stains of Fe oxide/hydroxide coatings. Small percentages of heavy minerals are seen in this sand column. In two locations, TRV1 and TRV4, a layer of clay having a thickness of 50 cms are seen at a depth of 19-20m. Other than the stray occurrence of clay, this layer is nearly uniform to a depth of 29m, where lateritic pebbles were encountered in TRV1. The sand column extends further deep crossing 65 m, where the drilling was stopped due to low sediment recovery. This unit of sediments encountered beneath the former layer is considered as a singular unit extending to a thickness of >20 m and is considered as bottom layer. The presence of lateritic specs and rhyzolith at a depth of 29 m in TRV1 throws up two possibilities. That is, the laterites and rhyzoliths are either deposited then or the bore hole has crossed the datum plane between the Quaternaries and Tertiaries.

Towards the eastern boarder of study area, closer to the base of laterite hills, the above discussed 3-layer sequences are not in prompt. The bottom and middle Litho Units, described above, are absent in T5, T6, K2 K3, K4, K5 and K6. Though the top layer is uniform in the area, it is seen mixed with brownish silty sand and silty clay in T1-T4, T7, T8, P1-P6. Here, in all locations, laterite underlies the sediment sequence. In locations like K4 and K6, a thick column of highly coarse sand has been recovered. The variation in lithological column along the eastern margin of the study area, down to a depth of 5-6m falls in the cultural horizon. It should be regarded as the product of anthropogenic activities during early civilizations and due to human encroachment in the later phase of urban development.

The systematic arrangement of the sediment column correlated with their occurrence in boreholes brings to light the fact that in the study area, there exist a minimum of three different Litho Units which were designated as bottom, middle and upper Litho Units. In order to systematize it, three identifiable names, namely Litho Unit 1, Litho Unit 2 and Litho Unit 3 are ascribed to the lower, middle and top most units respectively in the discussion here onwards. As per the Principle of Super Position, in an undisturbed terrain, the oldest of sequence lays at the bottom, while the youngest at the top and the numbering from bottom-onwards.

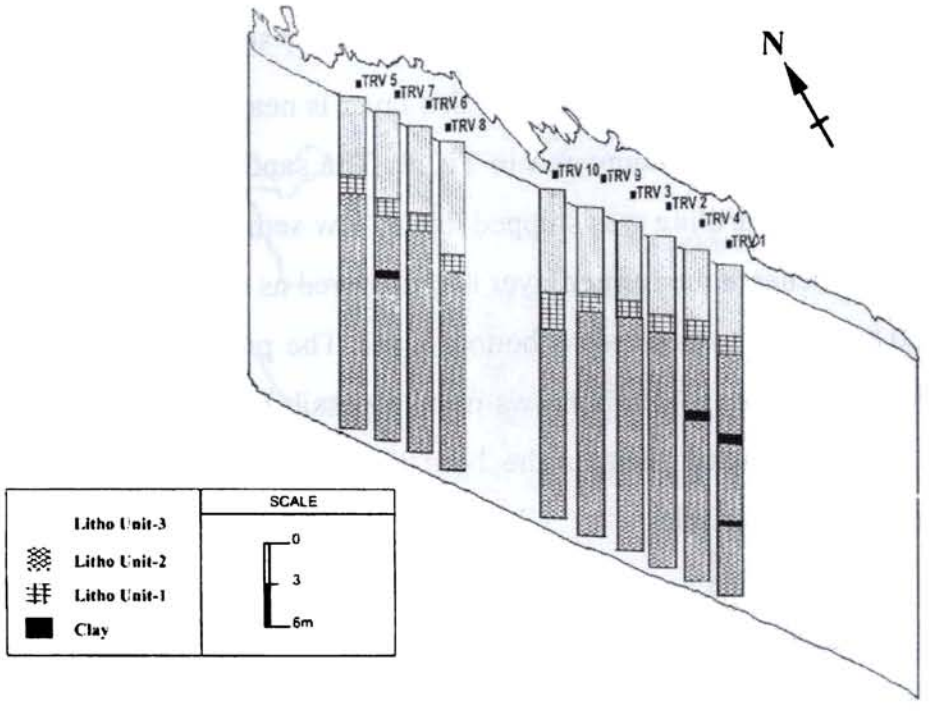

Figure 2.7. Subsurface lithostratigraphy of the central part of the study area where stratigraphic horizons are delineated.

In stratigraphy a sediment unit is considered stratum when it occurs undisturbed and its pack is repeated all throughout the region. From the present study it is understood that the Litho Units 1 to 3 do not show any sort of mixing up or overlapping or sequence reversals in the boreholes studied along the middle region of the study area (TRV 1 – 10). Therefore the three Litho Units identified can be regarded as stratigraphic horizons (Figure 2.7), covering a larger part of the study area. While towards the eastern periphery, where the overall thickness of sediment column is less, mixed sediment sequences are observed as expected. Therefore the approach in the subsequent chapters is to further characterize the three Litho Units established here, to understand their age, environment of depositions and other factors involved in their evolution.

Chapter III

Geochronology

3.1. Introduction

Geochronology is an essential component of geology, it deciphers the absolute time of the formation of a rock or any geologic event and has wide applications. Various methods are employed to determine the age of a rock, like the radioactive nuclide dating methods, fission-track datings, varve layering dating methods and luminescence dating methods. The selection of the method of dating depends upon the factors like suitability, possibility and utility.

Carbon-14 (^{14}C) dating method and Optically Stimulated Luminescence (OSL) dating method are employed in the present study. ^{14}C dating method was chosen specifically to date Litho Unit 2, since it is rich in organic carbon. But the absence organic carbon in Litho Unit 1 and Litho Unit 3 limited the application of ^{14}C dating in those layers. Therefore OSL dating technique was adopted to decipher the age of deposition of these two Litho Units.

3.2. Radiocarbon geochronology

Recent scientific work has demonstrated the capability of peat mires and organic rich muddy sand to store information of past environments with a high temporal resolution (Goodsite et al., 2001). Peat sections have served as archives of heavy metal pollutants of the atmosphere (Shotyk et al., 1998; Benoit et al., 1998) and yielded records of both climate and atmospheric CO_2 content (White et al., 1994; Martínez-Cortizas et al., 1999). The capability of determining age using ^{14}C in peat helps to bring out a time based documentation of peat lands.

^{14}C dating estimates the age of any organic material as old as 50,000 years. Commonly it is obtained on wood, charcoal, marine and fresh-water shell, bone and antler, peat and organic-bearing sediments carbonate deposits such as tufa, caliche, and marl, and dissolved carbon dioxide and carbonates in ocean, lake and ground-water sources.

^{14}C is radioactive and is produced when ^{14}N is bombarded by cosmic rays in the atmosphere (Figure 3.1). The newly formed ^{14}C drifts down to earth and get absorbed by plants and enters the food chain. When a living organism dies, it stops absorbing ^{14}C thereby the carbon begins to disintegrate. The quantity of ^{14}C disintegrated and it remaining within in the died object are assessed. ^{14}C decays at a slow but steady rate and reverts to ^{14}N.

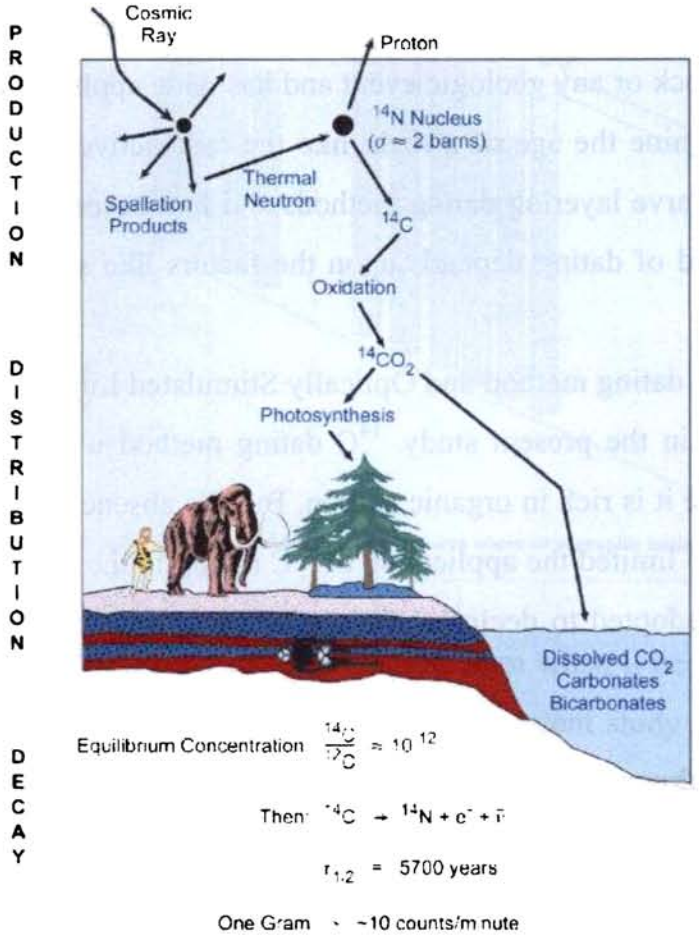

Figure 3.1. Graphical representation of the production, distribution, and decay of natural C (after Donahue et al., 1997).

A measurement of the radiocarbon content of an organic sample will provide an accurate determination of the age of the sample under the following assumptions:

1. the production of radiocarbon by cosmic rays has remained essentially constant long enough to establish a steady state in the $^{14}C/^{12}C$ ratio in the atmosphere;

2. there has been a complete and rapid mixing of radiocarbon throughout the various carbon reservoirs;

3. the carbon isotope ratio in the sample has not been altered except by radiocarbon decay; and

4. the total amount of carbon in any reservoir has not been altered.

In addition, the half-life of radiocarbon must be known with sufficient accuracy, and it must be possible to measure natural levels of radiocarbon to appropriate levels of accuracy and precision and ^{14}C has a half-life of 5730 years. Basically this means that half of the original amount of ^{14}C in organic matter will disintegrate in 5730 years after the organism dies and half of the remaining ^{14}C will disintegrate after another 5730 years and so forth. After about 50,000 years, the amount of ^{14}C remaining will be so small that the fossil cannot be dated reliably.

In radiocarbon geochronology, to determine how much ^{14}C remain in the carbonaceous matter, the number of β- radiations given off per minute per gram of material is counted. Modern ^{14}C emits about 15 β–radiations per minute per gram of material, but ^{14}C that is 5730 years old will only emit half that amount per minute. So if a sample taken from an organism emits 7.5 radiations per minute in a gram of material, then the organism must be 5730 years old. The accuracy of radiocarbon dating was tested on objects with dates that were already known through historical records such as parts of the Dead Sea scrolls and some wood from an Egyptian tomb. Based on the results of the Carbon 14 test the analysis showed that ^{14}C ages agreed very closely with the historical information. The natural radiocarbon activity in the geologically recent contemporary "pre-bomb" biosphere was approximately 13.5 disintegrations per minute per gram of carbon.

3.2.1. Methodology

The sample preparation and analysis of 6 samples from 3 lithologs were done at radiocarbon lab at Birbal Sahni Institute of Paleobotany, Lucknow. The process of radiocarbon dating involves two steps - benzene preparation from the sample and counting of benzene. The former is performed in the benzene system and the latter with the scintillation counter.

3.2.1.1. Benzene Preparation

Pre-treatment of the sample

Pre-treatment technique varies according to the nature of the sample. For sediments, carbonate impurities are removed by the pre-treatment. In this process, sample is taken in a beaker and is heated with 10% HCl, at 95°C, in a water bath, for one hour. Then it is washed with deionised water, to remove its acidity, which can be checked with pH paper. Sample is washed again, until it is neutralized. After complete neutralization, the sample is put in an oven, at 90°C, until it becomes dry. For wood, paper, charcoal, peat, cloth etc, sample is heated with 1%HCl, 1.5%NaOH, and then with 1% HCl at 95°C in a water bath for one hour and wash it with deionised water, until it is neutralized. For marine samples such as shells, and melliolites, the sample will be treated with 1% HCl for 5 minutes, to remove the impurities.

Extraction of CO_2 from the pre-treated sample

There are three techniques for CO_2 preparation, depending on the nature of the sample:- (1) Wet oxidation, (2) Hydrolysis and (3) Dry combustion.

Wet oxidation is done only for standard purposes. It is affected by a strong oxidant. In some cases, the untreated oxidant is measured by back titration and in some others, the evolved CO_2 is measured directly.

Hydrolysis is done, if the sample is carbonate such as shells. Dry sample is taken in a magnetic stirrer and is treated with 10% HCl to get CO_2.

$$CaCO_3 + 2HCl \rightarrow CaCl_2 + H_2O + CO_2$$

The whole system is checked for leak, using a mercury manometer. For vacuum measurement, PIRANI vac-gauge (~50 microns) was used. Silicon grease is used for the fixing of the apparatus instead of carbon grease. This is to prevent any contamination of the sample by external carbon. Older materials are extremely sensitive to contamination by younger carbon.

Combustion method is used, if the sample is peat, charcoal, sediment, wood, paper, cloth etc. The Sample is placed inside a quartz tube. Reusable quartz wool is placed in both sides of the sample, inside the quartz tube. Thus the heat will concentrate within the quartz wool. After putting glass wool inside the tube near the ends, the two ends are closed using rubber cork and sealed with sealing wax. Glass wool prevents the rubber cork from damage, since the rubber cork is very sensitive to heat. Quartz tube is slided inside an external electric heater. at 750°C is used for 1.5 hours. System is checked for leak. Then commercial O_2, (grade≈99%) from a cylinder is passed through 15% NaOH solution to remove the CO_2, associated with O_2:

$$2NaOH + CO_2 + O_2 \rightarrow H_2O + Na_2CO_3 + O_2..$$

Water vapor is removed by passing the gas through conc.H_2SO_4, which is a good dehydrating agent. Then pure O_2 is passed through the quartz tube. The temperature inside the heater, which we can read at the periphery of the heater, is maintained as 950°C, for one hour. Carbon in the sample reacts with O_2 to form CO_2. The CO, formed due to the partial combustion of carbon is converted to CO_2 by passing the gas through Cu_2O, which is a good oxidant. CO_2, evolved is passed through acidified $KMnO_4$ solution for complete oxidation, and through 5% acidified $K_2Cr_2O_7$ to remove nitrogen and sulfur. The gas is then passed through 1%$AgNO_3$ to remove the halogen impurities. CO_2 is again passed through acidified $KMnO_4$ solution through a spiral tap.

CO_2 gas, produced during hydrolysis or combustion is then passed through molecular sieve, of size 3A°, at -22°C to-30°C, under slush which is a mixture of liquid nitrogen and ethyl alcohol. It is then passed through silica gel at 0°C and is condensed using liquid nitrogen whose temperature is -196.4°C. The condensed CO_2 will make a pressure change from a highest to 0 cm in the manometer. It is kept for half an hour. The remaining gases are pumped off the system, through vacuum pumps. Condensed CO_2 is heated up to room temperature, and is stored in storage bulbs and labelled. The pressure has to be maintained below 50 cm during the whole process, as the system will blast if the pressure exceeds atmospheric pressure.

Acetylene preparation

The collected CO_2 is condensed using liquid nitrogen and heated to room temperature. Then it is treated with molten Li, at 550°C, inside a reaction vessel. Li combines with CO_2 to form Li_2C_2, in presence of Cr_2O_3 and Al_2O_3, which are kept inside the reaction vessel. After cooling to room temperature, deionised water is slowly supplied to Li_2C_2, which under hydrolysis yields C_2H_2, H_2, and H_2O. The mixture is then passed through empty trap, under slush, at -80°C.To remove the water vapor, C_2H_2 is passed through P_2O_5 and ascribe, whose mesh seize is 8 to 20. Then the gas is stored and condensed using slush.

Trimerisation of C_2H_2 to yield benzene.

For this process, we degas the catalyst, vanadium pentoxide at 550°, for one hour and then cooled to 80°C. Acetylene is then passed through the catalyst. C_2H_2 will trimerise to benzene using the degassed catalyst at about 80°C and left for one hour for the completion of the reaction. Benzene is then withdrawn in a separate detachable trap. It is cooled, using liquid nitrogen and the catalyst is heated at 90°C for one hour. Benzene is separated in a bottle and is then kept in a freezer at 40°C to minimize the evaporation loss.

3.2.1.2. Counting of benzene

Counting of benzene is done in the scintillation counter (Quantulus Liquid Scintillation Counter- Wallac 1220). It is only benzene that produces scintillation when it decays to half of its initial amount. Here, we count each sample 25 times. As the number of counting increases, errors in age decreases. We have to have three types of benzene. They are dead benzene or old benzene (anthracitic benzene), benzene from the sample, and standard benzene (butyl PBD). Pure benzene or spectrometric grade benzene cannot produce scintillation. So we add 15gm/L butyl PBD to pure benzene. In counting benzene, the following steps are involved:

(1) Sample ID is noted.

(2) Weight of counting box is taken

(3) 0.013gm of butyl PBD is added to it and the weight is noted down

(4) 0.7348 of anthracitic benzene is added and the weight is noted

(5) the sample benzene is added and the weight is noted

(6) Box is taken outside and closed.

(7) the sample is loaded in the scintillation counter, which is connected to software, for recording and processing the counts.

3.2.1.3. Standard error

Statistical analysis is necessary in radiocarbon dating because it is not possible to measure the entire radioactivity in a given sample. Each radiocarbon date is released as a conventional radiocarbon age with 'standard error'. This is the '±' value and by convention is ± 1 sigma. The standard error is based principally upon counting statistics.

According to Stuiver and Pearson (1992), the majority of laboratories report the measured counting statistics as a laboratory standard error. Many laboratories today calculate a laboratory error multiplier to account for all errors account for routine variation in reproducibility in radiocarbon dating. According to Stuiver and Pearson (1993), the error multiplier is a measure of the laboratory reproducibility, incorporating the errors resulting from the preparation of gas, its loading, memory effects and counting statistics and is defined as the actual standard error divided by the quoted standard error and is usually generated through repeat dating of a standard of known age or consensus age.

3.2.2. Results of radiocarbon dating

The following table shows the result of radiocarbon dating of two horizons in three different spatially separated bore holes, namely TRV1, TRV6 and TRV 10.

3.2.3. Age-depth models of organic rich mud sections

Age-depth models were constructed for each borehole to translate depth measurements to age measurements (Bennett, 1994). They make it possible to compare the temporal course of events in different sequences, assuming that the sedimentation rate between dated depth points were constant.

In the present study, the age-depth models for Litho Unit 2 from TRV 1,6 and 10 were made and deposition time and sedimentation rate are deduced using computer programme DEP-AGEZ, version 4 (Maher and Thompson, 1992). The deposition time is the time elapsed during accumulation of unit sediment thickness (in (radiocarbon years)/ cm) and sedimentation rate is the rate at which accumulation has taken place, which is the inverse of deposition time.

Table 3. 1. Radiocarbon ages of top most and bottom most part of Litho Unit 2

Depth (in meters)	Age (in B.P.)
a. Borehole No. TRV 1	
8	7730 ± 290
10	9460 ± 260
b. Borehole No. TRV 6	
10	7500 ± 350
12	9560 ± 250
c. Borehole No. TRV 10	
12	7230 ± 200
16	10,700 ± 210

Table 3.2. The deposition time and accumulation rate of organic rich mud in the location of boreholes

Borehole	**Deposition Time (radiocarbon years/ cm)**	**Accumulation Rate (cm/ yr)**
TRV 1	8.65	0.116
TRV 6	10.3	0.097
TRV 10	8.68	0.115

3.2.4. Discussion

The ^{14}C dates obtained are in good agreement with the sedimentation sequences enabling paleogeographic interpretations. The thick organic rich mud column, represented by Litho Unit 2, indicates a change in the sedimentation. The absence of organic materials above and below this layer remarkably points to the fact that, time span between 10,700 and 7230 B.P. was dramatically favouring intensive growth and accumulation of organic matter in the region. High vegetal productivity develops in an environment of low energy

and calmness, like lakes and ponds. Therefore, the Litho Unit 2 could have an origin attributed to these environments. Absence of marine shells and microfossils in this Litho Unit is noticeable, which confirms that the source and support of the organic regime was primarily continental. Thus it can be deduced that a fluvio lacustrine basin existed in the study area between 10,700 years and 7230 years B.P.

From radiocarbon dating of organic rich muddy sand obtained from depth samples from the study area gives the initial and final stages of wet-span experienced (Table 3.1.a-c) samples dated from the designated bore holes give a range of age from 10,700 B.P. to 7230 B.P. years. The span of wet spell, deduced from the age data ranges from 1730 years to 3470 years. The lowest extend of mud recorded from lower levels in TRV 1 between 8m and 10m, while the longest span was of TRV 10 between 12m and 16m.

The radiocarbon dates from organic rich sand layers in the area brings the following conclusions:

- TRV 10 borehole data points to a major environmental change around 10,000 yrs B.P. in the study area at the base of Litho Unit 2. Organic sediment formation should rather be considered as the result of change in the prevailing environment. Peat is formed in low energy or stagnant water bodies, supported by high nutrient supplementation. This is possible only when the regular flow of continental water is physically objected and pooled. It is established elsewhere that during Pliestocene Holocene boundary (approximately around 11,300 yrs B.P.), the rising sea level had reduced the riverine discharges into the sea, thereby creating low energy basins of water pooling along the coast. Pooling of high nutrient water could turn to be the nest of peat forming organic materials. Thus the Pliestocene-Holocene boundary in the area can be taken as coinciding with the base of Litho Unit 2.
- Among all the boreholes peat occurs at a deeper portion in TRV 10. Age wise the bottom part of peat layer in this borehole gives the oldest radiocarbon date. These facts fairly point to the physiographiy of the region at the Pliestocene – Holocene transition. The location of TRV10 could then be a low lying region of the pre-Holocene surface, compared to the other borehole sites, representing the deepest part of the basin.

- There was a gradual increase in the extent of organic rich sedimentation across the study area starting from 10,700years B.P. to 7730 years B.P. This enabled the peat formation to extent into geographical regions located at higher levels surrounding the central part of the basin.
- There was a sudden retreat of peat forming phase during 7730 years B.P. (location TRV 1) to 7230 years B.P. (location TRV 10). It is observed that in southernmost borehole (TRV 1) the organic mud formation ceases at 7730 years at depth of 8m whereas in TRV10 it ceases at 7230 years B.P. at 12m depth indicating that there was a retreat of the pooling condition towards central portion. Similar waxing and waning of sedimentation of the organic rich layer can be traced out in TRV6 also. Therefore it could be concluded that upper horizon of Litho Unit 2 follows in concurrence with drying up of the lake from south and north towards the locii near TRV10.
- Age-Depth model enabled to infer the deposition time and accumulation rate of the peat in Litho Unit 2. The northern part of the study area, where borehole No TRV 6 falls in, had experienced the lowest accumulation rate. It took about 10.63 radiocarbon years for the deposition of 1cm of peat. As where the southern part of the study area, boreholes TRV 1 and 10, the deposition time is around 8.68 radiocarbon years for accumulating 1 cm of the layer.

3.3. Luminescence geochronology

The Luminescence techniques enable to determine ages from one or two hundred years to about 400 ka with an error of around 10%. The method is quite unique in Quaternary dating techniques because it uses the constituent mineral grains of the sediment itself (quartz, feldspars) instead of the associated material (as carbon in ^{14}C dating method). In the study area, the radiocarbon dating is not feasible due to lack of organic materials especially in Litho Unit 1 and 3. The silica sand flats do not bear any other mineral material that could fruitfully date the age of deposition. Therefore luminescence dating has to be totally relied upon.

The term 'luminescence dating' covers a range of analytical methods that can be applied over different time periods to different minerals and in different environmental

settings. Luminescence is certainly a complex topic, but in essence the use of the phenomenon for dating Quaternary events is very simple (Duller, 2004).

Many common minerals, including quartz and most feldspar, are able to store energy within their crystal structure. Energy is deposited within the crystal mainly by ionizing radiation (e.g. alpha, beta and gamma radiations) from the environment, but there is also a contribution from cosmic rays. Some part of this energy is stored by electrons or holes becoming trapped in excited states above the valence band. The energy stored increases with the amount of radiation to which a crystal is exposed, and this provides a 'clock' that is the basis of all luminescence (and electron spin resonance) dating methods. In the laboratory, the energy stored in the crystal can be released by stimulating it, and some portion of the energy is released in the form of light. This light is known as luminescence. Such measurements can be used to estimate the dose of radiation that the crystal has absorbed; this quantity is the 'equivalent dose' (ED or De) and is measured in the SI unit of grey (Gy; 1 Gy = 1 J/kg). The only additional information required to calculate an age involves assessing the radioactivity of the sample and its surroundings using chemical or radiometric methods, and estimating the radiation contributed by cosmic rays. The rate at which the sample was exposed to radiation in the environment, the 'dose rate', is measured in Gy/ kyr, and dividing one quantity by the other yields the age

$$\text{age (ka)} = \frac{\text{equivalent dose(Gy)}}{\text{dose rate (Gy/kyr)}}$$

Although there are a wide range of luminescence dating methods, they all use above equation, and the only major difference is the process that sets the luminescence 'clock' to zero, related to the event that is being dated. There are four processes that will result in resetting of the luminescence signal: (i) formation of the mineral by crystallization (e.g. from a magma, or by biological processes), (ii) subjecting the mineral to extreme pressure, (iii) heating the crystal above 200-300 degrees C or (iv) exposing the crystal to light. Of these processes, the first is rarely used in dating applications, and the effectiveness of the second remains controversial. For archaeological applications, the third process is frequently appropriate where it is the heating of the material either deliberately during firing (e.g. pottery) or inadvertently in hearths (e.g. stones) that is the event being dated. This was

the first application of luminescence dating and has been thoroughly discussed elsewhere (Roberts, 1997). For luminescence dating of Quaternary sediments, it is the exposure of the mineral grains to daylight prior to deposition that is the event being dated. Exposure of the crystal to daylight causes stored energy resulting from previous radiation exposures to be released, thus leaving the crystal such that it has a low, or residual, luminescence signal.

For dating Quaternary sediments two methods of stimulating luminescence have been used, thermal and optical. Early measurements in the 1980s involved heating the sample from room temperature to approximately 500^0C to generate a thermoluminescence (TL) signal (Wintle and Catt, 1985). Optical stimulation is preferable for dating sediments and generates an optically stimulated luminescence (OSL) signal. Optical dating has the advantage over TL dating that preferential measurements are made of that part of the luminescence signal that is most sensitive to light, and so the OSL signal is reset to zero by exposure to light far more rapidly and completely than is the TL. This has two implications: firstly that sediments require much shorter periods of exposure to daylight at deposition to be dated using OSL than TL, and secondly that because the uncertainty in the degree to which the signal is reset to zero is smaller, younger samples can be dated.

Optical stimulation requires an intense light source that emits within a narrow wavelength region. Quartz is efficiently stimulated using green or blue light sources (ca. 420–550 nm wavelength), and it emits strongly in the blue and ultraviolet part of the spectrum. This ultraviolet emission (centred at ca. 365 nm) is separated from the stimulation light using glass filters and detected using a photomultiplier tube. A system based on filtering the blue-green light from a white halogen bulb was developed by Bøtter-Jensen and Duller (1992) and has been used by number of workers (like Olley et al. 1998; Hilgers et al. 2001 and others). However, the fully software-controlled green and blue LEDs have simplified OSL measurements on quartz.

3.3.1. OSL dating technique

Luminescence dating is based on quantifying both the radiation dose received by a sample since its zeroing event, and the dose rate which it has experienced during the

accumulation period. As a general rule, the intensity of the luminescence signal increases as the radiation dose to which it has been exposed is increased. It is this which allows us to use luminescence to calculate the equivalent dose for use in the age equation. However, two factors complicate this calculation. Firstly, the relationship between the radiation dose to which a sample has been exposed and the intensity of the luminescence signal is not an absolute one, and each sample requires calibration using a laboratory radiation source. Secondly, the relationship between dose and luminescence intensity is non-linear, with the signal growing asymptotically towards a maximum level. These two factors are dealt with by characterizing the luminescence response of a sample to known radiation doses administered in the laboratory. Traditionally a 'multiple aliquot' approach was used in which measurements were made on many different subsamples (aliquots) of a sample—typically 24 to 48 in number. These aliquots are given different laboratory radiation doses, and the results from all the aliquots are combined to define a 'growth curve' that defines the luminescence response of the material to radiation. From these 24–48 aliquots, a single estimate of De could be made. For grains ca. 200 mm in diameter, each aliquot would typically contain 500– 1000 mineral grains, implying that in total up to 48 000 mineral grains weighing as much as 0.5 g were required to generate one De value and subsequently an age.

Multiple aliquot approaches have a number of potential disadvantages. Firstly, because each aliquot may have a different number of mineral grains, or grains with different luminescence brightness, some form of normalisation between aliquots is necessary. This introduces a potential source of noise into the data, and there has not been agreement about which method of normalisation is appropriate. Secondly, because of the large amount of effort involved in making these measurements, it is normally not feasible to make more than one estimate of De for a sample. As well as making it difficult to check that a set of measurements are reproducible, it means that the uncertainty on De has to be determined from the mathematical uncertainty with which the luminescence growth curve is defined. Finally, and more significantly, this multiple aliquot approach assumes that each aliquot has the same De, and this is a difficult assumption to check using multiple aliquot measurements.

Duller (1991) developed analytical procedures for measurements necessary to construct a growth curve for a single aliquot were first produced for feldspars and later Murray and Roberts (1997) developed it for quartz. The development of single aliquot methods had two profound implications. Firstly, as all the measurements are made on a single subsample, the analytical precision is greatly high. Secondly, these single aliquot procedures can be automated using computer controlled luminescence equipment so that it becomes possible for routine dating of samples to involve the determination of multiple replicates of De.

The single aliquot regenerative dose (SAR) procedure developed by Wintle and Murray (2000) is a method for determining De using a single aliquot of quartz. The natural OSL signal i.e. that resulting from the radiation exposure the sample has undergone during burial is measured first. This measurement of the OSL signal removes all of the readily bleachable luminescence that would be expected to be removed by exposure to daylight during sedimentary processes. The response of the aliquot to radiation is measured by applying known laboratory doses to regenerate the luminescence signal. The first regeneration dose (R1) and the OSL signal resulting from this radiation is then measured (L1), and once again most, if not all, of the luminescence signal is removed during this measurement. This process is then repeated for a different radiation dose (30 Gy), and for any number of additional doses. The luminescence sensitivity of the aliquot is measured after each measurement (Lx) by giving a fixed radiation dose and measuring the resulting OSL (Tx). As the radiation dose given is always the same, the OSL signal should also be the same if the luminescence sensitivity has not altered. In practice the luminescence sensitivity does alter, but this can be allowed for by plotting a graph not of the growth of the luminescence signal Lx as a function of laboratory dose, but the ratio of Lx/Tx as a function of laboratory dose.

The key advantage of OSL dating is that the luminescence of quartz and feldspar grains is reduced to a low definable level after a few minutes of sunlight exposures versus hours for the corresponding thermo luminescence response. This level, called the residual level, is the point from which the geological luminescence accumulated after burial. OSL dating uses light of a particular wavelength or range of wavelengths, usually blue, green or infrared light, releasing rapidly the lightest sensitive trapped electrons from the crystal lattice

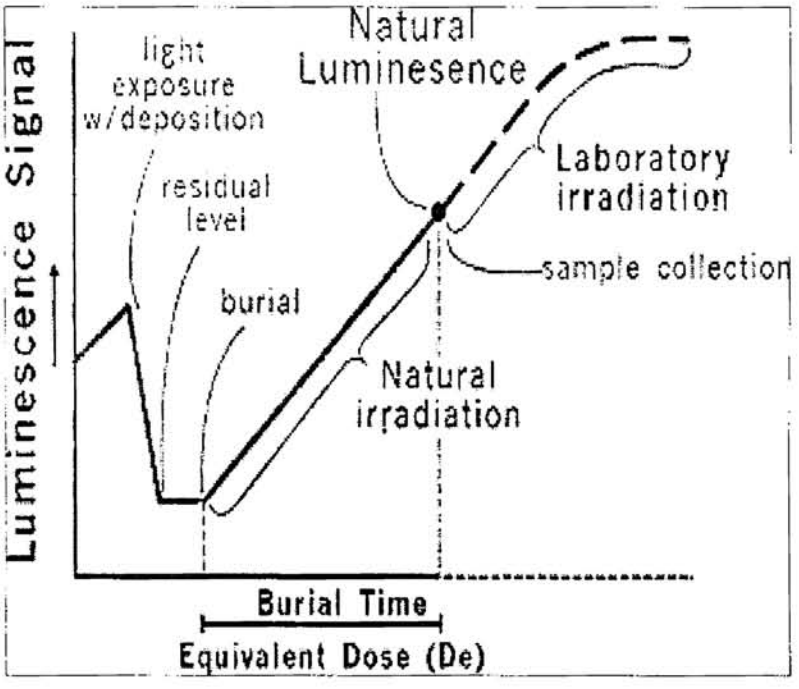

Figure 3.2. Diagrammatic representation of OSL Dating processes (after Aitken, 1998)

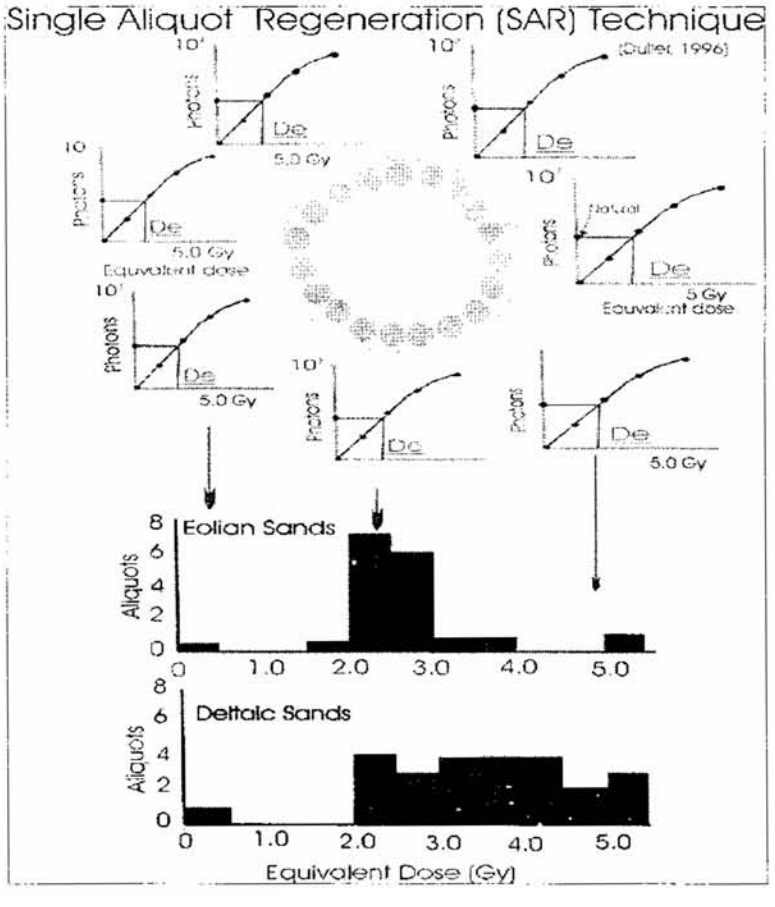

Figure 3.3. Diagram showing SAR technique (after Aitken, 1998)

3.3.1.1. Luminescence age equation:

Optically stimulated luminescence (OSL) is a trapped electron dating technique, based on the ability of natural semiconductors (such as quartz or feldspar) to accumulate a population of trapped electrons arising from atoms ionized by the ambient radiation flux. The size of the trapped electron population provides a measure of the dose received by the grain since it was last zeroed, which usually occurs with sunlight exposure during transport. Determination of the concentration of radionuclides within the deposit allows calculation of the dose rate to which the grain(s) was exposed. Thus in simple words:

$$\text{Age} = \text{Paleo Dose} / \text{Dose Rate}$$

$$\text{Age} = De / Dr$$

(**De** is measured in grays (absorbed dose) and commonly known as the Equivalent Dose or paleodose. **Dr** is measured in gray/Ka and commonly comprises of K, U, Th, Rb, and cosmic ray components. The dose rate is usually in the range 0.5-5 grays/1000 years).

3.3.2 Methodology

3.3.2.1 Sample collection and processing:

The samples for OSL dating were collected to fulfill three critical objectives, they being:

- Paleodose evaluation
- Dose rate determination
- Estimation of moisture content.

For paleodose evaluation:

It is of critical importance that the grains of this sample are not exposed to daylight, let alone sunlight; a few seconds of the latter is liable to reduce the dating signal very substantially and hence also the apparent age. One approach is to collect at night, first of all scraping off the surface layer and then putting the sediment in an opaque black plastic bag for transportation; the black bags must be thick

Another approach in case of consolidated sediments is to carve out a lump the sides of this are cut off in very strictly controlled lighting conditions. A more generally approach is to push or hammer a steel or PVC cylinder into a vertical section of the sediment, having first scraped off the surface sediment while shielding from direct sunlight. A convenient size of cylinder is about 60mm diameter by 100 mm long. In selecting the location from which the sample is to be extracted it needs to be borne in mind that gamma rays emitted at a distance of up to 0.3 (~ 1ft) contribute to the dose rate. Thus he paleodose sample should have been covered by at least that thickness of overburden for almost the whole of its burial period.

For dose rate determination:

It is not always necessary to take a separate sample for this purpose but for some facilities (e.g. beta dosimetry by means of TL, high resolution gamma spectrometry) a greater quantity than is available from the paleodose sample may be needed, perhaps approaching a kilogram.

For moisture content:

A sample for the evaluation of present day moisture content can be conveniently obtained in a small plastic container; it should be extracted from deep enough in the section to avoid the possibility of drying out having taken place and then tightly sealed.

Sample collection procedure followed in the present study

Sediments for OSL studies were collected by the same sampling procedures that followed for making of the litho log of the subsurface, explained in Chapter2. For the collection of samples unexposed to sunlight, special mobile black room was set up. A pick-up auto-rickshaw was covered with 3mm thick black resin, leaving provisions for the door. The cabin of the vehicle was painted black, so as to reduce internal luminescence due to white light. A red Zero Watt lamp used inside the cabin to facilitate the transfer of sample. A special black glow, with 6 layers of 1mm thick black coloured polyester cloth was designed to cover the spilt-spoon sampler while taking it from the drilling site to the mobile black room setup in the field itself.

Once the sampler is brought inside the black room, a 10cm long, 5cm diameter black pipe with one end closed is pushed into the sampler and the sample is transferred as such into the pipe. The other end is closed and the sample tube is properly logged and named for OSL studies.

Subsequent sample preparation and measurement were carried out in OSL laboratory facilities at Indian Institute of Technology, Roorkee, under subdued red light to avoid photo – bleaching of the thermo– luminescence. The outer layer~ 10 mm of the samples was removed first to estimate the portions that were sun bleached during the sampling. The inner core was processed either for the extraction of the fine sediments (4-11μm) or for the coarse grain minerals separates (100-150μm quartz or the feldspar).

Measurements are carried out on the custom build TL / IRSL / OSL reader (Daybreak Nuclear Instrument ver.1996). The instrument is equipped with IRSL/OSL sources for the photo-luminescence measurement and also heating arrangement to measure thermo optical luminescence. The IRSL sources is composed of the 30 IR diodes connected in an array from, emitting light at 880 +/- 20 nm, delivering ~ 50 mW/cm ^{2} power at the sample position Fig. The visible excitation is carried out at 514 nm band using 300W Xenon source filtered through the pack of the interference filters fig. The transmitted light is uniformly focused on the sample position the light guide and the other optical arrangements. The illumination power at the sample position using is about 45 mW/cm ^{2} at 514 +/- 34 n. The power supply to the optical sources is servo controlled to stabilize the beam intensity. The source intensity fluctuation at the sample position is less then 1%. Illumination (excitation) timings are controlled using the electronic shutter arrangements. The sample position, heating controlled, optical excitation sources are controlled using the inbuilt software interfaced with the system, and the computer. Standard TL/IRSL/OSL soft-wares are used in the data reduction and analysis.

For the detection of the OSL emission, the photo multiplier tube (EMI 9335 QA) with an associated electronics for the low level of the photon counting is used Fig. The output signal from photon counting system was transmitted to Pentium PC using an interface system. The sample luminescence was filtered either by UG 11 (~ 260-360nm) or

by BG 39 filter combination (~400-600nm). The filter before the photomultiplier tubes are needed to screen the scattered excitation light, mineral selectivity and optimize signal to noise ratio. In TL luminescence measurements, prior to the sample heating the sample chamber is evacuated to 10μm Hg and then it is filled with the inert gas (99.999% N_2) to the atmospheric pressure. The measurements are carried out 10^0C/sec ramp rate from the room temperature to 400^0C. For irradiation, an alpha irradiator system capable of the irradiating 5 samples at a time with pressure of 10^{-3} torr and for beta irradiation a microprocessor controlled beta irradiator system are used.

The irradiation dose received by a results from the radiation flux emitted by the radioisotopes (^{238} U, ^{232} Th and ^{40} K) within a sphere of the radius 30 cms , and a cosmic ray contribution (Wintle et. al.,1992). The dose rate was measured using the thick source of the alpha counter Th and U derived dose and the atomic absorption spectrometry (K derived dose). For the thick source alpha counting, the sample was crushed to about 10μm grain size and then evenly spread in a visually thick and uniform layer on a zinc sulphide screen which was placed at the base of the circular Perspex container. Equal counts were assumed for the U-Th series and also the series were assumed to be in radioactive equilibrium. Repeat measurements were carried out to minimize the statistical error and to improve the confidence limit. The intensity of the alpha particles arising from the sample depends on the concentration U and Th (K does not emit alpha particles). Each alpha particle reaching the zinc sulphide screen produces a flash of the light, which is counted by a photomultiplier tube facing the base of the screen. Each flash is recorded as an alpha count. All the measurements were made using the daybreak 583 alpha counter. For the measurements of the background, in the place of the sample zinc sulphide screen was covered using a thick Perspex plate and the Perspex container is air sealed. In the analysis, the BG counts were subtracted from the signal.

For the ^{40}K percentage 0.5gm sample was taken as powder (< 200 mesh size) in a Teflon beaker, 10.0 ml HF+ 5.0 ml HNO_3 + 1.0 ml $HCLO_4$ was added and heated for 24 hrs at 90^0C and latter the content were heated at 120^0C.Then 10.0 ml of HNO_3 was added to the beaker and was heated till the content are completely evaporated (dryness). When the fumes stopped coming, 10.0 ml HCl + 20.0 ml distilled water was added to make it to 100 ml for

analysis of the K the quantitative estimation of the K was done by Atomic Absorption spectrometry (Van loon, 1985).

The results of dose determination and the water contents measured for the samples that were collected adjacent to the OSL samples are reported in Table 3.3. These values have been used to adjust the dry dose rates, measured water contents, which were assigned uncertainties of F5%, are representative of those pertaining to the full period of sample burial. The cosmic-ray dose rates were calculated from Prescott and Hutton (1995). Beta-attenuation factors were taken from Mejdahl (1979), and the effective internal alpha dose rate (applied to all samples) has been estimated using an alpha-efficiency a value of 0.04F0.02, as measured previously for quartz grains from south-eastern Australia (Bowler et al., 2003)

3.3.3. Results

The lithogenic radionuclide concentrations for the samples are summarized in Table 3.3. These measurements were made on dried and powdered samples. Dry dose rates were calculated using the conversion factors of Stokes et al. (2003).

Table 3.3 and Figures 3.4 a & b give the OSL ages for 13 samples from the five bore hole sections in the study area. It gives the following picture. Amongst the sediments dated the youngest gave an age of 1444 $\pm$ 268 years B.P. in bore hole TRV 6 at 2m depth, while the oldest sediment from bore hole TRV 10 at depth 27m, dated back to 23.554 $\pm$ 4.185 Ka.

Six sediment samples from depths 2m, 5m, 8.5, 11.5m, 19.75m and 22m of TRV 1 were dated. Their ages fall sequentially from 1790 $\pm$ 328, 4087 $\pm$ 702, 6074 $\pm$ 1307, 10,018 $\pm$ 2278, 14,263 $\pm$ 2345 to 18,057 $\pm$ 3276 yrs B.P. respectively. Another seven samples dated fall belonged to boreholes, TRV 6 (four samples), TRV 7 (one sample) and TRV 10 (two samples). The dates are sequential and can be mutually correlated. The OSL ages characterizes the litho stratigraphy drawn for the study area.

Table 3.3. OSL Dates of sand grains from bore holes TRV1, TRV 6, TRV 7 and TRV 10

Sample Location	Depth (m) ± 0.08m	K %	Th (ppm)	U (ppm)	Cosmic Dose rate (Gy/Ka)	Moisture	ED values	Dose Rate (Gy/Ka)	Age (Ka)
TRV 1	2	3±1.2	28.9 ± 6.3	29.98 ± 5.7	150 ± 30	10 ± 3	2.61E1 ± 1.0068	150 ± 30	1.79 ± 0.328
	5	2.10 ± 0.89	26.32 ± 5.4	4.67 ± 1.23	150± 30	8 ± 2	2.87E1 ± 1.1212	7023 ± 1172	4.087 ± 0.702
	8.5	3.12 ± 1.02	21.44 ± 5.50	18.80 ± 6.32	150 ± 30	9 ± 2	7.77E1 ± 2.1657	12809 ± 2732	6.074 ± 1.307
	10.5	1.45 ± 0.62	8.54 ± 3.2	3.21 ± 1.02	150 ± 30	12.00 ± 3	3.59E1 ± 2.5946	3584 ± 776	10.018 ± 2.278
	19.75	4.3 ± 1.2	22.9 ± 6.5	19.01 ± 4.6	150 ± 30	9 ± 2	2.02E2 ± 7.368	14162 ± 2276	14.263 ± 2.345
	22	1.89 ± 0.76	24.87 ± 5.43	3.8 ± 1.32	150 ± 30	8 ± 3	1.14E2 ± 4.3536	6313 ± 1120	18.057 ± 3.276
TRV 6	2	4.6 ± 1.02	21.76 ± 5.43	18.87 ± 5.71	150 ± 30	8 ± 3	2.06E1 ±1.2393	14264 ± 2526	1.444 ± 0.269
	5	0.99 ± 0.33	9.98 ±2.54	7.8 ± 1.87	150 ± 30	10 ± 4	3.77E1 ± 2.7477	7197 ± 12.92	5.169 ± 0.849
	11	1.54 ± 0.6	16.76 ± 4.3	6.7 ± 2.3	150 ± 30	10 ± 3	5.26E1 ± 1.0270	6020 ± 1315	8.738 ± 1.916
	20	1.09± 0.23	8.72 ± 2.78	13.76 ± 3.12	150 ± 30	10 ± 4	1.23E2 ± 2.3650	7398 ± 13.19	16.626 ± 2.98
TRV 7	13	4.98 ± 1.78	27.86 ± 5.76	23.65 ± 3.78	150 ± 30	12 ± 4	2.30E2 ± 7.8352	16472 ± 2414	13.966 ± 2.100
TRV 10	26	6.54 ± 1.54	20.54 ± 5.43	26.54 ± 6.54	150 ± 30	10 ± 3	3.89E2 ± 1.44E1	18664 ± 3049	20.842 ± 3.491
	27	2.56 ± 0.78	23.64 ± 2.93	6.89 ± 5.11	150 ± 30	8 ± 3	1.89E2 ± 7.5328	8024 ± 1387	23.554 ± 4.185

3.3.4 Discussion

The OSL dates obtained during the present study span over a period of twenty two thousand years the oldest date being 23,554 ± 4185[for 27m depth in sediment borehole TRV10 and youngest date being 1444 ± 269 (for 2m depth sediment in borehole TRV 6). The oldest dates are obtained for samples that are recovered from the central part of the

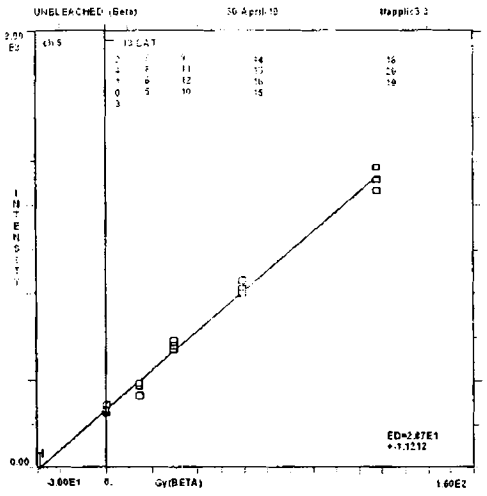

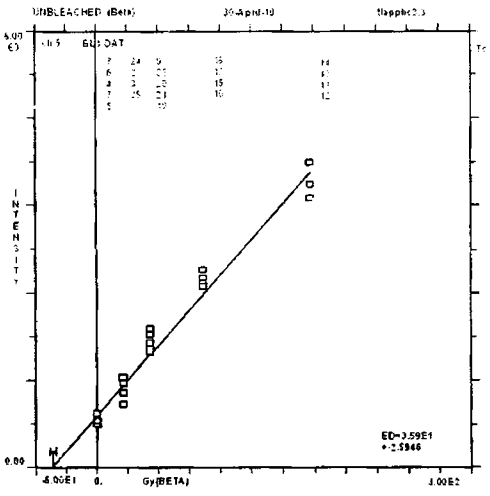

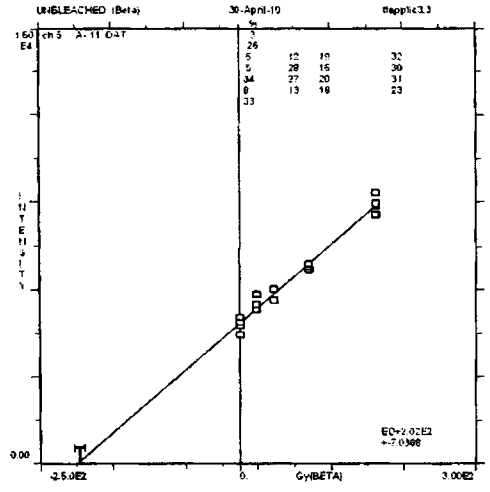

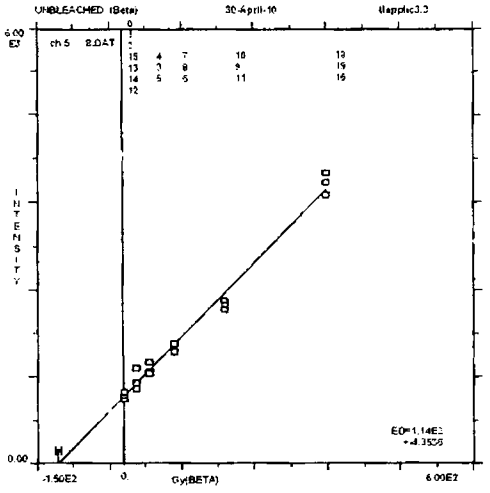

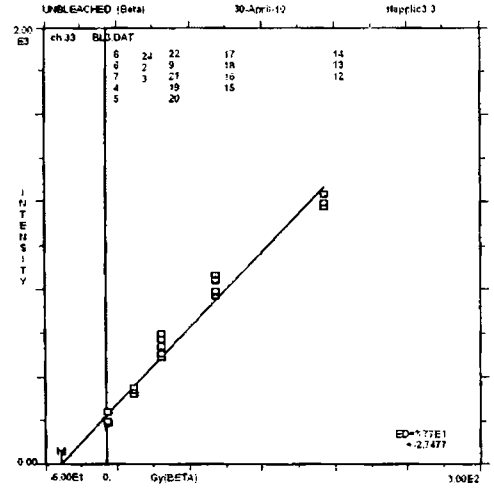

Figure 3.4a: Additive dose growth curve for samples processed from borehole TRV1 [Refer Table 3.3]

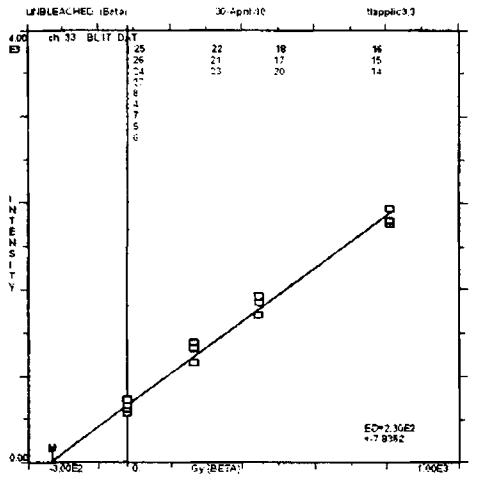

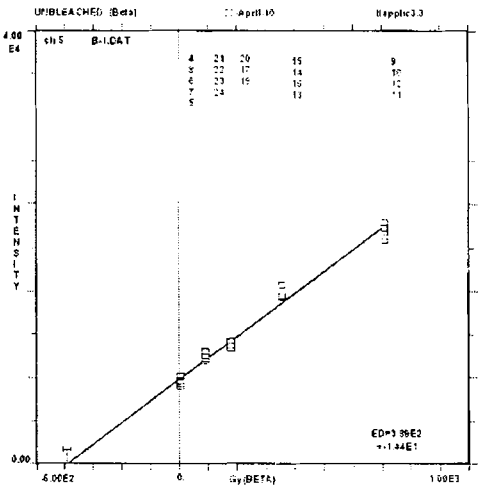

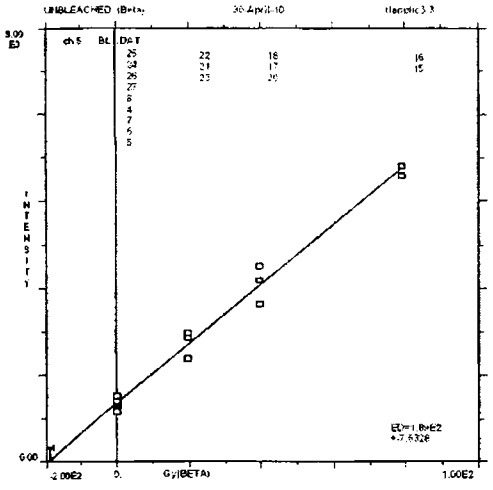

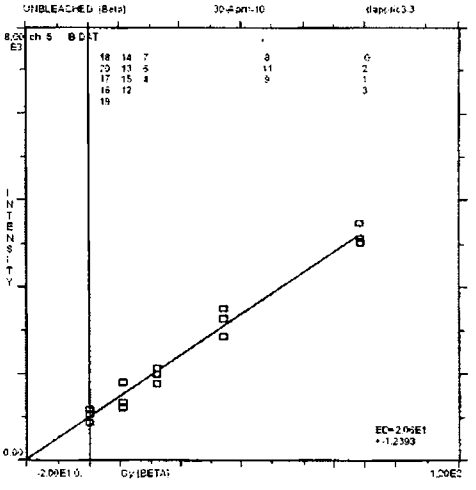

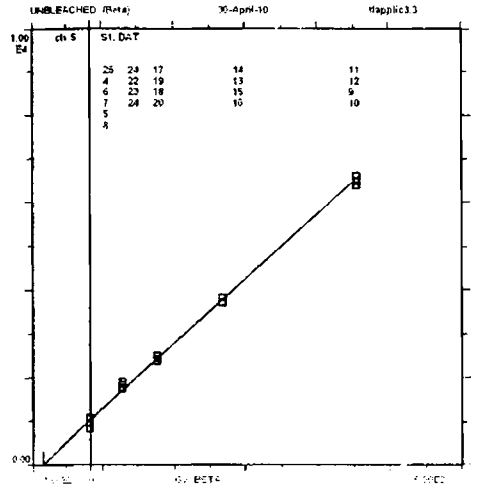

Figure 3.4b: Additive dose growth curve for samples processed from borehole TRV6, 7 and10 [Refer Table 3.3] Detailed plots in Appendix-1

study area. The youngest date at 2m depth is consistent throughout the terrain as the ages 1444 ± 269 years is obtained at the northern part of the study area and 1790 ± 328 is obtained towards the southern part of the study area.

Table 3. 4. Lithostratigraphy and OSL ages of sand grains.

Litho stratigraphic Position	Depth of the contact in m	Age in 1000 yrs B.P
Base of Unit 3	8 – 12 m	6.074 ± 1.3 to 8.738 ± 1.75
Base of Unit 2	10 – 16m	10.018 ± 2.278 to 12.468 ± 2
Oldest date in Unit 1	At 27m	23.554 ± 4.185
	30m and more	Depth at which OSL dates were not received

The borehole TRV1 bears more number of dates falling in ascending sequence down depth. The dates give an inconsistent rate of sedimentation/accumulation especially in unit 1 of the litho stratigraphic sequence. A similar pattern in the rate of sedimentation is observed in TRV6. In borehole TRV1 the average accumulation rate is seen to be high towards the top part of Litho Unit 1, with 0.217 cm/year (Table 3.5). In Litho Unit 2 (between 850cm and 1050cm) the accumulation is very slow at 0.051 cm/year and in Litho Unit 3 it is rather fast at 0.15 cm/year.

Table 3. 5 The deposition time and accumulation rate of sediments in borehole TRV 1

Depth range in borehole (cm)	year/cm	cm/year
200– 500	7.65	0.131
500 – 850	5.67	0.176
850 – 1050	19.7	0.051
1050 – 1950	4.59	0.217
1950 – 2200	13.8	0.072

3.4 Salient outcome of ^{14}C and OSL dating

On comparison of the dates from the two methods of dating employed, here, reasonable correspondence is seen between the two data sets. The timing of sediment deposition in the five boreholes fit mutually and can be laterally linked. The age-depth relations in the samples dated support the vertical accretion of sediments in the central belt of Thiruvananthapuram coastal plain. The OSL dates 6074 $\pm$ 1307 and 8738 $\pm$ 1752 from the contact of Litho Unit 3 and Litho Unit 2, cannot be fixed either to the beginning of the time span of Litho Unit 2 or to the end of Litho Unit 2. The Litho Unit 2 is rich in vegetal matter, produced out of slow accumulation of organic and mineral matter in standing or slow moving water. Mineral sediment introduced to such an environment can be arrived by a later aeolian activity which has allowed sufficient time for exposure. Another option is that the sediment, both quartz grains as well as the organic material, formed during 7730 $\pm$ 290 years before present would have remained exposed to sunlight till 6074 $\pm$ 1.307 years before present. Therefore OSL dates of quartz grains from lithological unit 2 would give an age which is post-depositional to organic sediments itself (Table 3.3). In later case, a maximum sedimentation rate of 0.3mm/year can be computed between the 7730 years and 6074 years before present considering that the 20cm of sediment overburden is necessary to keep any grain hidden from sun, no erosion has succeeded after the deposition of grains at 8.5 m depth and the date of deposition of sand grain is congruent to the time of formation of biota at this layer.

In summary it can be stated that the 20-30 m thick sand-dominated sediment pile along the central belt of the Thiruvananthapuram coastal plain were deposited during Late Pleistocene to Late Holocene.

Further discussion based on this tentative depositional history in chronometric terms is attempted in Chapter VIII.

Chapter IV

Texture and Mineralogy

4.1. Textural studies

The transportation and deposition processes are reflected from the population of grain sizes in sediment. Parameters like roundness, sphericity, surface texture, detrital heavy mineral ratio, biogenic components and syngenetic minerals, that quantify grain, further aid to identify the environment (Folk and Ward, 1957; Friedman, 1979; Martins, 1965).

The focus of textural studies is to discriminate between sediment layers based on the environment of deposition, like riverine, aeolian, beach sands and gravels. Grain size distribution bears fundamental relationship with the physical forces involved in mechanism of transport and deposition of sediments. The coarser sediments are found in high-energy environments while finer sediments clog at low energy regimes. Similarly weathering processes like, abrasion and corrosion of grains and sorting processes during transport and deposition are deciphered in the studies detailed by Folk and Ward (1957), Mason and Folk (1958), Folk (1966); Friedman (1961 and 1967) and Moiola and Weiser(1968).

For computations, sedimentologists have adopted the logarithmic Udden–Wentworth grade scale (Udden, 1914; Wentworth, 1922) as standard, where the boundaries between successive size classes differ by a factor of two.

4.1.1. Grain size parameters

There are generally four- statistical parameters used to describe the grain size distribution measuring

(a) The average size (mean)

(b) The spread (sorting) of the sizes around the average (standard deviation)

(c) The symmetry or preferential spread (skewness) to one side of the average

(d) The degree of concentration of the grains relative to the average (kurtosis).

In addition to these, the median and mode are also of great importance in understanding the grain size variations.

a) Mean grain size (Mz)

Mean is the statistical average expressed in phi (∅) units. Different workers have suggested different formulas but the widely accepted one is put forward by Folk and Ward (1957).

$$Mz\ (\varnothing) = \frac{\varnothing 16 + \varnothing 50 + \varnothing 84}{3}$$

Sediments can be classified into different grades using Wentworth (1922) scale as shown below:

Size class	Wentworth Scale (mm)	∅ Scale
Very coarse sand	2 - 1	-1 - 0
Coarse sand	1 - 0.5	0 - 1
Medium sand	0.5 - 0.25	1 – 2
Fine sand	0.25 - 0.125	2 – 3
Very fine sand	0.125 - 0.064	3 – 4

b) Median

The median is mid lying value and may not be a measure of average size. It is based on only one point of the cumulative curve.

c) Mode

No good mathematical formula exists for accurate determination of the mode. The best approximation is probably that given by Croxton and Cowden (1939)

d) Standard deviation (σ_1)

Standard deviation is a measure of sorting. Uniformity within a sample of sediment can be measured by the standard deviation. It is one of the most useful parameter mediums

in separating grains.

$$\text{Standard deviation } (\sigma_I) = \frac{(\varnothing 84 - \varnothing 16)}{4} + \frac{(\varnothing 95 - \varnothing 5)}{6.6}$$

According to Folk and Ward (1957) the divisional points based on standard divisions are as given below:

Standard deviation (∅)	Sorting
<0.35	Very well sorted
0.35 - 0.50	Well sorted
0.50 - 0.71	Moderately well sorted
0.71 - 1	Moderately sorted
1 - 2	Poorly sorted
2 - 4	Very poorly sorted
>4	Extremely poorly sorted

e) Skewness

The asymmetry of the grain size distribution in a sediment sample is measured by skewness and it can be sensitive indicator of sub-population mixing. In the sedimentological point of view, skewness is a measure extremely sensitive to the type of transport or deposition agent.

The skewness index by Folk and Ward (1957) is the best skewness measure, as it covers the full curve.

$$\text{Skewness (Sk)} = \frac{\varnothing 16 + \varnothing 84 - 2\varnothing 50}{2(\varnothing 84 - \varnothing 16)} + \frac{\varnothing 5 + \varnothing 95 - 2\varnothing 50}{2(\varnothing 95 - \varnothing 5)}$$

Sign of skewness is related to the environmental energy (Duane, 1964). Negative skewness (coarse skewness) is correlated with high energy and winnowing action (removal of fines) and positive / fine skewness with low energy levels (accumulation of fines).

The limits of skewness as given by Folk and Ward (1957) are as follows:

Skewness value	Type of skewness
>0.30	Very finely skewed
0.30 to 0.10	Finely skewed
0.10 to -0.10	Nearly symmetrical
-1.1 to -0.30	Coarse skewed

f) Kurtosis

Kurtosis is considered as one of the important textural parameters to distinguish various environments as explained by Duane (1964) and Mason and Folk (1958). It is a measure of the contrast between sorting observed in the central part of the particle size distribution with that of the tails. Kurtosis compares the sorting grade of the curve, central part with the two tails. A normal curve is mesokurtic or the sorting agent was uniform for the entire grain size distribution. Leptokurtic values have a central part better sorted than the tail, while platykurtic values indicate tails better sorted than the central portion. These values are indicators of differences in the sorting agents for the entire curve

$$\text{Kurtosis (kG)} = \frac{\phi 95 - \phi 5}{2.44(\phi 75 - \phi 25)}$$

The limits of kurtosis as given by Folk and Ward (1957) are as follows:

Kurtosis value	Type of Kurtosis
<0.67	Very platykurtic
0.67 - 0.90	Platykurtic
0.90 - 1.11	Mesokurtic
1.11 - 1.50	Leptokurtic
1.50 - 3	Very leptokurtic
>3	Extremely leptokurtic

Skewness represents the degree to which the particles are concentrated near the centre of the curve (Platykurtic- excessively flat curves, mesokurtic- middle and leptokurtic- excessively peaked curves) many curves designated as "normal" by the skewness measure turn out to be markedly non-normal when the Kurtosis is computed.

4.1.2. Environment of deposition

Palaeo environment can be interpreted from grain size analysis of sediments (Alimen and Bender, 1960; Real and Shepard, 1956; Bradley, 1999; von Engelhardt, 1940; Shepard 1960). von Engelhardt, 1940 and Shepard 1960 have distinguished beach sand from dune sand and from river sands. In their work, beach sand and dune sand were identified by deploying the binary plots, by computing the skewness, the distribution curve and by their sorting characteristics. In detail study on various sand deposition environments, Friedman (1961) found that when skewness of distribution was plotted against mean – phi value, the dune sands, ocean beach sands and the lake beach sands shows a clear complete separation. Sahu (1962, 1964) has employed Linear Discriminant Functions for finding the relation between variances exhibited by parameters.

The said discriminant relation can be brought out between aeolin, beach and shallow marine environment based on mean, standard deviation, skewness and kurtosis, which is as follows:

$$Y1\ aeolian : beach = -3.5688\ (Mean) + 3.7016\ (Standard\ Deviation)^2 - 0.0766(Skewness) + 3.1135\ (Kurtosis)$$

$$Y2\ beach: sh.\ marine = 15.6534(Mean) - 8.7604\ (Standard\ Deviation)^2 - 4.8932(Skewness) + 18.5043\ (Kurtosis)$$

$$Y3\ sh.marine : sh.agitated = 0.2852(Mean - 8.7604(standard\ deviation)^2 - 4.893(Skweness) + 0.0482\ (Kurtosis)$$

If Y1 $\geq$ -2.7411, then the environment of deposition falls within beach and less than the number described it is aeolian. If Y2 < 65.3650, then beach conditions are confirmed, if Y2 $\geq$ 65.3650, then shallow agitated conditions are expected. When Y3 $\geq$-7.4190, confirms shallow marine environment, while Y3<-7.4190 indicates fluvial environment

4.1.3. Methods of study

A total number of 230 sediments including 80 surface samples and 150 subsurface samples were selected for textural analysis. The samples were repeatedly washed, dried, and thoroughly mixed. By successive coning and quartering on a piece of paper a specific weight was taken (80gm). Dry samples were placed in the uppermost sieve and covered in a set of stacked sieves. The stack of sieves arranged in order so that the coarsest sieves at the top with finer ones below (with a pan at the bottom to catch any sediment that pass through the lowest and finest sieve). The sieves set are therefore placed on a shaking machine. The arrangements of sieves are as following-10, 14, 18, 25, 35, 60, 80, 120, 170, and 230 mesh numbers. The sample was then sieved for 15minutes in ro-top mechanical sieve shaker using a standard ASTM Erode colt sieve at half phi intervals. The sand that has retained on each sieve and pan was collected and weighed using a balance having an accuracy of 0.0001gm and cumulative weight percentage was calculated. After shaking, the sieve was inverted and cleaned. The calculation was made for weight percentage and cumulative weight percentage and was noted down. The data was plotted in order to obtain cumulative frequency curves. The grain size in phi values were plotted against cumulative weight percentage on a probability chart and different percentile values of 5, 16, 25,50,75,84 and 95 (ϕ) were obtained from the graph and noted in phi-units. The conventional method suggested by Folk and Ward (1957) was followed and different size parameters were calculated.

Grain size analysis is an essential tool for classifying sedimentary environments. The calculation of statistics for many samples can, however, be a laborious process. A computer program called Gradistat (Blott and Pye, 2001) has been used for the rapid analysis of grain size statistics from the standard measuring techniques. Mean, mode, sorting, skewness and other statistics are calculated arithmetically and geometrically (in metric units) and logarithmically (in phi units) using moment and Folk and Ward graphical methods. Method comparison has allowed Folk and Ward descriptive terms to be assigned to moments statistics. The results of Folk and Ward measures, expressed in metric units, provide the most robust basis for routine comparisons of compositionally variable sediments. The program runs within the Microsoft Excel spreadsheet package and is extremely versatile.

accepting standard and non-standard size data, and producing a range of graphical outputs including frequency and ternary plots.

4.1.3.1. Frequency distribution

Skewness and kurtosis characterize frequency distribution of the sediments. Many well-known distribution functions, to which observed data approximates, possess characteristic statistical values. Thus the Normal or Gaussian distribution may be completely described by its mean and variance; as the normal distribution symmetrically fall around the mean, its skewness is zero and its kurtosis possess values of 3, hence there is no necessity to list the skewness and kurtosis the frequency distribution is known to be normal. Generally however, this is not known, but suspected and it is necessary to attempt to establish that an observed set of data represents a sample drawn from some normal population. In which case the observed statistics, based on the sample value may be tested against those expected under the hypothesis that the population from which the sample was drawn is normally distributed. This is one of the most useful applications of statistical analyses and may be considered a part of the process of curves filling by means of moments.

4.1.3.2. Scatter plots

The scatter diagrams plots the statistical parameters of the distribution of grain size. The scatter plots among different size parameters have geological significances and an attempt has been made to bring out the mode and environment of deposition. The bivariant plot of Mean versus Sorting, after Friedman (1967) significantly demarcates sediments from dunes and river sand. The positive skeweness exhibited by the dune sands and negative skewness of the ocean beach sands enable to use skewness versus mean grain size bi-variant plot as a categorizer of those two environments. Friedman (1968) had succeeded in using skewness versus mean bi variant plots to distinguish dune sands from coastal sands. Later, Moiola and Weiser (1968) has added the regime of river sands into the same plot. River sands can be differentiated from beach sands in a bivariate plot where sorting of grains is plotted against skewness Friedman (1961).

Friedman (1961) and Moiola and Weiser (1968) pointed out that kurtosis and skewness of of a given sediment population when plotted against each other is an efficient tool to differentiate the environment of deposition of sediments. Accordingly, the above two parameters of the sediments from three different Litho Units were plotted each other.

4.1.3.3. Linear discriminant analysis

According to Sahu (1964), the variations in the energy and fluidity factors seem to have excellent correlation with different processes and the environment of deposition. Sahu's linear discrimnant functions of Y1 (aeolian and beach), Y2 (beach and shallow agitated water) and Y3 (shallow marine, fluvial) were used to decipher the process and environment of deposition.

Table 4.1 Grain size parameters (range and average) of sediments in three Litho Units (details in Appendix 2)

Litho Unit	Mean ϕ		Standard Deviation		Skewness		Kurtosis	
	Range	Average	Range	Average	Range	Average	Range	Average
3	1.294 to 1.934	1.43	0.621 to 0.798	0.68	-0.048 to 0.449	0.16	3.018 to 3.730	3.41
	Medium sand	Medium sand	Moderately sorted to well sorted	Moderately well sorted	Nearly symmetrical to very finely skewed	Finely skewed	Extremely leptokurtic	Extremely leptokurtic
2	1.86 to 2.86	2.27	0.678 to 0.932	0.79	-2.099 to 0.172	-0.73	3.144 to 8.291	3.89
	Medium to fine sand	Fine sand	Moderately well sorted to moderately sorted	Moderately sorted	Coarse skewed to finely skewed	Coarse skewed	Extremely leptokurtic	Extremely leptokurtic
1	0.87 to 1.904	1.4	0.678 to 1.163	0.91	-0.452 to 0.598	0.34	1.857 to 3.868	2.78
	Coarse sand to medium sand	Medium sand	Poorly sorted to moderately well sorted	Moderately sorted	Coarse skewed to very finely skewed	Very finely skewed	Very leptocurtic to extremely leptokurtic	Very lepokurtic

4.1.4. Results:

The grain size parameters of the sediments namely mean, standard deviation, skewness and kurtosis obtained for the three different Litho Units are summarised in Table 4.1 (Complete data is given in Appendix 2).

Mean:

There is significant variation in the mean size from Litho Unit to Litho Unit. It ranges between 1.151 to 1.904 ϕ for the bottom layer (Litho Unit 1), 1.855 to 2.855ϕ for the middle layer (Litho Unit 2) and 1.33 to 1.521ϕ for the upper layer (Litho Unit 3).

Standard Deviation (Sorting)

Though all the sediments studied can be classed as moderately sorted category in terms of standard deviation, there is slight difference between the three units in terms of their ranges. Litho Unit 1 shows a sorting value ranging from 0.727 to 1.163, Litho Unit 2 has sorting values ranging from 0.678 to 0.899 and topmost layer litho Unit 3 has sorting ranging from 0.621 to 0.798. Thus unit 3 has a very narrow range in standard deviation.

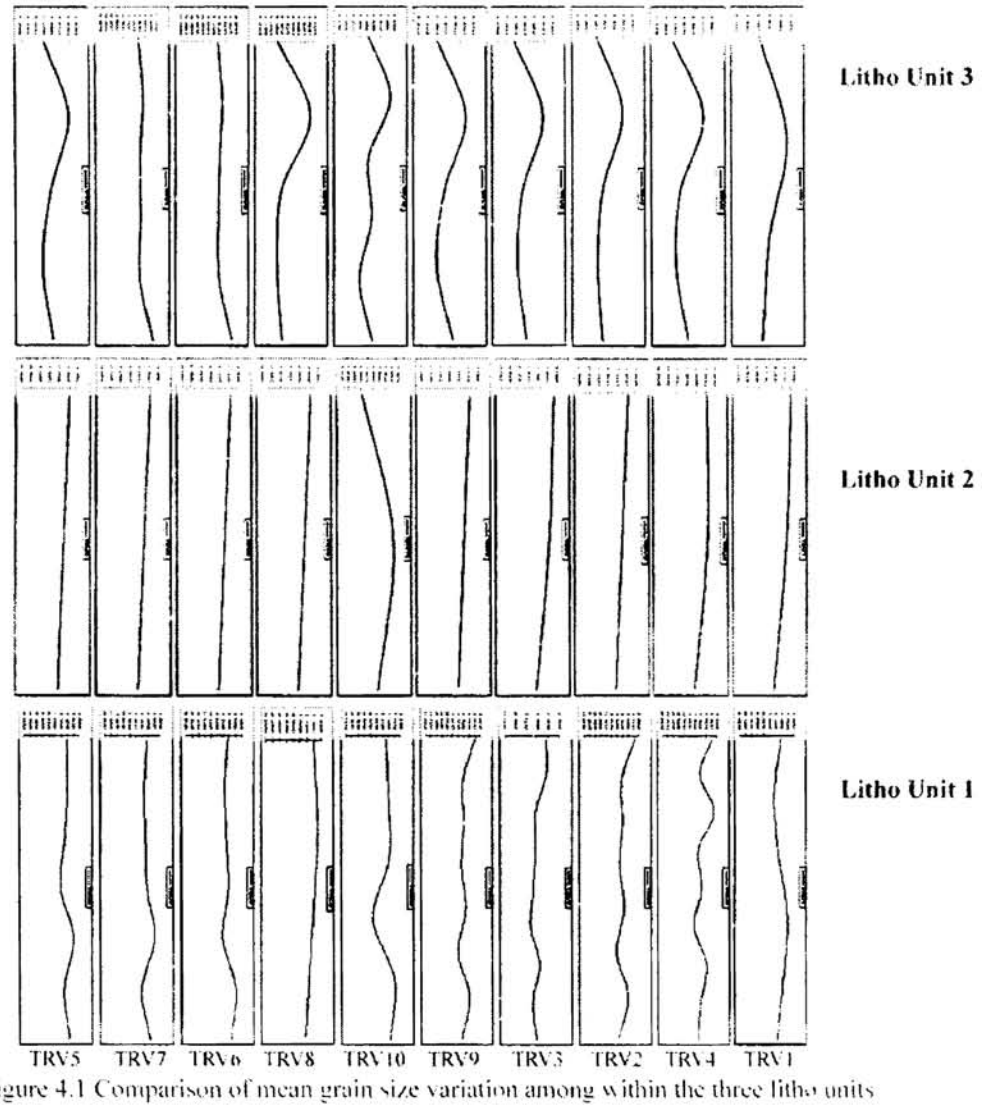

Figure 4.1 Comparison of mean grain size variation among within the three litho units

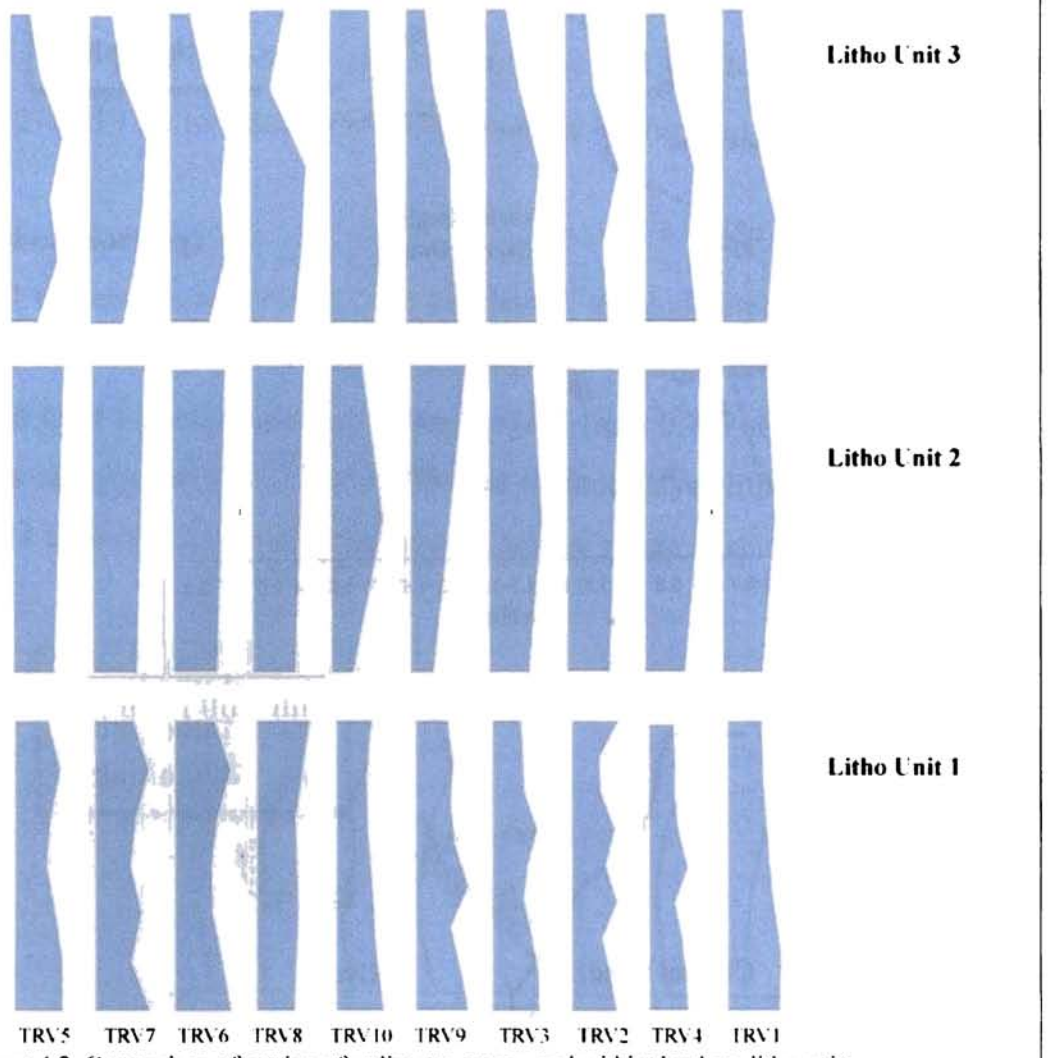

Figure 4.2 Comparison of sorting of sediments among and within the three litho units

Depth wise variation in mean and sorting

When the variation of mean size is analysed with depth (Figure 4.1.) it is seen that there is an undulatory change in Litho Unit 1, while in Litho Unit 2 there is a gradual coarsening upwards and in Litho Unit 3, there is a initial fining upwards followed by a pronounced coarsening upwards (reaching the highest values at a depth of ~ 5m) and then fining upwards. Though there is a correspondence with these in the sorting also with depth (Figure 4.2.) the variations are that distinct.

Skewness:

The skewness of sediments in Litho Units under study varies significantly from one Litho Unit to another. In Litho Unit 1 it is largely symmetrical to finely skewed, in Unit 2 it

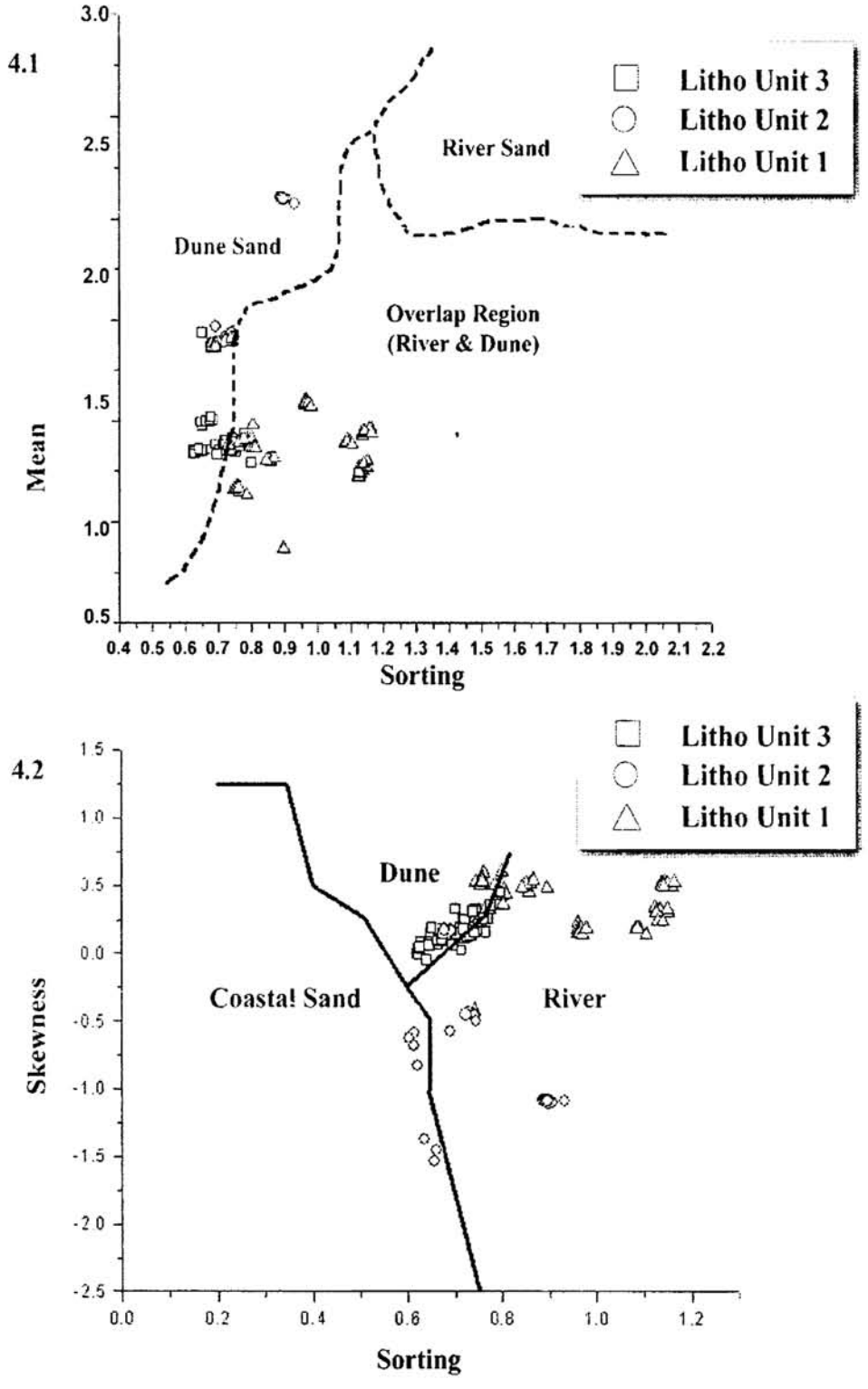

Figure 4.3 Bivariant plot of Mean vs Sorting demarkating dune sand and river sand(after Friedman(1961). The sands of Litho Unit 3 falls specifically under the Dune Sand regime. While the sands of Litho Unit 1 falls in the Overlap regime.

Figure 4.4 Field of Coastal sand, river sand and dune sand plotted in a Sorting-Skewness bivariant diagram(after Friedman(1961). The majority of sands of the Litho Units fall clearly in three different environment of deposits.

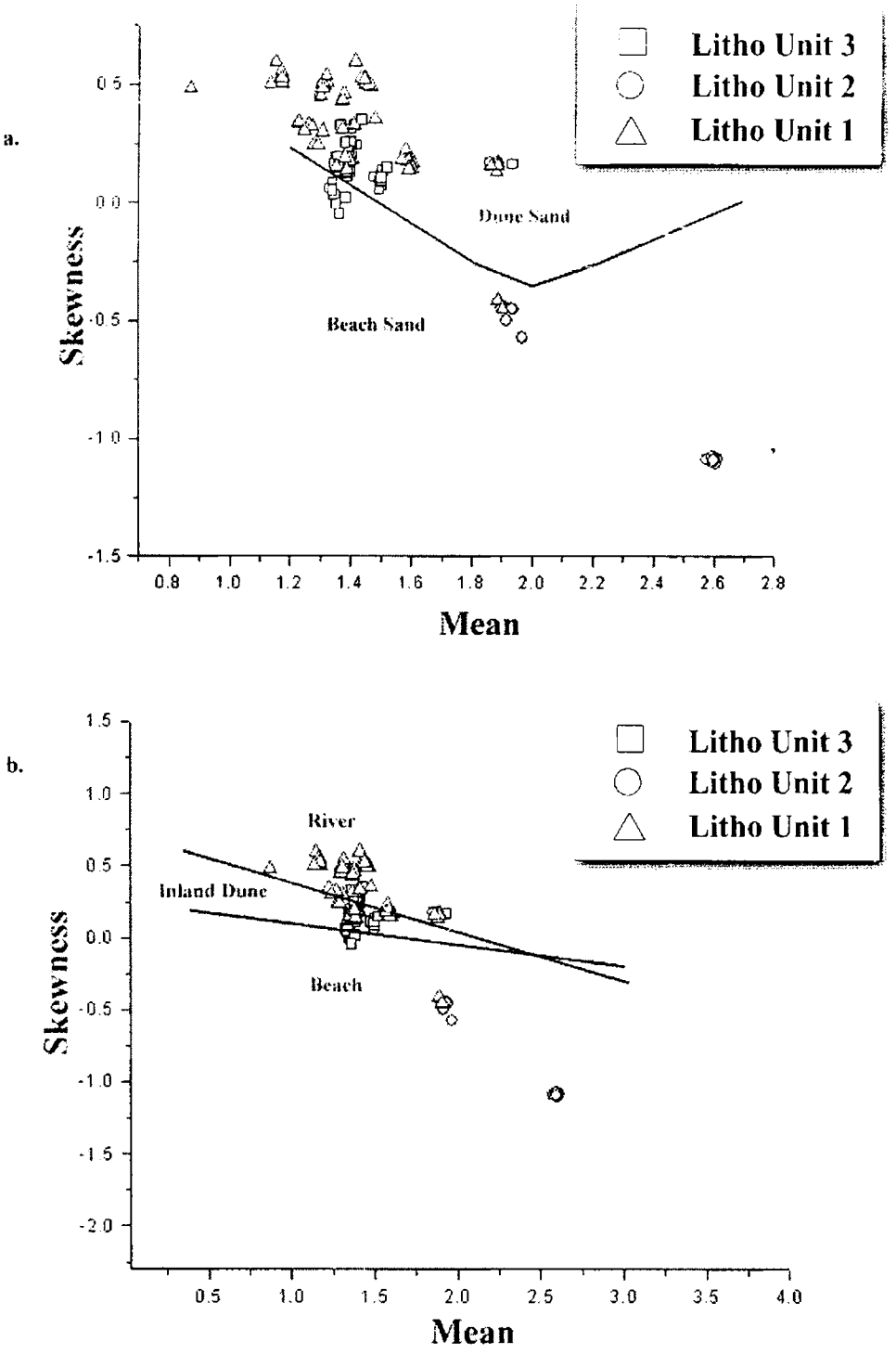

Figure 4.5. Bivariant plots, where mean plotted against skewness using Phi scale to discriminate the environement of deposition.

(a) Regimes of dune and beach sands after Friedman (1961). The plots of litho units 1 and 3 fall in the dune regime, while that of litho unit 2 fall in the coastal regime.

(b) Regimes of dune, beach and river sands after Moiola & Weiser (1968). Majority of plots of the three litho units fall, separatly. Litho unit 1 and 3 are further categorised into riverine regime and dune regime.

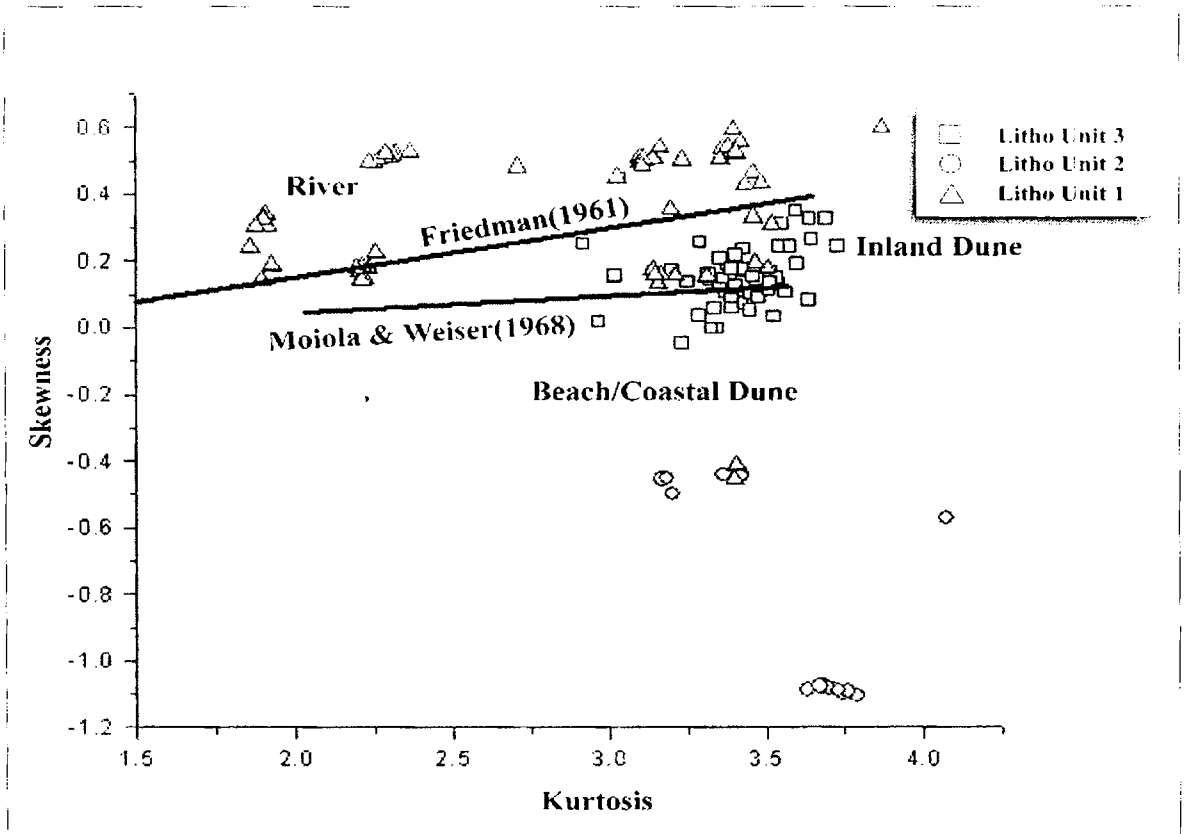

Figure 4.6 Kurtosis plotted against Skewness showing three diferent regions of sand deposit after Friedman(1961) and Moiola & Weiser(1968)

is largely coarse skewed to finely skewed and sediments of Unit 3 bears coarse skewed to symmetrical skewness. The skewness values ranges from -0.452 to 0.598 in Litho Unit 1, -2.099 to 0.172 in Litho Unit 2 and -0.048 to 0.449 in Litho Unit 3. Unit 1 is nearly symmetrical, while Unit 2 is largely negative skewed and Unit 3 is more positive skewed.

Kurtosis:

The kurtosis of sediment distribution in Unit 1 shows leptokurtic to mesokurtic towards lower depths and turns platykurtic at depths. In Unit 2, it is more leptokurtic and rarely mesokurtic and in Unit 3, it is mesokurtic to leptokurtic. The values of kurtosis ranges from 1.857 to 3.868 in Litho Unit 1, from 3.144 to 8.291 in Litho Unit 2 and from 3.018 to 3.691 in Litho Unit 3.

Bivarient plots of mean vs sorting, mean vs skewness, sorting vs skewness and kurtosis vs skewness gave a better picture of the variations mentioned above.

Sorting vs Skewness

The plots of sorting against skewness (Figure 4.4) of grain populations in the three Litho Units differentiate the Litho Unit 2 from rest two. Like in previous plot between mean and skewness, Litho Unit 2 falls in coastal sand regime of the bivarite diagram designed by Friedman (1961). Majority of the plots of Litho Unit 1 and 3 fall very close to each other, while there are a few which shows distinct riverine character and dune character.

Mean vs Skewness

In the present study the skewness versus mean plotting of the grains (Figure 4.5.a and Figure 4.5.b) of three different Litho Units fall within the bivariant field established by Friedman (1968) and Moiola and Weiser (1968). Majority of the grains of Litho Unit 1 falls in the the domain of river sands, the grains of Litho Unit 2 shows that the sand grains have more closeness to coastal sand domain in the plot . The plots of skewness with mean of Litho Unit 3 exclusively fits it to dune regime.

Kurtosis vs Skewness

The sediment population of Litho Unt 1 falls in the riverine regime of the plot(Figure 4.6), differentiated from dune in Friedman (1961). Litho Unit 2 having high negative skewness fall in the lower part of the plot and those of Litho Unit 3 spread around the center. The graphical discrimination between inland and coastal dune by Moiola and Weiser (1968), similarly differentiates Litho Unit 3 into inland dunes and coastal dunes. The sediments recovered from lower depths in Lihto Unit 3 fall in the coastal field of the graphical discriminant used. It is striking that the sediments of Litho Unit 2 too fall in the coastal dune regime. The Table 4.2 gives the process and environment of deposition of three Litho Units encountered in the study area as per the linear discriminant analysis (Sahu, 1964).

Table: 4.2 Interpretation of process and environment of deposition by Linear Discriminant Function (after Sahu, 1964)

Litho Unit	Mean	Sd	Sk	K	Y1	Y2	Y3
3	1.38	0.73	0.13	3.36	7.5	121.1	-4.76
2	2.58	0.76	-2.1	3.29	2.34	105.24	6.22
1	1.3	0.86	0.45	3.03	7.47	132.74	-8.12

The linear discriminant analysis shows that the majority of sediments of Litho Unit 1 falls in riverine and shallow agitated environment of deposition. The sediments of Litho Unit 2 fall in shallow marine agitated environment with proximities to beach. The sediments of Litho Unit 1 largely are of beach deposited in a shallow agitated environment and near shallow marine condition. The interpretation cannot be helpful to ascribe the site of formation; the discriminant analysis of the three in terms of degree of agitation is useful.

4.1.5. Discussion

The mean values of sediments does not vary considerably among Litho Units 1 and 3, they being of medium sand. The sediments of Litho Unit 1 shows variable sorting index. Towards the bottom of the cores it is poorly sorted, while towards the top of the unit, sediments are moderately sorted. The coarser and poorly sorted sediments that are encountered towards the bottom of Unit 1 could be indicative of either a near source or an action which was quick and instable. In Litho Unit 1 the grain population is symmetrical and the distribution of sediment population is meso-leptocurtic. Meanwhile Litho Unit 2 has predominantly fine sand admixed with medium sand. Sediments are largely coarse skewed at the top of the unit , while they are finely skewed in the remaining. The change in skewness could therefore indicate the action of a process responsible for draining away of the finer particles in the sediments deposited. It indicates that that the sources of sediments in Litho Unit 1 and 3 were of or greater than 0.5 to0.25 mm. In Litho Unit 2, the sediments are moderately sorted and have grain size 0.25 to 0.0625 mm. Litho Unit 2 it is prominently leptocurtic. While in Litho Unit 3 sediments are well sorted. In Litho Unit 3, the grains are symmetrical to coarse skewed. Here also, coarse skewness indicate high energy regime of the agent taking away the finer particle. In Litho Unit 3, the grain population shows leptokurtic sorting other than in the top most part of this layer. The top most part of this Litho Unit, which shows extreme and uniform well sorting also, bears the signature of coastal dunes.

4.2. Mineralogical studies

Mineral and their associations are hallmarks of different stages involved in formation of rocks and their sediments. Mineral associations and their textural composition give clue

to the earth surface processes that are responsible for the making up of a sedimentary deposit. Assemblage of minerals, taking account of their grain shape, size and degree of surface smoothness, in sedimentary deposits have been used by earth scientists for many years to unravel the source provenance, transportation history and depositional environment of sediments. The relative abundance of mineral fractions, in comparison with their physical properties, in sediments can speak about the geological agents responsible for the development and sustenance of sedimentary environment.

Mineral constitution of sediments supplemented by the textural characteristics bear the characteristics of the depository environment. In many published literatures minerals are examined in several fractions of sediments to represent the entire mineralogical assemblage of sediments. This is so because minerals are deposited according to the difference in size, shape and density and hence a single size fraction seldom represents the entire mineralogical composition of the sediments (Rubey, 1933; Rittenhouse, 1943; Friedman, 1961; Blatt et al. 1980 and Patro and Sahu 1977). The size frequency distribution of individual minerals is essential to understand the interaction between physical properties of minerals and the physical processes operated in the accommodative space. The lack of heavy minerals in the section poses a serious threat to the usual way of collecting information on source, distribution and dynamics spread across the study area.

4.2.1. Methodology

4.2.1.1. Microscopic studies

Microscopic studies were done with both reflective microscope and refractive microscope. Grain sample sets for microscopic studies were designated from samples procured from every one meter depth by coning and quartering. The result thus obtained was abridged by taking average of the contents of each mineral for each Litho Unit designed in the study area.

A reflective microscope (model LEICA 12.5, with magnification up to 5x) was used to identify the mineral, as well as to select mineral grains for SEM characterizations. The sediment grains were spread over a counting tray of dimensions 9x 5 cm calibrated to 45 equal squares and was observed under the microscope.

A refractive microscope (MEIJI, ML 9300, with magnifications, 4x, 10x and 40x was used for identifying the sediment grains. The mineral grains were mounted on a glass plate for refractive microscopic studies. In order to facilitate the studies, following method prescribed by Lewis (1984) was employed. The grains has been sieved and cleaned. A thin coating of canada balsam was applied over the glass slide and heated so that bubbles on the coating disappear. The grains were then scattered evenly over canada balsam and a cover slip was carefully pressed over the slide until bubbles were eliminated, again it was cooled and labelled. The minerals were identified and quantity of individual minerals were estimated by grain counting.

4.2.1.2. Powder X-ray Diffraction

Powder X-ray Diffraction (XRD) is one of the primary techniques used by mineralogists and solid state chemists to examine the physico-chemical make-up of unknown solids. This data is represented in a collection of single-phase X-ray powder diffraction patterns for the three most intense D values in the form of tables of interplanar spacings (D), relative intensities (I/Io), and mineral name.

The XRD technique takes a sample of the material and places a powdered sample in a holder, then the sample is illuminated with x-rays of a fixed wave-length and the intensity of the reflected radiation is recorded using a goniometer. This data is then analyzed for the reflection angle to calculate the inter-atomic spacing (D value in angstrom units - 10^{-8} cm). The intensity (I) is measured to discriminate (using I ratios) the various D spacings and the results are to identify possible matches. This method is based on identifying the presence of basal and prism peaks from the X-ray diffraction pattern and corresponding relative intensity values.

About 95% of all solid materials can be described as crystalline. When X-rays interact with a crystalline substance (Phase), one gets a diffraction pattern. The X-ray diffraction pattern of a pure substance is, therefore, like a fingerprint of the substance. The powder diffraction method is thus ideally suited for characterization and identification of polycrystalline phases.

When an X-ray beam hits an atom, the electrons around the atom start to oscillate with the same frequency as the incoming beam. In almost all directions we will have destructive interference, that is, the combining waves are out of phase and there is no resultant energy leaving the solid sample.

However the atoms in a crystal are arranged in a regular pattern, and in a very few directions it will have constructive interference. The waves will be in phase and there will be well defined X-ray beams leaving the sample at various directions. Hence, a diffracted beam may be described as a beam composed of a large number of scattered rays mutually reinforcing one another.

An X-ray beam incident on a pair of parallel planes P1 and P2 is separated by an interplanar spacing d. The two parallel incident rays 1 and 2 make an angle (θ) with these planes. A reflected beam of maximum intensity will result if the waves represented by 1 and 2 are in phase. The difference in path length between 1 to 1' and 2 to 2' must then be an integral number of wavelengths λ. This relationship can be expressed mathematically in Bragg's law as

$$2d\sin\theta = n\lambda$$

The process of reflection is described here in terms of incident and reflected (or diffracted) rays, each making an angle θ with a fixed crystal plane. Reflections occur from planes set at angle θ with respect to the incident beam and generates a reflected beam at an angle 2θ from the incident beam. The possible d-spacing defined by the indices h, k, l are determined by the shape of the unit cell.

Bragg's law can be rewritten as

$$\sin\theta = \lambda/2d$$

Each reflection is fully defined when we know the d-spacing, the intensity (area under the peak) and the indices h, k, l. If we know the d-spacing and the corresponding indices h, k, l we can calculate the dimension of the unit cell.

4.2.1.3. Scanning Electron Microscope (SEM) and Energy Dispersive Spectrometry (EDS)

The finer minerals that were unable to be identified under normal microscope were observed under scanning electron microscope and their presence is also incorporated in the mineral list under each Litho Unit. On the basis of techniques described above alone it may not be possible to distinguish finer sediment grains, especially those adhered to larger grains as coatings. Identification of such coatings and other micro-scale minerals adhered to the mineral surfaces could give more information regarding the deposition/ digenesis. Energy dispersive X-ray microanalysis is made possible using Scanning Electron Microscope and Energy Dispersive Spectrometer (SEM-EDS), with high resolutions, effectively, timely and economically.

The SEM permits the observation of materials in macro and submicron ranges and EDS perform an elemental analysis on microscopic sections of the material or contaminants that may be present on the surface (Goldstein et al., 2003)

In EDS a semi conductor detector is used to classify X-radiation in terms of its energy rather than its wave length. This type of detector usually consists of a single- crystal disc of Li-drifted Silicon, 3 to 5 mm thick with an active area of between 10 to 30 mm. The energy of X-ray photons coming from the specimen after bombardment by an electron beam and impinging on the crystal are converted into pulses of current proportional to the energy of photons. The pulses are amplified, counted, digitized and fed into a multichannel analyzer, from where they can be imaged into a series of charts.

SEM/EDS analyses are performed utilizing a JEOL JSM 820 SEM with magnification capabilities up to 200000X, coupled with a Tracor Northern TN5502 series II analyzer with a Rembrandt Model 3500F Computer Graphics film recorder and attached Kevex Energy Dispersive Spectrometer (EDS) facility at Michigan Tech University, Houghton, USA was availed for the purpose of SEM and EDS studies. It uses a cold field emission high resolution scanning electron microscope, which is configured to detect secondary and backscattered electrons as well as characteristic X-rays. The system is fully automated and is operated via easy-to-use menu driven software. Secondary electron image

photomicrographs are recorded with a digital camera. Images being captured on Polaroid prints and negatives. Images are digitally stored in tiff format. EDS spectra are acquired using count times of 1-2 minutes.

4.2.2. Results

4.2.2.1. Microscopic studies

The minerals from the study area, identified by both reflective and refractive microscopes are listed below. Among the grains, quartz is the most predominant mineral identified in the study area in different depth at three Litho Units, namely Litho Unit 3 (upper), layer 2(middle) and layer 1 (lower), as given in Table 4.3.

Table: 4.3. Mineralogical Composition of three sub surface layers in the study area

	Quartz (%)										Feldspar(%)									
Well No.	TRV										TRV									
	1	2	3	4	5	6	7	8	9	10	1	2	3	4	5	6	7	8	9	10
Litho Unit3	99	99	98	99	99	98	99	99	99	99	<1	<1	~1	<1	<1	~1	<1	<1	<1	<1
Litho Unit2	92	94	93	92	93	92	94	91	92	90	5	5	4	6	4	4	3	6	4	7
Litho Unit 1	97	96	95	96	94	95	93	96	93	96	-	--	1	--	-	1	2	1	2	--
	Ilmenite (%)										Others(%)									
Well No.	TRV											TRV								
	1	2	3	4	5	6	7	8	9	10	1	2	3	4	5	6	7	8	9	10
Litho Unit3	--	--	--	--	--	--	--	--	--	--	-	--	<1 *	--	--	<1 *	--	--	--	--
Litho Unit2	2	1	2	2	2	3	2	2	3	2	<1	--	1#	--	<1#	1#*	<1 #	<1 #	<1 #	<1#
Litho Unit1	2	3	3	3	4	3	3	2	3	3	1 + ^	1+	1#^	1+ *	<2+* ^	1+*	1+*	1-*	1-* ^	1+*

* Zircon , # Mica, + Sillimanite, ^ Haematite

But comparatively, Quartz present in Litho Unit 3 in the range of 98-99% is maximum followed by Litho Unit 1 which contains 93-97% and Litho Unit 2 contains 90-93% quartz.

Litho Unit 3: Quartz is followed by Feldspar. Ilmenite is absent in Litho Unit 3.

Litho Unit 2: In Litho Unit 2 Feldspar, Mica and Ilmenite follow quartz having percentage less than 5 percentages.

Litho Unit 1: In Litho Unit 1 Ilmenite, Zircon and Hematite shows dominance next to quartz while feldspar is absent in some of the locations in this layer.

Table 4.4 shows depth wise distribution of dominant minerals and minor minerals precisely with the help of XRD studies.

Litho Unit	Quartz	Biotite	Haematite	Ilmenite	Oligoclase	Rutile	Sillimanite	Zircon	Kaolinite	Garnet
3	√									
	√									
	√									
2	√	√							√	
	√	√							√	
	√	√								
1	√									
	√						√			
	√						√	√		
	√						√	√		
	√			√	√		√	√		
	√	√		√			√	√	√	
	√			√	√		√	√		
	√				√		√	√		
	√	√	√	√		√	√	√	√	√
	√		√	√	√	√	√	√		
	√			√			√	√		√
	√	√					√	√		

4.2.2.2. XRD Studies

The minerals identified from XRD are as follows:

Quartz:

Quartz, is the most resistant mineral in soil, Quartz, because of its very low aqueous solubility, may be considered unreactive, and it is one of the residual minerals remaining in soil after other minerals have altered or dissolved.

In the XRD, quartz is easily noticable with prominent peaks (Figures 4.7 a, b and c).

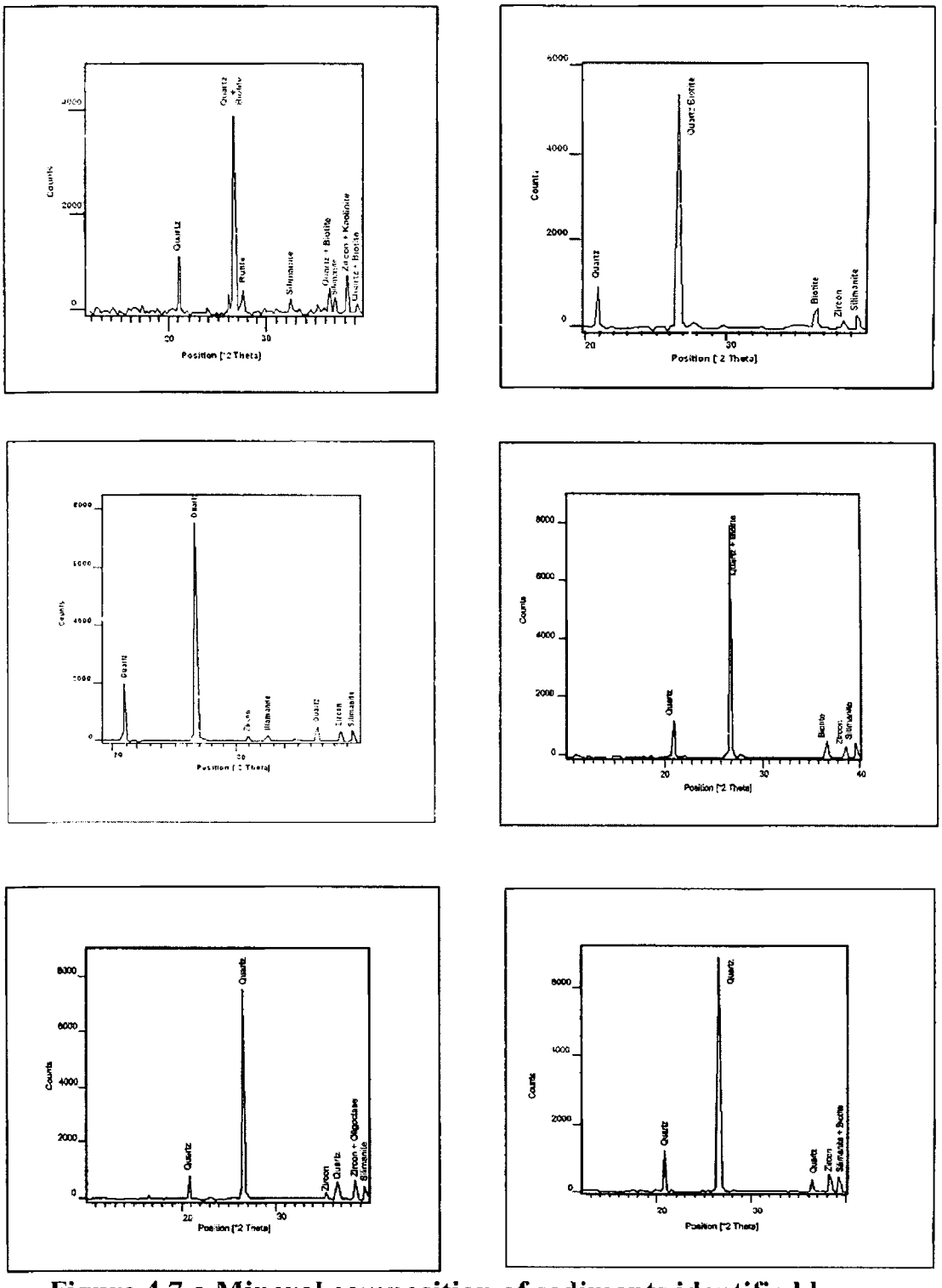

Figure 4.7 a Mineral composition of sediments identified by XRD technique of Litho unit 1

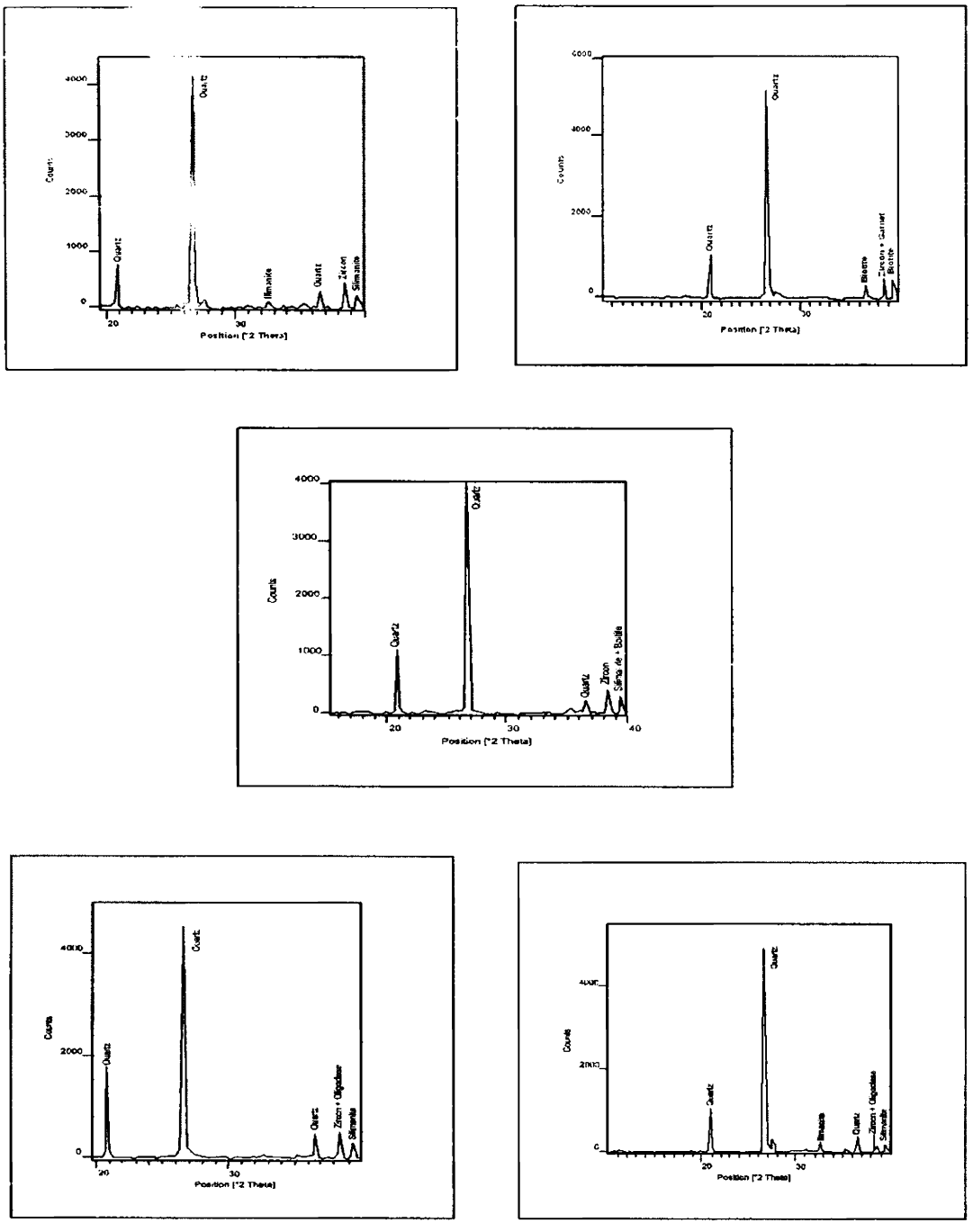

Figure 4.7 a (Cont.) Mineral composition of sediments identified by XRD technique of Litho unit 1

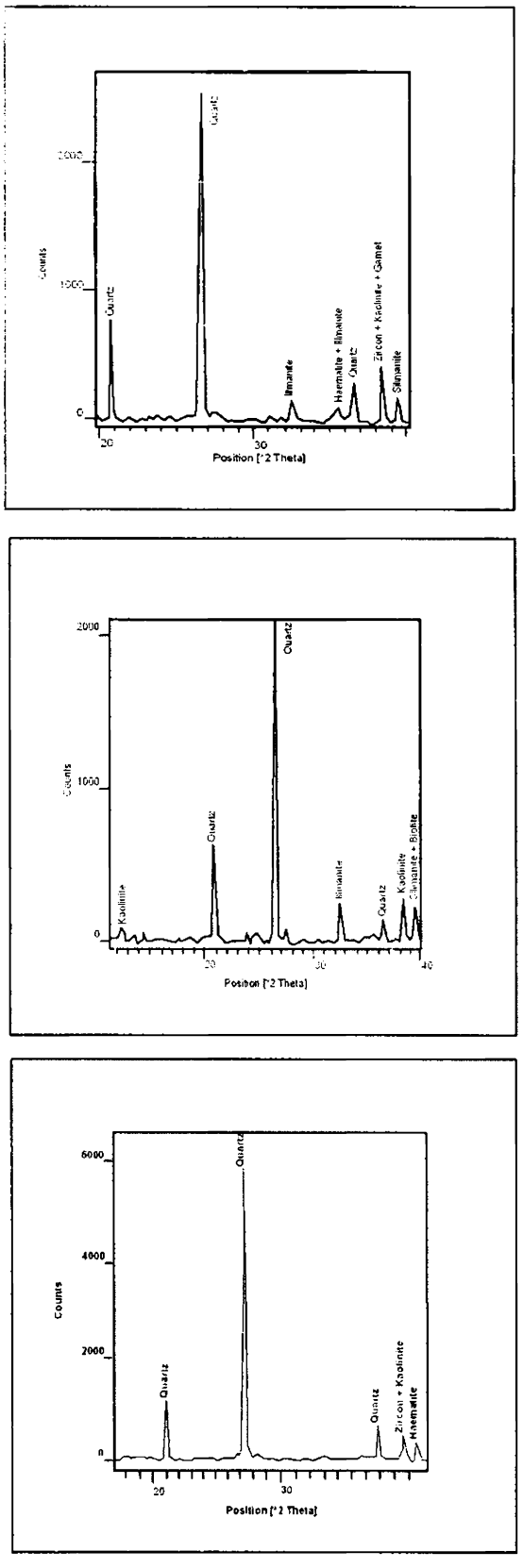

Figure 4.7 b Mineral composition of sediments identified by XRD technique of Litho unit 2

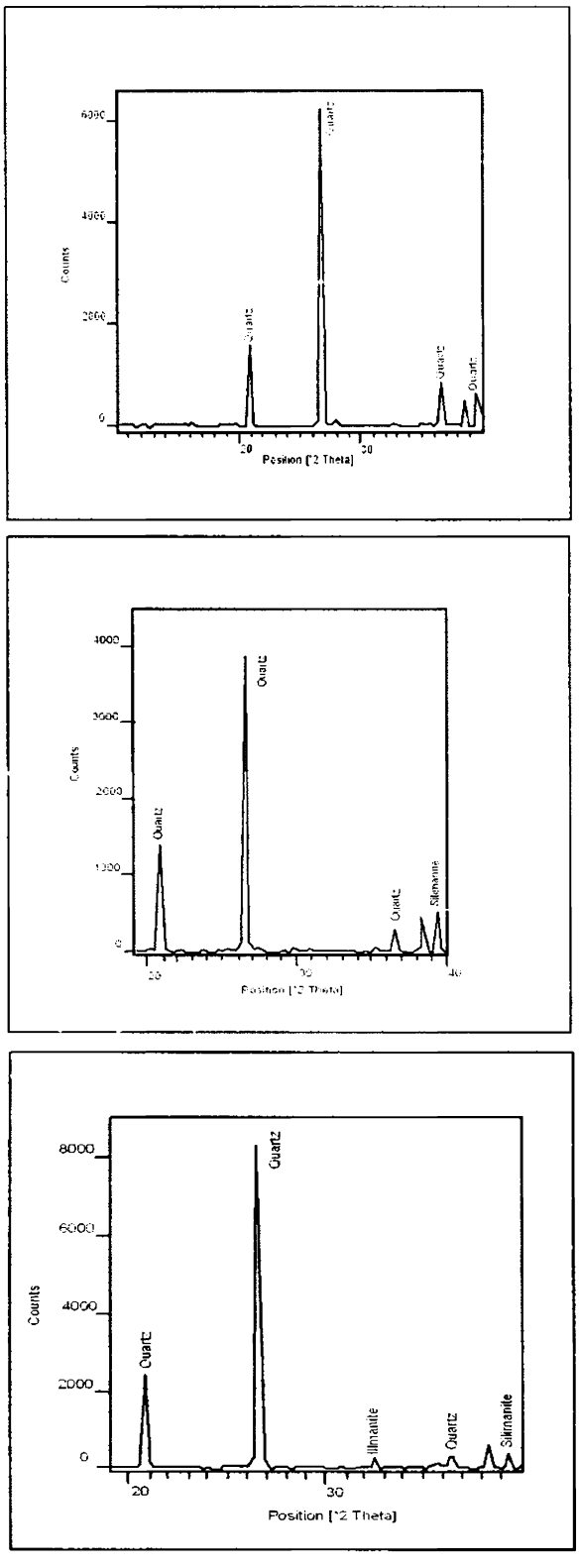

Figure 4.7 c Mineral composition of sediments identified by XRD technique of Litho unit 3

Biotite:

Presence of biotite indicates a restricted evaporitic environment during deposition of sedimentary rocks. In the study area, biotite is found in notable amounts in all the size fractions at depth ranging up to 10m. From 10m to 19 m it is absent and again found in Litho Unit 3 at some depths.

Hematite:

The post sedimentary phenomena and processes in sandstones include formation of rim cements comprising hematite, feldspar, quartz and chalcedony. The influence of the fluvial-marine transitional depositional environment on the digenesis is best reflected by the areal restriction of cement types fitting into the palaeogeographical framework. Observation of modern hematite concretion growth in a natural sedimentary setting provides a rare glimpse of conditions at the time of formation. It is hypothesis that the iron that composes the hematite concretions was originally sourced from weathering of the underlying bedrock The abundance of red iron oxide grain coatings in the sediments suggests a fairly oxidized system. Hematite is absent in Litho Unit 3 and Litho Unit 2. It is found at depth of 20m in Litho Unit 1 in discontinues manner.

Ilmenite:

Heavy minerals are important indicators which can tell us the type of rocks that existed in the sediment source area. Ilmenite is deficient at depth upto 13 m which include layer 3 and layer 2. Below 13 m up to 36 m that is Litho Unit 1 it is present.

Feldspar:

Feldspar is absent at depth upto 10m. It can be seen at 11m. Thereafter it is found below 19m depth which forms the part of Litho Unit 1.

Rutile:

Rutile is a common accessory mineral in high-temperature and high-pressure metamorphic rocks. In the sandstone, meteoric water alters ilmenite to rutile. Rutile is absent in Litho Unit 3 and Litho Unit 1. It is reported in Litho Unit 2 at depth of 9m. This indicate that an environment supportive of weathering of ilmenite to rutile was prevalent in the deposition of Litho Unit 2.

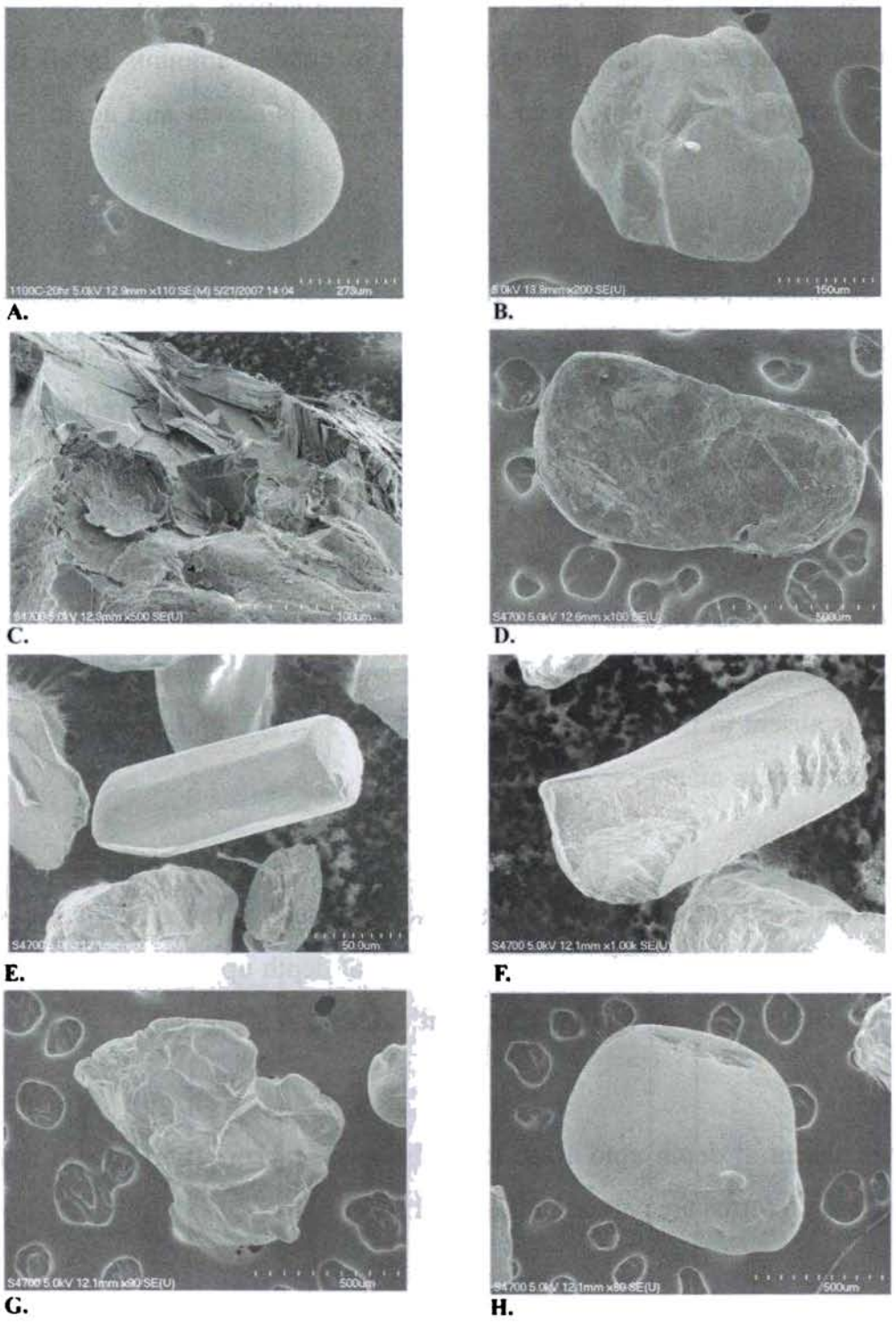

Figure 4.8. SEM Photomicrographs of minerals from three different lithological units. A & B: Quartz grains which forms 99% of Litho Unit 3, C: a grain of Graphite, D: a grain of Biotite and E: Rutile found in Litho Unit 2, F: Silliminite and G & H: Quartz in Litho Unit 1

Kaolinite:

Kaolin is a product of early digenesis involving meteoric water below the water table. In the sandstone, meteoric water flow alters feldspars to kaolin, thus yielding commercial silica sand deposits. Kaolinite is present in Litho Unit 3 from 2m up to 9m .It is absent in Litho Unit 2. In Litho Unit 1 it is found only at depths of 20m and 24 m.

Garnet:

Garnet is absent at all depths of Litho Unit 3 except 9m. It is totally absent from Litho Unit 2. In Litho Unit 1 it is found at depth of 24m. High grade metamorphic provenance for the sediment is inferred from the presence of garnet.

Zircon:

Zircon is found in notable amounts in almost all the size fractions and in all layers, at all depths but abundant in Litho Unit 1. These grains are mostly colorless and sometimes with brownish tint. Zoning and inclusions are exhibited by some of these grains.

Sillimanite and graphite:

Sillimanite is absent at depth up to 11m (that is Litho Unit 3). But it is prominently present thereafter up to 37m. Graphite is identified by SEM-EDS in sample from Litho Unit-2.

4.2.2.3. SEM-EDS Analysis

The sand grains in the Litho Units were analysed with SEM-EDS gives an idea of the dynamics of elemental leaching during or after the time of deposition. Here the analysis gives the detailed information about the materials that are adhered to the surface of grain.

EDS studies shows that the incidence of encountering precipitation/coatings on the surface of quartz grains is more in grains of Litho Unit 1. Many quartz here bear coatings of Si, Ca, Al, O (Figure 4.9.1.a), Al, Si, O, Zr (Figure 4.9.1.b), O, Al, Si, Ti (Figure 4.9.1.c) and O, Ti (4.9.1.d). In Litho Unit 2 the composition of the coating on the quartz are slightly different, O, Al, P, Ca, Sr (Figure 4.9.2.a), O, Mn, Fe (Figure 4.9.2.b) and C, O, Mg, Al, Si, Fe (Figure 4.9.2.c). The quartz grains in Litho Unit 3 are devoid of any coatings (The above figures are representative spectrographs, the remaining are attached in Appendix 2).

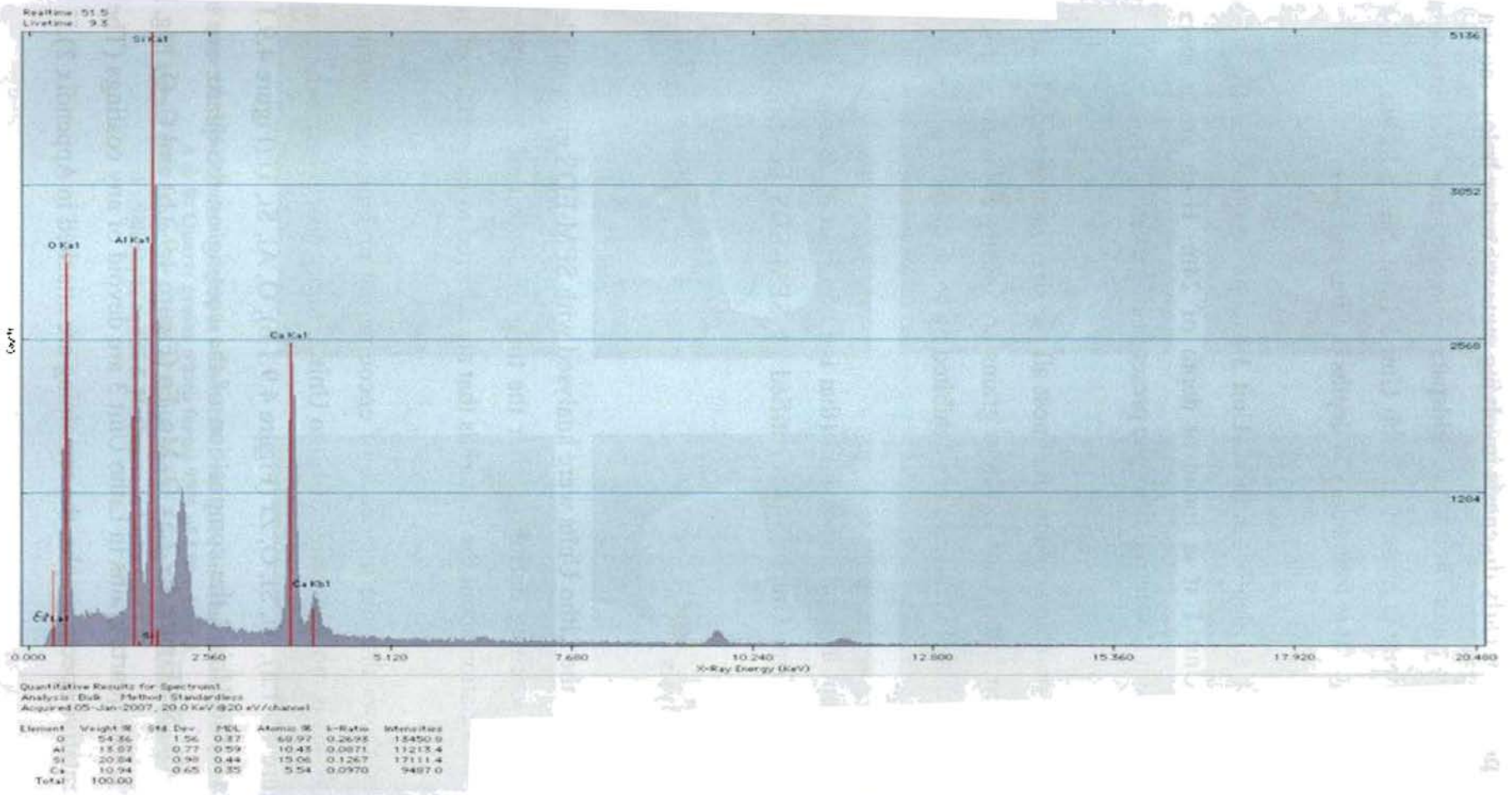

Figure 4.9.1.a. SEM-EDS Spectrograph of coatings on quartz grain from Litho Unit 1. The coating contain O, Al, Si, Ca.

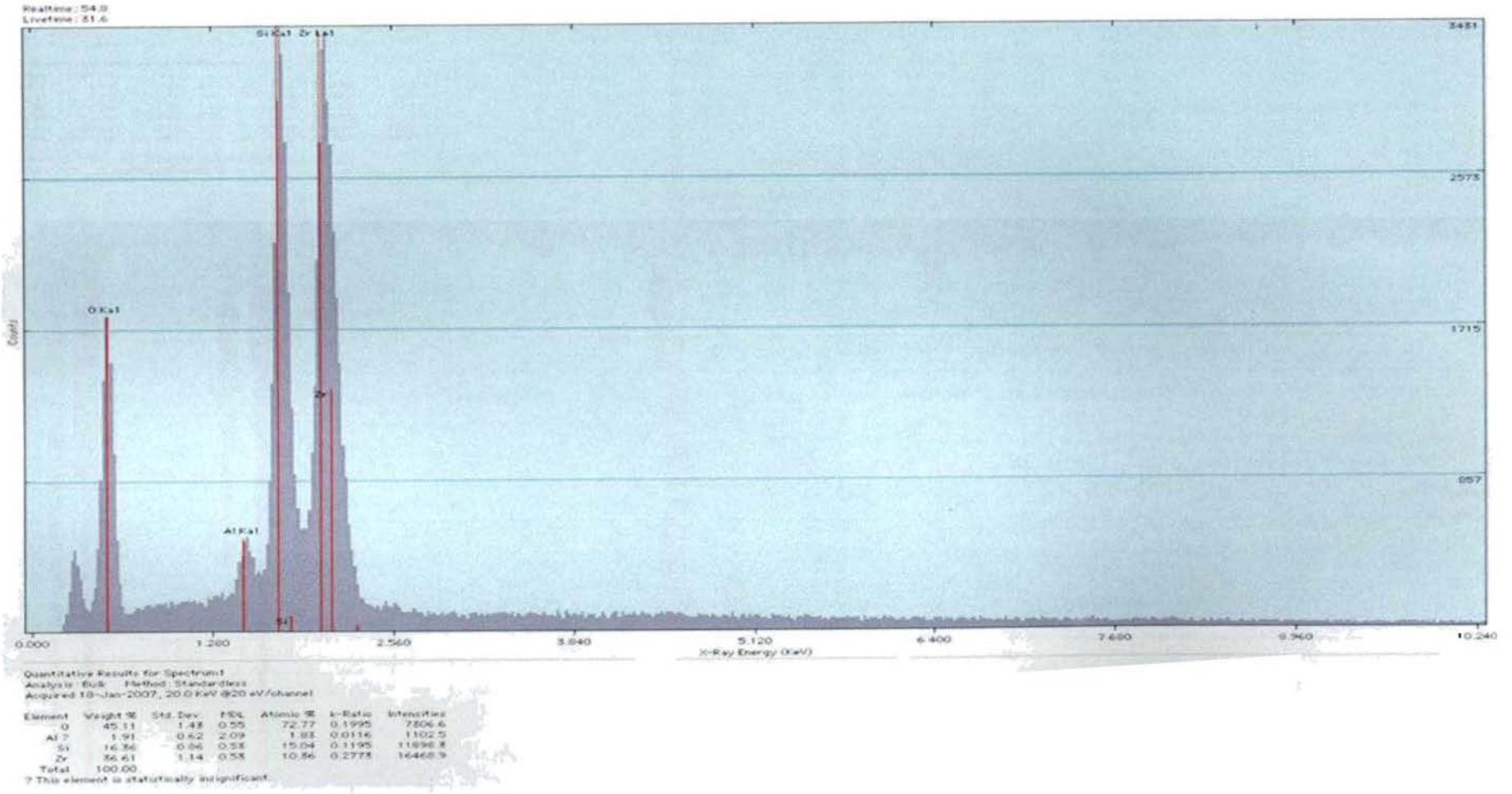

Figure 4.9.1.b. SEM-EDS Spectrograph of coatings on quartz grain from Litho Unit 1. The coating contain O, Al, Si, Zr.

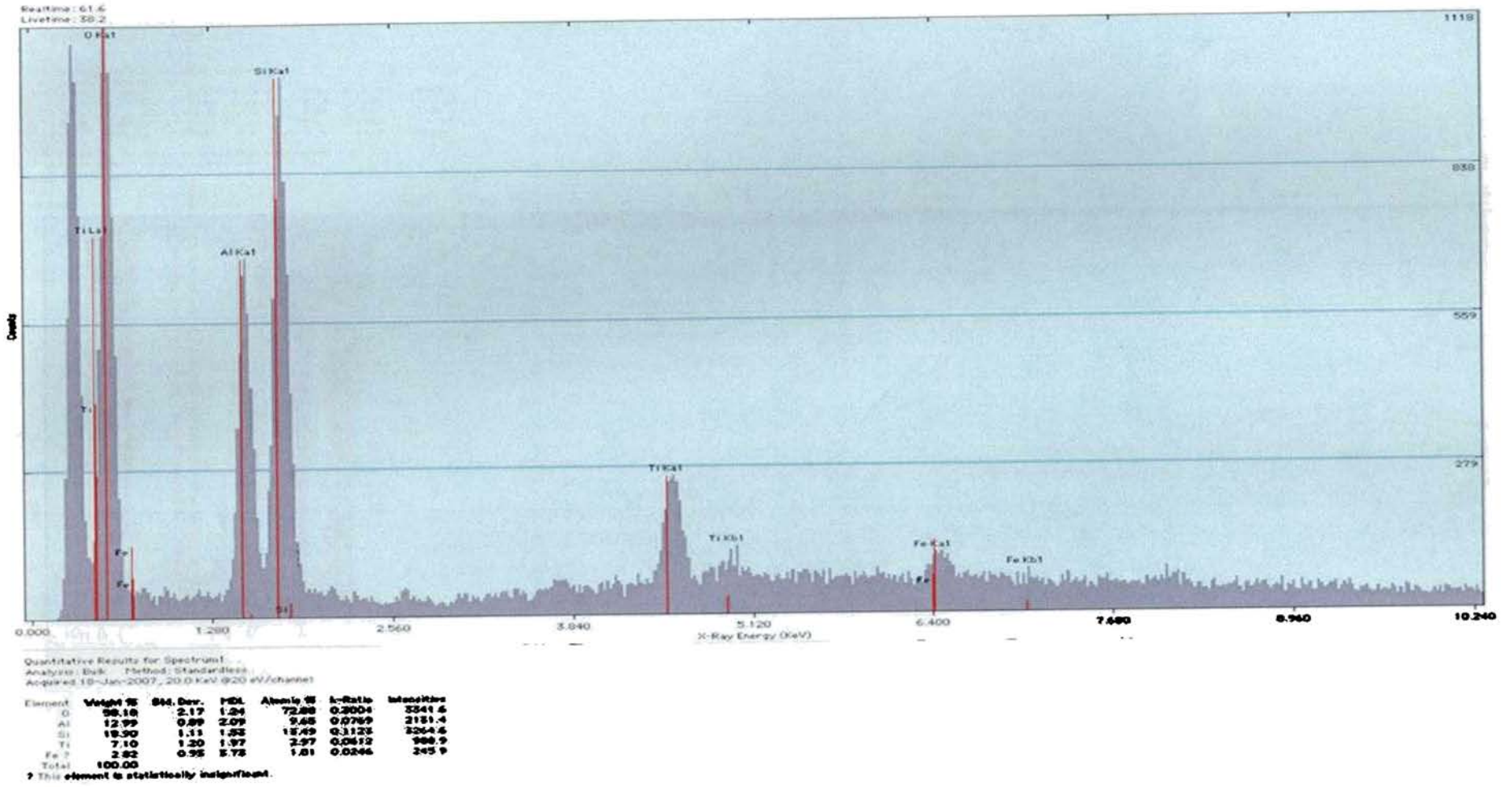

Quantitative Results for Spectrum1

Analysis : Bulk Method : Standardless

Acquired 19-Jan-2007, 20.0 KeV @20 eV/channel

Element	Weight %	Std. Dev.	MDL	Atomic %	k-Ratio	Intensities
O	58.18	2.17	1.24	72.88	0.2004	3341.6
Al	12.99	0.89	2.07	9.65	0.0799	2181.4
Si	19.50	1.11	1.82	13.49	0.1125	3264.6
Ti	7.10	1.20	1.97	2.97	0.0512	980.9
Fe ?	2.82	0.95	5.73	1.01	0.0246	245.9
Total	100.00					

? This element is statistically insignificant.

Figure 4.9.1.c. SEM-EDS Spectrograph of coatings on quartz grain from Litho Unit 1. The coating contain O, Al, Si, Ti.

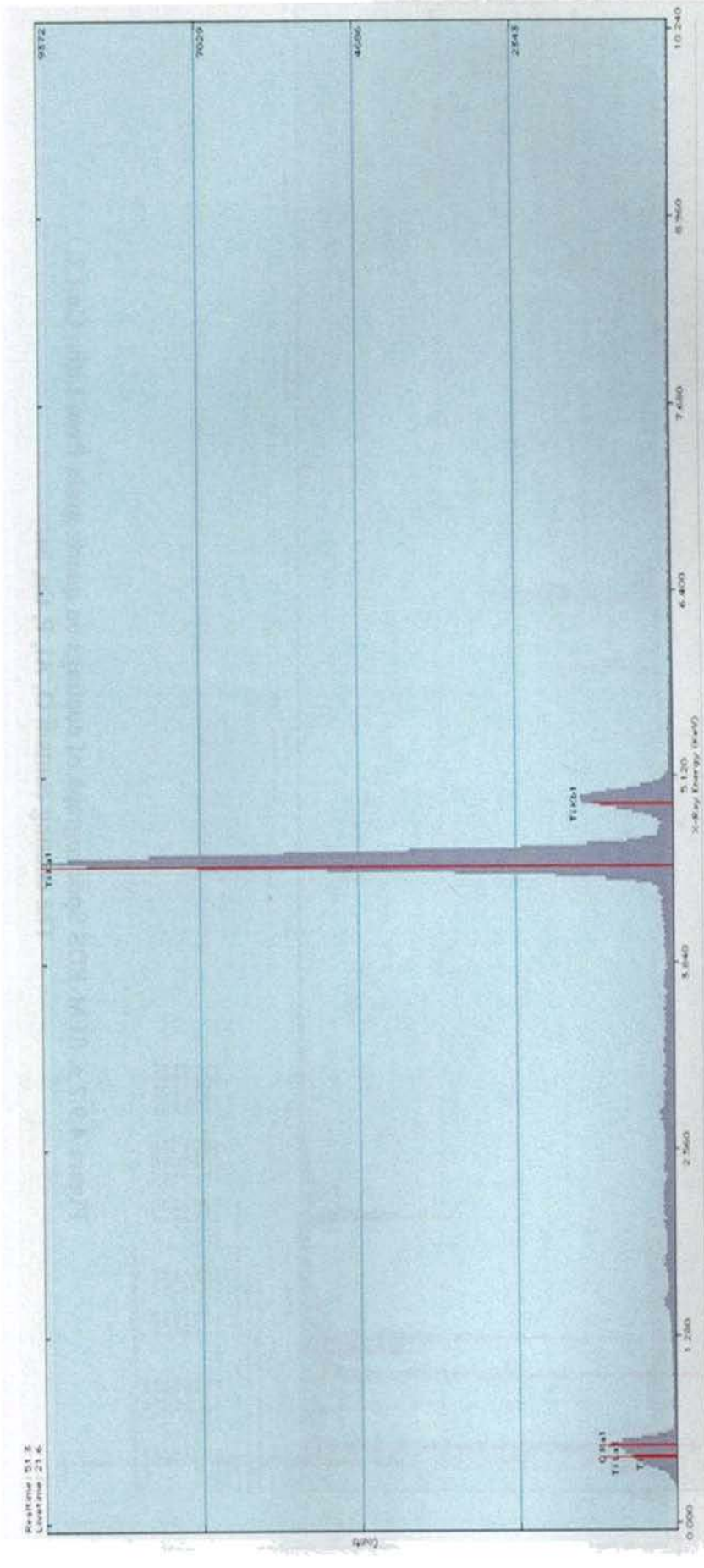

Figure 4.9.1.d. SEM-EDS Spectrograph of coatings on quartz grain from Litho Unit 1. The coating contain O, Ti.

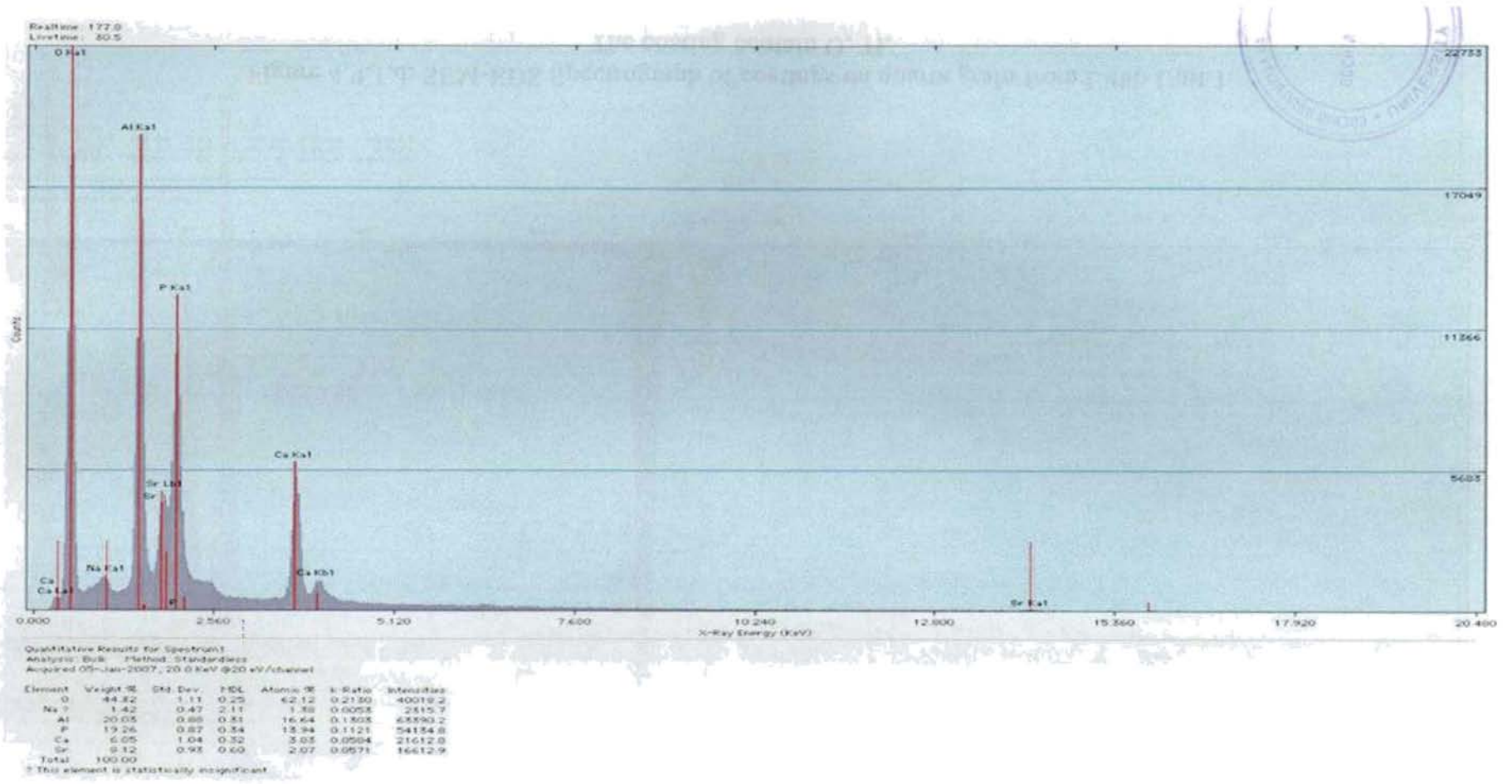

Figure 4.9.2.a. SEM-EDS Spectrograph of coatings on quartz grain from Litho Unit 2. The coating contain O, Al, P, Ca, Sr.

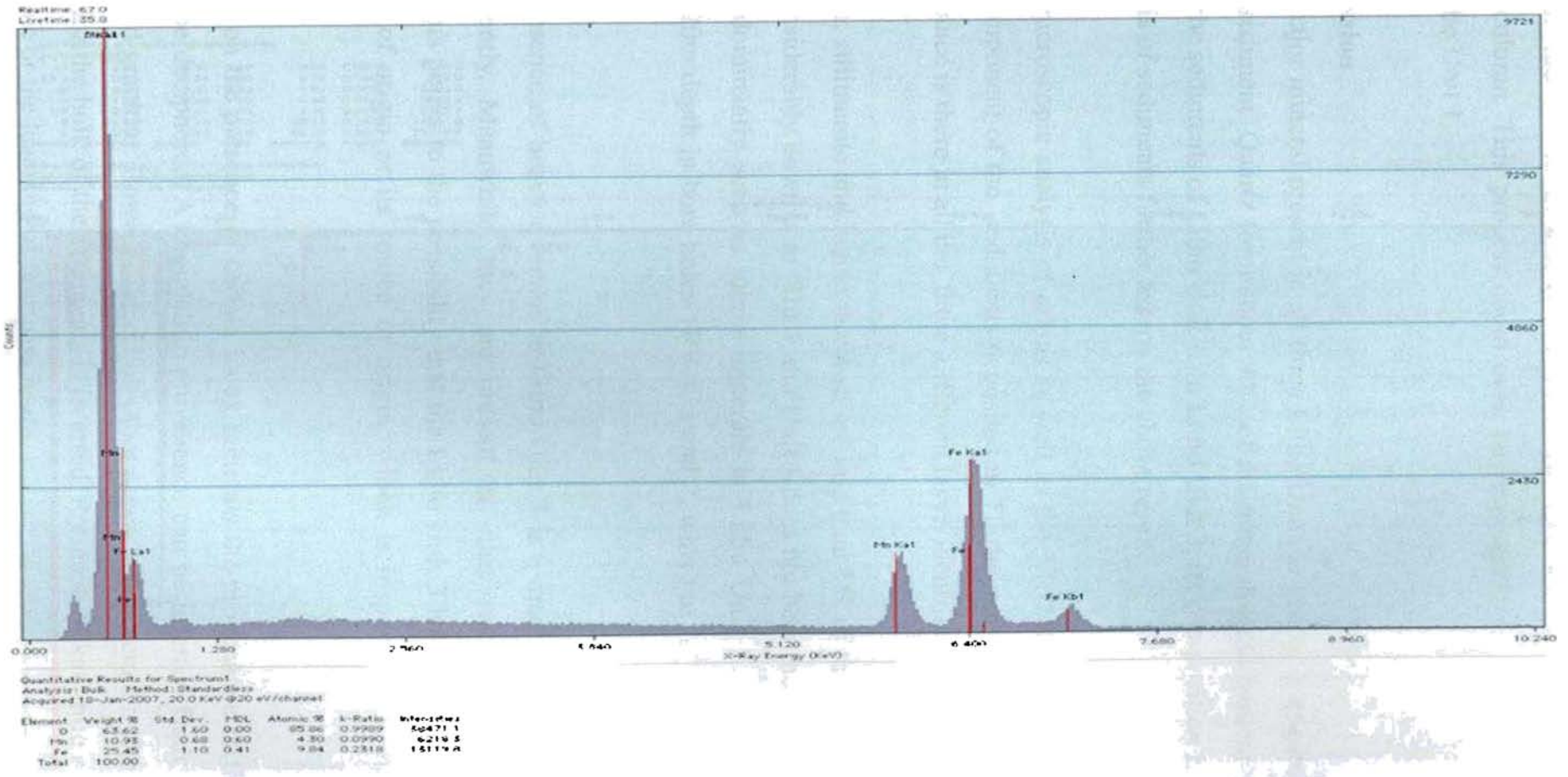

Figure 4.9.2.b . SEM-EDS Spectrograph of coatings on quartz grain from Litho Unit 2. The coating contain O, Mn, Fe.

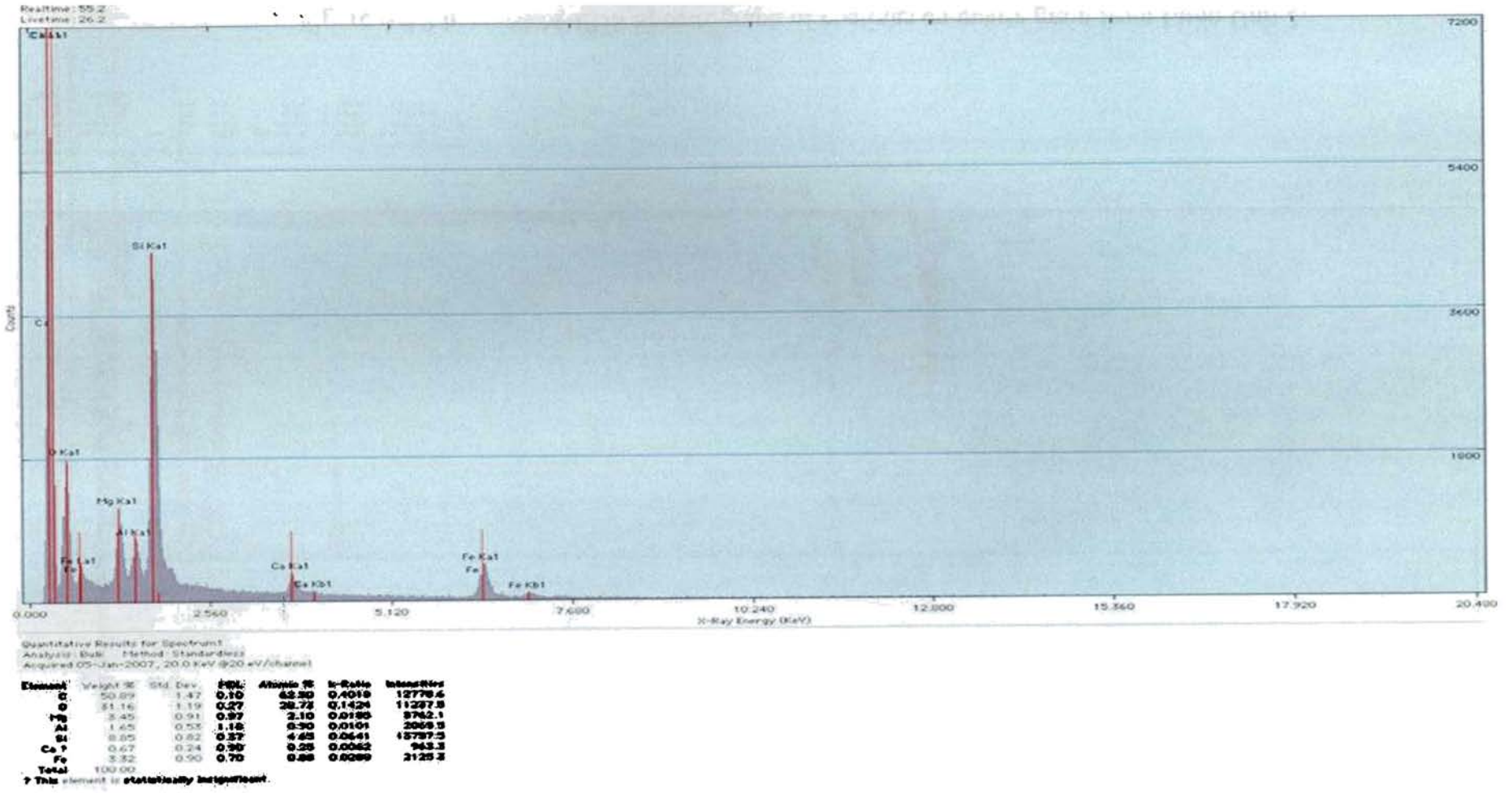

Quantitative Results for Spectrum1
Analysis: Bulk Method: Standardless
Acquired:05-Jan-2007, 20.0 KeV @20 eV/channel

Element	Weight %	Std. Dev.	MDL	Atomic %	k-Ratio	Intensities
C	50.89	1.47	0.10	62.50	0.4019	12778.4
O	31.16	1.19	0.27	28.72	0.1424	11287.8
Mg	3.45	0.91	0.97	2.10	0.0186	3762.1
Al	1.65	0.53	1.18	0.90	0.0101	2069.5
Si	8.85	0.82	0.37	4.65	0.0641	15787.3
Ca ?	0.67	0.24	0.90	0.25	0.0062	943.3
Fe	3.32	0.90	0.70	0.88	0.0289	3125.3
Total	100.00					

? This element is statistically insignificant.

Figure 4.9.2.c. SEM-EDS Spectrograph of coatings on quartz grain from Litho Unit 2. The coating contain C, O, Mg, Al, Si, Fe.

The EDS analysis shows that the coating intensity increases down the core. Therefore it can be concluded that mineral dissolution and re-precipitation has taken place in the lithological column. This process could even be responsible for increasing the purity of quartz in Litho Unit 1.

4.2.3. Discussion

The major mineral present in all three Litho Units is quartz. It constitutes more than 90% of the sediment. Quartz form about 99% of the mineralogical content of Litho Unit 3 and 94% of the sediments of Litho Unit 1. In Litho Unit 2, its composition falls to 90%. The XRD analysis of sediments further asserts the above result.

The microscopic analysis of grains as well as the XRD data confirms the quartz is the major component of the sediments deposited in Thiruvananthapuram coastal plain and its predominance is there in all the three different layer, identified there.

Zircon, sillimanite and hematite constitute lass than 1% of the sediment samples and they vary considerably down core. The Litho Unit 3 does not bear the heavy minerals, while they are predominantly seen as minor minerals in Litho Unit 1. Kaolin is identified at between 18-20m depth in bore holes TRV 1, 3 and 7, where as in TRV 1, it is seen at 25m depth too.

The absence of heavy minerals in Litho Unit 3 is a marked feature in the columns, studied presently. Meanwhile, they are present in other two units, though in minor quantities. This points to the possibility that the Litho Unit 3 has difference in either of its environment of origin or its source of origin, which is responsible in resultant mineral constituents.

Based on the presence of certain index minerals the provenance of the sediments in general can be deciphered. A khondalitic provenance can be inferred from the presence of sillimanite and graphite. However, based on other accessory minerals a gneiss /charnockite provenance for the bulk of the sediments is inferred. Presence of kaolinite either indicates a lateritic source or the leaching of feldspars insitu.

4.2.4. Estimation of Silica sand Quantity

For industrial and manufacturing applications, deposits of silica yielding products of at least 95% SiO_2 are preferred. Silica is hard, chemically inert and has a high melting point, attributable to the strength of the bonds between the atoms. These are prized qualities in applications like foundries, filtration systems, glassmaking and ceramics. Industrial sand's strength, silicon dioxide contribution and non-reactive properties make it an indispensable ingredient in the production of thousands of everyday products.

Table: 4.5 The qualitative utility of silica sands in various industries (after BS 2975, 1985)

Sl.No	Industry	SiO_2 (%)	Al_2O_3 (%)	Fe_2O_3 (%)	Alkalis (%)
1	Glass	100 - 98	0 - 0.4	0.0 – 0.5	0 – 0.32
2	Chemical Production	100 -97	0.2 – 0.8	0.2 – 0.5	0 – 0.3
3	Foundry	98 - 90	1 – 5	1 – 1.5	0.5 – 1.5
4	Metallurgy	95 - 90	1.5 - 4	1.2 – 1.6	0.5 – 1.5
5	Other industries	90- 85	2-3	1.5 -2	1 -1.5

The glass industry has established standard specifications for the silica sand intended for seven types of glass as per grades set out in British Standard methods 2975 (British Standard Methods, 1988) for sampling and analysis.

4.2.4.1. Estimation of tonnage

A preliminary estimate of the tonnage of the silica sand deposit in the study area is given in Table 4.8. The calculation is based on least thickness, which has been encountered in the well sections.

Table: 4.6 Grades of Silica sand for glass industry and the maximum limit of ferric oxide content

Grade of Silica	Use in industries	Iron content (as ferric oxide %)
A	Optical and ophthalmic glass	0.0
B	Tableware and lead crystal glass	0.05
C	Borosilicate glass	0.1
D	Colourless (or clear) container glass	0.15
E	Clear flot glass	0.2
F	Coloured container glass	0.25
G	Glass for insulating fibres	0.3

Table : 4.7 Average oxide content in silica sands of three Litho Units and their possible end use

Litho Unit	**Thickness**	**SiO_2**	**Al_2O_3**	**Fe_2O_3**	**Total Alkali**	**Quality**
3	8 to 16m	97.23	0.7	0.26	0.06	Useable for glass and chemical production industry
2	2 to 4m	86.22	4.21	0.07	0.28	Useable in other industries like paint, ceramics, filtering of water etc.
1	15 – 20 m	93.77	1.71	0.64	0.10	Good for foundry and metallurgic industries.

Table 4.8 Tonnage of silica sand in the study area up to a depth of 26m.

Litho Unit	Volume (million m^3)	Tonnage (in millions metric tonne)
3	240	288
2	60	72
1	480	576

Chapter V

Quartz-Grain Morphoscopy

5.1. Introduction

Quartz-grain morphoscopy is the statistical determination of the different types of quartz grains in sandy deposits (Cailleux, 1942). The method has been widely used in resolving problems of Quaternary geology, paleoclimatology and geomorphology with timely modifications incorporating the methodology adopted by Kuenen and Perdok (1962), Krinsley and Doornkamp (1973), Borger (2000), Mahaney et al. (2001) and Mahaney (2005).

Quartz-grain morphoscopic studies focus to bring out the history of the evolution of quartz grain since its detachment from the country rock. It is deduced from analyzing the available surface scars and markings, indicative of peculiar exogenic agents, like glacial, pluvial, fluvial, aeolian, coastal, mass wasting and insitu breaking. The study especially determines transport mechanisms undergone by sand grains and it discerns its deposition environments. The surface texture is examined most precisely under scanning electron microscope and it draws out the conclusion from the analysis of a large number of grains.

In quartz grain morphoscopy, to distinguish ancient deposition environments, the surface grain texture of quartz from contemporary environments were studied by Miller and Olson (1955), who divided all properties of contemporary environments into three groups.

The first include properties that exist only in contemporary sediments and not in the lithology; the second includes the properties that can be analyzed both in modern and ancient sediments, but which change over time with diagenetic process; and the third group encompasses properties that are the same in both modern sediments and lithology.

The surface micro textures fall in the second and third group. The correspondence between the modern and ancient micro-textures may be very close depending upon the original textural imprints, grain age and all the digenetic process that operated during post deposition time. If the origin of particular micro-texture is well understood environments can be delineated with a fare degree of certainty. The knowledge of physical and chemical parameters that influenced or created characteristic surface micro-textures can lead us to the exact environmental discrimination. The atlas of Krinsley and Doornkamp (1973) and Mahaney (2005) remains a useful source of illustration of textures.

5.2. Environment of deposition and quartz surface texture

Mahaney (2005) enlists forty-one different micro textures exhibited by quartz surface encrypting the records of events overprinted with time. Often it is possible to reconstruct the entire environment history of a grain as well as related time involved by studying closely the pre-weathering and weathering features. The parameters that had created different surface micro textures in different environments are discussed below.

Sand grains usually travel as saltating or creeping bed load (Bagnold, 1941) and may be subjected to a succession of high energy collisions. During collisions, the kinetic energy of each particle is converted, at least partially into elastic energy in the grain. The energy wave or vibration may bounce back and forth within a given grain a number of times, although it is not known how this affects the grain surface. The result of these collisions, termed "abrasion fatigue" by Pascoe (1961), is a disrupted lattice type of structure on grain surface. This makes the surface of the grains physically and chemically reactive and may cause small silt and clay particles to attach to the grains until they are removed by additional abrasion.

The shape of grains in the deposit regardless of their size depends on a number of factors, including:

- The initial shape of the grain
- Physical and chemical features
- The duration of the process

- Character and environment of transport
- The type and intensity of weathering following the sedimentation.

The two pre-deposition factors usually affecting the grains are rounding and surface frosting. Their degree depends upon the source of the grain, transportation factors and the intensity of the agent. Thus the character of rounding and surface frosting of the grain is an indicator of the transport environment and of the subsequent digenesis of deposits. The sand grain surface features of the three principal environments viz. aeolian, fluvial and glacial are summarized below.

5.2.1. Aeolian grains

The sediments are transported by wind, i.e. the aeolian transport, when the strength of wind crosses the threshold strength of the immobile loose material that retains it over an immobile surface (Bagnold, 1941; Pye & Tsoar, 1990; Barndorff-Nelson and Willets,1991; Boggs, 1995). Direct dislodgement from outcrops by wind is also important in grain transport (Greeley & Iverson, 1984; Anderson et al. 1991; Boggs, 1995). As grains are moved by wind, they collide with other grains in transport as well as on the surface below. If collision is sufficiently energetic, portions of grains may chip off, or they may shatter. Various types of cracks and plates may form on the parent grains. Much fine material of silt (63 μm) and clay (<2μm) may be mechanically produced in wind sediments that are transported long distances.

The micro texture observed on aeolian sand grains using SEM in the secondary mode includes:

- Upturned plates, parallel ridges approximately 0.5-10μm or thicker
- Elongate depressions
- Polygonal cracks
- Smoothed over depressions, low relief and ridges
- Bulbous projection

The upturned plates produced are probably the result of sand grains being frequently modified in the desertified environment by solution and precipitation of silica (Margolis & Krinsley, 1971; Krinsley et al. 1976). Plates appear to be sized from 0.1μm to 1um. Equidimensional or elongate depressions may be the result of glancing impact between saltating or creeping grains. They are observed on grains of sand size larger than about 400μm and are approximately 20μm (or less) to 250μm in diameter, producing medium relief. As grains saltate they also rotate; the effect of this behaviour on abrasion is unknown but it may assist in rounding grains and in the genesis of the bulbous edge.

Arcuate, circular and polygonal cracks (about 0.5μm to several tens of micrometers in length) are observed on most large quartz grains which are typical indicators of Aeolian. Smoothening of all the above mentioned features resulting in low relief is almost ubiquitous in modern desert grains. In the final stage of Aeolian transport a rolling topography is created which generally encompass the entire grain, often resulting in the production of bulbous edges.

5.2.2. Fluvial Grains

The most diagnostic micro feature of the fluvial process is the V-shaped percussion fracture. Well preserved in quartz, percussion scars are also found on other grains, including heavy minerals. The higher the flow regime, the greater the frequency with which this micro-texture appears on a random sample of grains. It is also, present on glacial grains, especially grains emplace by warm based glaciers, where water is available within and at the base of the ice, and moves material at high velocity (Mahaney & Kalm, 1996). The presence of these micro features is taken as evidence of near-catastrophic flow; however, much more work needs to be done with respect to correlating micro-textures with increasing stream velocity (Mahaney, 2005).

Abrasion seen primarily as a rounding factor with quartz is also important in wearing fracture down to plane surface and in some cases obliterating them. The available evidence indicates that upper flow regimes produce greater degrees of abrasion and rounding than middle or lower flow regimes and tend to obscure any previous micro texture signature.

especially over long transport distances. From the data available it appears that low regimes do not appreciably change the shape of grains inherited from till outcrops.

5.2.3. Glacial Grains

Among all type of sediment grains the glacial grains carry the greatest range of micro-textures than grains affected by other geologic agents. Unlike the Aeolian and fluvial grains, glacial grains are generally held in bondage by the ice or by other grains in rigid suspension resulting in the ultimate grinding of the grain as the glacier moves down. Aeolian and fluvial grains are capable of random motion. Therefore while they are undergoing high-energy collisions, they are not subjected to the concentration of this high energy specifically at one point as glacial grains do. In short the scars and imprints on grain surfaces that have undergone fluvial or Aeolian activities would be less intensive than that exhibited by grains from glaciated environment. Mahaney (2005) ascribes the features like angular grain shape, deep entrenchment of conchoidal and linear fractures and deep groves and frequent directionality of troughs and striations as unique to grains emplaced by glacial transport.

5.3. Methodology

SEM (Scanning Electron Microscopy) imaging capabilities

The SEM (Scanning Electron Microscopy) permits the observation of materials in macro and submicron ranges. The instrument is capable of generating three-dimensional images for analysis of topographic features. When used in conjunction with EDS the analyst can perform an elemental analysis on microscopic sections of the material or contaminants that may be present. An SEM generates high energy electrons and focuses them on a specimen. The electron beam is scanned over the surface of the specimen in a motion similar to a television camera to produce a rasterized digital image.

Electrons are speeded up in a vacuum until their wavelength is extremely short, only one hundred-thousandth that of white light. Beams of these fast-moving electrons are

focused on a sample and are absorbed or scattered by the specimen and electronically processed into an image.

EDS (Energy Dispersive Spectrometer) analytical capabilities

Viewing three dimensional images of microscopic areas only solves half the problem in an analysis. It is often necessary to identify the different elements associated with the specimen. This is accomplished by using the "built-in" spectrometer called an Energy Dispersive X-ray Spectrometer. EDS is an analytical technique which utilizes x-rays that are emitted from the specimen when bombarded by the electron beam to identify the elemental composition of the specimen. To explain further, when the sample is bombarded by the electron beam of the SEM, electrons are ejected from the atoms on the specimens surface A resulting electron vacancy is filled by an electron from a higher shell, and an x-ray is emitted to balance the energy difference between the two electrons. The EDS x-ray detector measures the number of emitted x-rays versus their energy. The energy of the x-ray is characteristic of the element from which the x-ray was emitted. A spectrum of the energy versus relative counts of the detected x-rays is obtained and evaluated for qualitative and quantitative determinations of the elements present

Modern SEM/EDS instruments are operated using very sophisticated software. These software programs allow unattended feature analysis and "mapping" of the composition of the elements on the surface of the specimen. Methodology involved in the present study has been elaborated elsewhere (Section 4.2.1.3).

5.3.1. Sample Collection

A sample collected in the field is only a representation of a population that may or may not be homogeneous. The sampling plan dictates the number of samples required to estimate sampling error and to characterize a population.

After deciding where to collect and with what intensity, the researcher normally considers some of his or her samples as "representative" for the purpose of microscope

analysis. Thus, we have the concept of the most "typical" site and sample, which in the collector's mind provides reliable information on the population. Representative samples are collected on the basis of color, mineral content, particle size, or some other easily determined property in the field, and may or may not represent the population.

5.3.1.1. Sub sampling

In sub sampling the sample is divided into a smaller portion to carry out a particular test, such as particle size, moisture content determinations or pH. The test is then carried out, presumably with a "representative" portion of the bulk sample (i.e., with splits or sub samples of the sand fractions) or with various fractions of sand recovered from wet sieving following particle size analysis. In any case, it is necessary to wash samples prior to selection for SEM-EDS analysis.

The various fractions to be analyzed may be recovered following particle size analysis where sand is wet sieved and dried. Individual sand fractions may be analyzed, from very coarse (1-2mm), coarse (1mm-500μm), medium (250-500μm) to the fine (250-125μm) and very fine (125-63μm) grade sizes.

A representative sub sample can be prepared with a sample splitter, or by spreading the sample out on weighing paper, and then using a micro spatula to select small amounts at more or less random intervals to produce the desired weight.

5.3.1.2 Processing the sample

Samples selected for SEM/EDS analysis are first cleaned using toluene and methanol to remove hydrocarbon residue, and then dried in a vacuum oven. The samples are broken to expose fresh interior surfaces. Samples are then cemented to an aluminium stub with epoxy. Carbon paint is used to cover the base of the sample and the epoxy to improve conduction and reduce charging effects in the SEM. Samples is sputter coated with platinum for 5 minutes.

5.3.2. Statistical Tests

The most basic means of summarizing micro textural data is to plot histogram or bar graph showing the frequency of occurrences of individual micro texture.

One means of analyzing bar graph summaries (frequency distribution) of micro texture observations on sediment grains is to quantify similarities or differences among samples in order to compare them. Specifically one may compare samples from three distinct environments of deposition.

The bar graph has different shapes, suggesting immediately that there is distinct signature for each environment. Quantitative analysis of observation on individual grains from all three environments would be required to show these relationships, which is something that would require principal components analysis or classical cluster analysis

5.4. Observations

The micromorphic textures of quartz grain surfaces show immediate variation among three sub surface Litho Units described in the study area under the scanning electron microscope and they bear the following imprints. Selected SEM photographs of microtextures on quartz of the three litho unit are given in Figures 5.1-5.3. The complete set of data is given in Appendix 3.

In Litho Unit 1

- The morphology and surface features of the quartz grains of this unit essentially show fluvial characteristics (Figure 5.1).

- The grains are smooth and round. The grains tend to attain ellipsoidal shape. Micropercussion cracks formed out of material collision and impact pits are identified.
- No specific stages of maturity can be identified.
- Some of these grains bear the imprints of an early aeolian phase modified under

fluvial environment, identified by the incidences of micro percussion cracks, impact pits and other fluvial features over bulbous projections, which is typical of aeolian surface mould. The imprints of higher regime aeolian grain surface at the back drop of fluvial print over further limits the commentary on the grade of maturity under fluvial activities.

- More heavy minerals are seen in this sediment fraction, with classic fluvial marks.
- Finer grains in this regime, exhibits more fluvial characters.

In Litho Unit 2

- The quartz grains of this unit show mixed characteristics.(Figure 5.2).
- Micro features like etching and chemically altered (weathered) surfaces are observed in grains from this Litho Unit
- Some of the grains from this unit show history of aeolian transport before being altered under the present one.
- Overprinted grains are more abundant indicating a lake environment.

In Litho Unit 3

- The activity of wind predominating over the accommodative space throughout the time of its deposition is identified. The aeolian micromorphic features imprinted on the quartz grains over print erstwhile surface textures (Figure 5.3).
- The grain surfaces range from youth to matured stages
- The grains procured from 2 to 3 m below the ground surface give geographical concentration of textural features. The coarser and fresher grains are seen closer to the backshores (to the west of study area) and matured and reworked grains towards the hinder land (Eastern part of study area).
- Predominantly, the grain surfaces are characterized by bulbous projection, percussion cracks, and roundness of edge, elongate depression and wind abrasion imprints. Other feature like upturned plates, precipitates, polygonal cracks are encountered infrequently.
- Among the micromorphic features seen the incidence of bulbous projections is the most, followed by edge roundness and abrasion imprint

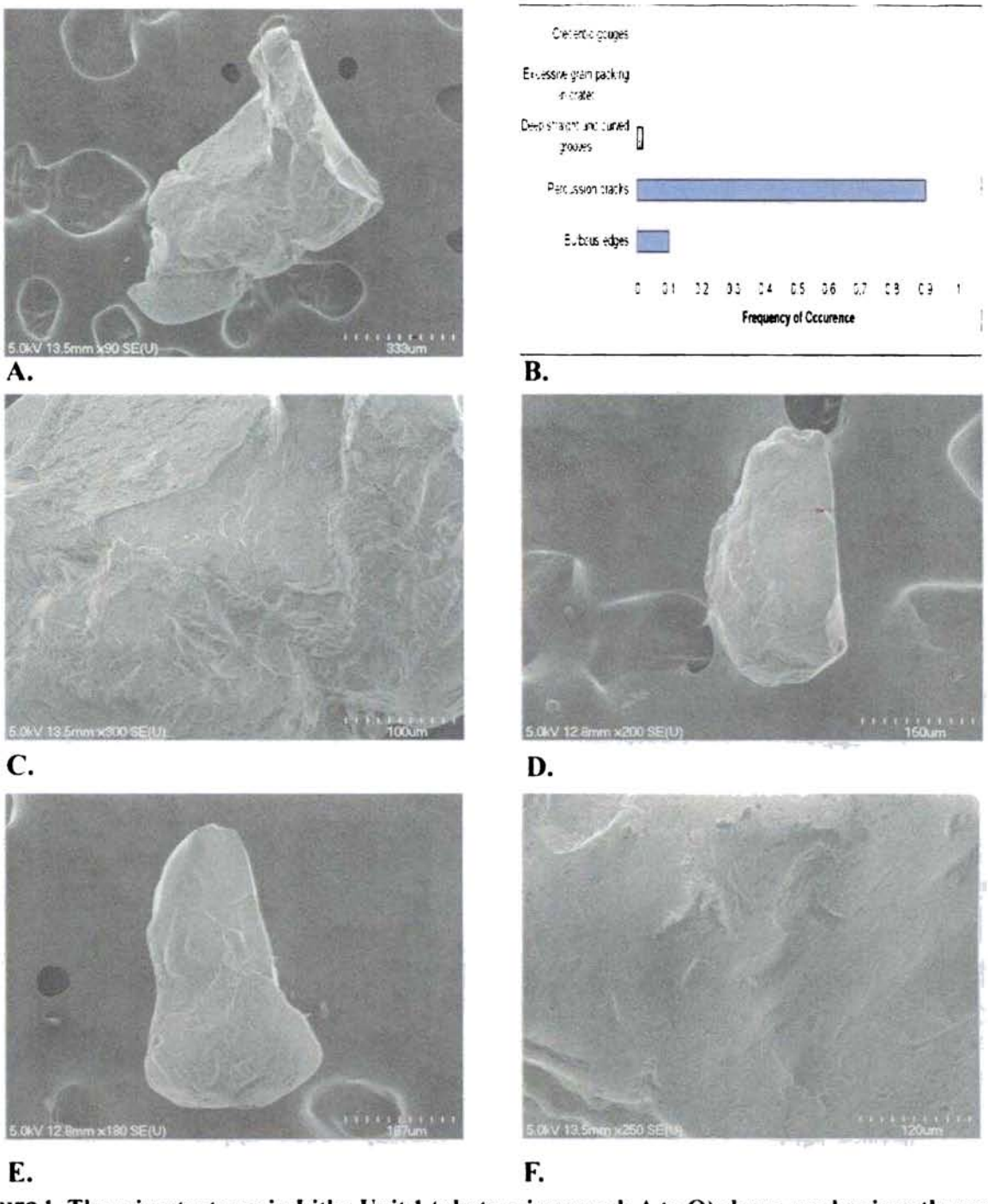

Figure 1. **The microtextures in Litho Unit 1 (photo micrograph A to O) shows predominantly percussion cracks (graph B)an indicative of fluvial environment. The grains show low relief, fracture faces, sub parallel linear fractures, linear steps, mechanically upturned plates, abrasion features, v shaped percussion cracks, edge rounding, over printed grains and ridges and troughs. Angular grain, precipitates on top ledge, bulbous edge on lower left, clear sharp fracture face to right, preceded**

coating in the upper left part of grain and deep trough in gain A and C, Fracture face front, old etched sub-parallel fractures to left, V-shaped deep scars- indicating upper flow regime current in D and E , angular--fracture faces, deep v-shaped scars in F.

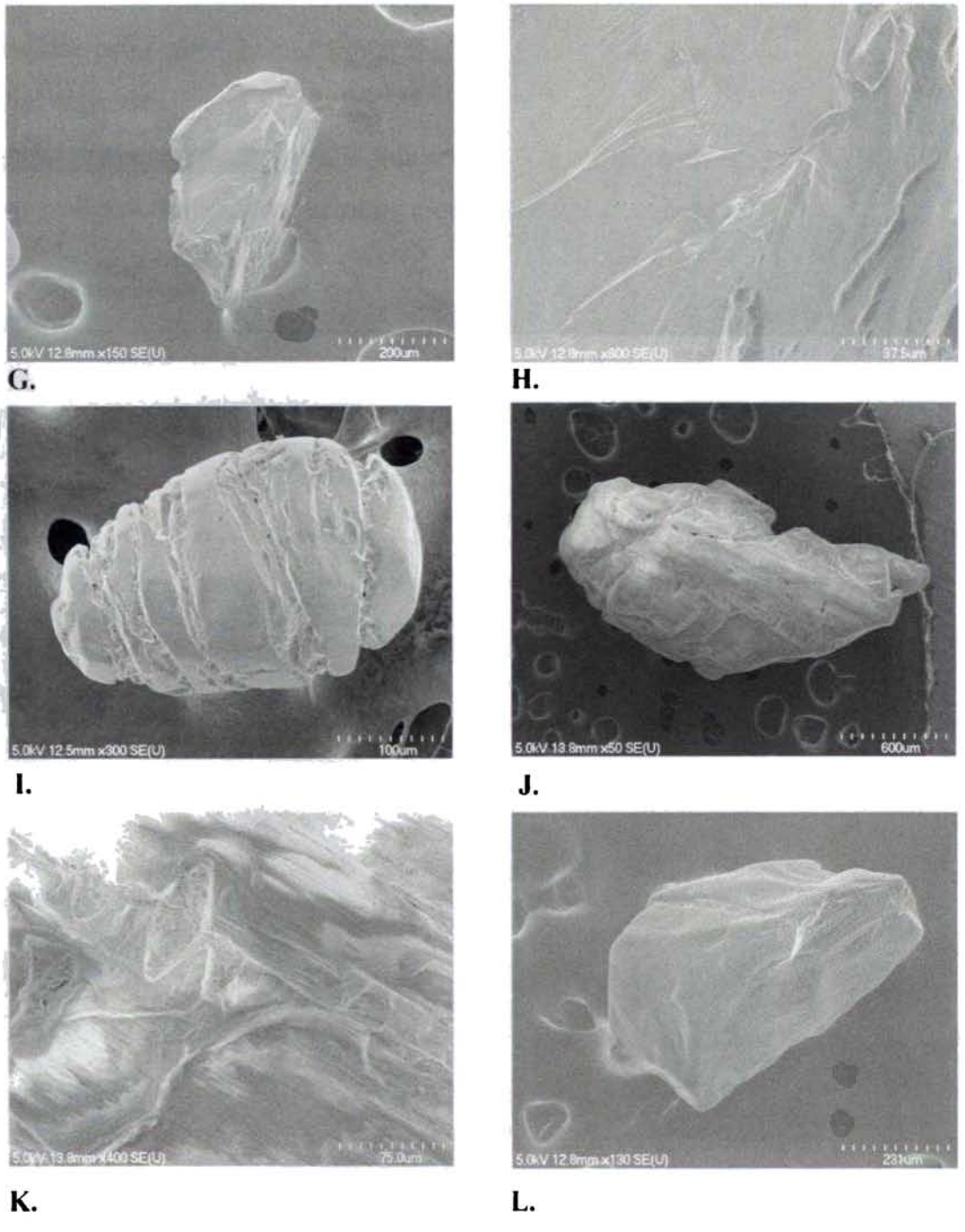

Figure 1 (contd) Angular grain with preserved weathering surface and etched surface in G, ablation ridges, cone shaped surface ruptures in H, Sharp edges, some v-cracks, minor edge rounding in J, laminations, minor etching and some pre-weathering in K, subrounded edges, and V shaped percussion cracks in L.

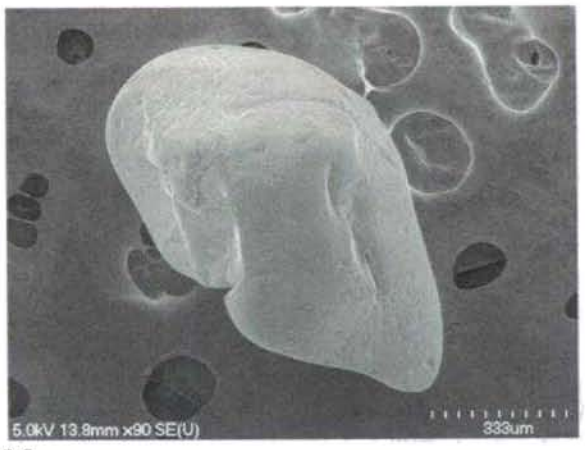

M.

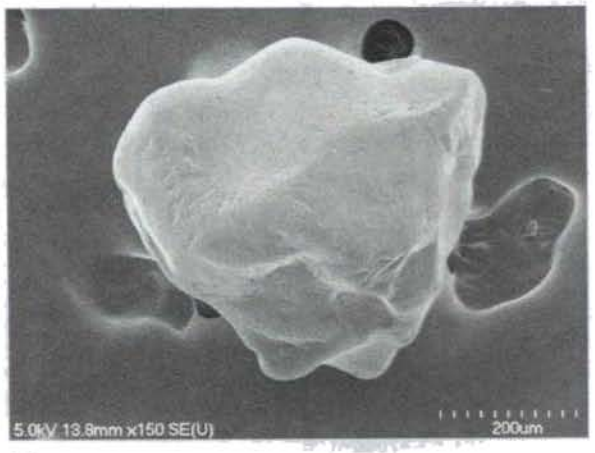

N.

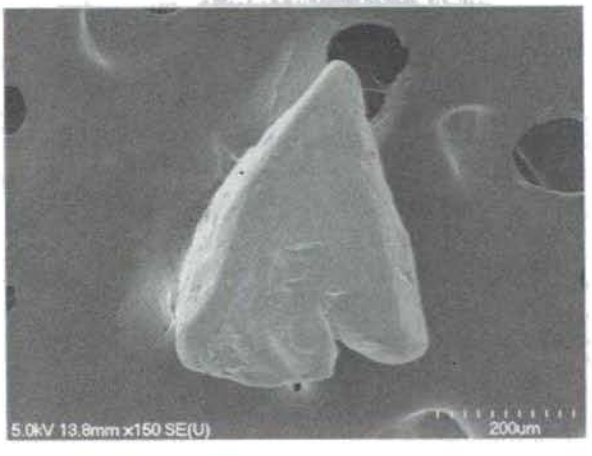

O.

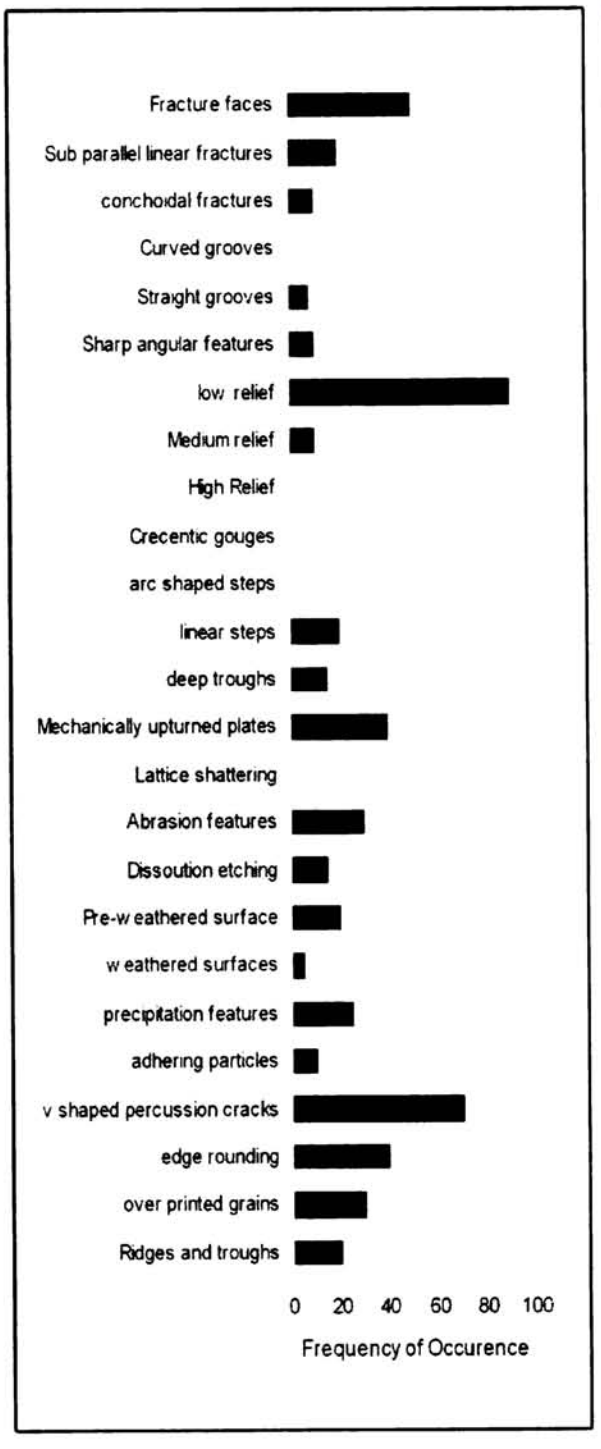

P.

Figure 1 (contd) Subrounded grain, dissolution etches, v shaped percussion cracks with precipitates in M, bulbuos subrounded smooth surfaces in N and angular grain with dissoultion etching with slight weathering in O

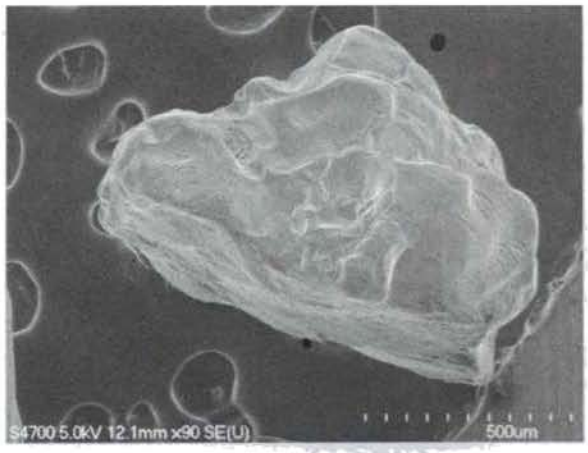

A.

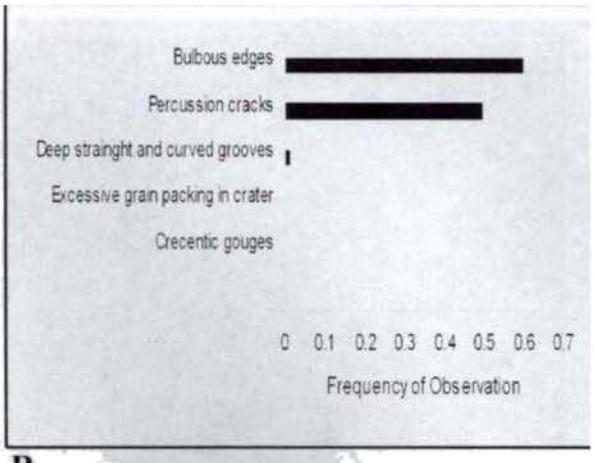

B.

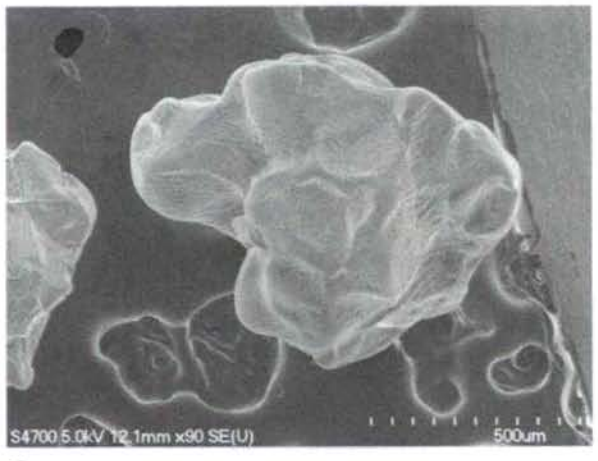

C.

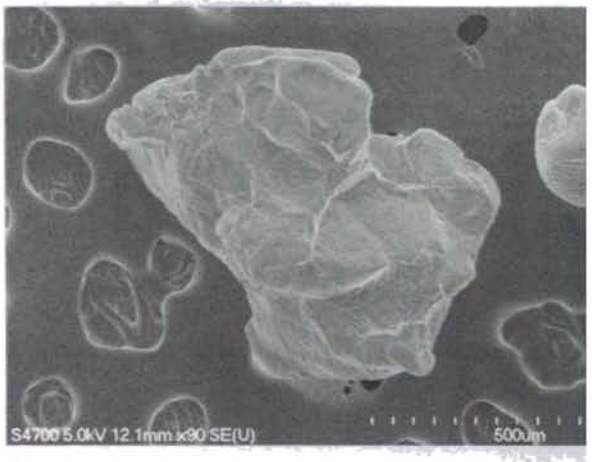

D.

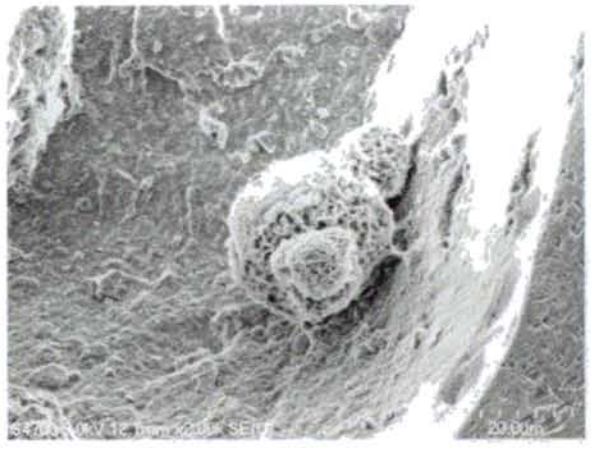

E.

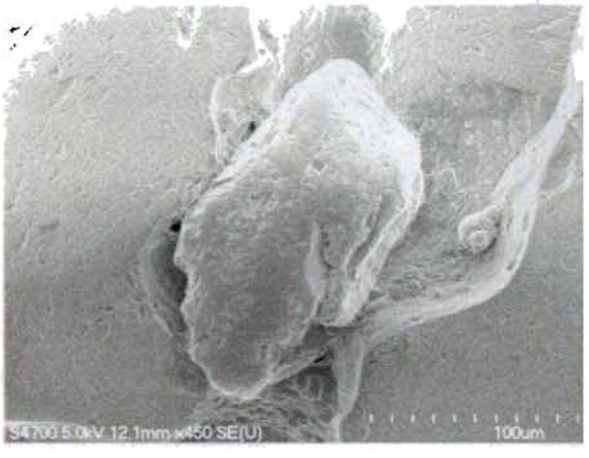

F.

Figure 2. The microtextures in Litho Unit 2 (photo micrograph A to O) shows predominantly bulbous and percussion cracks (graph B) an indicative of a mixed environment of deposition, namely aeolian and fluvial. The grains show low relief, fracture faces, sub parallel linear fractures, linear steps, mechanically upturned plates, abrasion features, v shaped percussion cracks, edge rounding, over printed grains, dissolution features, etching, edge rounding, abrasion features and ridges and troughs.

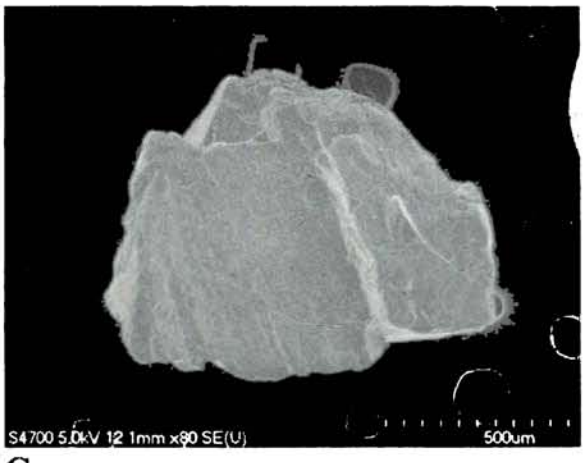

G.

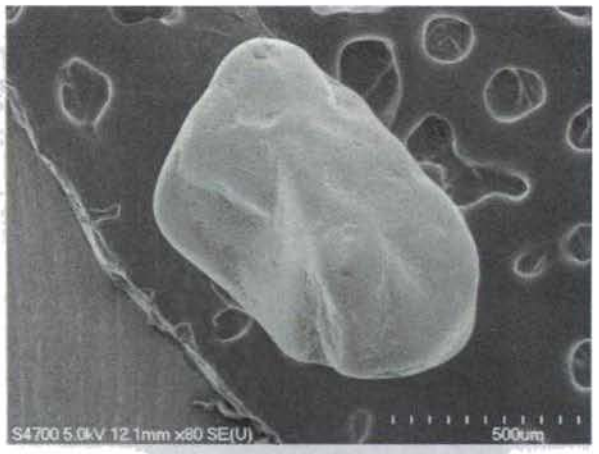

H.

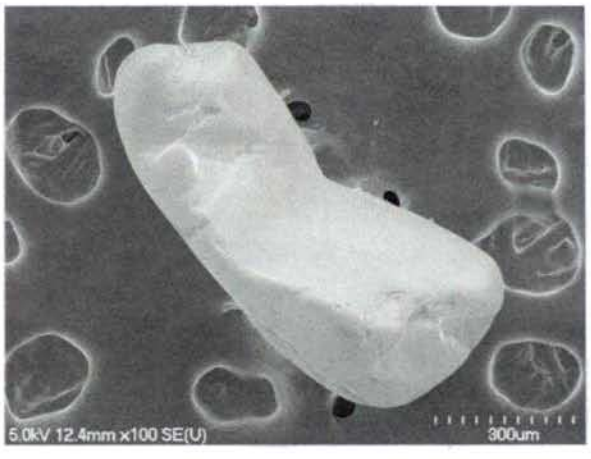

I.

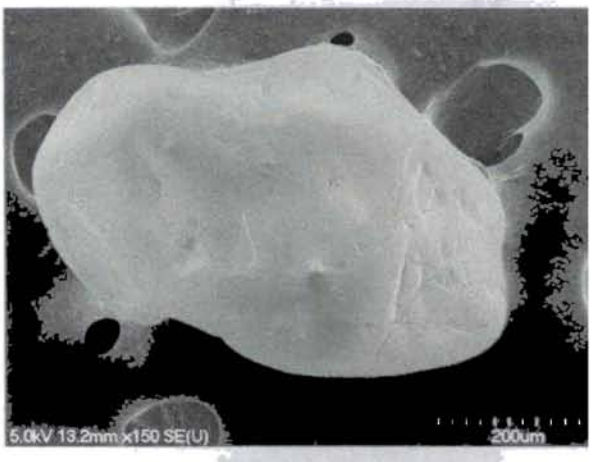

J.

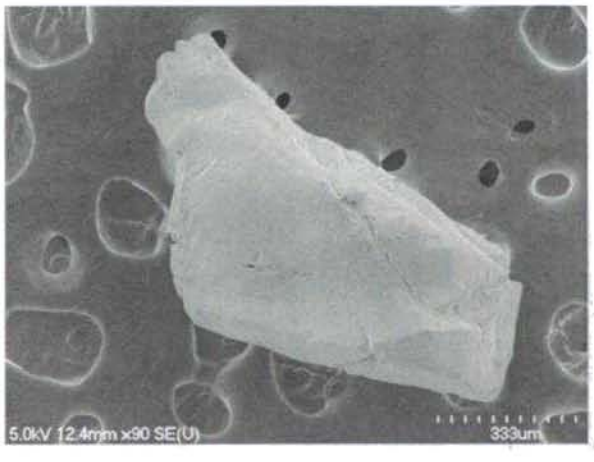

K.

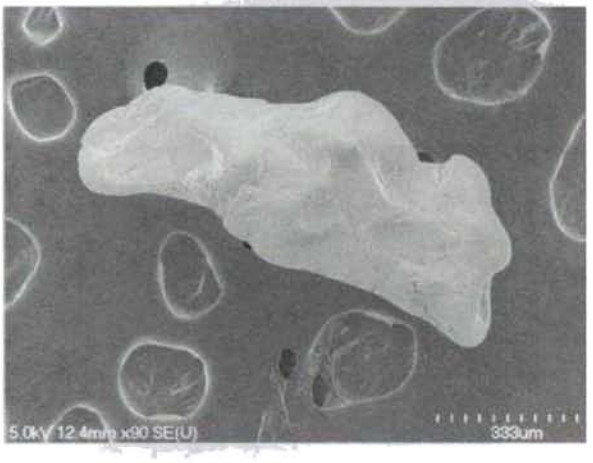

L.

Figure 2 (contd). The grains show low relief, dissolution features, etching, edge rounding ridges and troughs, V- shaped percussion marks and linear fractures (G- L) and precipitate features (K and L).

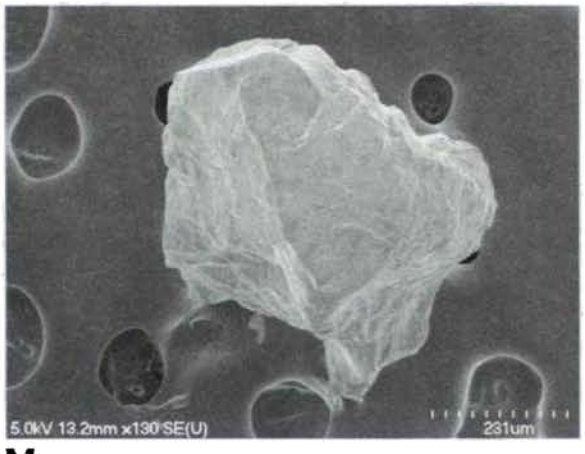

M.

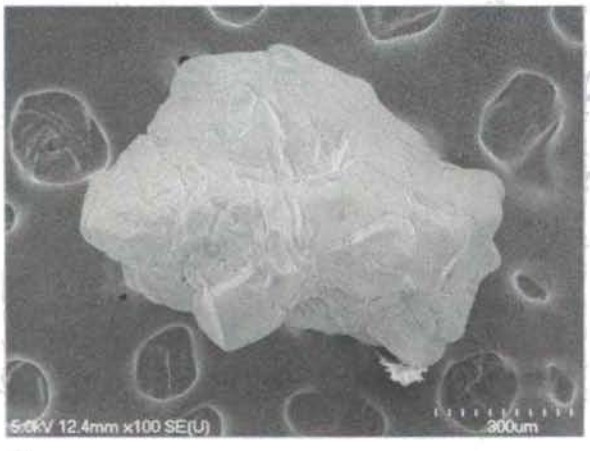

N.

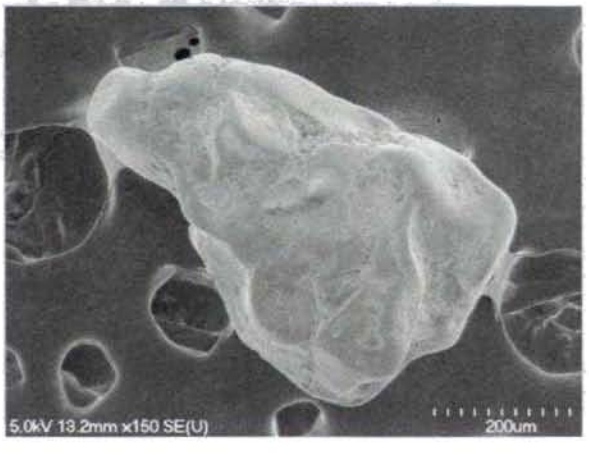

O.

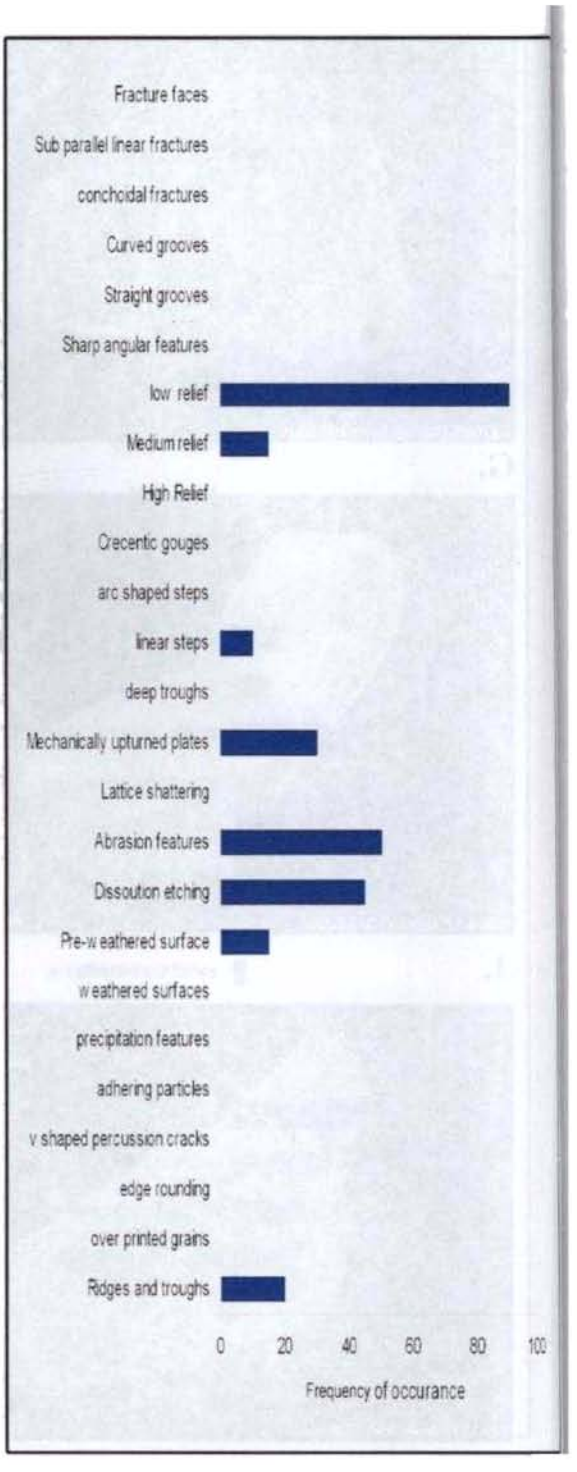

P.

Figure 2 (contd). Angular to sub angular edges (M), linear fractrure and parallael striations (N) and waethered surface with precipitates (O).

A.

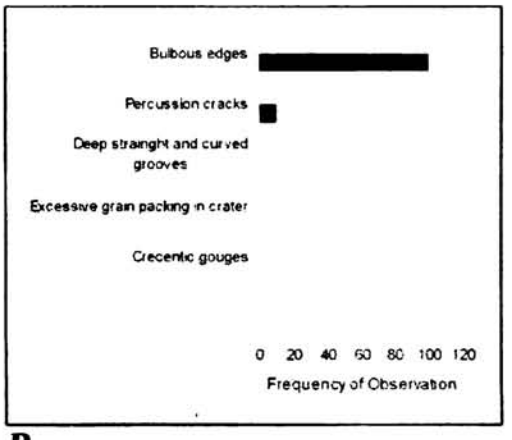

B.

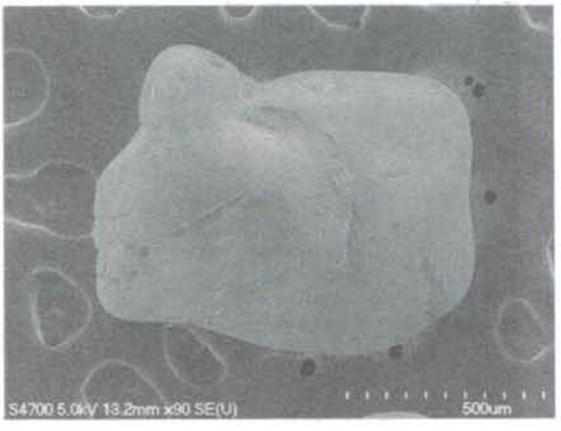

C.

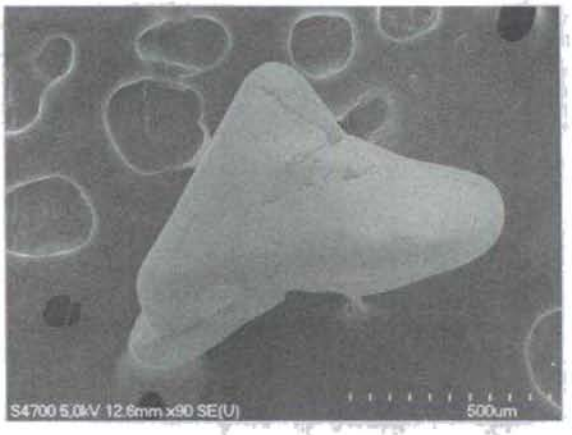

D.

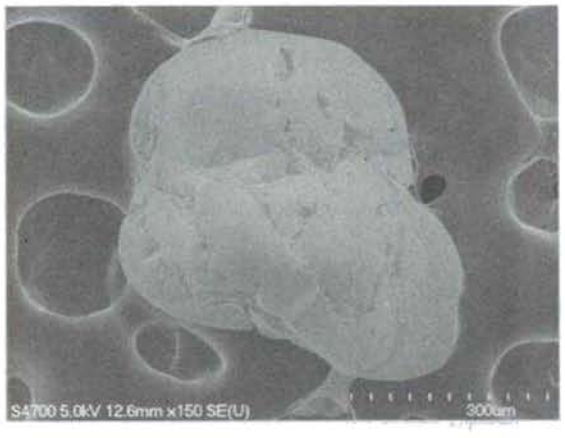

E.

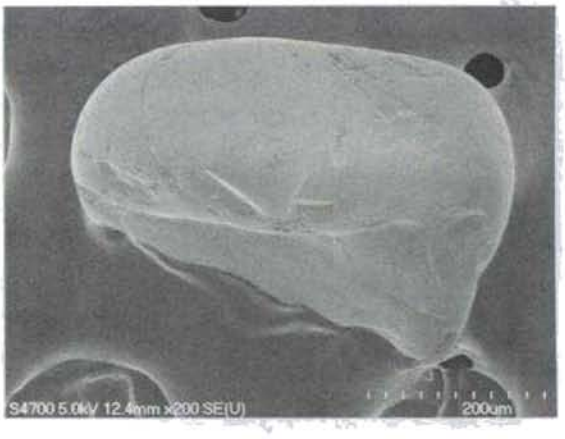

F.

Figure 3. The microtextures in Litho Unit 3 (photo micrograph A to O) shows predominantly bulbous texture(graph B) an indicative of aeolian environment. The grains show low relief, dissolution features, etching, edge rounding ridges and troughs, V- shaped percussion marks and abrasion features (A, C to F) , sub parallel linear features (B), weathered surfaces (A and F) and over printed surfaces (A).

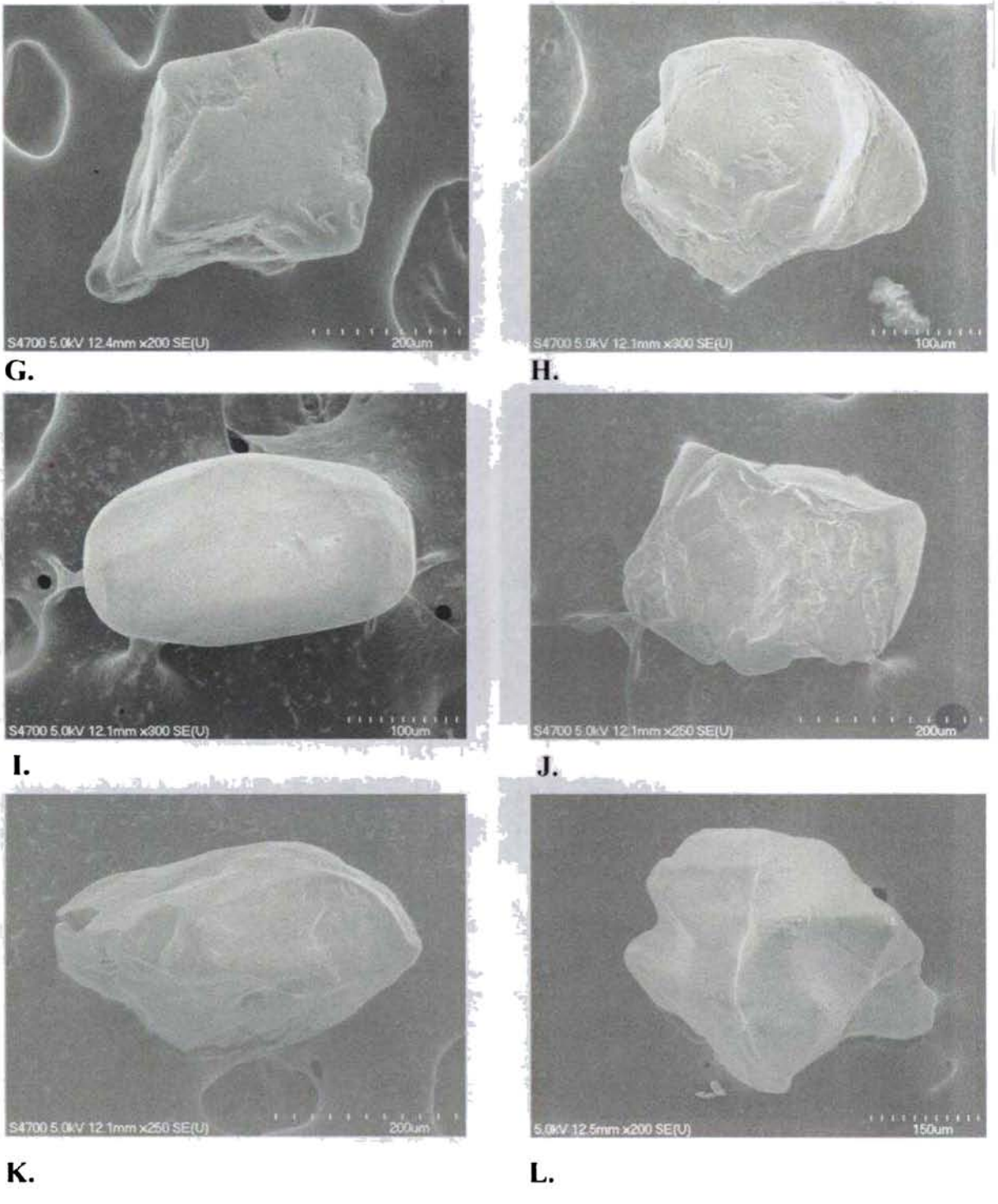

Figure 3 (contd). The grains show low relief, dissolution features, etching, edge rounding ridges and troughs, V- shaped percussion marks and abrasion features (G to L). Fresh surfaces and upturn plates are well seen in J and K. Parallel striations are dominantly observed in K and smooth depressions of aeolian action is explicit in L

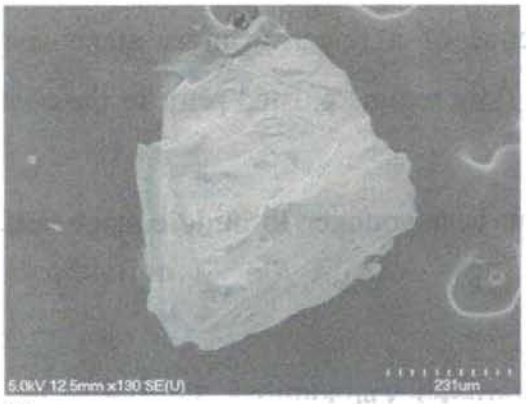

M.

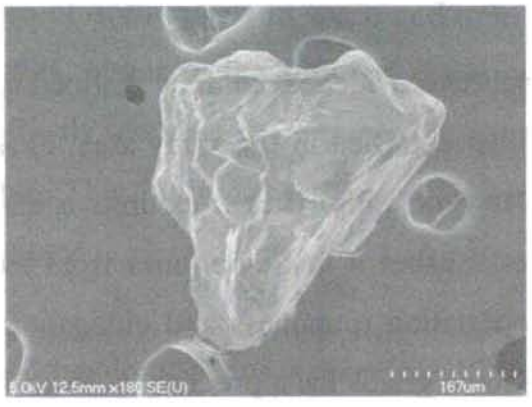

N.

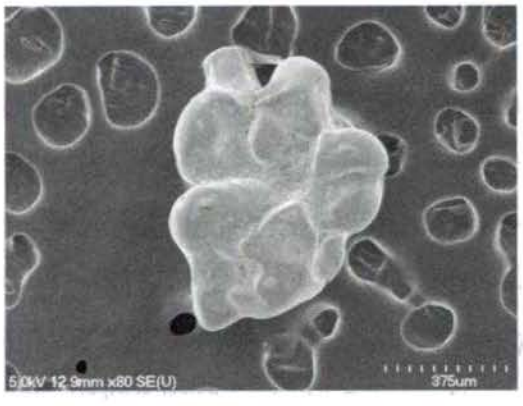

O.

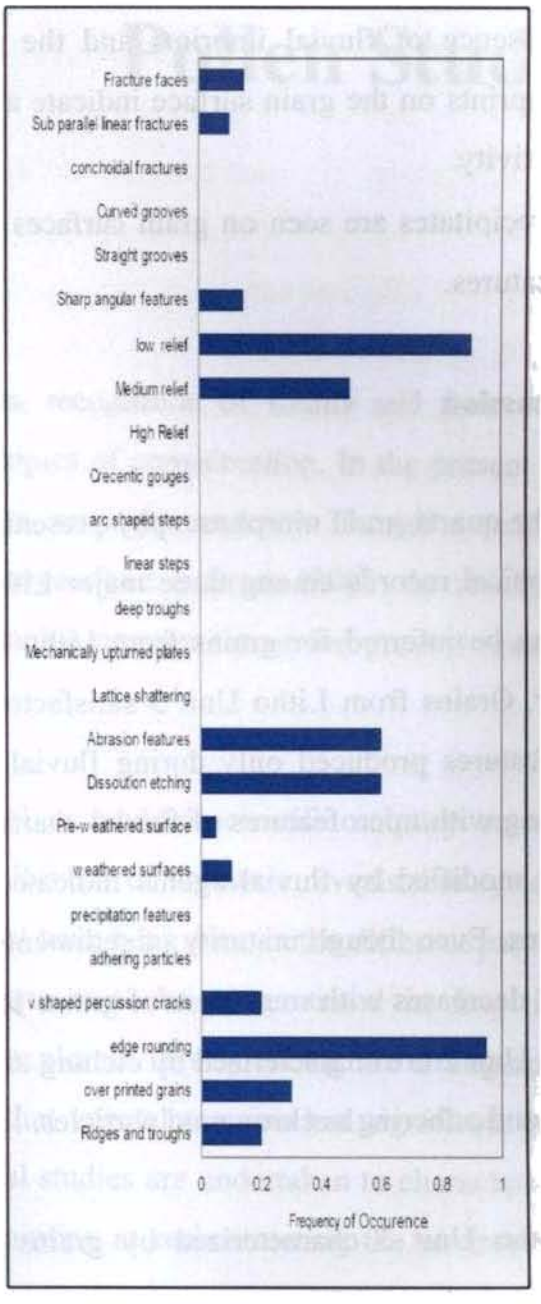

P.

Figure 3 (contd). The grains show low relief, dissolution features, etching, edge rounding ridges and troughs, V- shaped percussion marks and abrasion features (M to O). Note that parallel ridges are prominent in M. The probability of occurrence are plotted against major surface micro textures exhibited by the quartz grain (P), shows that the imprints predominantly are of wind action.

- In mature sediments the incidences of features of abrasion are quite low and the grain is almost round or near roundness.
- Absence of fluvial imprints and the presence of a fewer younger stage coastal imprints on the grain surface indicate a low flow regime existed prior to the aeolian activity.
- Precipitates are seen on grain surfaces which bear younger to middle stage surface features.

5.5. Discussion

The quartz grain morphoscophy presents supportive evidences to draw distinction in stratigraphical records among three major Litho Units identified in the study area. Fluvial origin can be inferred for grains from Litho Unit 1 while Litho Unit 2 exhibits a mixed character. Grains from Litho Unit 3 satisfactorily establishes it to fluvial ones from those impact features produced only during fluvial transportation roundness and elongation of grain along with microfeatures of fluvial character. Some grains have pre history of aeolian transport modified by fluvial agents indicated by micro percussion cracks over bulbous projections. Even though maturity of sediments cannot be identified relief of microfeatures observed decreases with roundness of grains indicating severe fluvial action. Quartz grains for Litho Unit 2 are characterized by etching and weathered surface as well as from the clay particles and adhering neckron mud particles. It conforms to a lacustrine environment.

Litho Unit 3 characterized by grains showing severe wind action. Most of the features via bulbous projection, percussion cracks roundness of edge, elongate depression, and wind abrasion imprints etc. are indicating the particular Litho Unit to be of aeolian. Migration of sand from around the shore towards hinterland along the wind direction is evident from maturity of grains features observed, which varies from younger features along the shore to matured ones as it nears later, as well as from the fining of grains.

The change in the medium clearly deciphered from quartz grain morphoscopy reflects the climatic hitory of the region in general. Further discussion on this aspect is presented in Chapter VIII.

Chapter VI

Pollen Studies

6.1. Introduction

In describing sedimentary environments, recognition of fossils and their relative position of occurrences in space and time are topics of consideration. In the present study, no fossils, either in the form of shells or casts, were encountered. Though a search for microfossils was also done as per the methods prescribed in Green (2001) the results were negative. This limited the scope of biostratigraphic component of the present study into palynology.

Palynology forms a very significant tool in modern scientific enquiry on natural vegetation and environmental reconstructions. Review of literature reveals that systematic palynological surveys to identify the plant habitat have been done in the different part of the world. However, in India, extensive work appears to be concentrated in few limited geographical centres. Vast area yet remains unexplored. In sequencing the stratigraphy of Thiruvananthapuram coastal plain, it is found that vegetal remains had significant part in making of Litho Unit 2. Therefore, palynological studies are undertaken to characterize the habitat nature prevailed during its deposition, aiming at reconstructing the environmental conditions of the time.

Palynology is the science of palynomorphs, which are resistant spores and pollen easily transported by wind and water in a dispersed state (Hyde and Williams, 1944). The spores of bacteria, fungi, algae and protists are rarely preserved but those of terrestrial plants are very common fossils because they produce extremely resistant spores and pollen. Pollens are produced by seed plants, both angiosperms and gymnosperms and are the carriers of male gametes. They are not simply the part of plant but are the haploids (half set of chromosomes) of the diploid (full set of chromosomes) plant body. Pollens have a

cellulose wall around the protoplasm called the intine, outside this is the sporopollenin layer which is inert, very tough and resistant to bacterial attack, this layer is called the exine. The pollen of several gymnosperm genera is saccate; that is, grains bear one, two or rarely three air sacs attached to a central body or corpus. Angiosperm pollen is extremely diverse and covers a multitude of combinations of features. Individual pollen grains may be inaperturate, or provided with one or more pores (monoporate, diporate, triporate, etc.), slit-like apertures or colpi (monosuclate, tricolpate, etc.), or a combination of pores and colpi (tricolporate, syncolporate etc.).

Pollens bear excellent transport characteristics. During their transport, they are completely separated from the parent plant and are perfectly designed to resist hostile environmental stresses. The shape, size, type, position of aperture and pollen wall characteristics - their structure and sculpture are the main adaptation parameters that the pollens imbibe to counter the expected stresses against performing their role in nature. These parameters mark their uniqueness and valuable indices in pollen identification (Willard and Edwards, 2000).

The botanical information from pollens are limited but in fossil studies they have proved exceptionally useful as biostratigraphic indices, providing information on stratigraphy and paleo-environment. They are particularly valuable in freshwater environments, in evaporitic deposits and situations where marine and freshwater facies interdigitate. Palynological data obtained from the subsurface sediments are valuable signpost in identifying ecological complexes and environmental preferences (Erdtman, 1952), especially to evaluate the long-term response of terrestrial ecosystems to paleoenvironmental changes (Willard, 1994).

6.2. Methodology

6.2.1. Light microscopy

Analysis of pollen grains using light microscopy includes preparation of the reference slides and preparation of sample slides. Multiple techniques and methods should be used when investigating pollen grains in order to provide comprehensive and accurate

information and help to avoid misinterpretations. The selection of procedure is based on the composition of the sediments and palynological materials that has to be analysed. In order to get usable image in the microscope the specimen must be properly illuminated.

6.2.1.1. Preparation of sample slides

Clay, silt and sand present in the sample are broken down physically into less than five millimetre fragments. The sample is then placed in a plastic beaker in a fume cupboard and covered in hydrochloric acid to remove carbonates. To concentrate the pollen and spores present in the material and to make them as much visible as possible with their morphological details , samples were treated with 10 % KOH solution, and were heated up to boiling point. After boiling, they were allowed to cool up to room temperature. Beakers with samples were filled with water and sieved using an150 mesh sieve. Sieved samples were transferred to separate labelled jars. Then the jars were kept for half a day for settling of pollens. Samples were washed three times at an interval of six hours.

The washed samples were treated with 40 % HF solution to remove sand particles (silica) and were stirred well with polythene rods, for three times at an interval of three hours. Liquid was decanted and the material was kept in HF solution for three days for the complete removal of silica.

After decanting water from the jars, samples were centrifuged. Water was again decanted from the tubes. To remove further water particles in the samples, equal quantities of concentrated glacial acetic acid (dehydrating agent) was added using a dropper, and mixed well using separate glass rods. Samples were again centrifuged and water was decanted. Acetolysis is an indispensable method for illustrating pollen grains with the Light Microscopy. Untreated or stained pollen grains will hide much of the important information for the description of a pollen grain. Pollens are colorless. In order to make the pollens visible under the microscope, we have to color them by a process called acetolysis. For acetolysis process, concentrated acetic anhydride was mixed with sulphuric acid in the ratio 9:1. Equal amounts of the mixture were then added to each sample and were stirred well with a glass rod. Then water was taken in a beaker and the samples were put in it in such a

way that, the level of the sample in the centrifuge tubes should be below the level of water in the beaker. Beakers were heated for half an hour using a heater. After boiling the water inside the beaker, centrifuge tubes were taken outside and were allowed to cool up to room temperature.

After decanting water from the samples, they were again treated with concentrated glacial acetic acid, mixed well and were centrifuged. Then the samples were again treated with concentrated glacial acetic acid, washed and were decanted. Then to remove the fine debris from the sample, they were sieved through 600 mesh. Samples were then treated with a mixture of glycerin and a few drops of phenol and transferred into separate bottles which were kept for half a day for settling the pollens.Once all acid treatment and separation processes are complete the sample is mounted by strewing onto cover slips and allowing to dry. The inverted cover slip is then glued onto a slide using a proprietary glue of sufficient refractive index and now they are ready to be examined under microscope.

6.3. Results

Pollens identified from the vegetal matrix of Litho Unit 2, having thickness of 2 m in two of the boreholes, namely TRV1 and TRV 6 are listed and described briefly in Figures 6.1.(1-20). About twenty different plant species are identified and are listed in Table 6.1.a-f. Among them 8 pollens are of trees, 1 pollen of shrub, 5 pollens of herbs, 3 pollens of ferns and 3 pollens of fungi. Their geographical affinities are summarized in Table 6.2 and discussed below.

Evergreen flora

Trees

1. Syzygium cumunii

Syzygium cumunii is commonly known as Jamun is a varity of large glabrous evergreen tree. *Syzygium* is seen growing all over in the tropical and subtropical terrains of India mostly as windbreak and as an avenue tree along the highways considering its height parameters.

Semi evergreen – moist deciduous flora

Trees

1. *Terminalia bellerica*

Terminalia bellirica is a deciduous tree common on plains and lower hill found in south east Asia, where it is also grown as avenue tree. *Terminalia bellerica* belongs to the family *"cumbertaceae"* commonly known as Bellerica myrobalan. In India it is found specifically to tropical climate.

2. *Semecarpus anacardium*

Semecarpus anacardium is known as 'marking nut tree' is a flowering plant of the family *Anacardiaceae*. The plant is very specific of tropical climate. *Semecarpous anacardium* is a rainy season bloomer. The tree is adapted to fly pollination but bees and other insects also pollinate.

3. *Salmalia malabaricum*

Salmalia malabaricum is known as 'silk cotton tree' is the largest and most common tree of the Indian sub continent. Alternate scientific name of this tree is *Bombax malabaricum*. It belong to the *Malvaceae* plant family. It grows and flourishes quite easily in low hills (height ranging from 200 to 1200m) and in the plains. The family consist of about 22 tropical genera and 150 species and the largest genera is Bombax. *Salmalia malabaricum* is specific of moist tropics.

Dry and moist deciduous flora

Trees

1. *Emblica officinalis*

Emblica officinalis is 'Indian gooseberry(Amla)'. The tree is small to medium sized, reaching up to 8 to 18 m in height, with a crooked trunk and spreading branches. It grows in plain land with sandy soil drain by water. It is specifically a tropical plant.

Aquatic flora

Herb

1. *Poaceae (*grass family)

The *Poaceae,* a flowering plant, are mostly herbs comprises one of the largest families with about 500 genera and 800 species. Wet lands form the typical habitat of *Poaceae.*

2. *Polygoum*

Polygoum identified as herb, is rarely shrubby at the base. The cosmopolitan genus includes over 150 species. They are widely distributed throughout western Asia. The said variety is found in open usually wet places at low and medium altitude.

Dry climate flora

Herb

1. Chenopodiaceae

The *Chenopodiaceae* type includes nearly all of the species *Chenopodiaceae* and genera *Amranthus.* This pollen grains are very common in wind pollinated area and are well transported and are observed mainly in arid areas and desert. The presence of *Chenopodiaceae* is an indicative of dry climate (Ge-lin, 1995)

2. *Amaranthaceae*

Amaranthaceae is a cosmopolitan subfamily of approximately 80 herbaceous plant species in the *Amaranth family.* Several species are aquatic plant in habit, but most are spreading stoloniferous plant (some time used as the ground cover). Most of these species are herbs or subshurbs very few are trees or climbers. Mostly found in subtropical and tropical regions although many species belong to cool temperate region.

Table 6.1. Pollen grains their species and associated habitat

No	Binomial	Family	Geographical Distribution
		Evergreen flora	
1	*Syzygium cumuni* (L.) Skeels.	*Myrtaceae*	Indo-Malaysian
		Semi Evergreen and Moist deciduous flora	
1	*Terminalia bellirica* (Gaertn) Roxb.	*Combretaceae*	Indo- Malaysian
2	*Semecarpus anacardium* L.f.	*Anacrdiaceae*	Africa, Indo-Malaysia, China, Australia
3	*Bombax malabaricum* DC. *(Salmalia malabarica) (Elavu, kapok tree)*	*Bombacaceae*	Tropical Asia and New Guinea
		Dry and Moist deciduous flora	
1	*Phyllanthus emblica* L (*Emblica officinalis* Gaertn.)	*Euphorbiaceae*	Pan tropical
		Arid flora	
1	*Chenopodiaceae*	*Chenopodiaceae*- family with fleshy perianth parts	Not reported from southern India
2	*Amaranthaceae*	*Amaranthaceae* - similar to *Cenopodiaceae* but with dry chaffy perianth	
		Aquatic flora	
1	*Poaceae*	Grass	Cosmopolitan advanced group
2	*Polygoum*	*Polygonaceae*	Tropics and temperate
		High altitude/ temperate flora	
1	*Alnus*	*Betulaceae*	Himalayas and China (*Alnus nepalensis* noted in S India)
2	*Betula*	*Betualcaeae*	Temperate parts of Europe America Asia.
3	*Pinux roxburghii*	*Pinaceae*	Native to himalaya
4	Artemisia – 2spp in kerala *Artemisia japonica* Thunb. *Artemisia nilagirica* (Clarke) Pamp	*Asteraceae*	India, Pakistan Nepal,Myanmer, Afghanistan, Japan, India , South china
		Species whose habitat is not determined	
1	Fern *Trilete*	*Trilete* spores traceable from late Ordovician , results from meiotic division of a spore mother cell to form a tetrad	
2	Fern *Monolete*	Herbs with broad but highly dissected leaves and no flowers.	
3	Fungus spores	Unicellular or multicellular, reproductive or distributional cells developing into a number of different phases of the complex life cycles of the fungi. They live on dead stems of herbaceous plants, and twigs and branches of many different kinds of trees.	
4	*Tetraploa*	*Tetraploa* species comprise a very small proportion of the fungal biota, it lives at leaf bases and stems just above the soil on many kinds of plants and trees. A fungal species known to cause keratitis in man.	
5	*Microthyriaceae*	Fungi seen in higher and wetter altitude (Ryan, 1924)	
6	*Tubliflorae*	Tropical shrub seen specifically in lacustrine environment.	

High Altitude/ Temperate Flora

Tree

1. *Alnus*

Alder is the common name of a genus of flowering plants (*Alnus*) the brich family *Betulaceae* .The genus comprises about 30 species of monoecious tree and shrubs are distributed throughout the temperate zone and are mainly wind pollinated but also visited by the bees to a small extend.

2. *Betula* (Indian paper Birch)

The temperate pollen belong to the family *Betulaceae,* genus *Betula.*It habitats forest at the upper height limit of tree growth, rarely found below 3000m. The plant prefers light (sandy), medium (loamy) and heavy (clay) soil and requires well drained soil and can grow in heavy clay soil. It can grow in semi shade (light wood) or even without shade

Table 6. 2. The distribution of pollens with respect to their present geographical habitat

	Evergreen	Semi evergreen and moist deciduous	Dry and moist deciduous	Aquatic	Dry climate	Tropical high altitude/ temperate	Pollens whose geographical limits not determined
Tree	1	3	1	*	*	3	*
Shrub	*	*	*	*	*	*	1
Herb	*	*	*	2	2	1	*
Fern	*	*	*	*	*	*	2
Fungi	*	*	*	*	*	*	3

3. *Pinus roxburghii* (Chir pine or Himalayan long needle pine)

Pinus roxburghii sargut Himalayan long needle pine is a valuable timber resin tree of the central-western Himalayan region. It is also a wind pollinated species. Pollen grains could migrate up to 2500 to 2000 m. The species generally form large trees reaching 30-50 m.

Name: *Syzygium cumunii*
Size: 55 µm (large size)
Shape: Triangular (polr view)
Aperture: Angulaperturate

Name: *Termilia bellerica*
Size: 45µm (medium size)
Shape: Polygonal
Aperture: Stephano aperturate(aperture situated at the equator)

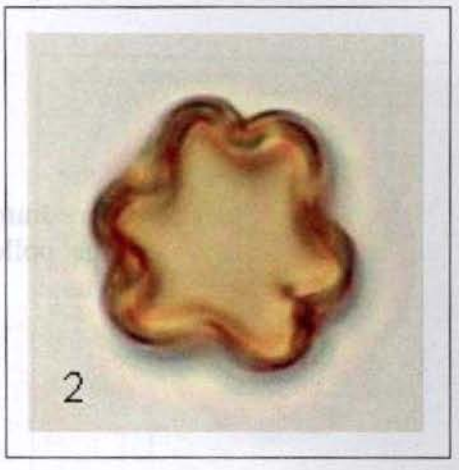

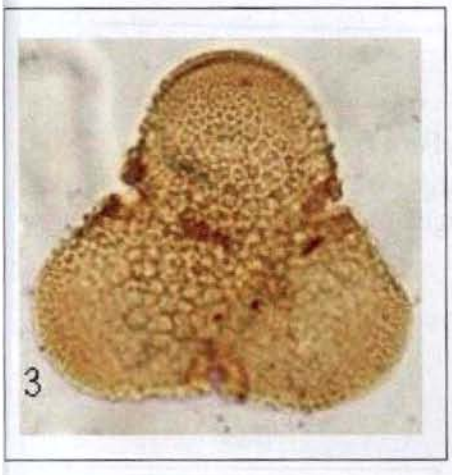

Name: *Salmalia malabaricum*
Size: 65µm (large size)
Shape: Outline triangular
Aperture: Planaperture (pollen grain with an angular outline where the apertures are situated in the middle of the side)

Name: *Semecarpus anacardium*
Size: 60µm (large size)
Shape: Prolate (pllen grain with polar axis larger than the equtorial axis)
Aperture: Stephanocolporate

Figure 6.1. Pollen micrographs(1 to 4)

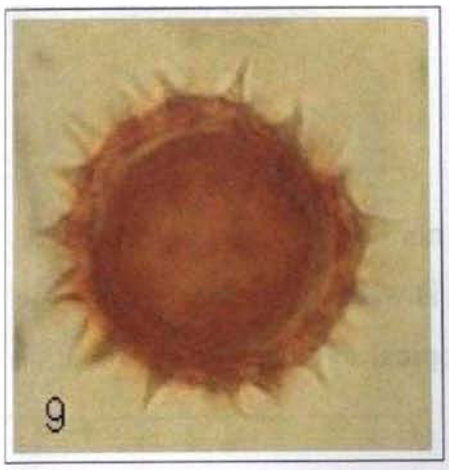

Name:*Tubliflorae*
Size: 50µm (medium size)
Shape: Spheroidal
Aperture: Pantoaperturate

Name: *Artemisia sp.*
Size: 50µm (medium size)
Shape: Saccus (exinous forming an air sac)
Aperture: pollen grain with three colpi

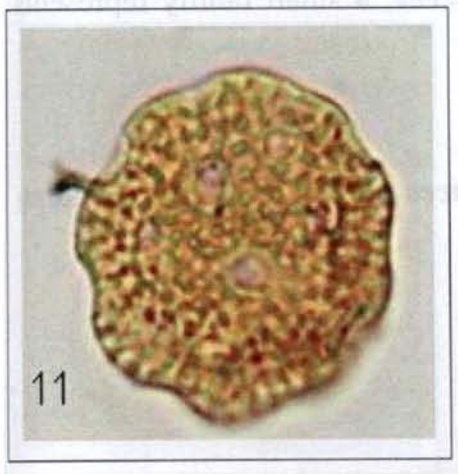

Name: *Amaranthaceae*
Size: 60µm (large size)
Shape: Outline circular
Aperture: Stephanoaperturate

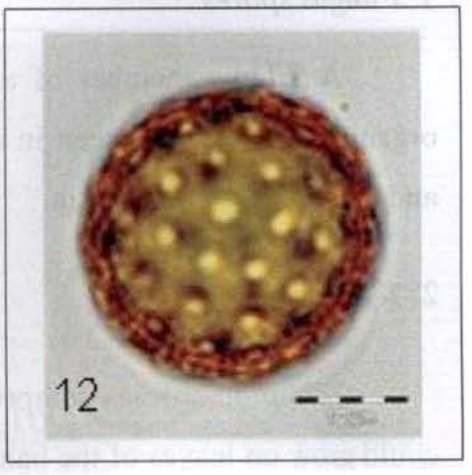

Name: *Chenopodiaceae*
Size: 50µm (medium size)
Shape: Sheroidal
Aperture: Pantoaperturate (pollen grain with apertures distribution more or less regularly over the whole surface)

Figure 6.1. Pollen micrographs (9 to 12)

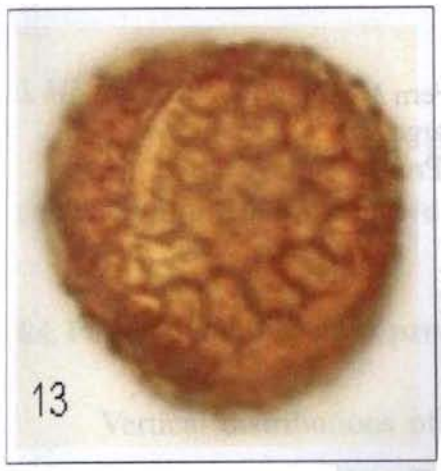

Name: *Polygonum serrulatum*
Size: 60µm (large size)

Name: *Poaceae*
Size: 50µm (medium size)
Shape: Outline, pollen infoldings, irregular
Aperture:Ulcus

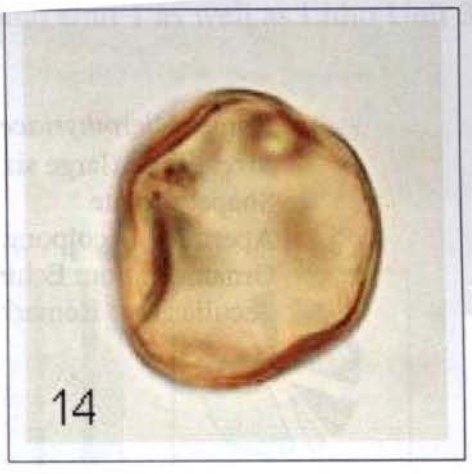

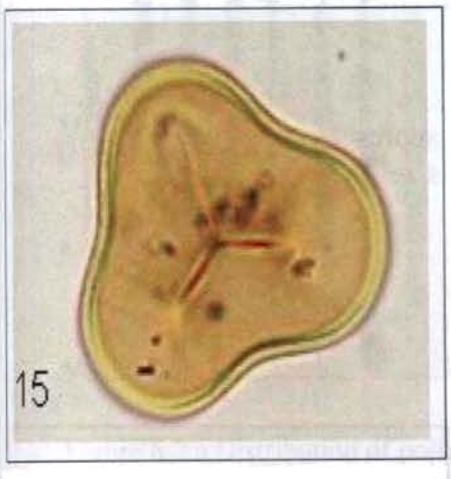

Name: *Trilete* (Fern spore)
Size: 55µm (large size)
Shape: Outline triangular

Name: ***Trilete***
Size: 55µm (large size)
Shape: Outline triangular

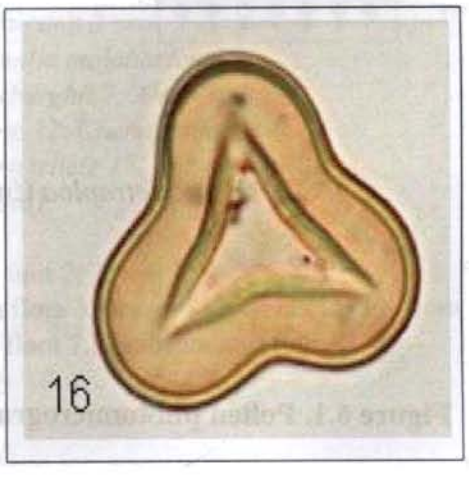

Figure 6.1. Pollen micrographs (13 to 16)

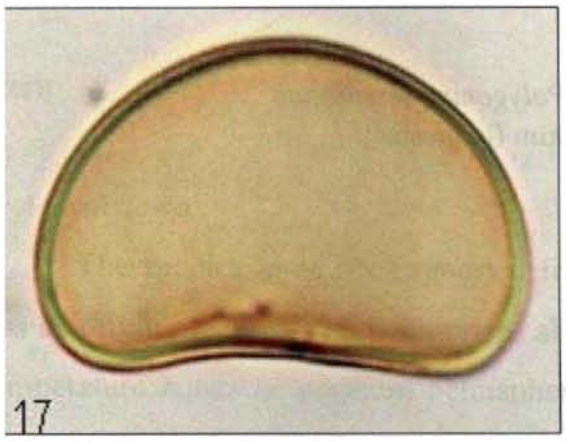

Name:Fern *Monolete*
Size: Large size
Shape: Prolate

Name: *Microthyriaceae* (fungi)
Size: 60µm (large size)
Shape: Prolate
Aperture: Tricolporate
Ornamentation: Echinate
Peculiarities: Remarkable endoaperture

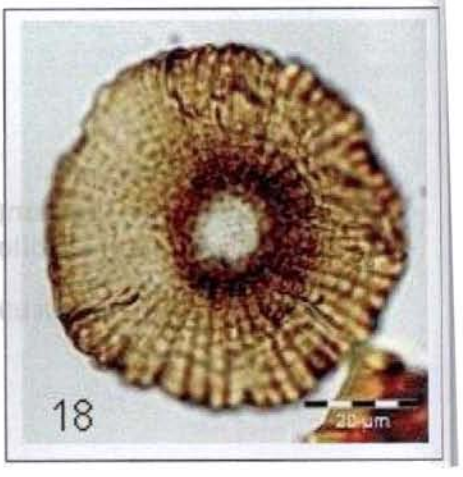

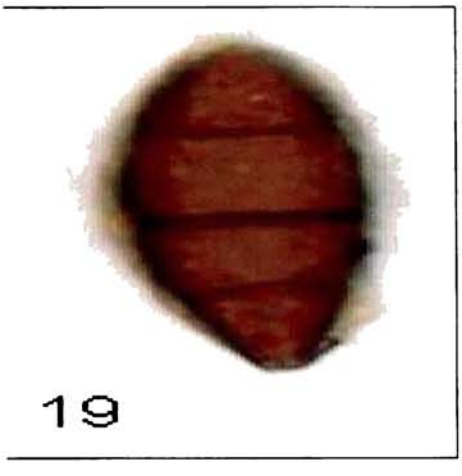

Name: Fungal spores
Size: Medium size

Name: *Tetraploa* (fungal)

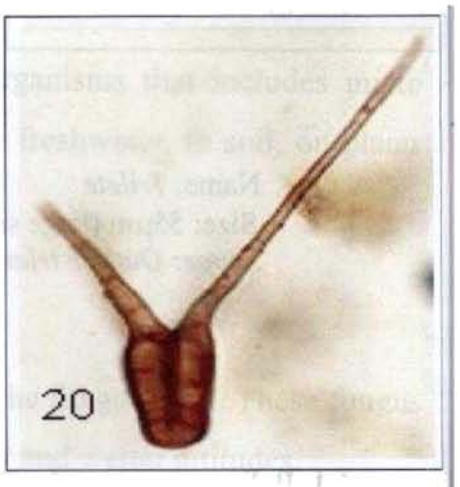

Figure 6.1. Pollen photomicrographs (16 to 20)

Herb

1. *Artemisia sp.*

The species have been reported from some areas in north-western India. The genus has its origin in Eurasia and comprises about 280 species. It is wildly distributed in the cold temperature zones of northern hemisphere scarce in the tropical and subtropical or in the southern hemisphere.

Flora with unidentified geographical spread

Shrub

1. *Tubliflorae*

Tubliflorae a common tropical shrub mainly seen in lacustrine environment.

Fern

1. *Trilete*

Trilete fern spore from the botanical family *Shizaeaceae*, a small family represents tropical environments.

2. *Monolete*

Monolete fern from the botanical family *Polypdiacea* grows in large spreading colonies on borders between sunlight and shade.

Fungi

1. *Fungus spores*

A fungus member of a large group of eukaryotic organisms that includes micro organisms. Fungii are seen in any habitat from sea water to freshwater, in soil, on plants and animals, on human skin.

2. *Tetraploa*

Tetraploa species comprise a very small proportion of the fungal biota. These fungus could grow on leaves of the bamboos or other grasses at higher and wetter altitudes.

3. *Microthyriaceae*

The *Mycrothyriaceae,* an interesting part of the fungal flora, whose distribution is practically limited to the native plants and to the higher and wetter altitudes.

6.4. Pollen distribution in profile of TRV1 and TRV 6

Vertical distributions of the pollen grains recovered from boreholes, namely TRV1 and TRV 6 are pictured in Figure 6.2. The pollen population is seen concentrated for a column of 1 to 1.5 m in the 2 m thick Litho Unit 2. The Litho Unit 1 as well as Litho Unit 3 are devoid of pollens.

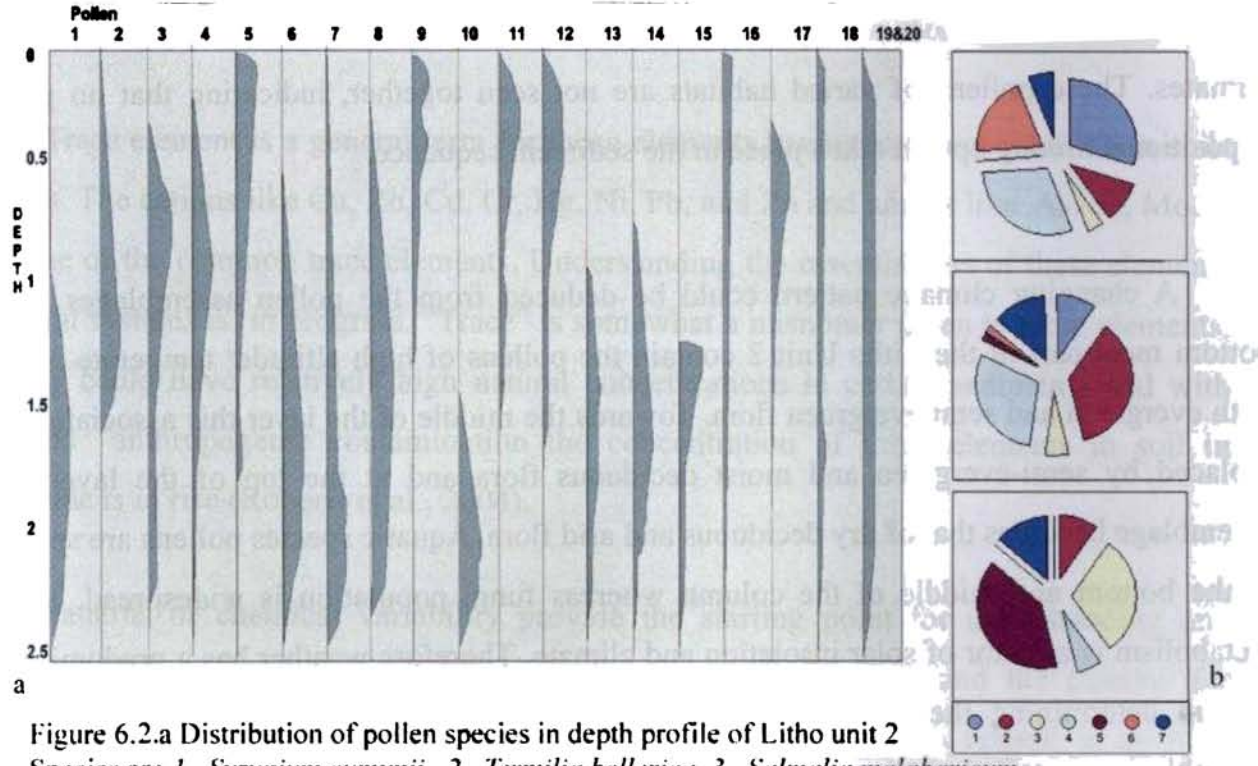

Figure 6.2.a Distribution of pollen species in depth profile of Litho unit 2
Species are *1. Syzygium cumunii 2. Termilia bellerica 3. Salmalia malabaricum 4. Semecarpus anacardium 5. Emblica officinalis 6. Pinus roxburghii 7. Alnus sp 8. Betula utalis 9. Tubliflorae 10. Artemisia sp 11. Amaranthaceae 12. Chenopodiaceae 13. Polygonum serrulatum 14. Poaceae 15. :Fern trilete 16. Fern trilete 17. Fern monolete 18. Microthyriaceae (fungi) 19. fungal spore 20. Tetraploa (fungus)*

b . Percentage wise distribution of flora in depth profile of Litho unit 2:
Legnd: 1.Evergreen flora 2.Semi-evergreen and moist deciduous flora 3.Dry and moist deciduous flora 4.Aquatic flora 5.Arid flora 6.Tropical high altitude / temparate flora 7.Non classified flora

Pollens of six different environments, with four overlaps, are identified. Majority of pollens, in Litho Unit 2 falls under deciduous (mainly, moist tropical) flora. In depth profile, pollens which are identified as high altitude / temperate are seen more towards the bottom of the 2m column. This is followed towards the middle of the layer by pollens of evergreen, semi-evergreen and moist deciduous flora, which further is overlain by pollens of dry deciduous and arid flora. Aqueous species are seen common to bottom and middle part of the Litho Unit 2.

6. 5. Discussion

Palynology of Litho Unit 2 (having a ^{14} C age of 7.5 to 9.5 Ka B.P. *refer Table 3.1*) brings out interesting aspects of pollen associations recovered from the Early Holocene sediments from central part of the Thiruvananthapuram coastal plain though largely have pollens of deciduous flora of tropics, but also bear pollens of evergreen, temperate and arid climates. These pollens of varied habitats are not seen together, indicating that no post-depositional mixing up had taken place in the sediment sequence.

A changing climatic pattern could be deduced from the pollen assemblages. The bottom most part of the Litho Unit 2 contain the pollens of high altitude/ temperate along with evergreen and semi evergreen flora. Towards the middle of the layer this association is replaced by semi-evergreen and moist deciduous flora and at the top of the layer the assemblage becomes that of dry deciduous and arid flora. Aquatic species pollens are spread in the bottom and middle of the column whereas fungi population is widespread. Plant metabolism is a factor of solar insolation and climate. Therefore weather has a predominant role in determining the plant growth. In the present study consistent variation in the assemblages of pollens indicates changing climate, from a cool wetter to hot arid. It could be a reflection of an overall drying up of land, which has been traced across the globe during early to mid Holocene (eg. Mayewski et al. 2004; Williams et al., 2009).

Chapter VII

Geochemistry

7.1. Introduction

Geochemistry is the functional characterization, evaluation of species distribution and concentration of chemical elements in the rock, soil and water. The study further includes understanding of chemical processes and reactions that govern the composition and chemical flux between various states (Kabata-Pendias and Pendias, 2001; Neuendorf et al., 2005). Much emphasis on geochemistry is related to chemistry of trace elements - its movements and distribution.

Trace element is a general term for those elements having low concentration in soils or rocks. The cations like Cu, Zn, Cd, Cr, Hg, Ni, Pb, and Zn and anions like As, Se, Mo, B are some of the common trace elements. Understanding the essentialness of these elements in natural systems is in progress. "Trace" is somewhat a misnomer given to these elements, but they could have relatively high natural concentrations in certain sediments and with increased anthropogenic contamination the concentration of these elements in soil in worldwide is in rise (Roberts et al., 2004).

Patterns of chemical variability provide the starting point for understanding and measuring differences between natural concentrations of elements and the reasons for anomaly effects. It provides an overview of background information related to sources, brings out logical structure for the reason behind anomalies, shed light into the geographical and geological conditions that aid sediment dynamics and elemental kinematics.

Background or native concentration of an element in sediment is related to the mineralogy of the parent material from which the sediment has developed and modified by pedogenic processes. Elements in native forms occur in primary sediments as components of the mineral structure. For example Cu, Co, Pb, Ni, and Zn are all present in a variety of

silicate and alumino silicate minerals such as olivine, pyroxenes, amphiboles, micas, and feldspars. The wide variety of parent materials creates a range in trace element content in sediments of 2 to 3 orders of magnitude for many elements. Also, there are specific parent materials that have extremely high concentrations of selected elements. For example, certain sedimentary deposits in west/ east coast of India (organic rich coastal sediments and marls) are high in Co, Ni, and Cr due to formation (i.e. regolith derived) from extensive belts of metamorphic rocks composed of serpentine minerals. Similarly, the presence of sulfidic materials (Chen et al. 2002; Gough et al. 1996) and geologic deposits rich in pyritic sulfur minerals contain enrichment of both As and Se (Strawn et al. 2002).

7.2. Literature Review:

Changes in weathering environments affect the pattern of trace element distribution (Kabata-Pendias, 2001). Nieboer and Richardson (1980) proposed the classification of ions based on their 'chemical nature and possible compounds in which they can exist under different environment conditions. The chemical nature means its electro negativity parameters and its ionic size. The Table 7.1 (after, Kabata-Pendias, 2001) tallies the affinity of trace elements to major elements in various geochemical environments. The elements with an ionic potential below 3 predominate as free ions, while the elements with an ionic potential between 3 and 12 tend to form hydrolysates or complex ions. Generally it is observed that the easily mobile elements usually produce smaller hydrate ions in aqueous solutions than the less mobile elements, which form larger hydrates. Like wise, the free energy needed for the formation of hydrates by the easily mobile ions seems to be less than the energy required for ion formation of less mobile elements. According to Trudgil (1988) the amounts of cations solubilized by biological activity and by chelate action are usually much greater than those mobilized by the action of water and hydrolysis alone. In other words, bacteria, fungi and plants are important in solubilizing minerals and adding chemical ion input into the sediments.

The concentration or depletion of elements in sediment columns are explained by thermodynamic equations describing the equilibrium conditions that could keep the composition of sediment phases constant. Bolt and Bruggenwert (1976) have presented

comprehensive mathematical models that describe chemical equilibria of different sediments. Figure 7.1 depicts the dynamic equilibrium between sediment components, which is governed by various interactions between the sediment, solution, biota and gases.

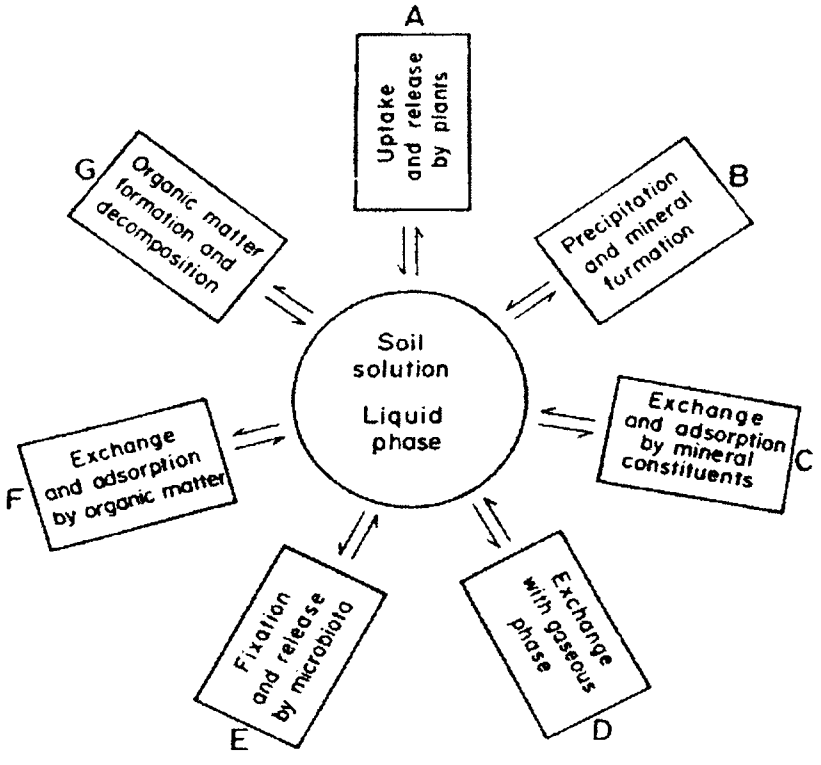

Figure 7. 1 Interactions between soil components and compartments. (after Kabata-Pendias, 2001)

The kinetics of reactions in the sediment system its principles, mechanisms, and models were described and proposed in recent years Spasito and Matigod (1980) and Sparks (1986). Sparks (1986) stated that thermodynamic data is more useful in predicting the final state of equilibrium of a geochemical system related to sediments from its initial non-equilibrium. The level of elemental mobilization in any environment is physically identified by the concentration factor of the element in the system. Thus, the concentration of elements (major/ minor/ trace) in sediment can give valuable insights into the kinetics of metals in specific environment for the sediment under consideration.

Many textbooks in geochemistry present stability diagrams for ionic species of elements as functions of pH and Eh (Garrels and Christ, 1965; Lindsay, 1979; Davies 1980). It is known that in natural soil conditions, pH ranges most often between 5 and 7, and Eh ranges between 400 mV and - 200 mV, except where there are high reduction states in

waterlogged soils (Table 7.1). Kabata-Pendias (2001) states that most mobile fractions of ions occur at a lower range of pH and at a lower redox potential, as illustrated in Figure 7.2. It leads to the anticipation that with increasing pH of the soil substrate, the solubility of most trace cations will decrease. In other words, the concentration of trace elements is lower in soil solutions of alkaline and neutral soils than in those of light acid soils.

Table 7.1 Geochemical association and some properties of trace and major elements (after Kabata-Pendias, 2001)

Major Elements (bold face) and Associated Trace Element.	*pH of Hydrous oxide Precipitation*	*Ionic Radii (A)*	*Electronegativity (kcal/g atom)*	*Ionic potential (charge/radius)*	*Diameter of Hydrated Ion Aqueous Solution (A)*
K^{+}	----------	1.7-1.6	0.6	0.6	3.0
Na^{+}	----------	1.2-1.1	0.9	0.9	4.5
Cs^{+}	----------	2.0-1.9	0.7	0.5	2.5
Rb^{+}	----------	1.8-1.7	0.8	0.6	2.5
Ca^{2+}	----------	1.2-1.1	1.0	1.8	6.0
Mg^{2+}	10.5	0.8	1.2	2.5	8.0
Sr^{2+}	----------	1.4-1.3	1.0	1.5	5.0
Ba^{2+}	----------	1.7-1.5	0.9	1.3	5.0
Pb^{2+}	7.2-8.7	1.5-1.4	1.8	1.9	4.5
Se^{3+}	----------	0.8	1.3	3.7	9.0
Fe^{2+}	5.1-5.5	0.9-0.7*	1.8	2.6	6.0
Cu^{2+}	5.4-6.9	0.8	2	2.5	6.0
Ge^{4-}	----------	0.5	1.8	8.3	----------
Mo^{4+}	----------	0.7	----------	5.5	----------
Mn^{2+}	7.9-9.4	1-0.8	1.5	2.0	6.0
Zn^{2+}	5.2-8.3	0.9-0.7	1.8	2.6	6.0
Fe^{3+}	2.2-3.2	0.7-0.6*	1.9	4.4	9.0
Co^{2+}	7.2-8.7	0.8-0.7	1.7	2.6	6.0
Cd^{2+}	8.0-9.5	1.03	----------	----------	----------
Ni^{2+}	6.7-8.2	0.8	1.7	2.6	6.0
Cr^{3+}	4.6-5.6	0.7	1.6	4.3	9.0
Mn^{4+}	----------	0.6	----------	6.5	----------
LI^{+}	----------	0.8	1.0	1.2	6.0
Mo	----------	0.5	1.8	12.0	----------
V^{5+}	----------	0.5	----------	11.0	----------
Al^{2+}	3.8-4.8	0.6-0.5*	1.5	5.6	9.0
Be^{2+}	----------	0.3	1.5	5.7	8.0
Cr^{6+}	----------	0.4	----------	16.0	----------
Ga^{3+}	3.5	0.7-0.8	1.6	4.9	----------
La^{3+}	----------	1.4-1.3	1.1	2.3	9.0
Sn^{2+}	2.3-3.2	1.3	1.8	1.5	----------
Y^{3+}	----------	0.9	1.2	3.1	----------
Si^{4+}	----------	0.4	1.8	12.0	----------
Ti^{4+}	1.4-1.8	0.7	1.5	5.8	----------
Zr^{4+}	2.0	----------	1.4	4.3	11.0

* values given for high and low spin, respectively.

It is found that the trace metals especially Cu, Cr and Zn increases in poorly aerated soils, which has low oxidation stage and Eh -100mV. The effect of redox potential on availability of Cu and to a smaller degree of Zn was reported by Gambrell and Patrick (1989). On conditions favouring metal solubilization, Chuan et al. (1996) found that acidic and reducing soil conditions are more favorable with the pH factor than that of redox potential. Smith and Huyck (1999) studied metal mobility under different environmental

conditions. Though it is difficult to predict element mobility in surficial environments, the authors referred to the capacity of an element to move within fluids after dissolution, exhibiting the conditions and behaviours of the metal compiled in Table 7. 2. In short, the Fe-rich particulates and hydrogen sulfides are among the abiotic factors most significant in controlling metal behaviour in the terrestrial environment.

Table 7.2 Behaviour of trace element in various weathering environment (after Rose et al., 1979)

Degree of Mobility	Environmental Conditions	Trace Elements
High	Oxidizing and acidic	B, Br and I
	Neutral or Alkaline	B, Br, F, I, Li, Mo, Re, Sc, U, V, W, and Zn.
	Reducing	B, Br and I
Medium	Oxidizing and acidic	Li, Cs, Mo, Ra, Rb, Se, Sr, F, Cd, Hg, Cu, Ag and Zn.
	Mainly acidic	Ag, Au, Cd, Co, Cu, Hg and Ni.
	Reducing with variable potential	As, Ba, Cd, Co, Cr, F, Fe, Ge, Li, Mn, Nb, Sn, Sr, Ti, U and Y.
Low	Oxidizing and acidic	Ba, Be, Bi, Cs, Fe, Ga, Ge, La, Li, Rb, Si, Th, Ti and Y.
	Neutral or Alkaline	Ba, Be, Bi, Co, Cu, Ge, Hf, Mn, Ni, Pb, Si, Ta, Te and Zr.
Very low	Oxidizing and acidic	Al, Au, Cr, Fe, Ga, Os, Pt, Rh, Ru, Sc, Sn, Ta, Te, Th, Ti, Y and Zr.
	Neutral or Alkaline	Ag, Al, Au, Cu, Co, Fe, Ga, Ni, Th, Ti, Y and Zr.
	Reducing	Ag, As, Au, B, Be, Ba, Bi, Cd, Co, Cu, Cs, Ge, Hg, Li, Mo, Ni, Pb, Re, Se, Te, Th, Ti, U, V, Y, Zn and Zr

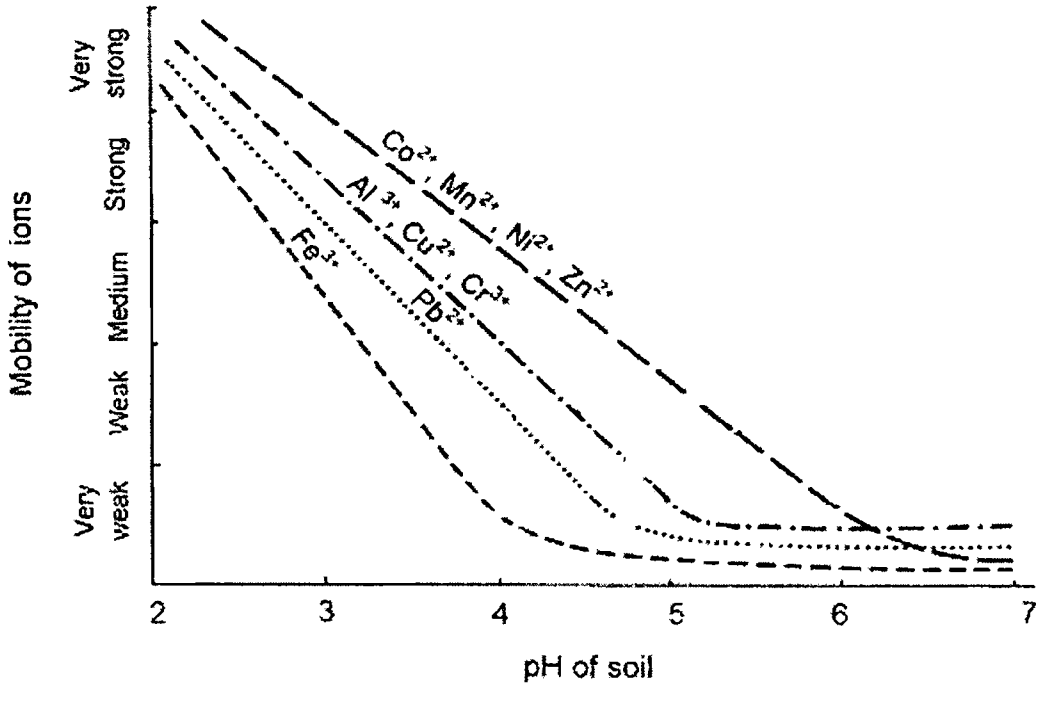

Figure 7.2 Schematic trends in the mobility of metals as influenced by soil pH. (Data for light mineral soil.) (Kabata-Pendias, 2001)

The liquid phase in soil is called *soil solution* and is composed of water with colloidal suspension and dissolved substances, which can be free salts and ions of these salts (Hodgson et al., 1966). The kinematics of soil solution determines the concentration of metal phases in different soils under same condition or same soil under different condition. The same physical situation is applicable to sediments which are fully or partially under the influence of earth's subsurface water. Such sediments will be drained by the subsurface water, carrying colloidal materials and free salts, infiltrated from above. Rainfall, evaporation, water percolation rate can change the metal content in the soil. When undergoing changes in physical conditions, the concentrations of trace ion vary tremendously where as the major ions (Ca, Mg, K, Na, NO_3, and P_2O_5) remain negligibly altered. The acidification increases the intensity by which trace metals are mobilized in soils. According to Kabata-Pendias (2001) the concentration of metals (the sum of Fe, Mn, Zn, Pb, Cu, and Cd) in the solution of the very acid soil was 9080 g/ L, whereas the solution of the same kind of soil, but with neutral range of pH, contained 17 g/L of these cations.

As sedimentation takes place, the hydrological dynamics in vadose zone and redoximorphic conditions result in trace element mobility in aqueous forms or with translocated soluble complex forms, bound to clay or organic compounds (Quantin et al., 2002; Sommer et al., 2000). For example Wilson (2004) points to the changing oxidation character of Cr with changing redox conditions. It affects the speciation, solubility, mobility and cohesion of element itself. But in such dynamics, one could observe that the trace elements could not perform the motion or translocation in isolation. In other words, there exists an interdependence of elemental cycles in natural systems, viz. interdependence of cycles of different elements in same environment. In sedimentary environments it is observed by various workers that trace elements are dependent upon major element cycles, but how remarkable they one from another.

Organic substances play a prominent role in biochemical weathering and thus in geochemical cycling of major and trace elements. Stevenson (1983) discussed evidence of humic and fulvic acids activity in metal ion mobilization from sediments. Halbach et al.

(1980), Stevenson (1983) and Thanabalasingam and Pickerings (1985) have described the solubilization and transport of some metals, such as Au, Hg, and U, mediated by humic substances.

Humic substances arise by the microbial degradation of plant and animal tissues and ultimately biomolecules (lipids, proteins, carbohydrates, and lignin) dispersed in the environment after the death of living cells. They are supramolecular structure of relatively small bio-organic molecules (having molecular mass <1000 Da) self-assembled mainly by weak dispersive forces such as Van der Waals force, π-π, and CH-π bonds into only apparently large molecular sizes (Piccolo and Cozzolino, 2002). Their colour is dark due to quinone structures formed in the oxidative soil conditions and remain trapped in the humic hydrophobic domains. In geological parlance, humic substances are the most stable fraction of organic matter in soils and persist for ten thousands of years Stevenson (1983). The present study looks into the geochemical variation of major and trace elements from sediments in study area.

7.3. Methodology:

7.3.1. XRF

XRF Spectrometry has a unique characteristic of being a non-destructive analytical technique and with a very rapid analysis feature. It has become a well-established technique for the analysis of geological materials due to its precision, accuracy, versatility, automation, sensitivity, and selectivity. Moreover as the analysis can be performed on both the solid as well as liquid samples, it is one of the most rapid and relevant method of Geochemical analysis for obtaining qualitative and quantitative elemental analysis.

XRF spectrometry is used for determining major, minor and trace elements present in geologic materials, which comprise of rocks, ores and minerals present in nature. Due to the presence of minerals in a heterogeneous way, the mineralogical effects, particle size effects and surface irregularities contribute to the error in XRF analysis. Reference rock samples play a major role in XRF analysis to reduce the complex matrix effects. No instrumental method of geochemical analysis can work without having the reference rock samples. The reference samples are essentially required to prepare the calibration curves for the

quantitative estimation of chemical elements and to check the accuracy of the analytical data. No quantitative analysis can be performed without having the suitable reference samples of similar matrix. Accuracy of the analytical results, which are carried out by instrumental methods of analysis, to a large extent depends on the accuracy of the standards which are used as reference samples to prepare the calibration curves of the analyte.

A beam of x-rays is directed on to a sample of the substance causing secondary or fluorescent x-rays to be emitted. This secondary radiation contains wavelengths that are characteristic of each element present. X-ray spectrometry is suitable for all elements in the periodic table from atomic number 5 (Boron) to 92 (Uranium) at concentration levels of 100% to a few parts per million.

7.3.2. Sample Preparation by pressed pellets:

Pressed pellets are prepared by using collapsible aluminum cups. These cups are filled with boric acid and about 1g of the finely powdered rock sample is put on the top of the boric acid and pressed under a hydraulic press at 20 tons pressure to obtain a 40 mm diameter pellet.

7.3.3. Principle of XRF spectrometry

X-rays are electromagnetic radiations having a wavelength range of 10^{-5} A° to 100 A°. Practical XRF spectrometry deals with the specific region of 0.1 A° to 20 A°. Fluorescence is a phenomenon similar to luminescence. When an atom is excited by removing an electron from the inner K shell, an electron is transferred from outer shell to K shell. The difference in the energy of the two shells is emitted as x-ray photon. These x-rays, emitted from an excited element, have the wavelength characteristic of that particular element and its intensity is directly proportional to the number of excited atoms or the concentration of that element present in the rock sample.

XRF spectrometry is a group of non-destructive instrumental method of qualitative and quantitative chemical analysis based on the measurement of the wavelength and intensity of their x-ray spectral lines emitted by secondary excitation. In Wavelength

Dispersive x-ray fluorescence spectrometry, x-ray spectral lines of all the elements in the samples are excited simultaneously and then separated on the basis of their wavelengths prior to detection. WD-XRF spectrometry is the most widely used system for the analysis of geological samples.

7.3.4. Instrumentation

Philips PW 2440 microprocessor controlled, sequential x-ray fluorescence spectrometer with 4.5 kw x-ray generator and 166-position automatic sample changer to load and unload the samples in the spectrometer housed at the petrology laboratory, Centre for Earth Science Studies, Thiruvananthapuram was used to measure different peaks and background counts for elements. Software used in computer is able to take care of dead time correction, background and line overlap corrections and matrix effects giving the output directly as the concentration in weight percentage or in ppm after converting the counts into concentration with the help of calibration curves.

Operating Parameters

A Spinner was used to spin the sample inside the spectrometer while measuring the counts to have uniform counts and to remove in homogeneity effect from the pressed sample. A 32mm primary beam aperture mask was used to restrict the x-ray beam to the sample surface only. Flow and scintillation detectors were used to count the x-ray photons. The major and minor element data estimated by XRF are reproducible with a precision range of 5%.

7.4 Results

The concentration of major and trace elements of 190 samples covering all the three Litho Units were analysed which is abridged in Table 7. 3 and detailed data is presented in Appendix 4. The elemental variations were studied using statistical measures and the correlation matrices are plotted in Table 7.4a and b.

7.4.1 Major Oxides

Silica

The concentration of SiO_2 is more than 90% in most of the sediments analysed. In Litho Unit 1, it ranges between 89.12 to 97.28, with an average of 93.7 %, in Litho Unit 2 it is 82.04 to 89.88, with a mean of 86.02 % and in Litho Unit 3 it is 95.09 to 99.54, with a mean of 98%.

Alumina

The concentration of Al_2O_3 shows striking variation among the samples of different litho units of the present study. In Litho Unit 3 it ranges between 0.06 to 3 % (mean = 0.7%), in Litho Unit 2 it varies from 3 to 4.57% (mean = 1.59%) and in Litho Unit 1 from 0.52 to 4.59 % (mean = 1.22%). It does not show significant variation in the correlation coefficients with the concentration of major elements other than SiO_2. Al_2O_3 and SiO_2 show negative correlation in Litho Unit 3, almost no relation in Litho Unit 2 and high positive correlation in Litho Unit 1.

Sodium

The concentration of Na_2O varies between 0.01 and 0.13%. The concentration demarcates the Litho Unit 2, with comparatively higher concentration of the oxide (0.12% to 0.13%). The inter-oxide correlation of major elements show that Na_2O is positively correlated with all other oxides down core, but it shows noticeable negative correlation with Fe_2O_3 in Litho Unit 2.

Sodium is a lithophile element and has affinity for forming compounds with oxygen and the halogens and forms predominantly as dissolved salt. There are no low-solubility salts of Na, so once the element is in solution it tends to remain in the dissolved form, although its mobility may be reduced by adsorption on clay minerals with high cation-exchange capacities. The normal amount of sodium in residual sediments is considerably less in terrestrial sediments, less than one per cent of Na_2O by weight, but its concentration is high in sediments rich in soda feldspar or kaolin.

Sodium from the sediments of study area shows the characteristics of terrestrial sediments. The higher values of Na in Litho Unit 2 can be linked with the occurrence of feldspar and kaolin, identified from mineralogical studies.

Table 7.3 Summary of major element distribution in three Litho Units (see appendix 4 for complete data)

	SiO2	TiO2	Al2O3	Fe2O3	MnO	CaO	MgO	Na2O	K2O	P2O5	Org C	Lol
Litho Unit 3 (avg)	98	0.64	0.7	0.26	0.01	0.09	0.02	0.04	0.02	0.01	0.40	0.14
	99.54	1.9	3.0	0.88	0.01	0.5	0.16	0.13	0.14	0.02	1.34	0.32
Range (n=64)	95.09	0.05	0.0	0.0	0.0	0.0	0.0	0.0	0.0	0.0	0.0	0.0
Litho Unit 2(avg)	86.02	1.16	4.26	0.07	0.01	0.3	0.03	0.1	0.19	0.02	5.43	2.04
	89.88	1.45	4.81	0.17	0.01	0.45	0.07	0.15	0.3	0.02	6.76	3.8
Range (n=26)	82.04	0.87	3.0	0.0	0.0	0.17	0.0	0.05	0.03	0.01	4.5	0.15
Litho Unit 1(avg)	93.71	1.59	1.76	0.63	0.01	0.14	0.02	0.04	0.06	0.02	0.54	0.61
	97.28	4.54	4.57	2.12	0.02	0.49	0.15	0.12	0.25	0.04	2.6	3.8
Range (n=100)	89.12	0.39	0.4	0.0	0.0	0.05	0.0	0.0	0.0	0.01	0.0	0.0

Potassium

The concentration of K_2O varies between almost nil to 0.29%. Its average concentration is high in Litho Unit 2 (0.03 to 0.14%). Like Na_2O, K_2O also shows positive correlation with all other oxides down core, but it differs from this trend in Litho Unit 2 with Fe2O3, with showing a senile relation there.

Potassium is a typical lithophile element with its large ionic radius and is found in sub ordinate amounts in residual sediments. The average K concentration in sand, sandstone and non-detrital siliceous sediments is <1%. Once released through the weathering of feldspar minerals, K is very soluble and occurs as the simple cation K^+ over the entire stability field of natural water (Brookins, 1986). The geochemistry of potassium has an interesting aspect in connection with formation of evaporite sediments, and therefore indicative of evaporate environment.

In the study area the concentration of potassium falls within the range of that in detritus. There is relatively high concentration of K in Litho Unit 2, still falling within the regime of normal sediments.

Magnesium

The concentration of magnesium varies between almost nil to 0.16% . Its average concentration does not vary among the Litho Units. It is highly correlative with the concentration of other major elements.

Magnesium is common metallic element associated to the weathering of ferro-magnesium minerals. Magnesium occurs in sediments either as a solute in pore water or as an important component in the formation of late stage digenetic chlorite and dolomite (Wedepohl, 1978). In the residual sediments, such as quartz sand and sandstones, it is represented only rather sparingly, probably mostly as detrital chlorite. Among different sediment types, the hydrolysates, oxidates and residuates sediments are rather poor in magnesium. But in carbonate and evaporate sediments they occur strikingly higher in concentration.

Consistency of Mg in the sediments irrespective of physical differences exhibited by the three Litho Units of the study area, indicates the absence of Mg contributing parent rocks/ minerals or that such minerals were lost in solution before they reach the site of deposition.

Calcium

CaO ranges from almost nil to 0.50% with slightly higher values in Litho Unit 2 (0.36% to 0.50%). Locations TRV3 and TRV6 have the highest values.

Calcium, like magnesium is a major electropositive constituent of the universe and the Earth's crust. In residual sediments the amounts of calcium are always small-as a rule less than 1 per cent. Hydrolysate sediments are also generally very poor in CaO, the amount not usually exceeding 1 per cent, apart from admixed calcium carbonate or dolomite.

In the present study CaO is negatively correlated with SiO_2 in Litho Unit 3 and 2 positively correlated in Litho Unit 1. The positive correlation in the bottom most unit indicates that Ca in this unit is silica bound, which is supported by the presence of feldspar in it. Whereas the Ca in the upper units are not silicate bound, and may be of non-detrital origin.

Table 7.6 Major element correlation matrix

	SiO2	TiO2	Al2O3	Fe2O3	MnO	CaO	MgO	Na2O	K2O	P2O5	Or.C	Lol	
SiO2	1												
TiO2	-0.58	1											
Al2O3	-0.91	0.68	1										
Fe2O3	-0.01	-0.41	-0.41	1									Lith Unit 3
MnO	-0.65	0.71	0.90	-0.74	1								
CaO	-0.62	0.28	0.82	-0.58	0.86	1							
MgO	-0.65	0.21	0.79	-0.42	0.77	0.97	1						
Na2O	-0.17	-0.69	0.21	0.46	-0.24	0.27	0.41	1					
K2O	-0.59	0.22	0.21	0.75	-0.19	-0.24	-0.13	0.17	1				
P2O5	-0.43	-0.05	0.02	0.88	-0.40	-0.34	-0.21	0.35	0.96	1			
Or.C	0.27	-0.78	-0.61	0.89	-0.86	-0.54	-0.40	0.66	0.41	0.64	1		
Lol	-0.95	0.39	0.83	0.09	0.58	0.68	0.77	0.40	0.52	0.41	-0.14	1	

	SiO2	TiO2	Al2O3	Fe2O3	MnO	CaO	MgO	Na2O	K2O	P2O5	Or.C	Lol	
SiO2	1												
TiO2	0.11	1											
Al2O3	-0.79	0.52	1										
Fe2O3	0.15	0.999	0.49	1									
MnO	0.40	-0.87	-0.88	-0.85	1								
CaO	0.00	-0.99	-0.61	-0.99	0.92	1							Litho Unit 2
MgO	0.27	-0.93	-0.80	-0.91	0.99	0.96	1						
Na2O	0.05	-0.99	-0.65	-0.98	0.94	1.00	0.98	1					
K2O	-0.35	0.90	0.85	0.88	-0.998	-0.94	-1.00	-0.43	1				
P2O5	-0.93	0.28	0.96	0.24	-0.72	-0.38	-0.61	-0.43	0.68	1			
Or.C	-0.81	-0.67	0.28	-0.71	0.22	0.59	0.35	0.55	-0.28	0.52	1		
Lol	-0.9999	-0.12	0.78	-0.16	-0.39	0.02	-0.25	-0.04	0.33	0.92	0.81	1	

	SiO2	TiO2	Al2O3	Fe2O3	MnO	CaO	MgO	Na2O	K2O	P2O5	Or.C	Lol	
SiO2	1												
TiO2	-0.31	1											
Al2O3	-0.88	0.12	1										
Fe2O3	-0.09	0.92	0.04	1									
MnO	-0.20	0.95	-0.07	0.83	1								
CaO	-0.50	-0.12	0.26	-0.44	0.03	1							
MgO	-0.40	0.11	0.24	-0.18	0.24	0.87	1						
Na2O	-0.45	-0.24	0.21	-0.53	-0.07	0.94	0.74	1					
K2O	-0.79	-0.11	0.77	-0.28	-0.24	0.38	0.27	0.46	1				Litho Unit 1
P2O5	-0.41	0.94	0.15	0.76	0.95	0.19	0.41	0.07	-0.03	1			
Or.C	-0.21	-0.41	0.19	-0.62	-0.25	0.76	0.59	0.69	0.02	-0.17	1		
Lol	-0.50	-0.18	0.53	-0.28	-0.29	0.09	-0.07	0.24	0.85	-0.18	-0.23	1	

As one of the main constituents of the Earth's crust, Al in rocks commonly ranges from 0.45 to 10%. During weathering of primary rock minerals a series of Al hydroxides of variable charge and composition, from $Al(OH)_2$ to Al , is formed and they become the structural components of clay minerals. It has a low mobility under most environmental conditions, although below pH 5.5 its solubility increases as it is released from silicate rocks (Shiller and Frilot, 1996). In acidic environments only very small amounts of aluminium are to be found in true residue. Because of its amphoteric nature, aluminium may also be mobilised in anionic form under strongly alkaline conditions at pH values above 8 (Shiller and Frilot, 1996).

Very low content Al_2O_3 in Litho Unit 3 can be attributed to the absence of aluminium bearing minerals in the sediments. Higher concentration of aluminium in Litho Unit 2 is due to the presence of clay minerals and feldspars. In Litho Unit 1 it further increases with the incidence of more feldspar and clay.

Iron

The concentration of Fe_2O_3 varies in Litho Unit 3 between 0.1 to 0.3 averaging 0.18 percentage, in Litho Unit 2 it varies between 0.03 to 0.16 averaging 0.09 and Litho Unit 1 it ranges between 0.11 and 1.90 averaging around 0.71 percentage. The variation of Fe_2O_3 down the core shows low concentration in Litho Unit 3 with extreme depletion in Litho Unit 2 and high concentration in Litho Unit 1. The positive correlation between iron and titania points to their association in minerals like ilmenite, while a negative correlation in the other two Litho Units indicates that the two oxides have different phases.

Manganese

The concentration of MnO is constant all throughout the core. But its correlation with the concentrations of other elements is quite interesting. MnO seems to have no correlation with any oxides in the Litho Unit 3, while it exhibit a high negative correlation with SiO_2, and Fe_2O_3 and positive correlation with other oxides in Litho Unit 2. In Litho Unit 3, MnO varies positively with all oxides, including SiO_2 and Fe_2O_3, other than TiO_2. As the variation in MnO among the samples is insignificant, no meaningful analysis can be done on these correlations.

7.4.2. Trace Elements

The trace element data for 190 samples covering the chief lithounits identified were obtained and the same are presented in Table 7.3

Vanadium

Vanadium is one of the lightest members of transition elements. It is a lithophile metallic element at low pressure, but it is a siderophile at the elevated pressures and is incompatible in most silicate minerals, although is moderately compatible in some pyroxenes (Snyder et al., 2000). The geochemical characteristics of V are strongly

dependent on its oxidation state (+2, +3, +4, and +5) and on the acidity of the media. It usually does not form its own minerals, rather replaces metal in crystal structure and get precipitated in along with Pb, Zn and Cu. In residual sediments the amount of vanadium is generally low, very much lower than in the average of the upper lithosphere. The low vanadium content of sandstones are due to two important main factors viz the raw materials of such rocks is to a great extent derived from granite and quartz diorites, which represent late stages of magmatic evolution and are poor in vanadium and during oxidative weathering most of the vanadium has been removed as the soluble vanadate ion. Vanadium content of sedimentary rocks reflects primarily the abundance of detrital Fe oxides, clay minerals, hydrous oxides of Fe and Mn, and organic matter. Vanadium in floodplain sediment has a very strong positive correlation with Fe2O3 and Ti2O, a strong correlation with Al2O3, Ga, Co, Nb, Ce, La, Eu, Sm, Gd and Y, and a good correlation with Li, Ta, Cu, Th and the remaining REE. Distribution of V on the stream sediment map is very similar to that of Fe.

Concentration of V shows variation along down core. In Litho Unit 3 it ranges between 151ppm to 160ppm , in Litho Unit 2 it varies between 132ppm to 136ppm and in Litho Unit 1 the concentration is 159ppm to 167ppm. Litho Unit 2 has lower concentrations of V compared to the top and the bottom Litho Units. It does show striking high positive correlation with Zr, Nb and Pb and moderately positive with Zn, Y and Ce, in Litho Unit 3. Meanwhile in Litho Unit 2 ,V shows only a moderate positive correlation with Zr and negative relation to Zn and Ce. In Litho Unit 1, V is high negative correlation with Ba.

Chromium

The Cr content of soil and sediments is highly variable (0-1000 ppm) and the highest concentrations are seen in argillaceous sediments or soil derived from ultramafic rocks. The behavior of soil Cr has been extensively studied by Bartlett and Kimble, (1976) Bartlett and James, (1979); Cary et al., (1977); Bloomfield and Pruden, (1980) ; Grove and Ellis, (1980); James et al., (1997) and Bartlett (1997) . Mukherjee (1998) has detailed the Cr balance in environment that Cr^{3+} is slightly mobile only in very acid media and at pH 5.5 it is almost completely precipitated, into very stable compounds in sediments in soils. It is found that the bulk of Chromium in sedimentary sequence occurs common in marine hydrolysate sediments.

Table 7.7 trace element distribution in three Litho Units

Litho Unit 3 Bore hole no.	V	Cr	Co	Ni	Cu	Zn	Ga	Rb	Sr	Y	Zr	Nb	Ba	La	Pb	Ce	Nd
trv1	160	216	6	11	12	75	14	80	42	480	654	217	bd	121	29	396	159
trv2	156	220	6	11	13	71	14	81	43	480	434	189	30	108	29	350	119
trv3	151	205	7	6	13	70	14	81	43	430	419	171	bd	108	27	388	134
trv4	157	215	6	11	13	72	14	80	45	506	436	193	bd	108	31	346	120
trv5	156	213	6	11	13	71	15	81	41	503	450	192	bd	94	29	374	135
trv6	148	210	6	11	13	68	14	82	43	430	245	153	10	98	23	300	118
trv7	156	213	6	10	13	71	14	82	41	503	450	192	bd	106	29	374	121
trv8	157	204	7	10	12	74	14	80	42	477	496	199	bd	81	28	391	140
trv9	148	210	6	14	13	71	14	82	43	430	245	153	10	98	23	272	118
trv10	154	206	6	13	14	75	14	83	53	417	310	180	20	88	28	349	109

Litho Unit 2 Well No	V	Cr	Co	Ni	Cu	Zn	Ga	Rb	Sr	Y	Zr	Nb	Ba	La	Pb	Ce	Nd
trv1	136	245	10	50	28	97	16	96	125	bd	259	29	528	47	bd	101	42
trv2	136	255	14	86	37	143	17	107	203	bd	189	14	423	53	bd	121	55
trv3	135	246	9	9	37	85	20	98	134	bd	190	31	155	40	2	101	37
trv4	136	245	10	50	28	97	16	96	125	bd	259	29	227	47	bd	101	42
trv5	136	255	14	86	7	143	17	107	203	bd	180	14	528	53	bd	121	55
trv6	136	255	bd	86	bd	120	26	110	220	bd	180	18	300	45	bd	121	50
trv7	136	255	14	13	37	143	18	107	203	bd0	180	14	528	53	bd	121	55
trv8	138	210	6	23	24	83	15	99	118	63	454	71	227	41	29	97	39
trv9	136	255	14	70	37	85	26	110	220	bd	180	18	300	45	bd	121	50
trv10	132	255	14	86	38	143	17	107	203	4	160	14	434	55	28	124	50

Litho Unit 1 Well No	V	Cr	Co	Ni	Cu	Zn	Ga	Rb	Sr	Y	Zr	Nb	Ba	La	Pb	Ce	Nd
trv1	159	223	6	13	11	71	14	82	50	428	1354	194	136	127	29	467	176
trv2	164	216	7	11	11	80	14	80	45	410	1500	213	0	154	32	537	205
trv3	167	206	6	6	12	78	14	80	46	444	1329	196	0	138	29	473	182
trv4	164	21	7	11	11	80	14	80	45	410	1500	213	0	154	32	537	205
trv5	159	223	6	12	11	79	14	81	45	431	1364	210	136	134	32	467	162
trv6	167	206	6	13	14	74	14	81	46	444	1329	196	0	138	32	457	182
trv7	159	222	6	23	11	77	14	82	50	428	1354	194	136	140	32	467	176
trv8	161	196	8	23	16	89	14	85	75	388	1348	178	0	146	32	473	188
trv9	167	206	6	12	13	74	13	81	46	444	1329	196	0	138	32	473	182
trv10	167	214	6	10	11	78	13	81	49	388	1586	211	0	164	32	573	215

Table 7.8 Trace element correlation matrix of three units

	V	Cr	Co	Ni	Cu	Zn	Ga	Rb	Sr	Y	Zr	Nb	Ba	La	Pb	Ce	Nd
V	1																
Cr	0.41	1															
co	-0.04	-0.68	1														
ni	-0.10	0.23	-0.70	1									UNIT	3			
cu	-0.42	-0.11	-0.37	0.26	1												
zn	0.67	-0.09	0.05	0.27	-0.19	1											
ga	0.15	0.12	-0.17	0.03	0.06	-0.12	1										
rb	-0.60	-0.26	-0.36	0.38	0.80	-0.22	-0.07	1									
sr	-0.10	-0.30	-0.17	0.37	0.70	0.43	-0.26	0.52	1								
y	0.75	0.59	-0.18	-0.11	-0.41	0.11	0.37	-0.60	-0.52	1							
zr	0.89	0.33	0.19	-0.37	-0.68	0.53	0.10	-0.75	-0.38	0.65	1						
nb	0.99	0.35	0.03	-0.16	-0.51	0.68	0.14	-0.63	-0.16	0.71	0.94	1					
ba	-0.21	0.28	-0.35	0.42	0.50	-0.03	-0.23	0.47	0.47	-0.37	-0.41	-0.28	1				
la	0.25	0.66	-0.30	-0.25	-0.22	-0.10	-0.21	-0.32	-0.31	0.26	0.45	0.28	-0.10	1			
pb	0.89	0.38	-0.02	-0.24	-0.10	0.49	0.19	-0.50	0.04	0.74	0.72	0.85	-0.17	0.25	1		
ce	0.78	0.10	0.41	-0.61	-0.38	0.42	0.14	-0.53	-0.19	0.49	0.84	0.82	-0.23	0.21	0.76	1	
nd	0.53	0.06	0.35	-0.38	-0.84	0.36	0.18	-0.72	-0.53	0.33	0.83	0.64	-0.57	0.34	0.26	0.60	1

	V	Cr	Co	Ni	Cu	Zn	Ga	Rb	Sr	Y	Zr	Nb	Ba	La	Pb	Ce	Nd
V	1																
Cr	-0.55	1															
co	-0.34	0.39	1														
ni	-0.33	0.51	0.09	1													
cu	-0.32	0.03	0.62	-0.38	1								UNIT	2			
zn	-0.41	0.58	0.39	0.48	-0.11	1											
ga	-0.03	0.43	-0.32	0.25	-0.23	-0.17	1										
rb	-0.22	0.58	0.16	0.58	-0.18	0.58	0.60	1									
sr	-0.31	0.72	0.24	0.62	-0.15	0.65	0.58	0.98	1								
y	0.49	-0.94	-0.32	-0.35	-0.07	-0.38	-0.34	-0.28	-0.45	1							
zr	0.63	-0.98	-0.37	-0.43	-0.08	-0.55	-0.46	-0.57	-0.71	0.91	1						
nb	0.55	-0.99	-0.44	-0.54	-0.03	-0.67	-0.35	-0.60	-0.75	0.91	0.96	1					
ba	-0.18	0.44	0.50	0.33	-0.05	0.71	-0.27	0.32	0.40	-0.34	-0.35	-0.52	1				
la	-0.48	0.59	0.64	0.51	0.10	0.91	-0.29	0.47	0.56	-0.43	-0.52	-0.69	0.80	1			
pb	-0.22	-0.56	-0.31	0.04	0.10	-0.12	-0.38	0.08	-0.08	0.71	0.48	0.52	-0.24	-0.11	1		
ce	-0.43	0.75	0.36	0.64	-0.08	0.76	0.43	0.94	0.98	-0.48	-0.73	-0.79	0.51	0.71	-0.05	1	
nd	-0.18	0.67	0.45	0.59	-0.12	0.84	0.20	0.84	0.88	-0.43	-0.60	-0.74	0.68	0.81	-0.23	0.92	1

	V	Cr	Co	Ni	Cu	Zn	Ga	Rb	Sr	Y	Zr	Nb	Ba	La	Pb	Ce	Nd
V	1																
Cr	-0.14	1															
co	-0.16	-0.37	1														
ni	-0.60	0.14	0.42	1													
cu	0.17	0.09	0.51	0.43	1							UNIT	1				
zn	-0.14	-0.22	0.85	0.40	0.46	1											
ga	-0.53	-0.14	0.30	0.23	0.03	0.22	1										
rb	-0.48	0.25	0.51	0.82	0.68	0.49	0.11	1									
sr	-0.31	0.10	0.72	0.70	0.74	0.71	0.13	0.94	1								
y	0.13	0.21	-0.66	-0.30	-0.10	-0.67	0.13	-0.41	-0.57	1							
zr	0.24	-0.35	0.17	-0.29	-0.47	0.18	-0.33	-0.34	-0.19	-0.69	1						
nb	0.20	-0.32	-0.26	-0.62	-0.76	-0.20	-0.16	-0.80	-0.74	-0.08	0.72	1					
ba	-0.84	0.33	-0.39	0.33	-0.44	-0.33	0.33	0.17	-0.10	0.24	-0.31	-0.05	1				
la	0.42	-0.36	0.38	-0.11	-0.11	0.46	-0.37	-0.17	0.05	-0.74	0.88	0.47	-0.60	1			
pb	0.06	-0.18	0.30	0.38	0.18	0.38	-0.25	0.11	0.10	-0.35	0.33	0.24	-0.22	0.51	1		
ce	0.35	-0.37	0.20	-0.35	-0.41	0.26	-0.40	-0.36	-0.18	-0.67	0.98	0.68	-0.43	0.93	0.29	1	
nd	0.52	-0.38	0.35	-0.24	-0.10	0.26	-0.38	-0.22	0.01	-0.67	0.86	0.41	-0.68	0.92	0.27	0.91	1

The Cr concentration in the sediment samples pictures that it varies down the core between 205ppm to 220ppm in Litho Unit 3, 210ppm to 255ppm in Litho Unit 2 and 196 ppm to 223ppm in Litho Unit 1. It shows only slight variation among the Litho Units. Cr is moderately positive to the concentration of La and negative to Co in Litho Unit 3. In Litho Unit 2, it is highly negative to the concentration of Y, Zr and Nb. Cr is moderately positive to Sr, Ce and Nd. In Litho Unit 1 Cr does not show any significant correlation with any of the trace metals.

Cobalt

Cobalt displays chalcophile and siderophile properties and is partitioned into a number of sulphide and sulpharsenide phases. Cobalt is most mobile in the surface environment under acidic and reducing conditions, where the formation of high valency phases of Fe and Mn is inhibited. It is rapidly removed from solution by co-precipitation and sorption in most oxidising, near-neutral or alkaline stream water as the dissolved Fe and Mn precipitate out as secondary oxides, hydrous Mn oxides having a particularly strong sorption affinity for cobalt. Divalent cobalt (Co^{2+}) is bioaccessible when it is organically bound, and cobalt may also bind to humic and fulvic acids and inorganic colloids. Certain bacteria are known to mobilise Co already complexed as chelate compounds (Kabata-Pendias, 2001). Cobalt does not form residual silicate minerals in soil.

In the Earth's crust, Co has a high concentration in ultramafic rocks (100 to 220 ppm) when compared to its content in acid rocks (1 to 15 ppm). In sedimentary rocks its concentration ranges from 0.1 to 20 ppm and is associated with clay minerals or organic matter. During weathering, Co is relatively mobile in oxidizing acid environments, but due to a high sorption by Fe and Mn oxides, and by clay minerals, this metal does not migrate in a soluble phase. In soils / sediments which contain certain bacteria which mobilizes Co - chelate compounds the Co is seen to be transported away (McKenzie, 1975). In hydrolysate sediments the content of Cobalt is same as that of average for the lithosphere. In reduced sediments Co distinctly exceeds the average for the upper lithosphere. The Co in reduced sediments is probably derived by precipitation of the sulphides of the solute elements in sea water. In oxidate sediments, the amount of cobalt is generally small mostly of an order distinctly lower than the average proportion of these elements to iron and

manganese in the upper lithosphere. In calcareous marine sediments its amount is exceedingly small, a few parts per million.

The concentration of Co does not show any significant variation in the study area. Down the core it varies between 0ppm to 14ppm, with averages of 6.5ppm in Litho Unit 3, 12.5ppm in Litho Unit 2 and 7ppm in Litho Unit 1. There is a slight enrichment of Co concentration in Litho Unit 2. Co is moderately negative to the concentration of Cr and Ni in Litho Unit 3. In Litho Unit 2, it is not with significant correlation with any trace metals. Co is highly positive to Zn, moderately positive with Sr in Litho Unit 1.

Nickel

The distribution of Ni, Co, and Fe in the Earth's crust, have some similarities. Like Co, the concentration of Ni is highest in ultramafic rocks (1400 to 2000 ppm), and decreases with increasing acidity of rocks, in granites the concentration of Ni is 5 to 15 ppm. Sedimentary rocks contain Ni in the range of 5 to 90 ppm, with the highest range being for argillaceous rocks and the lowest for sandstones. Geochemically, Ni is siderophilic and will join metallic Fe, wherever an accommodative phase is present. Ni is easily mobilized during weathering and then is co precipitated mainly with Fe and Mn oxides. However, unlike Mn and Fe, Ni is relatively stable in aqueous solutions and is capable of migration over a long distance. A large proportion of the Ni in stream sediment is held in detrital silicate and oxide minerals that are resistant to weathering Organic matter reveals a strong ability to absorb Ni; therefore, this metal is likely to be concentrated in humus, coal and oil. This concentration is apparently an effect of the precipitation of Ni as sulfides in sediments rich in organisms and under reducing conditions (Cataldo et al., 1978) Nickel is highly mobile under acidic, oxidising conditions.

Concentration of Ni varies significantly among the sediment samples analysed. In Litho Unit 3 Ni averages at 11.5ppm, in Litho Unit 2 it is 70ppm and in Litho Unit 3 it is 15ppm. Litho Unit 2 has higher concentrations of Ni compared to the top and the bottom Litho Units. Ni concentration shows a moderate negative correlation with Co and Ce in Litho Unit 3, moderately positive with Sr and Ce in Litho Unit 2 and highly positive with the concentrations of Rb, moderately positive with Sr and moderately negative with V and Nb in Litho Unit 1.

Copper

Cu is a chalcophile element forming several minerals and the most mobile of the heavy metals in hypergenic processes. but is more widely dispersed at trace levels in mica (biotite), pyroxene and amphibole, thus showing a greater affinity for mafic than for felsic igneous rocks. Copper can occur in its metallic form in nature It is abundant in rocks, with lowest content in carbonates. Cu minerals are simple and hence easily soluble in weathering processes and release Cu ions, especially in acid environments. Cu is a very versatile trace cation and in deposition materials it exhibits a great ability to chemically interact with mineral and organic components. The Cu ions can also readily precipitate with various anions such as sulfide, carbonate, and hydroxide. Thus, in soils Cu is a rather immobile element and shows relatively little variation in total content. ions. According to Bloom and McBride (1979) peat and humic acids strongly immobilize the Cu ion in direct coordination with functional oxygens of the organic substances. Humic and fulvic acids are likely to form stable complexes when Cu is present in small amount sand that organic matter can modify several Cu reactions with inorganic soil components.

The concentration of Cu is strikingly high in the humic rich Litho Unit 2 (31ppm) compared to Litho Unit 1(13ppm) and Litho Unit 1(14ppm). Cu is highly positive to the concentration of Rb and highly negative to Nd, moderately positive with Sr in Litho Unit 3. In Litho Unit 2, it is moderately positive with Co. Elements like Rb and Sr exhibit moderately positive correlation, while Nb shows moderately negative correlation with Cu in Litho Unit 1.

Zinc

Zinc is the heaviest member of the first row transition series of elements. The concentration of Zn in weathering solutions is controlled rather by adsorption (on clay minerals Fe, Mn Al hydroxides and organic matter) than by solubility of Zn carbonates, hydroxides and phosphates. Zinc mobility in the environment is greatest under oxidising, acidic conditions and more restricted under reducing conditions. Below pH 7.5–8.0, Zn occurs predominantly in the Zn^{2+} form.

Geochemically zinc distribution is somewhat closer to the range 60ppm to 90ppm, slightly varying from basic to acid rock. In argillaceous sediments and shales it ranges 80 to

120 ppm; while in sandstones and carbonaceous rocks, concentrations of this metal range from 10 to 30 ppm. Zinc in hydrolysate sediment is very imperfect, it is likely much of the zinc in circulation, has been collected in deep sea mud and in marine shales

Concentration of Zn is slightly high in Litho Unit 2. The ranges of Zn concentration in the stratigraphic delineated Litho Units are 68ppm-75ppm in Litho Unit3, 83ppm to 143ppm in Litho Unit 2 and 71ppm to 89ppm in Litho Unit 1. The correlation matrix of Zn shows that the metal is moderately positive to V and Nb in Litho Unit 3, while it is highly positive to Nd and La, moderately positive to Sr, Ce and Ba and moderately negative to the concentration of Nb in Litho Unit 2. In Litho Unit 1, Zn is highly positive to Co and moderately to Y.

Gallium

Ga is distributed rather uniformly in the major types of rocks and its common values in both magmatic and sedimentary rocks range from 5 to 25 ppm. In weathering, Ga behaves like Al and is usually strongly associated with Al minerals (e.g.,bauxites). This general tendency of Ga is reflected with Ga positively correlated with the clay fraction. The distribution of Ga in soils also shows a relation to Fe and Mn oxides. Ga is concentrated with Al in clay minerals during the weathering process, though some may remain in detrital feldspar. Gallium, like Al, is relatively immobile in the surface environment because of the low solubility of its dominant hydroxide, Ga(OH)3. It is most mobile under acid conditions and is found at relatively high levels in acid mine water, formed from the weathering of sulphides (Shiller and Frilot, 1996). Because of its correlation with Al, it is normally enriched in the clay fraction; it also has a relationship with Fe and Mn oxides, and soil organic matter.

In true residual sediments only very small amounts of gallium are to be expected. The hydrolysate sediments contained the bulk of gallium of the sedimentary sequence. After the sedimentation of the hydrolysate very little gallium can remain as solute. Concentration of Ga does not show much variation down core. In Litho Unit 3 Ga averages at 14.5ppm , in Litho Unit 2 it is 21 ppm and in Litho Unit 1 it is 13.5ppm. Litho Unit 2 has some enrichment of Ga. Ga concentration is moderately positive to that of Rb in Litho Unit 2. A negative affinity for V and Ce has been exhibited in Litho Unit 1. Otherwise Ga seems to be inert to remaining trace elements, considered in the present study.

Rubidium

Rb abundance in the major rock types reveals its geochemical association with Li, and therefore it has higher concentrations in acidic igneous rocks and sedimentary aluminosilicates. Rubidium is a lithophile metallic element that does not form any minerals of its own, but is present in several common minerals in which it substitutes for potassium. In sedimentary rocks, Rb is present mainly in K-feldspar, mica and clay minerals. In weathering, Rb is closely linked to K; however, its bonding forces to silicates appear to be stronger than those of K; therefore, the K:Rb ratio continually decreases in sedimentary processes. The behaviour of Rb in sedimentary processes is controlled mainly by adsorption on clay minerals. Franz and Carlson (1987) observed that Rb markedly decreased the rate and activation. In residual sediments such as quartz sandstone the amount of rubidium will certainly be small and approximately proportional to the amount of potassium.

The concentration of Rb show enrichment in Unit 2. Down the core it varies between 80ppm to 83ppm in Litho Unit 3, 96 ppm to 110ppm in Litho Unit 2 and 80ppm to 85ppm in Litho Unit1. Rb is highly positive with Cu, moderately negative to V, Y, Zr, Nd and Nd in Litho Unit 3. In Litho Unit 2, it is highly positive to Sr, Ce and Nd , moderately positive to Ga and moderately negative Nd. In Litho Unit 1, Ga is highly positive to Ni and Sr and moderately positive to Cu.

Strontium

Strontium is a lithophile metallic element and is a relatively common trace element in the Earth's crust and is likely to concentrate in mediate magmatic rocks and in carbonate sediments. In sedimentary processes, the distribution of Sr is affected both by strong adsorption on clay minerals, extensive substitution of Sr^{2+} for Ca^{2+} in carbonate minerals (aragonite>calcite) and Sr^{2+} for Ba^{2+} in sulphate minerals, as well as the amount of detrital feldspar. Strontium is easily mobilised during weathering, especially in oxidising acid environments, and is incorporated in clay minerals and strongly fixed by organic matter. The Sr content in soil is highly controlled by parent rocks and climate.

Geochemical characteristics of Sr are similar to those of Ca; thus, Sr is very often associated with Ca and to lower extent with Mg, in the terrestrial environment. A Ca:Sr ratio less than 8 indicates a possible toxicity of Sr. During the formation of calcareous and

sulfuric sediments, Sr is mobilized as easily soluble strontianite ($SrCO_3$), and later deposited as celestite ($SrSO_4$) (Oliver et al. 1996). The evaporates sediments are comparatively rich in strontium and the entrance of strontium into the minerals of marine salt sediments seems to be regulated by the calcium content of these minerals.

Concentration of Sr shows enrichment in Litho Unit 2. The ranges of Sr concentration in the stratigraphic delineated Litho Units are; 41ppm-53ppm in Litho Unit3, 120ppm to 203ppm in Litho Unit 2 and 45ppm to 74 ppm in Litho Unit 1. The correlation matrix of Sr shows that the metal is moderately positive to Cu Litho Unit 3, while it is highly positive to Ce, Nd and Rb and moderately positive to Cr, Ni and Zn and moderately negative to Zr and Nb in Litho Unit 2. In Litho Unit 1, it is correlated highly positive to Rb, moderately positive to Ni, Z and Cu and moderately negative to Nb.

Zirconium

Zircon, is relatively insoluble and hard mineral, concentrated in oceanic beach sand and sandstones, and these concentration seems preferentially to collect zircon varities. It can substitute for Ti in ilmenite and rutile, and is also present at trace levels in clinopyroxene, amphibole, mica and garnet. Zirconium displays very low mobility under most environmental conditions, mainly due to the stability of the principal host mineral zircon and the low solubility of the hydroxide $Zr(OH)_4$. This limits the concentration of Zr in most natural water A greater part of the zirconium is probably concentrated in hydrolysate sediments, such as clay and bauxite, either as very finally divided zircon and some secondary zirconium oxide or possibly, phosphate. A subordinate fraction of zirconium may be precipitated from solutions together with oxide sediments and even to a small extent with carbonate sediments. The circulation of dissolved zirconium compounds is of greater importance than has hitherto often been assumed. Colloidal zirconium is also readily absorbed by organic matter, macroplankton and siliceous material.

Concentration of Zr shows interesting character in the studied cores. Its average concentrations in the sub surface Litho Units are, Litho Unit 3 (1300ppm), Litho Unit 2 (210 ppm) and Litho Unit 1(1450ppm). There is a striking depletion of Zr concentration in Litho Unit 2. Zr shows highly positive correlation to V, Nb Ce and Nd, moderately positive to Y and Pb. moderately negative to Cu and Rb in Litho Unit 3. In Litho Unit 2, Zr is highly positive to Y and Ni and highly negative to Cr, moderately negative to Sr and Ce. In Litho

Unit 1, Zr is highly positive to La, Ce and Nd and moderately positive to Nb and moderately negative to Y.

Niobium

Niobium, is a lithophile metallic element. Niobium displays very low mobility under all, but the most extreme environmental conditions, due to the high stability and very low solubility of the oxide Nb_2O_5 and niobates derived from this (Brookins, 1986). However, the presence of citric, tartaric and oxalic acids increase the solubility of Nb through chelation. In sea water and most other surface water, Nb concentrations are likely to be much lower.

The amounts of Nb increase on the average in intermediate and acid magmatic rocks (15 to 60 ppm) and in argillaceous sediments (15 to 20 ppm). Its abundance in the Earth's crust is estimated at 24 ppm. In the subsequent stages of weathering and sediment evolution a certainly small fraction of the niobium remains in resistant minerals and is arrested in residual sediments such as sand and sandstones. Most of the niobium, is precipitated with hydrolysate sediments, such as clays and bauxites, along with most of the titanium and zirconium. In bauxite, niobium can be easily be shown to be concentrated almost in proportion to the aluminium of the primary rock.

Concentration of Nb is depleted in Litho Unit 2. The average concentration of Nb in Litho Unit 3 is 211ppm, Litho Unit 2 is 30ppm and Litho Unit 1 is 190ppm. Nb shows high positive correlation with V, Zr and Ce, moderately positive to Y and Nd, moderately negative to Rb in Litho Unit 3, highly positive to Zr, highly negative to Cr, moderately negative to Zn, Rb, Sr, Zr, La, Ce and Nd in Litho Unit 2 and highly negative to Rb, moderately positive to Zr and Ce, moderately Cu and Sr in Litho Unit 1.

Barium

Barium is a lithophile element and is the 14th commonest element in the Earth's crust. Barium released from weathered rocks is not very mobile since it is easily precipitated as sulphate and carbonate, strongly adsorbed by clays, concentrated in Mn and P concretions, and specifically adsorbed onto oxides and hydroxides (Kabata-Pendias , 2001).

The ionic radii of divalent barium (1.43A) and univalent potassium (1.33A) are sufficiently allow barium to be captured by potassium minerals. Various process eliminate solute barium from the sedimentary circulation. Most important is probably the precipitation of very insoluble $BaSO_4$, which we found often conspicuous concentration in many marine hydrolysate sediments, eg. shale. Another process of precipitation of barium takes place in oxidate sediments, especially in such as rich in manganese dioxide. Considerable amounts of barium are also found in many hydrolysate sediments, also probably held by absorption, and usually amounting to 200-600 ppm. BaO in marine sediments, and as low as 3-10 ppm. or even less in bauxites. Concentration of Ba is highly enriched in Litho Unit 2, ranging 300- 528 ppm. In fact it is relatively very low in other two Litho Units. In Litho Unit 2, Ba concentrations are highly positive correlative to La, moderately positive to Zn and Nd.

Lead

Lead is a chalcophile metallic element forming several important Pb minerals. It is also widely dispersed at trace levels in minerals like K–feldspar, plagioclase, mica, zircon and magnetite. In sedimentary rocks, the distribution of Pb is controlled by the presence of primary detrital minerals, such as feldspar, mica and sulphides, clay minerals and organic matter (Heinrichs et al., 2004, Heinrichs et al., 2001). Its ionic radius (Pb^{2+} 1.32A) makes it possible for lead to replace strontium (1.27A), barium (1.43A), potassium (1.33A), and in certain minerals even in calcium (1.06A). The concentration of lead from coarse clastic porous sediments under conditions suitable for oxidation. In residual sediments, such as quartz sands, sandstones, and quartz conglomerates lead is probably present in only very minute amounts. During weathering, Pb sulfides slowly oxidize and have the ability to form carbonates and also to be incorporated in clay minerals, in Fe and Mn oxides, and in organic matter. The geochemical characteristics of Pb^{2+} somewhat resemble the divalent alkaline-earth group of metals; thus, Pb has the ability to replace K, Ba, Sr, and even Ca, both in minerals and in sorption sites.

Lead is generally present in the aqueous environment as $Pb^{2+}(aq)$ below pH 6, but it also forms complexes with organic anions, chloride and hydroxide, and insoluble or poorly soluble compounds with sulphide, sulphate, hydroxy carbonate and phosphate anions. Lead mobility is restricted by sorption on clay, organic matter, secondary iron and manganese oxides, and the formation of secondary minerals with low solubilities. In lower alkalinity

and pH water, however, the dissolved Pb concentration can be significantly higher (Hem, 1976).

Concentration of Pb is depleted in Litho Unit 2. The average concentration of Pb in Litho Unit 3 is 26 ppm, Litho Unit 2 is 3 ppm and Litho Unit 1 is 31 ppm. Pb shows high positive correlation with V and Nb, moderately positive to Zr, Ce and Y in Litho Unit 3, no evident correlation with any trace metals in Litho Unit 2 and positive affinities to La in Litho Unit 1.

7.4.3. Chemical Weathering Indices

Chemical weathering indices are useful tools in characterizing weathering profiles and determining the extent of weathering and for comparing sediments with varied histories. Silicate weathering strongly affects the major-element geochemistry and mineralogy of siliclastic sediments (e.g., Nesbitt and Young 1982; Johnsson et al. 1988; McLennan 1993), where large cations (Al_2O_3, Ba, Rb) remain fixed in the weathering profile preferentially over smaller cations (Ca, Na, Sr), which are selectively leached (Nesbitt et al. 1980). These chemical signatures are ultimately transferred to the sedimentary record (e.g., Nesbitt and Young 1982; Wronkiewicz and Condie 1987) thus provide useful tools for monitoring the weathering conditions of source area. Silicate weathering indices, such as chemical index of alteration (CIA), plagioclase index of alteration (PIA), chemical index of weathering (CIW), weathering index of Parker (WIP) and simple molecular ratios such as, SiO_2/Fe_2O_3 (SF) and SiO_2/ Al_2O_3 (R) are widely used to interpret the weathering history of modern and ancient sediments (Jenny, 1941; Ruxton, 1968; Parker, 1970; Nesbitt and Young, 1982; Harnois 1988; Fedo et al. 1996; Colin et al. 1999; Tripathi and Rajamani 1999; Selvaraj and Chen, 2006; Ohta and Arai, 2007). The chemical weathering indices and the formula for calculation are given in Table 7.7. All these indices exploit Al_2O_3 as normalizing oxide on the assumption that its mass remained invariant during the weathering process. A clear advantage of these indices is that normalization enables the detection of changes in absolute elemental abundance during weathering (e.g., Chadwick et al., 1990; White et al., 2004).

Table 7.7. Chemical weathering indices used for characterizing weathering profile

Index	Formula (Molecular proportions of oxides)
CIA	$Al_2O_3 \times 100 / (Al_2O_3 + CaO + Na_2O + K_2O)$
PIA	$(Al_2O_3 - K_2O) \times 100 / (Al_2O_3 + CaO + Na_2O - K_2O)$
CIW	$Al_2O_3 \times 100 / (Al_2O_3 + CaO + Na_2O)$
WIP	$100[(2\ Na_2O / 0.35) + (MgO / 0.9) + (2\ K_2O / 0.25) + (CaO / 0.7)]$
SF	SiO_2/Fe_2O_3
R	SiO_2/Al_2O_3

According to Selvaraj and Chen(2006) and Ohta and Arai (2007), a good measure of the degree of weathering can be obtained by CIA using molecular proportions. Higher the CIA values indicate more removal of labile cations (Ca , Na , K) relative to stable residual constituents (Al ,Ti) during weathering (Nesbitt and Young 1982). Conversely, low CIA values indicate the near absence of chemical alteration and might reflect arid conditions (Fedo et al. 1995).

In addition, Nesbitt and Young (1982) and Nesbitt et al. (1996) used A-CN-K (Al_2O_3-CaO/Na_2O-K_2O) ternary plots to deduce the silicate weathering trends among sediments. Selvaraj and Chen (2006) has summarized the range of values chemical weathering indices show for different environments.

The Table 7.8 summarizes the chemical indices of weathering in the present study for three Litho Units. The CIA, PIA and CIW indices show a distinct field of index for Litho Unit 3, where as those fields of Litho Units 2 and 1 overlap. WIP, SF and R indices are very distinct for al the three Litho Units. There is a slight overlap of WIP indices of Litho Unit 3 and 1.

The CIA values of Litho Unit 3 are low and falls in the intermediate weathering index, classified by Selvaraj and Chen (2006) for aeolian sediments. Fedo et al., (1995) ascribes similar condition to reflect an arid climate. CIA values of Litho Unit 2 and 1 are high and fall closer to the extreme weathering indices, indicating that the sediments have undergone intensive leaching/ weathering and are matured.

Table 7.8. The Chemical weathering indices of Litho Units 1,2 and 3

Litho Units	CIA		PIA		CIW		WIP		SF		R	
	Range	Mean	Range	Mean	Range	Mean	Range	Mean	Range	Mean	Range	Mean
3	73.2-77.1	74.87	74.4-78.1	75.9	75.1-78.43	76.44	0.51-1.34	0.75	787–1246	1019	130-473	292.86
2	81.1-83.6	82.86	83.4-87.02	85.8	84.01-87.63	86.39	2.56-3.66	3.24	2671-4381	3470	29.7-37.2	35.08
1	79.23-83.26	81.45	81.84-84.88	83.54	82.62-85.24	84.08	1.2-1.5	1.3	297-642	409	82.2-118	94.99

The A-CN-K plot (Figure 7.3) for the Litho Units shows wide range of CIA values for Litho Unit 1 and concentrated plots for Litho Unit 2, but PIA index is concentrated for Litho Units 1 and 3. The WIP, SF and R values have considerable differences among the three Litho Units.

The Litho Unit 2 lake sediments show a narrow range of higher CIA values between 80 and 84, therefore, fall towards the apex A. It implies that with advanced weathering an aluminium-rich composition results. The presence of thick vegetation acts as an ideal site for soil development, and the considerable amount of humus material available in this region is probably responsible for the relatively low pH in soil solutions of lake catchments caused by production of organic acids. It has been shown by Colinet et al., (1999) that increasing vegetation cover in the flood plains during the summer monsoon reinforcement favors soil development. This inference indicates that acidic by-products of vegetation promote silicate weathering.

In A-C-N plot (Figure 7.4), sediments of the Litho Unit 2 Lake show very high PIA values (>80) and plot near the Al_2O_3 apex on the triangle, indicating their highly aluminous character. They are also virtually depleted in Ca and Na, but occur in small amounts because of feldspar (oligoclase, identified by XRD pattern) present. For the other two Litho Units PIA are comparatively away from the apex. For Litho Unit 3, the degree of weathering is intermediate. For Litho Unit 1 weathering might have proceeded to a stage in which significant amount of Ca and Na had been removed from the sediments because of copious

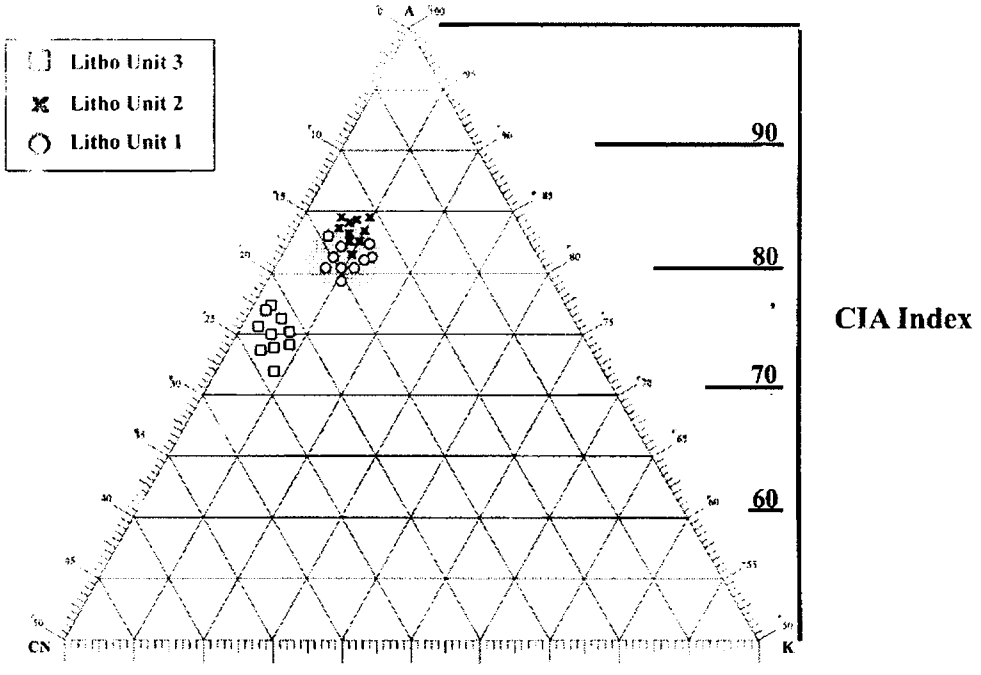

Figure 7.3. A-CN-K diagram (after Nesbitt and Young, 1984) with CIA Index showing the weathering regime of three litho units

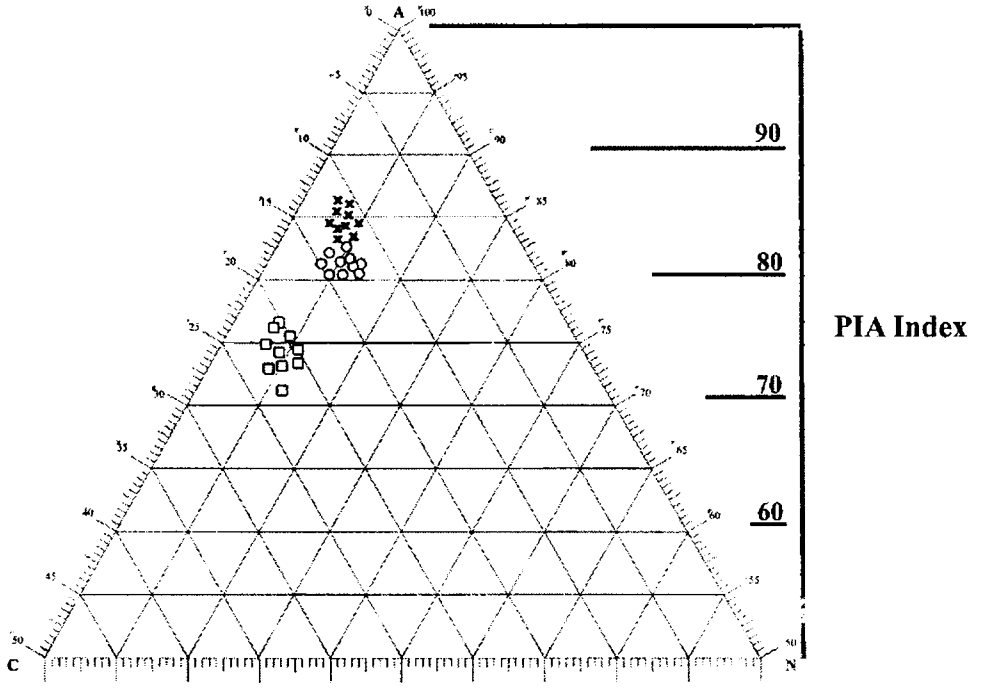

Figure 7.4. Triangular plot (after Fedo et al. 1995) showing Al2O3-K2O, CaO and Na2O with PIA index.

rainfall. The increase of rainfall in a period after the deposition of Litho Unit 1 is evident by the presence of vegetal matter in Litho Unit 2 and the sub-equatorial and tropical moist pollens present in the later formation.

According to Nesbitt et al. (1996), consistency exhibited by CIA and PIA values by sediment geochemistry suggests that, the degree of silicate weathering. Geochemists use the properties of large-ion lithophile elements (Rb, Sr, K, and Na) to understand the weathering characteristic of sediments. Increase in chemical weathering intensity rapidly leaches Sr compared to Rb (Nesbitt and Young 1982); therefore, the Rb/Sr ratio increases with increasing CIA (Ma et al. 2000). Likewise, it is found that with the increase in chemical weathering intensity, K will normally show depletion against Rb (Wronkiewicz and Condie 1989), thus leading to a lower K/Rb ratio. Rb has been considered to be primarily fixed in weathering residues and less reactive than Ca, Na, and Sr (Nesbitt et al. 1980). The Rb/Sr ratios of sediments and sedimentary rocks is therefore employed to monitor the degree of source rock weathering (McLennan et al. 1993).

In scatter plots of CIA vs Al/Na and molar K/Na vs Rb/Sr, discriminant tools for determining the degree of weathering (Selvaraj and Chen 2006), all the three Litho Units of the study area show different pattern of weathering. Figure 7.5 . In CIA vs Al/Na plot, the sediments of Litho Unit 2 and 1 show extreme weathering while Litho Unit 3 shows intermediate weathering. In Molar K/Na vs Rb/Sr plot, though all the lithounits fall in a regime moderate values. The simultaneous increase in Rb/Sr and K/Na ratios indicates heavy leaching and hence an identity of chemical alteration. The Litho Unit 3 shows lower K/Na and higher Rb/Sr, Litho Unit 2 has higher K/Na and lower Rb/Sr and Litho Unit 1 has moderately high K/Na and Rb/Sr indicating that the sediments have undergone higher level of leaching and hence more chemically altered.

The weathering indices and scatter plots of large-ion lithophile elements clearly distinguishes the Litho Unit 1 from Litho Unit 3.

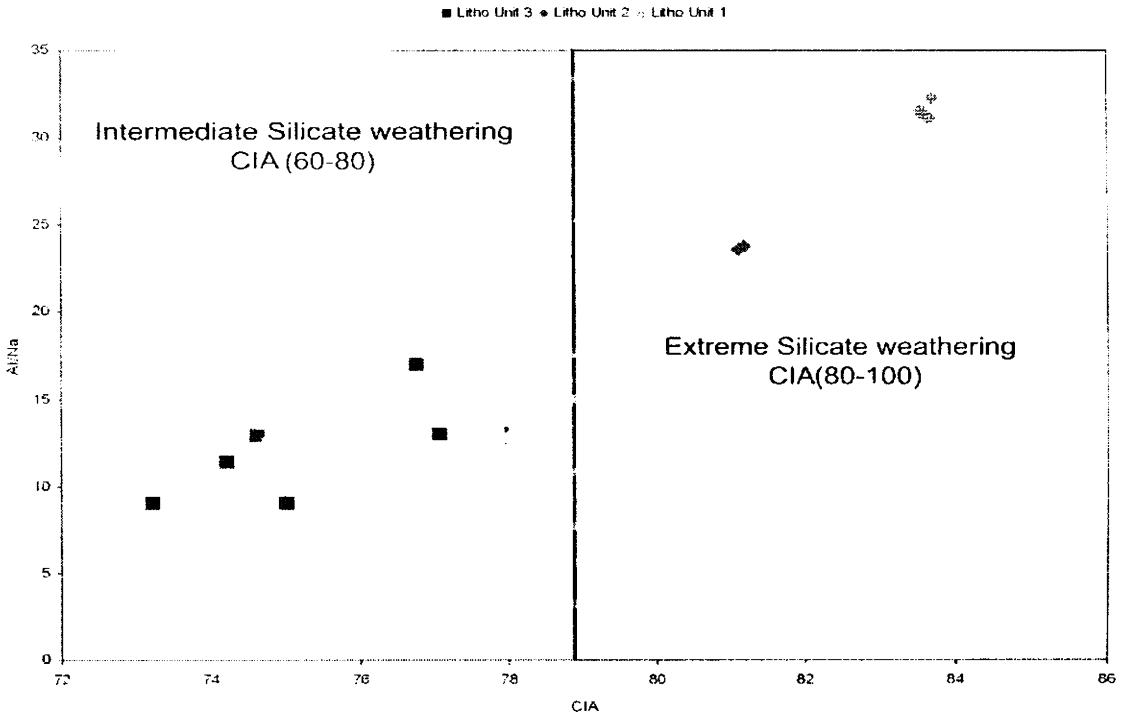

Figure 7.5 CIA vs Al/Na discriminate plot showing the degree of weathering.

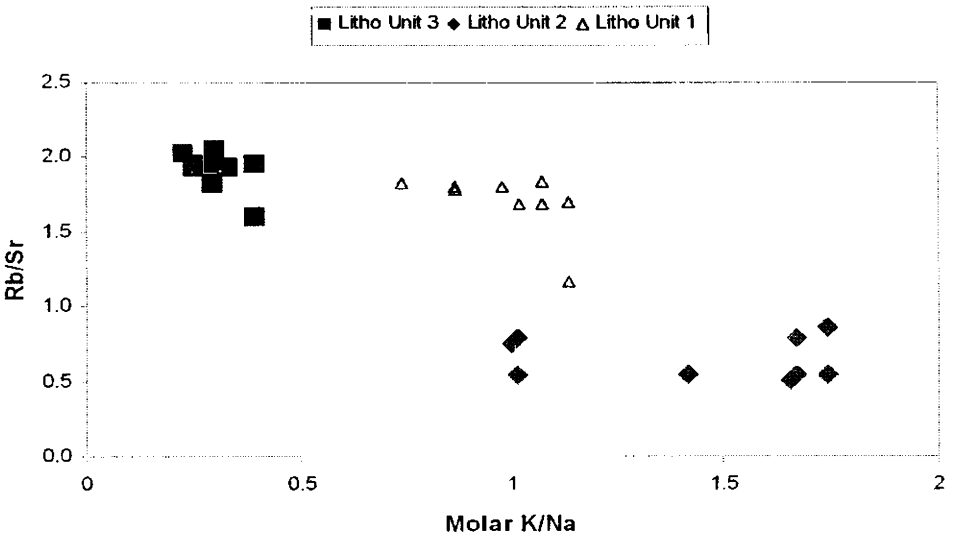

Figure 7.6 Molar K/Na vs Rb/ Sr discriminate plot

7.5. Discussion

The major and trace element data and the inter-element correlations presented above clearly depict the significant differences among the three Litho Units in terms of their geochemistry. In Litho Unit 1, concentration of Al_2O_3 is higher and it is positively correlated to CaO and SiO_2. It points into the transportation history of sediments indicating that they are feldspar/ insitu altered feldspar bounded. The relatively higher contents of LoI, organic carbon, Al_2O_3 and clay bound trace elements and lesser content of SiO_2 in Litho Unit 2 are inconformity with its lacustrine origin. The enrichment/ depletion of major and trace elements in Litho Unit 2 with respect to other units are shown in Figures 7.7 and 7.8. The trace elements can roughly be arranged in the order of decreasing enrichment in Litho Unit 2 as follows:

Ba > Sr > Ni > Cu > Zn > Co > Ga > Rb > Cr > V > La > Zr > Nb > Nd > Pb > Na > Y

Enriched *Depleted*

Similarly the major oxides also vary considerably among the three units (Figure 7.7.). The Litho Unit 2 shows relatively high concentrations of all major oxides other than SiO_2 and Fe_2O_3. The following pattern of oxide compositional variation are seen.

Al_2O_3	Litho Unit 2 > Litho Unit 1 > Litho Unit 3
CaO	Litho Unit 2 > Litho Unit 3 > Litho Unit 1
Na_2O	Litho Unit 2 > Litho Unit 1 ~ Litho Unit 3
K_2O	Litho Unit 2 > Litho Unit 1 > Litho Unit 3
MgO	Litho Unit 2 > Litho Unit 1 ~ Litho Unit 3
Fe_2O_3	Litho Unit 1 > Litho Unit 3 > Litho Unit 2
SiO_2	Litho Unit 3 > Litho Unit 1 > Litho Unit 2
TiO_2	Litho Unit 1 > Litho Unit 3 > Litho Unit 2
P_2O_5	Litho Unit 2 > Litho Unit 1 ~ Litho Unit 3
MnO	Litho Unit 2 > Litho Unit 1 > Litho Unit 3
Org.C	Litho Unit 2 > Litho Unit 1 ~ Litho Unit 3 = 0
LOI	Litho Unit 2 > Litho Unit 1 > Litho Unit 3

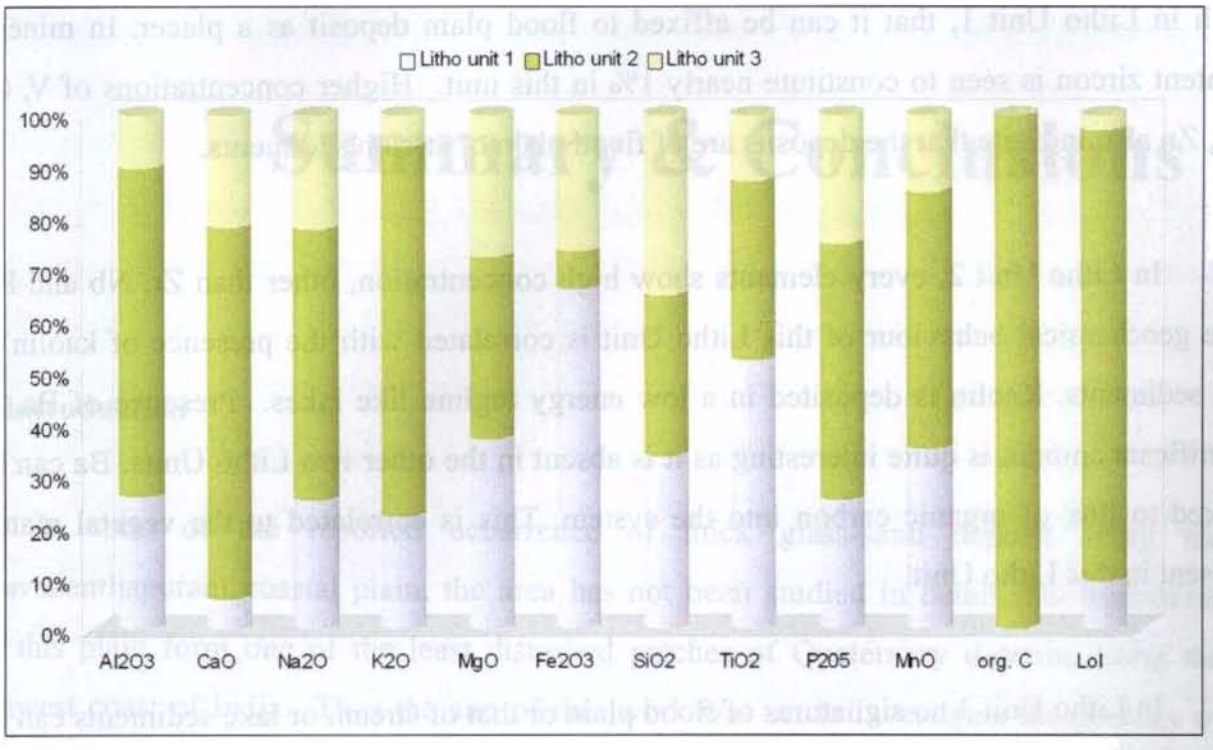

Figure 7.7. Relative variation of major oxides in sediments of three Litho Units.

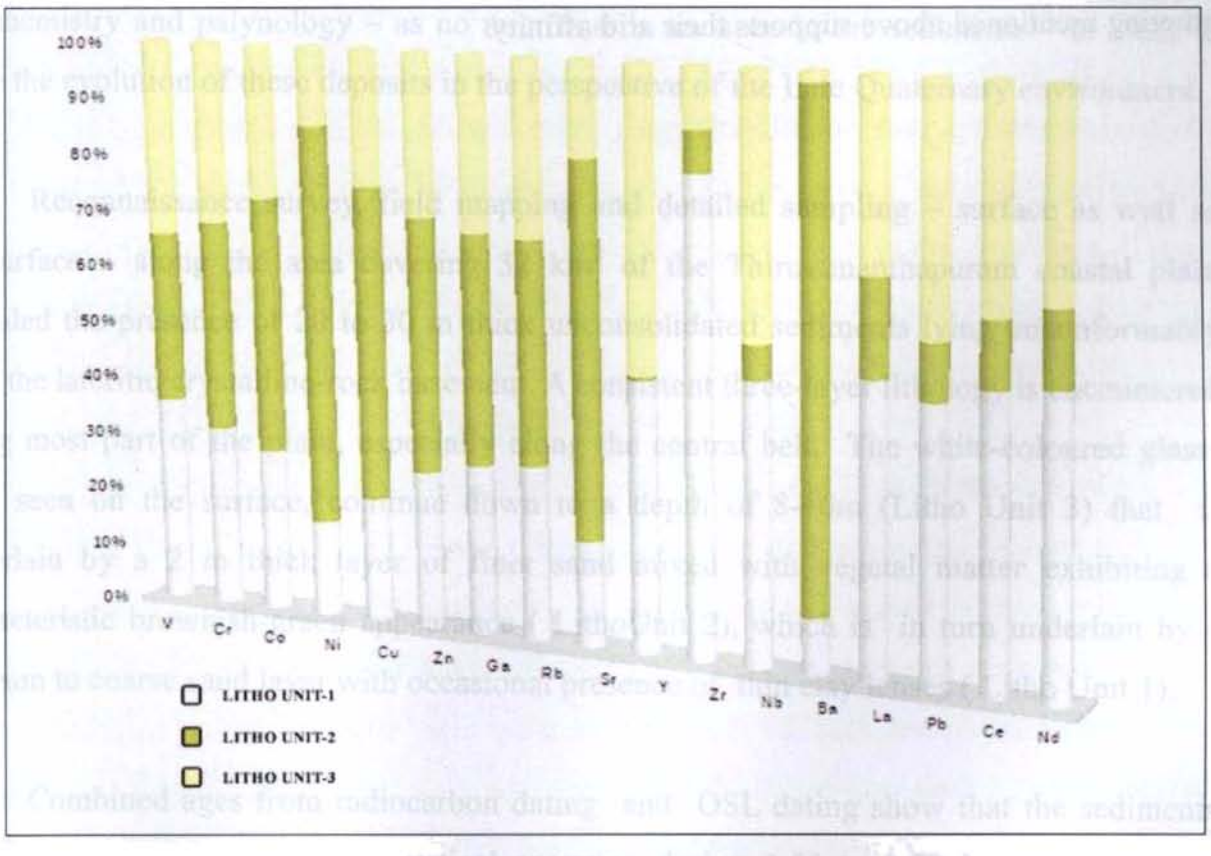

Figure 7.8 Variation of trace elements in sediments among three Litho Units

Among trace elements, Zr concentration exhibit anomaly. Its concentration is too high in Litho Unit 1, that it can be affixed to flood plain deposit as a placer. In mineral content zircon is seen to constitute nearly 1% in this unit. Higher concentrations of V, Cr, Co, Zn also indicate that the deposits are of flood plain or stream sediments.

In Litho Unit 2, every elements show high concentration, other than Zr, Nb and Pb. The geochemical behaviour of this Litho Unit is correlated with the presence of kaolin in the sediments. Kaolin is deposited in a low energy regime like lakes. Presence of Ba, in significant amount is quite interesting as it is absent in the other two Litho Units. Ba can be linked to flux of organic carbon into the system. This is correlated to the vegetal matter present in this Litho Unit.

In Litho Unit 3 no signatures of flood plain or that of stream or lake sediments can be deduced. Al_2O_3 exhibits negative correlation with SiO_2. Mineralogically this Litho Unit is quartz predominant (more than 95%). These chemical features along with the indices of weathering mentioned above supports their arid affinity.

Chapter VIII

Summary & Conclusions

8.1. Introduction

In spite of the reported occurrence of thick glass-sand deposit along the Thiruvananthapuram coastal plain, the area has not been studied in detail. The sediments over this plain form one of the least disturbed patches of Quaternary deposits along the southwest coast of India. Thus the aim of the ,work was set to investigate the geology of the glass-sand deposit and the associated sediments in the coastal plain of Thiruvananthapuram, in terms of their lithology, geochronology, texture, mineralogy, geochemistry and palynology – as no microfossils are seen in the sediments – in order to trace the evolution of these deposits in the perspective of the Late Quaternary environment.

Reconnaissance survey, field mapping and detailed sampling – surface as well as subsurface – along the area covering 32 km^2 of the Thiruvunanthapuram coastal plain revealed the presence of 20 to 30 m thick unconsolidated sediments lying unconformably over the lateritic/crystalline-rock basement. A consistent three-layer lithology is encountered along most part of the plain, especially along the central belt. The white-coloured glass-sand seen on the surface, continue down to a depth of 8-10m (Litho Unit 3) that is underlain by a 2 m thick layer of finer sand mixed with vegetal matter exhibiting a characteristic brownish-green appearance (LithoUnit 2), which is in turn underlain by a medium to coarse sand layer with occasional presence of thin clay lenses (Litho Unit 1).

Combined ages from radiocarbon dating and OSL dating show that the sediments got accumulated essentially by vertical accretion during 2.55 to 1.79 Ka B.P. Thus the sediments are of Late Quaternary age. The contact between Litho Unit 2 and Litho Unit 1 (which dates 12.47 -10.02 Ka as per OSL dating and 10.7-9.46 Ka as per radiocarbon

dating) marks the transition from Pleistocene to Holocene. The significant change in the depositional environment at the Pleistocene-Holocene boundary is reflected in the lithologic distinction of the sediments of the Litho Unit 2 deposited immediately succeeding it.

Mineralogically quartz forms the major constituent in the sediments, in all the three lithounits and in the upper and lower units the quartz percentage is high enough to be classed them as good quality glass-sand deposits (~ 99 and 95 % respectively). In Litho Unit 2 the quartz percentage is around 95 as it contains minor but significant amount (3-7 %) of feldspar and carbonaceous matter. Mica and kaolinite are noticed in the sediments of Litho Unit 2 whereas the common accessories in the other two units are mainly garnet, zircon, rutile, ilmenite, haematite and sillimanite. Texturally these sediments show the characteristics of aeolian and fluvial actions. The morphoscopic studies on quartz grains further aided to establish the environmental signatures of formation of these deposits and accordingly, the sediments of the Litho Unit 1 bear fluvial characteristics, those of the Litho Unit 2 bear lacustrine character and those of the Litho Unit 3 bear aeolian character. For instance, the grains of the Litho Unit 1 show smooth and rounded grains with classic fluvial marks, micropercussion and impact pits. The grains from the Litho Unit 2 show mixed fluvio-aeolian features with some evidences of chemical weathering like etching and over-printed grains indicating a lake environment. The grains of the Litho Unit 3 have surficial features indicating youth to mature stages of wind action, dominated by bulbous projections, elongated depressions and wind abrasion imprints, upturned plates and polygonal cracks. The mature grains from this unit from the eastern part of the area are finer and rounded.

The sediments of the Litho Unit 2 have abundant well-preserved spores and pollens which were studied and around twenty plant species were identified. Majority of the taxa identified are tropical with a few incidences of temperate. Most of the temperate species were from sediments representing the Pleistocene–Holocene transition. This is in agreement with the earlier interpretations of Holocene climate from southern India, inferred from vegetation history (Sukumar et al., 1993; Rajagopalan et al., 1997; Staubwasser and Weiss, 2007) which indicated a period of warming and aridity.

Geochemistry of the sediments ratifies the three-tier division attributed to the sediment column in the study area. The sediments of the Litho Unit 2 have more alumina (Al_2O_3 wt.% of ~4 compared to <2 in the other two units), Ca, Mg, Fe, while less silica (90%). Analysis of variations in major-element chemistry in terms of indices of alteration/weathering indicates that the sediments of Litho Unit 2 and 1 appear to have undergone extreme weathering than the sediments of Litho Unit 3. SiO_2 shows weak correlation with all the oxides in all the three Litho Units. It is more or less weak negative in the Litho Unit 1 and shows slight positive correlation with many of the oxide in Litho Unit 2. Al_2O_3 shows positive correlation with majority of oxides in Litho Unit 1(weakly positive) and 3. It shows inverse characters with oxides in Litho Unit 2 to that of Litho Unit 3. This can be attributed to the fact that Al in Litho Units 1 and 2 are silicate bound. Fe_2O_3 shows negative correlation with other oxides in Litho Unit 2, while in Litho Unit 1 and 3 it exhibits only weekly negative MnO shows negative correlation with oxides of alkali and earth metal in all three Litho Units, but in Litho Unit 2 they show prominently negative correlation. Na_2O and K_2O are positively correlated to other major oxides in Litho Unit 1 while Na_2O is negatively correlated to other oxides in Litho 2 and 3. Thus geochemical elemental variations clearly show distinction between all the three Litho Units. Organic carbon is extremely in Litho Unit 1 and three and high in Litho Unit 1.LoI is consistently high in Litho Unit 2 and is less in Litho Unit 1 and 3.

In terms of trace element abundances also the sediments of Litho Unit 2 stand out separately. There is significant enrichment of Ba, Sr, Ni, Cu, Zn, Co and Ga while depletion of La, Zr, Nb, Pb, Nd and Y in this unit compared to the others. .

More focussed discussions on certain significant findings from this work are attempted below.

8.2. Timing and duration of accumulation of sediments

The radiocarbon dates and OSL dates designate the absolute age of deposition of the sediment layers in the study area. ^{14}C dates specifically characterize the age of deposition and the rate of accumulation of sediments rich in organic/vegetal matter. Accordingly the Litho Unit 2, carrying high vegetal content, ages between 10,700 years B.P. (age of the lower part of the stratum) and 7730 years B.P. (age of the upper part of the stratum). The

rate of accumulation of the vegetal matter is found to vary between 0.097 cm/yr to 0.116 cm/yr, lowest in the northern section of study area and highest in the southern section.

The OSL dating technique is used to the sediments of Litho Units 1 and 3, which are devoid of organic carbon. The oldest age of 23,554 years B.P. is obtained from the quartz grains deposited at a depth of 27m in the central part of the study area. There exists a very good correlation with depth and age indicating that the sediments were accreted essentially in vertical fashion. The calculated sediment accumulation rates is 0.05 to 0.28 cm/yr. In borehole TRV 1 the dates of deposition of quartz at the base and top of the Litho Unit 2 have been estimated as 10,018 years B.P. and 6,074 years B.P respectively. It is found that the OSL dates of the bottom part of Litho Unit 2 are comparable well with the ^{14}C dates but the respective dates at the top of the same layer varies substantially . A few possible explanations can be ascribed to the variance of the dates at the contact of Litho Units 2 and 3: (It is to be noted that, while the radiocarbon dates give the age of decay of the organic/ vegetal remains, the OSL data give the date of the last exposure of sediment to the Sun.)

- A hiatus exist, indicating time gap in sedimentation after Litho Unit 2 prior to the accumulation of the Litho Unit 3, i.e. aeolian sand, the duration of the hiatus range between 150 to 1302 years;
- The quartz grains deposited in time concurrence with the vegetal matter, but were later exposed to the sunlight around 6,000 years B.P, changing the paleo-dose in the sediment; Or
- As the detrital sediment supply was feeble or intermittent, it took a long time for the concealing of the quartz grains from light (i.e., to build an overburden of 20cm), and thereby delaying the OSL clock compared to the ^{14}C clock.

The geochronology of the sediments of the study is summarised in Figure 8.3.

8.3. Lithostratigraphic Variations and Implications

The systematic arrangement of the sediment column correlated with their occurrence in boreholes establishes the existence of three layers, unique in their characters. The sand that is encountered on the surface is extending down to depth of 8m (TRV1 and TRV4) to 12m (TRV10) without any notable change in its physical properties like constituents, colour

and common appearance. This concludes that first 8-12 m depth from the surface constitute a single unit (Litho Unit 3).

The Litho Unit 2 is with finer sediments with greyish green color and more vegetal matter. One striking character exhibited by these sediments at the time of collection was its 'color fading', due to oxidation. It indicates that while the layer is deposited there existed an anaerobic condition.

The bottom-most is a sequence of medium to coarse sand with slight yellow/brown color. The color is washable and could be the stains of Fe coatings. Small percentages of heavy minerals are seen in this sand column. In two locations, TRV1 and TRV4, a layer of clay having thickness of 50cm are seen at a depth of 19-20m. Other than the stray occurrence of clay, this layer is nearly uniform to a depth of 29m, where lateritic pebbles were encountered in TRV1. The sand column extends further deep crossing 65 m, where the drilling was stopped due to low sediment recovery. A compilation litho-chrono stratigraphy, environment of deposition and geochemistry of the sediments is given in Figure 8.1.

The oldest date obtained falls in the Litho Unit 1, at a depth of 27m indicate that the sediment column upto that depth belongs to late Pliestocene . The base of Litho Unit 2 marks the beginning of Holocene. As per Steno's Principle of Later Continuity, an undisturbed terrain exhibit the lateral; continuum of the pack of sediments throughout the region without any change. In the study area, none of the layers show mixing ups, overlapping or sequence reversals. The Figure 8.2. deciphers the general lithological characteristics of each units for a time span since the peak of Last Glacial Maxima.

8.4. Holocene Sequence Map

A sequence map of the study area was prepared from the litholog in tandem with Streif (1978 and 1998), Bogemans and Baeteman(2003) and Bertrand and Baeteman (2005). Conventional geological maps represent the geographical distribution of

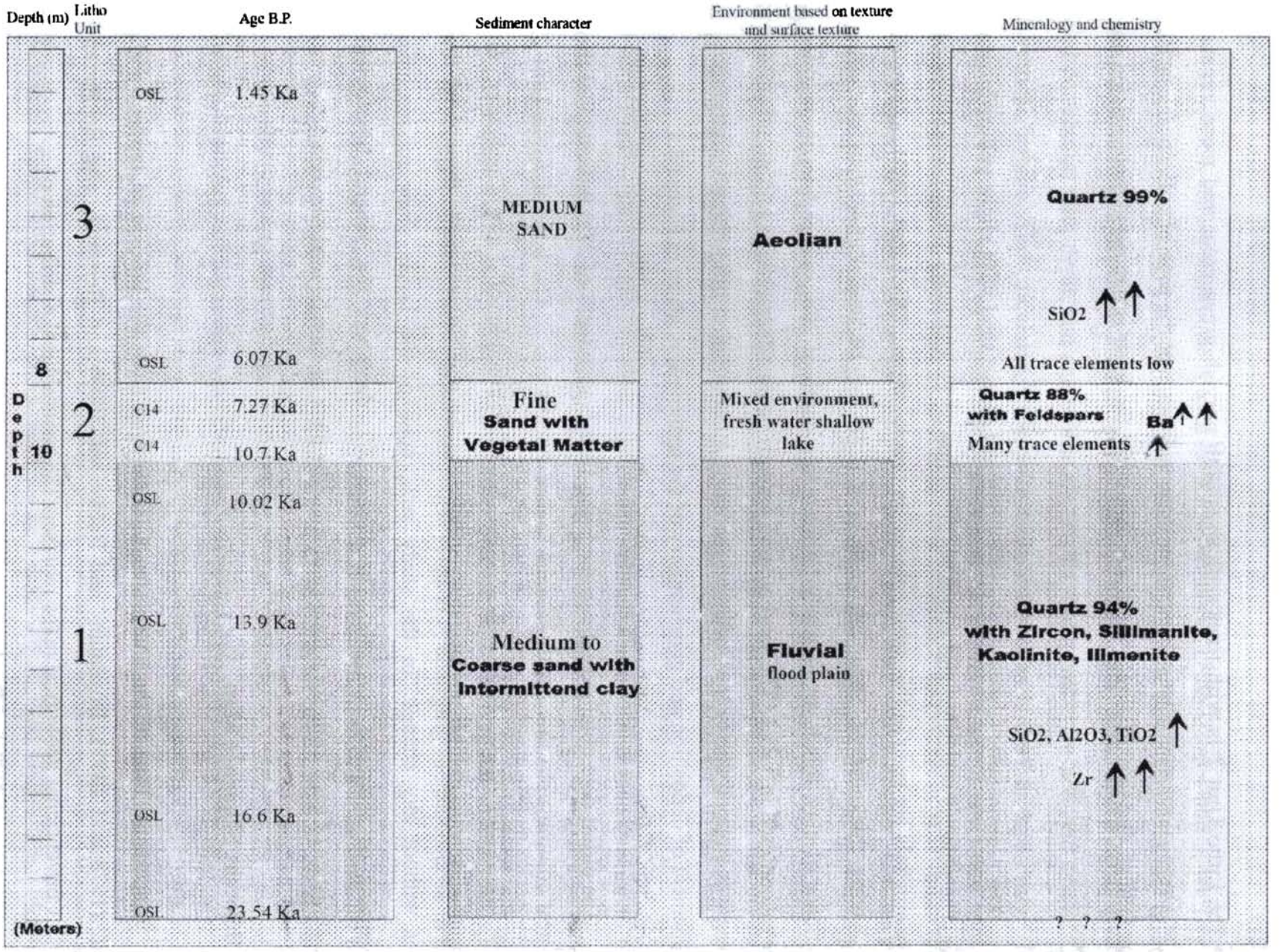

Figure 8.1 The compilation of litho-chrono stratigraphy, environment of deposition and geochemistry of the sediments

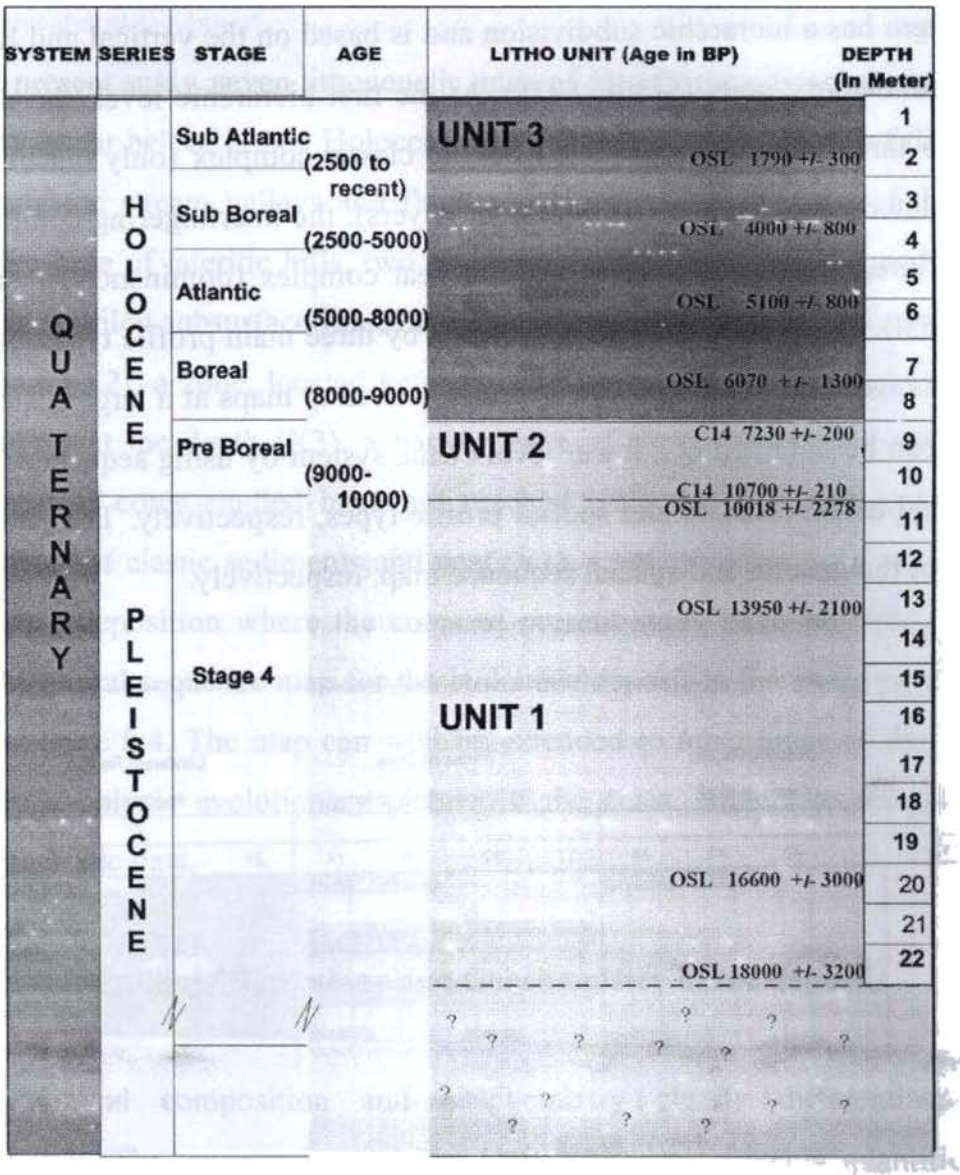

Figure 8.2 The litho-stratigraphic profile of the study area

outcropping deposits and it seldom gives information in terrain which are characterized by a high lateral and vertical variability. Hence a new classification system for coastal Holocene deposits and their representation in the form of profile types was developed by Streif (1978) and applied to the mapping of Niedersachsen, Germany (Barckhausen et al., 1977; Streif, 1978). Later, Streif (1998) introduced some minor modifications replacing lithogenetic units for describing the sedimentary units which later on were successfully used as mapping units (Bertrand and Baeteman, 2005). The classification system was applied to tidal areas, marshes and coastal fans. Based on this system a lithological map has been prepared for the Thiruvananthapuram coastal plain and adjacent areas.

The system has a hierarchic subdivision and is based on the vertical and lateral inter-fingering of sedimentary units (Streif, 1978). At the first hierarchic level, the deposits are subdivided into three complexes (Figure 8.3): the clastic complex (only clastic sediments with no intercalated peat/ organic rich sediment layers), the interfingering complex (clastic sediments and intercalated peat layers) and the peat complex (dominance of organic rich sediment material). The complexes are represented by three main profile types: X, Y and Z, respectively. The use of the main profile types is limited to maps at a large scale. A further differentiation can be obtained at a lower level of the system by using sequences and facies units, represented as subordinate and special profile types, respectively. The latter are then used to construct the general and special sequence map, respectively.

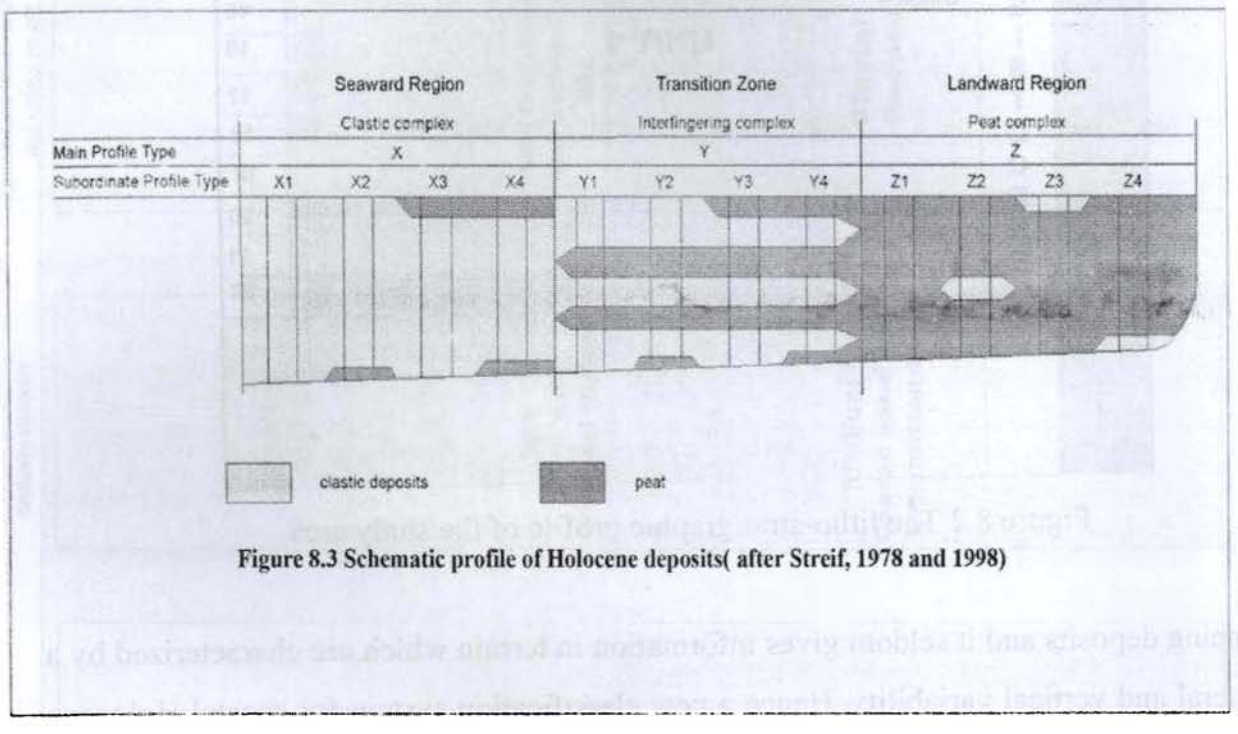

Figure 8.3 Schematic profile of Holocene deposits(after Streif, 1978 and 1998)

In Streif's classification a sequence is defined as a single layer or a group of sediment layers or peat/ organic rich sediments distinct from surrounding lithologies (e.g. clastic sequence, organic basal sequence, clastic cover sequence) (Streif, 1978). The possible combinations of the sequences build up the 12 sub-ordinate profile types (X1 to Z4) (Figure 8.3). The labels 1 and 3 added to the main profile types X and Y stand for the absence of basal peat; 2 and 4 for the presence of basal peat. The same principle applies for the absence or presence of a cover peat. A label 'u' has been added to the main profile types for boreholes that do not penetrating the entire Holocene sequence.

In the present study, seven lithogenetic units of Streif's classification were identified, namely a curvilinear belt of clastic Holocene deposits in the hinterland of of the coastal belt (X1) just along the stream valleys and flood plain in the southern part of the study area adjacent to the base of lateritic hills, two elongated lensoid patches (located one in north and another in soutiled subsurface lith of the study area) made up of clastic sediments with peat at the base (X2), a zone, located between X1 and X2 composed of peat followed by clastic sediments at the depth (X3), a narrow zone of clastic sediments along the coast, where the base of cores studied have not reached Holocene base (Xu) and pockets of alternating layers of clastic sediments and peat (Y1), single thin layer of peat lying above laterite and peat deposition where the cores of present study have not reached Holocene base (Zu). A general sequence map for the Holocene deposit in the study area is made and portriated in Figure 8.4. The map can well be extended to other areas of the SW coast of India to have a holistic evolutionary picture of the coast, subject to the availability of subsurface lithologic data.

8.5. Factors controlling Mineralogy and Geochemistry of the deposits

Both mineral composition and geochemistry clearly differentiate the three lithological layers. The topmost layer, Litho Unit 3, contain varying quantities of eolian sediments and are characterized by the presence of very fine grained pure quartz, with feldspars and other minerals forming 1% of whole. The high concentration of quartz is consistent across the study area and down within the Litho Unit. Geochemical relationship of Al and Si evince it.

Litho Unit 2 is characterized by higher vegetal content, imparting a brownish-green colour to the sediments in it. Mineralogical components include quartz, feldspar, ilmenite, kaolin and rutile. The mineral percentage of quartz is low compared to the layer above and below it. Geochemically, this layer bears high concentration of almost every trace element, but lack in Zr, Nb and Pb. The absence of Zr and Nb need to be further explored, while that of Pb can be a resultant of organic absorption. Ba , which is otherwise absent in the litho column is seen to have the average crustal concentration in this unit.

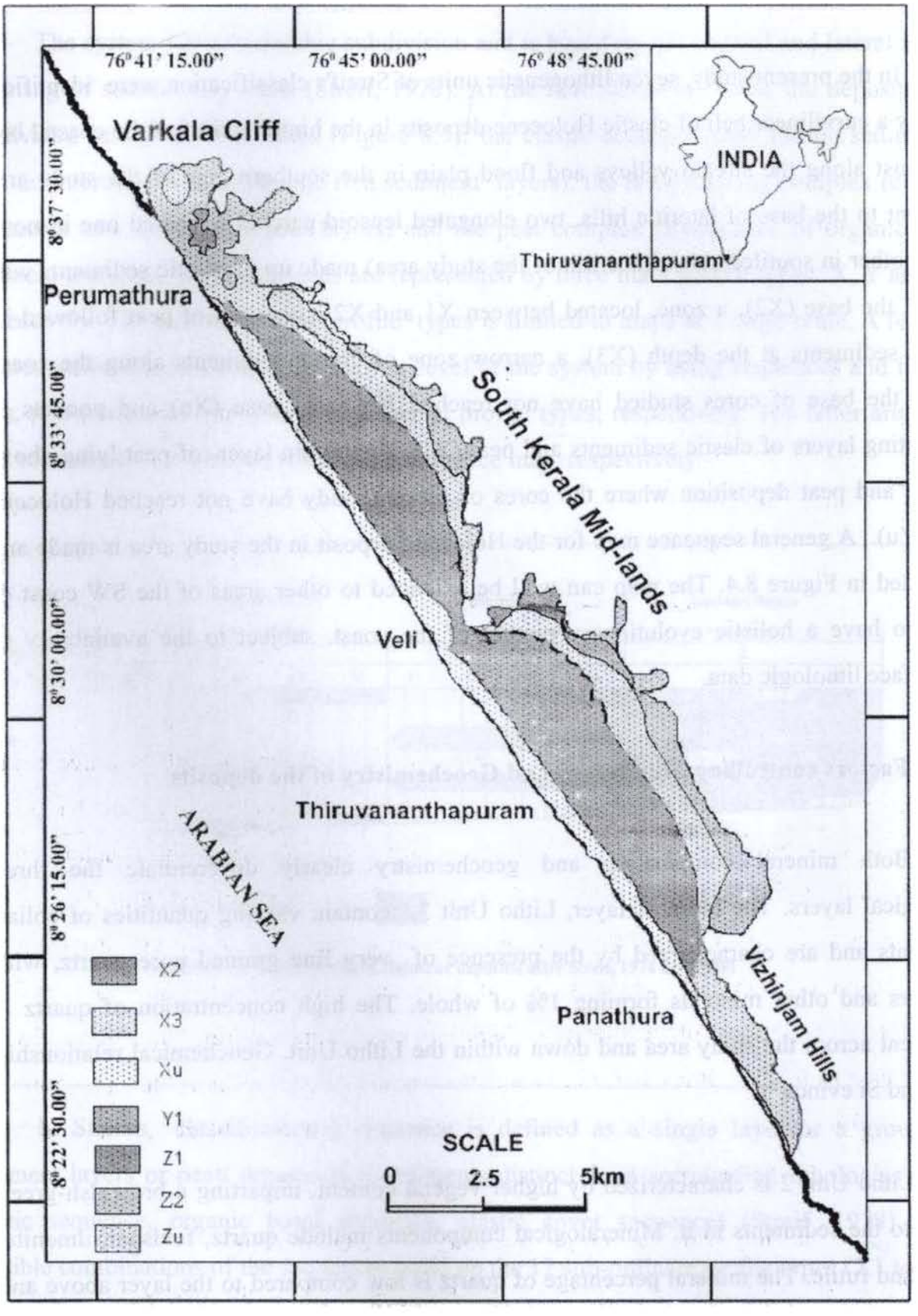

Figure 8.4: General sequence map of the Holocene deposits in Thiruvananthapuram coastal plain (X2, X3, etc are profie types as per Streif, 1998)

Litho Unit 1, the lower most layer, has a different mineral proportion in their make up. Quartz predominates like in Litho Unit 3 followed by ilmenite upto 3% and feldspar upto 2% of the count. Lack of clay or silt within the sandy layer indicate that the depo center of this unit bear the characteristics of high energy sedimentation. In two boreholes, a 50cm thick clay horizon is found within, hence localized. This association can be visualized in a flood plain environment with ox-bow lakes here and there. Geochemically this Litho Unit bears unique characteristics, which differentiates it from other layers. Al, Ca and Si are positively correlated among themselves for which the feldspar present is the source. Anomalous quantity of Zr, in this layer is due to the presence of accessory zircon. The plots of CIA and PIA index shows that the sediments fall in three different regimes. These plots proved that the there exist differences between the geochemical behavior of Litho Unit 1 and 3. Sediments of Litho Unit 1 are more matured and fall in a riverine regime, whereas the sediments of Litho Unit 3 is less matured and fall in the regime of loess, wind-blown sands.

8.6. Palynology and inferred paleo-environment

Though no micro fossils were obtained from the sediments of all the three Litho Units, pollens were noticed in Litho Unit 2. These pollen grains belong to plants that grow mainly in wet tropical climate with some transitional varieties showing, sub equatorial and dry tropical. Interestingly, four species of temperate flora are associated with the pollen assemblages at 10m depth. This assemblage wanes up the core and at the top of the Litho Unit 2, it is totally absent. The existence of temperate flora raises the question of their source. It gives a picture of temperate or high mountain climate prevalence in the study area prior to Holocene . It needs further confirmation at regional level. A changing pattern of climate from wet to dry spell has been deduced from pollen assemblages in tandem with observations from petrography and geochemistry.

8.7. Thiruvananthapuram coastal plain through Late Quaternary

Although quartz sand is abundant in all the three Litho Units, their natures differ. SEM characteristics, in particular, suggest a dominantly aeolian origin for the sand in Litho Unit 3 (largely rounded grains and absence of angular quartz grains) and fluvial in Litho Unit 1 (absence of rounded and abundance of angular shaped quartz grains with conchoidal

fractures and linear groves). According Krinsley and Doornkamp (1973), Culver et al. (1983) and Mahaney (2005) quartz grains lacking angular shape, rounded and upturned plates with dish shaped cavities characterizes aeolian deposit, while grains with conchoidal fractures and linear groves testify hydrodynamic transport, mostly fluvial. On the other hand the Litho Unit 2 shows a mixed character of fluvial and aeolian grains intermingled. The grains contain more precipitates indicating the incidences of surface adherence in stagnant environment. Overall it attests low energy deposition condition, like lake.

The pattern of sedimentation and accumulation rate has been brought out for a single core to a depth of 22m. The rates vary much showing that there was inconsistency of the agents or mechanisms operating during the time period. The lowest accumulation rate for clastic sediments was seen in Litho Unit 2, while the accumulation of vegetal matter was comparatively high. Accumulation of vegetal matter increases only when the intensity of the agents of erosion is too low. Therefore the sizable difference in the accumulation rate between clastic sediment and vegetal matter in Litho Unit 2 is a finger print of the prevalence of a very low dynamic environment of deposition, hence a lake.

In short, three environments are deciphered from the sediment characteristics, namely a fluvial, followed by a lacustrine and then an aeolian. The Litho Unit 1 further conforms to a flood plain – oxbow lake sedimentation with essentially coarse to medium sand deposits with localized thin lenses of clay. The thick accumulation of these sediments could have - due to slowly rising sea-level during Late Pleistocene.

The Holocene climatic changes inferred from the study in the Thiruvananthapuram coastal plains confirms the earlier deductions by Nair and Hashmi (1999) and Nair et al. (2006) who deduced the incidences of warmer conditions and two terrestrial runoff from the occurrences of oolitic limestone in the Kerala Shelf which dates 9-11 Ka. B.P.

8.8 Silica sand deposits : qualitative and quantitative aspects

Based on the lithological,mineralogical and geochemical data gathered in the present work, an estimation of the quantity and chemical quality of the quartz-rich sand deposits of the Thiruvannanthapuram coastal plain is attempted. Accordingly a silica sand reserve of

288 metric tonnes of high quality (SiO_2 >97%), which can be used in glass and chemical production industries, 576 metric tonnes of nearly high quality (93%<SiO_2 <97%), which can used foundry and metallurgic industries and 72 metric tonnes of 86%<SiO_2 <90% are available in the study area.

* * *

REFERENCES

Agarwal, D. P., Rajguru, S. N. and Roy, B. (1978) SEM and other studies on the Saurashtra miliolite rocks, Sediment. Geol., v20, pp. 41-47.

Agarwal, D. P. and Guzder, S. J. (1974) Quaternary studies on the western coast of India: Preliminary observations, The Paleobotanist, v21, pp. 216-222.

Ahmed, E. (1972) Coastal geomorphology of India. Orient Longman, New Delhi, pp. 222.

Aitken, M.J. (1998) Science-based Dating in Archaeology. Longman, England.

Anderson, R. S., Sorenson, M. and Willets, B.B. (1991) A review of recent progress in our understanding of aeolian sediment transport, Acta Mechanica Supplementum 1, Springer-Verlag, New York, pp. 1-19.

Bagnold, R. A. (1941) The Physics of Blown Sand and Desert Dunes, London, Methuen, pp. 265.

Baker, R. G. V. and Haworth, R. J. (2000) Smooth or oscillating late Holocene sea-level curve, Evidence from the palaeo-zoology of fixed biological indicators in east Australia and beyond. Marine Geology, v163, pp. 367–86.

Banerjee, M. and Sen, P. K. (1987) Paleobiology in understanding the change of sea level and coastline in Bengal Basin during Holocene period, Indian Jour. Science Special No. Modern Trends in Quaternary Geology, v14 (3-4), pp. 307-320.

Barndorff-Nelson, O. E. and Willets, B.B. (1991) Aeolian grain Transport 1- Mechanics, Springer-Verlag, New York.

Bartlett, R. J. and Kimble, J. M. (1976) Behavior of chromium in soils, I Trivalent forms. II. Hexavalent forms, Jour. Environ. Qual., v5, pp. 379-383.

Bartlett, R. J. and James, B. (1979) Behavior of chromium in soils. III. Oxidation, Jour. Environ. Qual., v8, pp. 31.

Bartlett, R. J. (1997) The chromium scene, in Chromium Environmental Issues, Canali, S., Tittarelli, F. and Sequi, P., Eds., FrancoAngel, Rome.Methods. Soil Sci. Soc. Amer. Book Series No. 5. Madison, WI: Soil Science Society of America, pp. 683–701.

Barnola, J.M., Raynaud, D., Korotkevich, Y.S. and Lorius, C. (1987) Vostok ice core provides 160,000-year record of atmospheric CO_2. Nature, v329, pp. 408–414.

Beal, M. A. and Shepard, F. P. (1956) A use of roundness to determine depositional environments, Journal of Sedimentary Petrology, v26, pp. 49-60.

Bednarik, R. G. (2007) The Late Pleistocene cultural shift in Europe, Anthropos, v102 (2), pp. 347-370.

Beerling, D. J. and Woodward, F. I. (1993) Ecophysiological Responses of Plants to the Global Environmental Change Since the Last Glacial Maximum, New Phytologist, v125, pp. 641-648.

Beerling, D. J., Lomax, B. H., Royer, D. L., Upchurch, G. R. and Kump, L. R. (2002) An atmospheric CO_2 reconstruction across the Cretaceous-Tertiary boundary from leaf

megafossils. Proceedings of National Academy of Sciences USA, v99, pp. 7836–7840.

Benoit, J. M., Fitzgerald ,W. F. and Damman, A. W. H. (1998) The biogeochemistry of an ombrotrophic bog: evaluation of use as an archive of atmospheric mercury deposition, Environmental Research, v78 A, pp. 118–133.

Bennett, A. (1994) The Last Glacial-Holocene transition in southern Chile. Science v290, pp.325–328.

Bertranda, S. and Baeteman, A. (2005) Sequence mapping of Holocene coastal lowlands: the application of the Streif classification system in the Belgian coastal plain, Quaternary International, pp. 151–158.

Bhaskara Rao, U. V. and Vaidhyanathan, R. (1975) Photogeometric study of Coastal Features between Visakhapatnam and Pudimadaka. In Andhra Pradesh, Jour. Ind. Soc. Photointerpretation, v111, pp. 43-46.

Bhatt, N. (2003) Quaternary carbonate deposits of Saurashtra and Kachch, Gujarat, Western India: A Review, Proc. Indian Nat. Sci. Acad., v6, pp.137–150.

Bhatt, N and Bhonde, U.A. (2003) Quaternary fluvial sequences of South Saurashtra, Western India, Current Science, v84, pp. 1065-1071.

Blatt, H. (1967) Original characteristics of clastic quartz grains, Jour. Sediment. Petrol., v37, pp. 401-424.

Blatt, H., Middleton, G. V. and Murray, R. C. (1980) Origin of Sedimentary Rocks, 2nd ed., Prentice-Hall, New Jersey, pp. 634.

Bloom, A. L. (1988) Glacial-eustatic and isostatic controls of sea level since the last glaciation. In: Turekian, K.K. (ed.), Late Cenozoic Glacial Age, Yale University Press, New Haven, pp. 355-379.

Bloom, P. R. and Mc Bride, M. B. (1979) Metal ion binding and exchange with hydrogen ions in acid- washed peat, Soil Sci. Soc. Am. Jour., v43, pp. 687.

Bloomfield, C. and Pruden, G. (1980) The behaviour of Cr (VI) in soil under aerobic and anaerobic conditions, Environ. Pollut., v23, pp.103.

Blott, S. J. and Pye, K. (2001) Gradistat a grain size distribution and statistics package for the analysis of unconsolidated sediments, Earth Surf. Process Landforms, v26, pp. 1237–1248.

Bogemans, F. and Baeteman, C. (2003) Toelichting bij de Quartairgeologische kaart Veurne—Roeselare 1:50,000. Ministerie van de Vlaamse Gemeenschap.

Boggs, S. Jr. (1995) Principles of Sedimentology and Stratigraphy, Prentice Hall, Eglewood Cliffs, New Jersy.

Bolt, G. H. and Bruggenwert, M.G.M. (1976) Soil Chemistry, A. Basic elements, Elsevier,

Amsterdam, pp. 525.

Bond, G., Heinrich, H., Broecker, W., Labeyrie, L., McManus, J., Andrews, J., Huon, S., Jantschik, R., Clasen, S., Simet, C., Tedesco, K., Klas, M., Bonani, G., Ivy, S. (1992) Evidence for massive discharges of icebergs into the North Atlantic ocean during the last glacial period, Nature, v360, pp. 245–249.

Borger, H. (2000) Mikromorphologic and Paleoenvironment, Gebruder Borntraeger. Berlin.

Borole, D. V., Rajagopalan, G. and Somayajulu, B. L. K. (1987) Radiometric ages of phosphorites of the west coast of India, Marine Geology, v78, pp. 161-165.

Botter-Jensen L. and Duller G.A.T. (1992) A new system for measuring optically stimulated luminescence from quartz samples, Nuclear Tracks and Radiation Measurements, v20, pp. 549–553.

Bowler J. M., Johnston, H., Olley, J.O., Prescottk J.R., Roberts, R.G., Shawcross, W. and Spooner, N.A. (2003) New ages for human occupation and climatic change at Lake Mungo, Australia, Nature, v421, No.20

Boyd, R. and Richerson, P. J. (1995) Why does culture increase human adaptability?, Ethology and Sociobiology, v16, No.2, pp. 125-143.

Bradley, R. S. (1999) Paleoclimatology: Reconstructing Climates of the Quaternary, Academic Press, San Diego.

Brookins, D. G. (1986) Geochemical behavior of antimony, arsenic, cadmium and thallium: Eh-pH diagrams for 25°C, 1-bar pressure, Chemical Geology, v54, No.3-4, pp. 271-278.

Bruckner, H. (1986) Stratigraphy, evolution and age of Quaternary marine terraces in Morocco and Spain, Zetschift fur geomorphologic, v6, pp.83-101.

Butzer, K. W. (1980) Holocene alluvial sequences: Problems of dating and correlation. In: Cullingford, R.A., Lewin, J. and Davidson, D. A. (eds), Timescales in Geomorphology, pp. 333-354.

Cailleux, A. (1942) Les actions eoliens periglaciaires en Europe, Memoirs, Societe Geologique France, pp .76.

Caratini, C., Delibrias, G. and Rajagopalan, G. (1990) The Paleomangroves of Kanara Coast (Karnataka) and their implications on late Pliestocene sea level changes, The Paleobotanist, v38, pp. 370-378.

Cary, E. E., Allaway, W. H., and Olson, O. E. (1977) Control of chromium concentrations in food plants, I.Absorption and translocation of chromium in plants, II.Chemistry of chromium in soils and its availability to plants, J. Agric. Food Chem., v25, No. I, pp. 300, No. II, pp. 305.

Cataldo, D. A., Garland, T. R., and Wildung, R. E. (1978) Nickel in plants, Plant Physiol., v62, pp. 563-566.

Chadwick, O.A., Olson, C.G., Hendricks, D.M., Kelly, E.F. and Gavenda, R.T. (1990) Quantifying climatic effects on mineral weathering and neoformation in Hawaii: Proceedings of the 15th International Soil Science Congress, v8A, pp. 94–105.

Chacko, T., Ravendrakumar, G. R. and Newton, R.C. (1987) Metamorphic P-T conditions of the Kerala (south india) Khondalite Belt a granulite-facies supracrustal terrain, Jour. Geol., v40, pp.1356-1361.

Chauhan, O. S., Borole, D. V., Gujar, A .R., Antonio, M., Mislanker, P. G. and Rao, C. M. (1993) Evidences of climatic variations during Late Pleistocene–Holocene in the eastern Bay of Bengal, Curr. Sci., v65(7), pp. 558–562.

Chen, M., Ma, L. Q. and Harris, W. G. (2002) Arsenic concentration in Florida surface soils: Influence by soil type and properties, Soil Science Society of America Journal, v66, pp. 632–640.

Chuan, M. C., Shu, G. Y. and Liu, J. C. (1996) Solubility of heavy metals in a contaminated soil: effects of redox potential and pH. Water Air Soil Pollut, v90, pp. 543–560.

Church, J.A., Gregory, J. M., Huybrechts, M., Kuhn, K., Lambeck, M. T., Nhuan, Qin, D. and Woodworth, P. L. (2001) Changes in sea level, Climate Change: The Scientific Basis, Contribution of Working Group I to the Third assessment Report of the Intergovernmental Panel on Climate Change, Cambridge University Press, Cambridge, U.K., pp. 639–693.

Colin, C., Turpin, L., Bertaux, J., Desprairies, A. and Kissel, C. (1999) Erosional history of the Himalayan andBurman ranges during the last two glacial-interglacial cycles, Earth Planet. Sci. Lett., v171, pp.647–660.

Cowling, S. A. and Sykes, M. T. (1999) Physiological significance of low atmospheric CO2 for plant–climate interactions, Quaternary Research, v52, pp.237–242.

Cronin, T .M. (1999) Principles of Paleoclimatology, Columbia University Press, New York.

Croxton, F.E. and Cowden, D.J. (1939) Applied General Statistics. New York.

Curray, J. R. and Moore, D. G. (1971) Growth of the Bengal Deep – Sea Fan and Denudation in the Himalayas, Geol. Soc. Am. Bull., v82, pp. 563–572.

Dansgaard, W., Johnsen, S., Clausen, H. B., Dahl-Jensen, D., Gundestrup, N. S., Hammer, C. U., Hvidberg, C. S., Steffensen, J. P., Sveinbjornsdottir, A. E., Jouzel, J. and Bond, G. (1993) Evidence for general instability of past climate from a 250-Kyr ice-core record, Nature, v364, pp. 218–220.

Davies, O. (1980) Last interglacial shorelines in the South Cape, Palaeontographica Africa, v23, pp. 153-171.

De Menocal, P. B. (2001) Cultural responses to climate change during the late Holocene, Science, v292, pp. 667-673.

Ditlevsen, P. D., Svensmark, H. and Johnsen, S. (1996) Contrasting atmospheric and climate dynamics of the last-glacial and Holocene periods. Nature, v379, pp. 810-812.

Donahue, W. F. and Schindler. D.W. (1997) Diel emigration and colonization responses of black flies (Diptera: Simuliidae) to ultraviolet radiation. Freshw. Biol. v40 pp.357–365.

Douglas, B. C. (1991) Global sea level rise, J. Geophys., Res. v96. pp. 6981-6992.

Duane, D. B. (1964) Jour. Sed. Petrol., v34, pp. 864-874.

Duller, G. A. T. (2004) Luminescence dating of Quaternary sediments: recent advances, Journal of Quaternary Science. v192, pp.183–192.

Duller G. A. T. (1991) Equivalent dose determination using single aliquots, Nuclear Tracks and Radiation Measurements, v18, pp. 371–378.

Emery, K. O. and Aubrey, D. G. (1991) Sea Levels, Land Levels, and Tide Gauges, Springer-Verlag.

Erdtman, G. E. (1952) Pollen morphology and plant taxonomy, Angiosperms, Stockholm, Almqvist and Wiksell.

Eronen, M. (1987) Global sea-level changes, crustal movements and Quaternary shorelines in Fennoscandia. Geological Survey of Finland, Special Paper, v2. pp.31-36.

Fairbridge, R. W. (1966) The Encyclopedia of Oceanography, pp. 116.

Fairbridge, R. W. (1983) The pleistocene-holocene boundary, Quaternary Science Reviews, pp. 215-244.

Farr, T. G. and Kobrick, M. (2000) Shuttle radar topography mission produces a wealth of data, Eos Transactions, AGU, v81, No. 48, pp.583–585.

Fedo, C. M., Nesbitt, H. W. and Young, G. M. (1995) Unraveling the effects of potassium metasomatism in sedimentary rocks and paleosols, with implicationsfor paleoweathering conditions and provenance, Geology, v23, pp. 921–924.

Fedo, C. M., Eriksson, K. A. and Krogstad, E. J. (1996) Geochemistry of shales from the Archean (□3.0 Ga), Buhwa Greenstone Belt, Zimbabwe: implications for provenance and source-area weathering, Geochim., Cosmochim., v60, pp. 1751–1763.

Flenley, J. R. (1996) Problems of the quaternary on mountains of the Sunda-Sahul region, Quaternary Science Reviews, v15, pp. 549-555.

Folk, R. L. and Ward, W. C. (1957) Brazos River Bar, a study in the significance of of grain size parameters, Jour. Sedimentory Petrology, v27, pp. 3-26.

Folk, R. L. (1966) A review of grain-size parameters, Sedimentology, v6, pp. 73-93.

Friedman, G. M. (1961) Distinction between dune, beach and river sands from their textural characteristics, J. Sediment. Petrol., v31. pp. 514–529.

Friedman, G. M. (1967) Dynamic processes and statistical parameters compared for size frequency distribution of beach river sands, J. Sediment. Petrol., v37, pp. 327 –354.

Friedman, G. M. and Sanders, J. E. (1978) Principles of sedimentology, Wiley, New York, pp. 792.

Friedman, G. M. (1979) Differences in size distribution of populations of particles among sands of various origin, Sedimentology, v26, pp. 859–862.

Franz, G. and Carlson, R. M. (1987) Effects of rubidium, cesium and thallium on interlayer potassium released from Transvaal vermiculite, Soil Sci. Soc. Am. Jour., v5, pp. 305.

Gambrell, R. P. and Patrick, W. H., Cu, Zn, and Cd availability in sludge-amended soil under controlled pH and redox potential conditions in Contaminants in the Vadose Zone, Bar-Yosef, B.

Garrels, R. M. and Christ, C. L. (1965) Solutions, Minerals and Equilibria. Harper and Row, New York, pp. 450.

Gayes, P.T., Scott, D.B., Collins, E.S. and Nelson, D.D. (1992) A Late Holocene sea-level irregularity in South Carolina, Society of Economic Paleontologists and Mineralogists, Special Publication, v48, pp. 154-160.

Ge-lin, Z. (1995) Origin, differentiation and geographic distribution of Chenopodiaceae, Acta Phytotaxonomica Sinica, v35, No. 5, pp. 486-504.

Giresse, P. (1989) Quaternary sea-level changes on the Atlantic coast of Africa, Sea-level changes, Basil Blackwell, London, pp. 249-275.

Glennie, K. (1970) Desert sedimentary environments, Developments in Sedimentology, Elsevier, Amsterdam, v14.

Goodsite, M. E., Rom, W., Heinemeier, J., Lange, T., Ooi, S., Appleby, P. G., Shotyk, W., Van der Knaap, W. O., Lohse, C. H. and Hansen, T. S. (2001) High-resolution AMS 14C dating of post-bomb peat archives of atmospheric pollutants, Radiocarbon, v43(2B), pp. 495–515.

Goldstein, J. (2003) Scanning electron microscopy and x-ray microanalysis, Kluwer Adacemic/Plenum Pulbishers, pp 689.

Goldstein J., Newbury D.E., Joy D.C., Lyman C.E., Echlin P., Lifshin E., Sawyer L.C. and Michael J.R. (2003) Scanning Electron Microscopy and X-ray Microanalysis. Kluwer Academic / Plenum Publishers, New York,p p 689.

Goring-Morris, A. N. and Belfer-Cohen, A. (1998) The Articulation of Cultural Processes and Late Quaternary Environmental Changes in CisJordan, Paleorient., v23(2), pp. 71-93.

Gornitz, V. and Lebedeff, S. (1987) Global sea-level changes during the past century. In Sea-Level Change and Coastal Evolution, SEPM Special Publication, No. 41.

Gornitz, V. and Seeber, L. (1990) Vertical crustal movements along the East Coast, North America, from historic and late Holocene sea level data. Tectonophysics, v178, pp.127-150.

Goudie, A. (1981) The Human Impact:Man's Role in Environmental Change, Blackwell Publishers,

Oxford, pp. 326.

Gough, L. P., Kotra, R. K., Holmes, C. W., Griggs, P. H., Crock, J. G. and Fey, D. L. (1996) Chemical analysis results for mercury and trace elements in vegetation, water, and organic-rich sediments, south Florida, USGS Open File Report, pp. 96-191.

Graham, L. C. (1974) Synthetic interferometer radar for topographic mapping, Proc. IEEE., v62, pp. 763–768.

Greeley, R. and Iverson, J. (1984) Wind as a geologic process, Cambridge University Press, New York.

Green, O. R. (2001) A manual of practical laboratory and field techniques in palaeobiology, pp 175.

GRIP (Greenland Ice-core Project Members). (1993) Climate instability during the last interglacial period recorded in the GRIP ice core, Nature, v364, pp. 203-207.

Grove, J. H. and Ellis, B. G. (1980) Extractable chromium as related to soil pH and applied chromium, Soil Sci. Soc. Am. J., v44, pp. 238.

Halbach, P., Borstel, D. and Gundermann, K. D. (1980) The uptake of uranium by organic substances in a peat bog environment on a granitic bedrock, Chem. Geol., v29, pp.117.

Haneeshkumar, V., Ramachandran, K.K., Suchindan, G.K., Samsuddin, M. and Singh, A.D. (1998) Morphostrati-graphic implications of Holocene landforms along the northern Kerala. Paper presented in National ymposium on Late Quaternary Geology and Sea Level Changes, held during November 4-6, at Cochin University of Science and Technology, Cochin, pp. 4.

Harnois, L. (1988) The CIW index, a new chemical index of weathering, Sed. Geol., v55, pp. 319–322.

Hashimi, N. H., Nigam, R., Nair, R.R. and Rajagopalan, G. (1995) Holocene sea level fluctuations on western Indian Continental margin: An update, Jour. Geol. Soc. India, v46, pp.157-162.

Heinrichs, M. L., Peglar, S. M., Bigler, C. and Birks, H. J. B. (2004) A multi-proxy palaeoecological study of Alanen Laanija¨rvi, a boreal-forest lake in Swedish Lapland, Boreas, v34, pp. 192–206.

Heinrichs, M. L., Walker, I. R. and Mathewes, R. W. (2001) Chironomid based paleosalinity records in southern British Columbia, Canada: a comparison of transfer functions, J. Paleolimnol., v26, pp. 147–159.

Hem, J. D. (1976) Geochemical controls on lead concentrations in stream water and sediments, Geochimica et Cosmochimica Acta., v40, pp. 599-609.

Hem, J. D. and Durum, W. H. (1973) Solubility and occurrence of lead in surface water, Journal of the American Water Works Association, v65, pp. 562-568.

Hendy, I. L. and Kennett, J. P. (1999) Dansgaard-Oeschger Cycles and the California Current System: Planktonic Foraminiferal Response to Rapid Climate Change in Santa Barbara Basin, Ocean Drilling Program Hole 893A, Paleoceanography, v15, pp. 30-42.

Hilgers, A., Murray, A. S., Schlaak, N. and Radtke U. (2001) Comparison of quartz OSL protocols using late glacial and Holocene dune sands from Brandenburg, Germany, Quaternary Science Reviews, v20, pp. 731–736.

Hodgson, J. F., Geering, H. R. and Norvell, W. A. (1966) Micronutrient cation complexes in soil solution, Soil Sci. Soc. Am. Proc., v29, pp. 665, v30, pp. 723.

Houghton, J. T., Jenkins, G. J. and Ephramus, J. J. Eds. (1990) Climate Change, The IPCC Scientific Assessmen, Cambridge University Press, New York.

Hyde, H.A. and Williams, D. A. (1944) The right word.,Pollen Science Circular, No. 8, pp. 6.

(IPCC) The Intergovernmental Panel of Climate Change (2007) The Fourth Assessment Report (AR4)

Jacob, K. and Sastry, V. V. (1952) Miocene foraminifera from Chavara near kollam, Travancore, Rec, Geol. Surv. India, v32, pp. 65-67.

James, B. R., Petura, J. C., Vitale, R. J. and Mussoline, G. R. (1997) Oxidation-reduction chemistry of chromium, relevance to the regulation and remediation of chromate-contaminated soils, J. Soil Contamin., v6, pp. 596.

Jayalakshmi, K., Nair, K.M., Kumai, H. and Santosh, M .(2004) Late Pleistocene-Holocene Paleoclimatic History of the Southern Kerala Basin, Southwest India, Gondwana Research, v7, pp. 585-594.

Jenny, H. (1941) Factors of soil formation: a system of quantitative pedology, McGraw-Hill, New York

Johnsson, M. J., Stallard, R. F. and Meade, R. H. (1988) First-cycle quartz arenites in the Orinoco River Basin, Venezuela and Colombia, J. Geol., v96, pp. 263–277.

Kabata-Pendias, A. (2001) Trace Elements in Soils and Plants, CRC Press, Boca Raton, Florida, pp. 365.

Kabata-Pendias, A. and Pendias, H. (2001) Trace elements in soils and plants (3rd ed.), Boca Raton, FL, CRC Press.

Kale, V. S. and Rajaguru, S. N. (1985) Neogene and Quaternary transgressional and regressional history of the west coast of India, An overview, Bull Decccan college, Res.Inst., v44, pp. 153-165.

Kerr, A. R. (2008) GEOLOGY: A Time War Over the Period We Live In, Science, v319, no. 5862, pp. 402 – 403.

Kraft, J. C., Belknap, D. F. and Demarest, J. M. (1987) In:Prediction of effects of Sea Level Changes from Paralic and Inner Shelf Stratigraphic sequences, Rampino, M. R.,

Sanders, J. E., Newman, W. S. and Konigsson, L. K.(Eds) Climate History, Periodicity and Predictability, Von Nostrand Reinhold Co, New York, pp. 166-192.

KrishnaRao, B., Bhanumurthy, P. and Swamy, A. S. R. (1990) Sedimentary Characteristics of Holocene beach in western delta of Krishna River, In sea level variation and its Impact on coastal environment, (Ed.) Rajamanikam, V., Tamil University, Tanjavur, Pub. No.131, pp. 133-148.

Krinsley, D. H. and Doornkamp J. C. (1973) Atlas of quartz sand surface textures, Cambridge University press, Cambridge, UK., pp. 91.

Krinsley, D., Friend, P. and Klimentides, R. (1976) Eolian transport textures on the surface of sand grains of early Triassic age, Geol. Soc. Am. Bull., v87, pp.130-132.

Kuenen, P. H. and Perdokw, G. (1962) Experimental abrasion 5, Frosting and defrosting of quartz grains, J. Geol., v70, pp. 648-658.

Lamb, H .F., Gasse F., Benkaddour A., Hamount, N., van der Kaars, S., Perkins, W. T., Pearce, N. J. and Roberts, C. N. (1995) Relation between century scale Holocene arid intervels in tropical and temperate zones, Nature, v373, pp. 134-137.

Lele, V.S. (1973) The miliolite limestone of Saurashtra, Western India, Sedimentary Geology, v10, pp.301–310.

Lewis, D. W. (1984) Practical Sedimentology, Van Nostrand reinhold Co. Inc., New York.

Lindsay, W. L. (1979) Chemical Equilibria in Soils, Wiley-Interscience, New York, pp. 449.

Limaye, R. B., Kumaran, K.P.N., Nair, K.M. and Padmalal, D. (2009) Cyanobacteria as potential biomarkers of hydrological changes in the Late Quaternary sediments of South Kerala Sedimentary Basin, India, Quaternary International (Article in Press)

Loveson V. J. and Rajamanickam G. V. (1999) Progradation as evidenced around a submerged ancient port, Periapatnam, Tamil Nadu, India, Indian J. Land Syst. Ecol. Stud., v12, pp. 94–98.

Ma, Y., Liu, C. and Huo, R. (2000) Strontium isotope systematics during chemical weathering of granitoids, importance of relative mineral weathering rates, J. Goldschmidt Conf. Abstr, v5, pp. 657.

Mahaney, W. C. (2005) Atlas of Sand Grain Surface Textures and Applications, pp. 221

Mahaney, W. C. and Kalm, V. (Eds.) (1996) field guide for the International Conference on Quaternary Glaciation and Paleoclimate in the Andes mountains, Quaternary Surveys, Toronto.

Mahaney, W. C., Dohm, J., Baker, V. R., Newsom, H., Malloch, D., Hancock, R. G. V., Campbell, I., Sheppard, D. and Milner, M. W. (2001) Morphogenesis of Antartic Paleosols, Mrtian analog, Icarus, v154, pp. 113-130.

Maher, B. A. and Thompson, R. (1999) Quaternary Climates, Environments, and Magnetism, Cambridge University Press, Cambridge, pp. 81–125.

Margolis, S. and Krinsley, D. (1971) Submicroscopic frosting on eolian and subaqueous quartz sand grains, Geol. Soc. Am. Bull., v82, pp. 3395-3406.

Margolis, S. V. and Krinsley, D. H. (1974) Process of formation and environmental occurence of microfeatures on detrital quartz grains, Am. J. Sci., v274, pp. 449-464.

Martínez-Cortizas, A., Pontevedra-Pombal, X., García- Rodeja, E., Nóvoa-Muñoz, J. C. and Shotyk, W. (1999) Mercury in a Spanish peat bog, archive of climate change and atmospheric metal deposition, Science, v284, pp. 939– 42.

Martins, G. R. (1965) Significance of skewness and Kurtosis, in environmental interpretation, Journal of sedimentary petrology, v35, pp. 768-776.

Mason, C. C. and Folk, R. L. (1958) Differentiation of beach, dune and eolian flat environments by size analysis, Mustang Island, Texas, Jour. Sed. Pet., v28, pp. 211-226.

Mathur, U. B. (2005) Quaternary Geology: Indian Perspective, Geol. Soc. India Memoir, v63, pp. 344.

Mayewski, P. A., Rohling, E. E., Stagerc, J. C., Karlend, W., Maascha, K. A., Meeker, D. L., Meyerson, E. A., Gasse, F., Van Kreveld, S., Holmgrend, K., Lee-Thorph, J., Rosqvist, G., Rack, F., Staubwasser, M., Schneider, R. R. and Steig, E. J. (2004) Holocene climate variability, Quaternary Research, v62, pp. 243 – 250

McKenzie, R. M. (1975) The mineralogy and chemistry of soil cobalt, in Trace Elements in Soil-Plant- Animal Systems, Nicholas, D. J. D. and Egan, A. R, Eds., Academic Press, New York, v83.

McLennan, S. M. (1993) Weathering and global denudation, J. Geol., v101, pp. 295–303.

McLennan, S. M., Hemming, S., McDaniel, D. K. and Hanson, G. N. (1993) Geochemical approaches to sedimentation provenance, and tectonics, In Johnsson, M. J. and Basu, A. (Eds.) Processes controlling the composition of clastic sediments, Geol. Soc. Am. Spec. Pap., v284, pp. 21–40.

Meijerink, A. M. J. (1971) Reconnaissance Survey of the Quaternary Geology of the Cauvery deltas, Journal Geol. Society, India, v12, pp. 113–124.

Mejdahl , V. (1979). Thermoluminescent dating: beta-dose attenuation in quartz grains. Archaeometry, v21, No.1, pp. 61.

Mejdahl, V., Butter-Jensen, L. and Murray, A. S. (1999) New light on OSL Quaternary Science Reviews, v18, No.2, pp. 303-309.

Miller, R. and Olson, E. (1955) The statistical stability of Quantitative properties as a fundamental criterion for the study of environments, J. Geol., v63, pp. 376-387.

Mishra, S. (1982) On the effects of basalt weathering on the distribution of Lower Palaeoliths sites in the Deccan, Bulletin of the Deccan College Post-Graduate and Research Institute, v41, pp. 107–151.

Mishra, S. P. (1982) New genetic model for base metals in the Aravalli Region, India, Symposium on Metall geny of the Precambrian, I.G.C.P., Project 91, pp. 63-70.

Moiola, R. J. and Weiser, D. (1968) Textural parameters, an evaluation, J. Sediment. Petrol., v38, pp. 45-53.

Morner, N. A. (1992) Sea-level changes and Earth's rate of rotation, J. Coastal Res.,v8, pp. 966-971.

Morner, N. A. (1980b) A 10,700 year's paleotemperature record from Gotland and Pleistocene/ Holocene boundary events in Sweden, Boreas, v9.

Morner, N. A. (1995) Rapid changes in coastal sea level, Journal of Coastal Research, v12, pp. 797–800.

Mukherjee, A. B. (1998) Nickel a review of occurrence, uses, emissions, and concentration in the environment in Finland, Environ., Rev., v6, pp. 173.

Murray, A. S. and Robert, R. G. (1997) Determining the burial time of single grains of quartz using optically stimulated luminescence, Earth and Planetary Science Letters, v152, pp. 163–180.

Nageswara Rao, J.(1979) Studies on the Quaternary Formation of the Coastal Plains Flanking Pulicat Lake, Geological Survey ot India, Misc. Publi., No.45, pp. 231-233.

Nageswar Rao, C. R., Stowe, L. L., McClain, E. P. and Sapper, J. (1988) in Aerosol and Climate (eds Hobb, P. V. and McCormick), Deepak Publication, Hampton, pp. 69-79.

Naidu, P. D. (1999) A review on Holocene climate changes in the Indian Subcontinent, Memoir Geological Society of India, No.42, pp. 303-314.

Nair, K. K. (1991) Geomorphological and Quarternary geological studies along the coastal plains in parts of Cannanore and Kasargod districts Kerala., Jour. Geol. Soc. India, v29, pp. 433-439.

Nair, M.M. (1974) Coastal geomorphology of Kerala, Jour.Geol.Soc.India, v29, No.4, pp. 450-458.

Nair, K. M. and Padmalal, D. (1998) Quaternary sea-level oscillations, geological and geomorphological evolution of South Kerala Sedimentary Basin. Project proposal submitted to Department of Science and Technology, New Delhi, pp. 1–36

Nair, K.M., Padmalal, D. and Kumaran, K.P.N. (2006) Quaternary Geology of South Kerala Sedimentary Basin– An outline, Journal of Geological Society of India, v67, pp. 165-179.

Nair, R.R. and Hashmi, N.H. (1990) Distribution and dispersal of clay minerals on the western continental shelf of India, Mar. Geol., v50, pp. M1-M9.

Nair R.R., Hashimi, N.H. and Gupta, M.V.S. (1974) Holocene limestone of part of the western continental shelf of India, Journal of the Geological Society of India, v20, pp.17-20.

Nair, R.R., Hashimi, N.H., Kidwai, R.M., Guptha, M.V.S., Paropkari, A.L., Ambre, N. V., Muralinath, A.S., Mascarenhas, A. and D'Costa, G.P. (1975) Topography and sediments of western continental shelf of India-Vengurla to Mangalore, Indian J. Mar. Sci., v7, pp. 224-230.

Nair, K. M. and Padmalal, D. (1995) Quaternary geology of South Kerala sedimentary basin – An outline., J. Geol. Soc. India, v67,No. 1, pp. 65–179.

Narayana, A.C., Priju, C.P. and Chakrabarti, A. (2001) Identification of a palaeodelta near the mouth of Periyar river in central Kerala, Journal of the Geological Society of India, v57, pp. 545-547.

Nakiboglu, S. M. and Lambeck, K. (1991) Secular sea-level change, Glacial Isostasy, Sea-Level and Mantle Rheology, Sabadini, R., Lambeck, K. and Boschi, E. (Eds.), Kluwer Academic, pp. 237–258.

Nambiar, A. R. and Rajagopalan, G. (1995) Radiocarbon dates of sediment cores from inner continental shelf off Taingapatnam, south west coast of India, Current Science, v68, pp. 1133-1137.

Nesbitt, H. W. and Young, G. M. (1984) Early Proterozoic climates and plate motions inferred from major element chemistry of lutites, Nature, v299, pp. 715–717.

Nesbitt, H. W., Markovics, G. and Price, R. C. (1980) Chemical processes affecting alkalis and alkaline earths during continental weathering, Geochim., Cosmochim.Acta., v44, pp. 1659–1666.

Nesbitt, H. W., Young, G. M., McLennan, S. M. and Keays, R. R. (1996) Effects of chemical weathering and sorting on the petrogenesis of siliclastic sediments, with implications for provenance studies, J. Geol., v104, pp. 525–542.

Neuendorf, K. K. E., Mehl, Jr., J. P. and Jackson, J. A. (Eds.) (2005) Glossary of geology (5th ed.), Washington DC, American Geological Institute.

Newman, W. A., Genes, A.N. and Brewer, T. (1985) Pleistocene geology of northeastern Maine, Geological Society of America, Special Paper, v197, pp. 59-70.

Nieboer, E. and Richardson, H. S. (1980) The replacement of the nondescript term 'heavy metals' by a biologically and chemically significant classification of metal ions, Environ. Pollut. Ser. B., v3.

Nigam, R. (1993) Foraminifera and changing pattern of monsoon rainfall, Current Science, v64, pp. 935-937.

Niyogi, D. (1975) Quaternary geology of the coastal plain in West Bengal and Orissa, Indian Journal of Earth Sciences, v2, pp. 51-61.

Ohta,T. and Arai,H.(2007): Statistical empirical index of chemical weathering in igneous rocks: A new tool for evaluating the degree of weathering. Chemical Geology, V 240, pp 280-297

Oliver, D. P., Tiller, K. G., Conyers, M. K., Slattery, W. J., Alston, A. M. and Merry, R. H. (1996)

Effectiveness of liming to minimize uptake of cadmium by wheat and barley grain grown in the field, Aust. J. Agric.Res., v47, pp. 1181.

Olley, J., Caitcheon, G. and Murray, A S. (1998) The distribution of apparent dose as determined by optically stimulated luminescence in small aliquots of fluvial quartz, implications for dating young sediments, Quaternary Geochronology (Quaternary Science Reviews) v17, pp. 1033–1040.

Page, S.J. and Stainton, M.P. (1998) Acid-induced changes in DOC quality in an experimental whole lake manipulation. Environ. Sci. Technol., v32, pp. 2954–2960.

Pandarinath, K., Verma, S. P. and Yadava M G. (2004) Dating of Sediment layers and sediment accumulation studies along the western continental margin of India, A review, Int. Geol. Rev. v46, pp. 939–956.

Parker, T.W.(1970) Allophane and halloysite formation in a volcanic ash bed under different moisture conditions. Soil Sci.,V 138 No.5 pp: 360-364

Paul, J. and Babu, D. S. S. (2008) Quaternary evolution of Thiruvananthapuram coast, Kerala, Earth System Dynamics, CESS annual report, 2006-2007.

Pascoe, K. J. (1961) An Introduction to the Properties of Engineering Materials, Blackie, London.

Partridge, T. C., Scott, L., Hamilton, J. E. (1999) Synthetic reconstructions of southern African environments during the Last Glacial Maximum (21–28 kyr) and the Holocene Altithermal, (8–6 kyr), Quaternary International, v57/58, pp. 207–214.

Patro, B. C. and Sahu, B. K. (1977) Discriminant analysis of sphericity and roundness data of elastic quartz grains in river, beaches, and dunes, Sed.Geol., v19, pp. 301-311.

Paulose, K. V. and Narayanaswamy, S. (1968) The Terrtiaries of Kerala coast. Mem. Geol. Soc. India, v2, pp. 300-308.

Peltier, W. R. and Tushinghan, A. M. (1989) Global sea level rise and the greenhouse effect. Might there be a connection? Science, v244, pp. 806-810.

Peltier, W. R. (2001) Global istostatic adjustment and modern instrumental records of relative sea level history. In:Douglas, B. C., Kearney, M. S. and Leatherman, S. P. (Eds.), Sea Level Rise — History and Consequences, Academic Press, pp. 65–95.

Peltier, W. R. (2004) Global isostacy and the surface of the ice-age Earth: The ICE-5G (VM2) model and GRACE. Ann. Rev. Earth Planet, Science, v32, pp. 111–149.

Pendias, A. K. and Wiacek, K. (1986) Effects of sulphur deposition on trace metal solubility in soils, Environ. Geochemistry, Health, v8, pp. 9.

Pendias, A .K. and Pendias, H. (2001)Trace elements in soils and plants 3rd ed., pp. 331.

Piccolo, A. and Cozzolino, A. (2002) Polymerization of dissolved humic substances catalyzed by peroxidase. Effects of pH and humic composition Organic Geochemistry, v33, No.3, pp.281-294.

Pirazzoli, A. P. (1991) World Atlas of Holocene Sealevel Changes, Elsevier, pp. 300.

Pirazzoli, P. A. (2005) A review of possible eustatic, isostatic and tectonic contributions in eight late-Holocene relative sea-level histories.

Potts, D. C. (1983) Evolutionary disequilibrium among Indo-Pacific corals, Bulletin of Marine Science, v33, pp. 619-632.

Potts, R. (1996) Evolution and climatic variability, Science, v273, pp. 922–923.

Powar, S.D., Venkataramana, B., Mathai, T. and Mallikarjuna, C. (1983) Progress Report, Geological Survey of India, Trivandrum

Prell, W. L. and Curry, W. B. (1981) faunal and isotopic indices of monsoonal upwelling, Western Arabian Sea,Oceanologica Acta, v4, No.1, pp. 91-98.

Prell, W .L., Marvil R E. and Luther, M.E. (1990) variability in upwelling fields in the northwestern Indian ocean 2, data model coparison at 9000 years B.P. Paleoceanography, v5, No.3, pp. 447-457.

Prell, W. L. and STREETER, H. F. (1982) Temporal and spatial patterns of monsoonalupwelling along Arabia, a modern analogue for the interpretation of Quaternary SST anomalies, Journal of Marine Research, v40, pp. 143-155.

Prescott, J. R. and Hutton, J. T. (1995) Environmental dose rates and radioactive disequilibrium from some Australian luminesce dating sites, Quaternary science Reviews, v14, pp. 439-448.

Prescott, J. R. and, Robertson, G. B. (1997) Sediment dating by luminescence, a review, Radiation Measurements, v27, pp. 893-922.

Priju, C. P. and Narayana, A. C. Evolution of Coastal Landforms and Sedimentary Environments of the Late Quaternary Period along Central Kerala, Southwest Coast of India, Journal of Coastal Research, v39, pp 1898 – 1902.

Prithviraj, M. and Prakash, T.N. (1991) Surface Microtextural study of detrital quartz grains off inner shelf sediments off Central Kerala coast. Indian Journal of Marine Science, v20, pp. 3-16.

Pye, K. and Tsoar, H. (1990) Aeolian sand and sand dunes. Unwin Hyman, Boston, MA.

Quantin, C., Becquer, T., Bouiller, J. H. and Berthelin, J. (2002) Redistribution of metals in a New Caledonia Ferralsol after microbial weathering, Soil Science Society of America Journal, v66, pp. 1797–1804.

Radhakrishna,T., Maluski, H.,Mitchell,J.G and Mathew , J. (1999) 40Ar/39 Ar and K-Ar Geoochronology of the dykes from the south Indian granulite terrane. Tectonophysics v.304. p.109-129

Radhakrishnan, B. P. (1998) Holocene Chronology and Indian pre-history. Jour. Geol. Soc. Indian.

v51, pp. 133-138.

Raha, P. K., Sinha Roy, S. and Rajendran, C.P. (1983) A new approach to the lithostratigraphy of the cenozoic sequence of Kerala, Jour. Geol. Soc. India, v24, pp. 114-115.

Rajamanickam, G. V. and Gujjar, A. R. (1992) Gtrain size studies on the near shore sediments of Jaigad Anbwah and Varvada Bays, Maharashtra, Journal of Geological Society of India, v49, pp. 567-576.

Rajamanickam G. V. and Gujar A. R. (1985) Indications given by median distribution and CM patterns on clastic sedimentation in Kalbadevi, Mirya and Ratnagiri bays, Maharashtra, India, Giorn. Geol., v47, pp. 237–251.

Rajamanickam, G. V. and Gujar A. R. (1984) Sediment depositional environment in some bays in central west coast of India, Indian J. Mar. Sci., v13, pp. 53–59.

Rajendran, C. P., Rajagopalan, G. and Narayanaswami, (1989) Quaternary Geology of Kerala, Evidence from Radiocarbon dates, Jour. Geo. Soc. India, v33, pp. 218-222.

Ramachandran, C. (1992) P-wave velocity in granulites from south India, Implications for the contnental crust, Geophysics, v201, pp. 187-198.

Ramakrishnan, M and Vaidyanathan, R. (2008) Geology of India, Geological Society of India, Bangalore, Vol. 2, p 850.

Rao, K. K. (1996) Foraminiferal fauna from the cochin Backwaters, Biological indicators of manmade changes in the environment, Jour. Aquatic Biol., v11, pp. 9-16.

Rao, P. S., Ramaswamy V. and Thwin S. (2005) Sediment texture, distribution and transport on the Ayeyarwady continental shelf, Andaman Sea, Mar. Geol., v216. No. 4, pp. 239–247.

Rao, V. P. and Thamban, M. (1994) Evidence of late quaternary climate change from the sedimentary rocks of the Western Continental Shelf of India, geoscience for energy and environment, Annual Convention, Indian Geophysical union, Hyderabad, pp. 20-22.

Rao, V. P., Veeryya, M., Thamban, M. and Wagle, B. G. (1996) Evidence of Late Quaternary neotectonic activity and sea-level changes along the western margin of India, Currrent Science, v71, pp. 213-219.

Rachna Raj and Yadava, M. G. (2009) Late Holocene uplift in the lower Narmada basin, western India Current science, v96, pp. 985-988.

Ravindrakumar, G. R. and Chacko, T. (1994) Geothermobarometry of mafic granukite and metapelite from the Palghat gap sout India, Petrolgical evidence for isothermal uplift and rapid cooling, Jour. Met. Geol., v12. No. 4, pp. 479-492.

Reddy, P.R., Venkateswarlu, N., Prasad, A.S.S.S.R.S. and Koteswara Rao, P. (2002) Basement Structure Below the Coastal Belt of Krishna-Godavari Basin: Correlation Between Seismic Structure and Well Information, Gondwana Research, v5, pp. 513-518.

Rittenhouse, G. R. (1943) Geol. Soc. Amer. Bull., v54, pp. 1725 -1789.

Roberts, N. (1998) The Holocene, an environmental history, Blackwell, Oxford, 2eds.

Roberts, N., Reed, J. M., Leng, M. J., Kuzucuog˘lu, C., Fontugne, M., Bertaux, J., Woldring, H., Bottema, S., Black, S., Hunt, E. and Karabıyıkog˘lu, M. (2001) The tempo of Holocene climatic change in the eastern Mediterranean region, new highresolution crater-lake sediment data from central Turkey, The Holocene, v11, pp. 721–736.

Roberts, N. and Rosen, A. (2009) Diversity and complexity in the first farming communities of Southwest Asia, new insights into the economic and environmental basis of Neolithic Çatalhöyü k, Current Anthropology, v50(3), pp. 393-402.

Roberts, N., Stevenson, T., Davis, B., Cheddadi, R., Brewster, S. and Rosen, A. (2004) Holocene climate, environment and cultural changein the circum-Mediterranean region, In Battarbee, R. W., Gasse, F., Stickley, C. (Eds.), Past Climate Variability through Europe and Africa. Springer, Dordrecht, pp. 343–362.

Roberts, R. G. (1997) Luminescence dating in archaeology, from origins to optical, Radiation Measurements, v27, pp. 819–892.

Rose, W. I., Jr., Grant, N. K. and Easter, J. (1979) Geochemistry of the Los Chocoyos Ash, Quezaltenango Valley, Guatemala. Geol. Soc. Am. Spec. Pap., v180, pp. 87-99.

Rubey, W. (1933) Settling velocities of gravel, sand and silt narticles, Am. J. Sci., v25, pp. 125-128

Ruxton, B.P. (1968) Rates of weathering of Quaternary volcanic ash in northeast Papua, Trans. 9th Int. Congr. Soil Sci. V 4 pp. 551–560

Ryan, W. (1924) The Microthyriaceae of Porto Rico, Mycological Society of America, pp. 177-179.

Sahu, B. K. (1964) Depositional Mechanisms from the size analysis of clastic sediments, J. Sediment. Petrol., v34, pp. 73-83.

Sambasiva Rao, M. (1982) Morphology and Evolution of modern Cauvery Delta, Tamil nadu, India,Transaction Institute of Indian Geographers, No.4, pp. 68-78.

Samsuddin, M. (1986) Textural differentiation of foreshore and breaker zone sediments on Northern Kerala coast, India, Sed. Geol., v46, pp. 135-145.

Samsuddin, M., Ramachandran, K. K. and Dora, Y. L. (1992) Quartz grains surface textures as indicators of deposited beach and strand plain sediments along the North Kerala coast. Jour. Geol. Soc. India, v40, pp. 501-502.

Santhosh, M. (1987) Cordierite gneiss of southern Kerala, India: petrology, fluid inclusions and implications for crustal uplift history, Contrib.Minera,.Petrol, v96, pp. 343-356.

Saraswathi, P. K., Roger, K. M. and Raja, R. (2006) Disequilibrium effect in oxygen and carbon isotopic composition of modern foraminifera from Lakshadweep, India, Journal of Geological Society of India, v68, pp. 1003-1007.

Satkūnas, J. and Stančikaitė, M. (2009) Pleistocene and Holocene palaeoenvironments and recent processes across NE Europe, Quaternary International, v207, pp.13.

Sen, P. K. and Banerjee, M. (1990) Palyno-plankton stratigraphy and environment changes during the Holocene in the Bengal Basin, India, Rev. Palacobot. Palynol., v65, pp. 25–35.

Schneider, S. H. (1972) Cloudiness as a global climatic feedback mechanism, The effects on the radiation balance and surface temperature variations in cloudiness. J. Atmos. Sci., v29, pp. 1413-1422.

Schulz, H., von Rad, U. and von Stackelberg, U. (1996) Laminated sediments from the oxygen minimum zone of the NE Arabian Sea. In: Kemp, A.E.S. (Eds.) Palcoeclimatology and Paleoceanography from Laminated Sediments, Geological Society, London, Special publications, v116, pp. 185- 207.

Schumm, S. A. (1969) Geomorphic implications of climate change. In, Chorley, R.J. (Ed.), Introduction to Fluvial Processes, Methuen, London, pp. 202–210.

Selvaraj, K. and Chen, C. T. A. (2006) Moderate Chemical Weathering of Subtropical Taiwan, The Journal of Geology, v114, pp. 101–116.

Semeniuk, V. and Semeniuk, C. A. (1997) A geomorphic approach to global classification for natural inland wetlands and rationalization of the system used by the Ramsar Convention – a discussion, Wetland Ecology and Management, v5, pp. 145-156.

Shepard, F.P. (1960) Rise of sea-level along north-west Gulf of Mexico, Recent sediments, In,Shepard, F.P., Phleger, F.B. and Van Andel, T.J.H. (Eds.) Recent Sediments, Northwest Gulf o f Mexico, American Association of Petroleum Geologists, Tulsa, pp. 338 - 344.

Shepard, F. P. (1963) Thirty-five thousand years of sea level, In Essays in marine geology,Univ. S. Calif. Press, Los Angeles.

Shiller, A. M. and Frilot, D. M. (1996) The geochemistry of gallium relative to aluminum in Californian streams Geochimica et Cosmochimica Acta, v60. No. 8, pp. 1323-1328.

Shotyk, W., Weiss, D., Appleby. P. G., Cheburkin, A. K., Frei, R., Gloor, M., Kramers, J. D., Reese, S. and van der Knaap, W.O. (1998) History of atmospheric lead deposition since 12,370 14C yr BP recorded in a peat bog profile, Jura Mountains, Switzerland, Science, v281, pp. 35–40.

Singh, A.D., Ramachandran, K. K., Samsuddin, M., Nisha, N. R. and Haneeshkumar, V. (2001) Significance of Pteropods in deciphering the late quaternary sea-level history along the southwestern Indian shelf. Geo-Marine Letters, v20. No.4, pp. 243-252.

Singh, G. (1971) The Indus vally culture seen in the context of postglacial climatic and ecological studies in the northwest India, Archaeology and physical Anthropology in Oceanica, v6, pp.177-189.

Sinha, R. and Friend, P.F. (1994) River systems and their sediment flux, Indo-Gangetic plains, northern Bihar, India. Sedimentology, v41, pp. 825-845.

Sinha, R. and Sarkar, S. (2009) Climate-induced variability in the Late Pleistocene–Holocene fluvial and fluvio-deltaic successions in the Ganga plains, India: A synthesis Geomorphology, v113, No.3-4, pp. 173-188.

Sinha, R., Tandom, S. K., Gibling, M. R., Bhattacharjee, P. S. and Dasgupta, A. S. (2005) Late Quaternary geology and alluvial stratigraphy of the Ganga basin, Himalayan Geology, v26 (1), pp. 223-240.

Smith, D. G. (1986) Anastomosing river deposits, sedimentation rates and basin subsidence, Magdalena river, northwestern Colombia, South America. Sediment. Geol., v46, pp.177–196.

Smith, K. S. and Huyck, H. L. O. (1999) An overview of the abundance, relative mobility, bioavailability, and human toxicity of metals; in Plumlee, G.S.,and Logsdon, M. J. (Eds.), The Environmental Geochemistryof Mineral Deposits, Part A, Society of Economic Geologists, Reviews in Economic Geology, v6A, pp. 29-70.

Sommer, M., Halm D., Weller, U., Zarei, M. and Star, K.(2000) Lateral podzolization in a granitic landscape, Soil Science Society of America Journal, v64, pp.1434–1442.

Snyder, C. T., Hardman, G. and Zdenek, F. F. (1964) Pleistocene Lakes in the Great Basin, U. S. Geological Survey Miscellaneous Geological Investigations Map, pp. 416.

Snyder, J. A., Werner, A., Miller, G. H. (2000) Holocene cirque glacier activity in western Spitsbergen, Svalbard, sediment records from proglacial Linne´vatnet. Holocene, v10, pp. 555–563.

Sparks, D. L. (1986) Kinetics of reactions in pure and mixed systems, in Soil Physical Chemistry, Sparks, D. L., (Ed.), CRC Press, Boca Raton, FL., pp. 83.

Sposito, G. and Matigod, S. (1980) Geochem, Computer Program for the Calculation of Chemical Equilibria in Soil Solutions and Other Natural Water Systems, University of California, Riverside, CA., pp. 92.

Srinivasa Rao, P., Krishna Rao, G., Durgaprasad Rao, N. V. N. and Swamy, A. S. R. (1990) Sedimentation and Sea level variations in Nizampatnam Bay, east coast of India. Indian Jour. Mar. Sci., v19, pp. 261-264.

Staubwasser, M. and Weiss, H. (2006) Holocene climate and cultural evolution in late prehistoric-early historic West Asia. Quaternary Research, v66, pp. 372-387.

Stevenson, F. J. (1983) Trace metal-organic matter interactions in geologic environments, in Trace Elements in Petrogenesis, Augustithis, S. S., (Ed.)., Theophrastus Publ., Athens, pp. 671.

Stokes, S., Child, A. and Bourke, M. C. (2003) Optical age estimates for hyper-arid fluvial deposits at Homeb, Namibia Quaternary Science Reviews, v22, No.10-13, pp. 1099-1103.

Strawn, D., Doner, H., Zavarin, M. and McHugo, S. (2002) Microscale investigation into the geochemistry of arsenic, selenium, and iron in soil developed in pyritic shale materials, Geoderma, v108, pp. 237–257.

Streif, H. (1978) A new method for the representation of sedimentary sequences in coastal regions, Proceedings of the 16th Coastal Engineering Conference, ASCE/Hamburg, West Germany, pp. 1245–1256.

Streif, H. (1998) Die Geologische Ku¨ stenkarte von Niedersachsen 1:25.000—eine neue Planungsgrundlage fu¨ r die Ku¨ stenregion, Zeitschrift fu¨ r angewandte Geologie, v44, pp. 183–194.

Stuiver, M. and Pearson, G. W. (1992) Calibration of the 14C time scale, 2500-5000BC. In, Radiocarbon Dating after Four Decades: An Interdisciplinary Perspective. R.E Taylor., Long, A., and Kra, R.S. (Eds.) Co-publication with Radicarbon, Springer-Verlag, NY, pp. 19-33.

Stuiver, M. and Pearson, G. W. (1993) High-precision bidecadal calibration of the radiocarbon time scale, AD 1950-500 BC and 2500-6000 BC. Radiocarbon, v35(1), pp.1-25.

Suchindan, G.K., Samsuddin, M., Ramachandran, K.K. and Haneeshkumar, V. (1997) Holocene coastal landforms along the northern Kerala coast and their implications on sea level changes. Paper presented in International Seminar on 'Quaternary sea-level variation, shoreline displacement and coastal environment' held at Tamil University Thanjavur.

Sukumar. (1993) Deforestation and Ecological imbalance in Palani Hills of Tamilnadu. Indian Geographical Journal, v67(2), pp. 85-87.

Sukumar, R., Ramesh, R., Pant, R.K.. and Rajagopalan, G. (1993) A C13 record of Late Quaternary climate change from tropical peats in southern India, Nature , v364, pp. 703-705.

Tanner. W. F. (1995) Environmental clastic granulometry,Florida, Geol. Surv.Special publ. No.40. pp. 1-144.

Thamban, M.,Kawahata, H., and Purnachandra Rao, V. (2007) Indian Summer Variability during the Holocene as Recorded in sediments of the Arabian sea, Timing and Implications Jornal of oceanography, v63, pp. 1009-1020.

Thamban, M., Rao, V. P., Schneider, R.R. and Grootes, P. M. (2001) Glacial to Holocene fluctuations in hydrography and productivity along the Southwest continental margin of india, Palaeogeorgr., v165, pp.113-127.

Thanabalasingam, P. and Pickering, W. F. (1985) The sorption of mercury II by humic acids, Environ. Pollut. Series B, v9, pp. 267.

Thrivikramji, K.P. and Ramasarma, M. (1983) Implications of sedimentary structural facies of a calcareous sandstone body, Jour. Geol. Soc. India, v24, pp. 203-207.

Tripathi, J. K. and Rajamani, V. (1999) Geochemistry of the loesic sediments on Delhi ridge, eastern Thar desert, Rajasthan: implication for exogenic proceses. Chem. Geol., V **155**, pp 265–278

Trudgill, S. T. (1988) Soil and Vegetation Systems, 2nd ed, Claderon Press, Oxford, Bolt, G. H. and Bruggenwert, M. G. M., Eds, Soil Chemistry. A Basic Elements, Elsevier, Amsterdam, pp. 281.

Tushingham, A. M. and Peltier, W. R. (1991) ICE-3G, A new global model of late Pleistocene deglaciation based upon geophysical predictions of post-glacial relative sea-level change. J. Geophys. Res., v96, pp. 4497–4523.

Tushingham, A. M. and Peltier, W. R. (1993) Relative Sea Level Database. IGPB Pages/World Data Center-A for Paleoclimatology Data Contribution Series, pp. 93-106, NOAA/NGDC Paleoclimatology Program, Boulder, CO, USA.

Udden, J.A. (1914) Mechanical composition of some clastic sediments. Bulletin of the Geological Society of America, v25, pp. 655–744.

Unnikrishnan, A. S., Rupa Kumar, K., Fernandes, S. E., Michael, G. S. and Patwardhan, S. K. (2006) Sea level changes along the Indian coast, observations and projections, Curr. Sci. v90, pp. 362–368.

Unnikrishnan, A. S. and Shankar, D. (2007) Are sea-level-rise trends along the coasts of north Indian Ocean coasts consistent with global estimates? Global and Planetary Change, v57, pp. 301-307.

Vaidhyanadhan, R. and Ramakrishnan, M. (2008) Geology of India, vI, pp.556, vII, pp. 994.

Van Loon, J. C. (1985) Selected Methods of Trace Metal Analysis: Biological and Environmental Samples. John Wiley and Sons, NewYork.

Vasudeva, C. (1983) Report on the exploration for industrial minerals in the palaeo and sub recent drainage channels in parts of Trivandrum , Report of Department of Mining and geology, Government of Kerala.

Velichko, A.A., Kurenkova E. I. and Dolukhano P. M. (2009) Human socio-economic adaptation to environment in Late Palaeolithic, Mesolithic and Neolithic Eastern Europe Quaternary International, v203. No.1-2, pp. 1-9.

Verma, K. K. and Mathur, U. B. (1988) Tertiary-Quaternary Stratigraphy area, southern Saurashtra, Gujarat, Geol. Surv. India. Pub., v11,pp. 333-345.

Verstappen, H. T. H. (1989) Geomorphology in S. and SE. Asia, Proceedings, Colloquim Royal Academy of Overseas Sciences, Brussels, Geo-Eco-Trop, v16, pp. 101-147.

Von Engelhardt, W. (1940) Die Anisotropie der Teilbarkeit des Quarzes' Nachr. Ahad'.Wiss. Gdtti,ngm. Math. Phys. Klasse, pp. 43-56.

Wagle, B.G. (1982) Geomorphology of the Goa Coast, Proceedings of the Indian Academy of Sciences (Earth-and Planetary Sciences), v91, pp. 105-117.

Wagle, B.G., Vora, K.H., Karisiddaiah, S.M., Veerayya, M. and Almeida, F. (1994) Holocene submarine terraces on the western continental shelf of India, implications for sea-level changes, Mar. Geol., v117, pp. 207-225.

Walker, M. J. C., Coope, G. R., Sheldrick, C., Turney, C. S. M., Lowe, J. J., Blockley, S. P. E. and Harkness, D. D. (2003) Devensian Lateglacial environmental changes in Britain: a multi-proxy environmental record from Llanilid, South Wales, UK. Quaternary Science Reviews, v22. No.5, pp. 475-520.

Wallace, R. E. (1977) Profiles and ages of young fault scarps, north-central Nevada, Geological Society of America Bulletin, v88, pp. 1267–1281.

Wallace, W. (2001) Stratigraphy and Distribution of Eolian Sand Dunes in the Glacial Lake, Hind Basin, Manitoba, Canada. M.Sc. thesis. University of Wisconsin-Madison, pp. 63.

Watts, W. A. (1980) Regional variation in the response of vegetation to late glacial climatic events in Europe, In, Lowe.

Wentworth, C.K. (1922) A scale of grade and class terms for clastic sediment. Journal of Geology, v30, pp. 77–392.

Wedepohl, K. H. (1971) Environmental influences on chemical composition of shales and clays, Physics and Chemistry of the Earth, Pergamon, Oxford, pp. 307-331. J. J. et al. eds. Studies in the Lateglacial of North-west Europe, Pergamon Press, Oxford, pp. 1-21.

Wedepohl, K. H. (1995) The composition of the continental crust Geochimica et Cosmochimica Acta, v59. No.7, pp. 1217-1232.

Wenchuan, Q. U., Morrison, R. J., West. and Chenwei, Su. (2006) Organic matter and benthic metabolism in Lake Illawarra, Australia Continental Shelf Research, v26. No.15, pp. 1756-1774.

White, S. (1977) Geological significance of recoery and recrystallization process in quartz. Technophysics, v39, pp. 143-170.

White, J. W. C., Ciais, P., Figge, R. A., Kenny, R. and Markgraf, V. (1994) A high-resolution record of atmospheric CO2 content from carbon isotopes in peat, Nature, v367, pp. 153–156.

White, J. C., Penny, D., Kealhofer, L. and Maloney, B. (2004) Vegetation changes from the late Pleistocene through the Holocene from three areas of archaeological significance in Thailand, Quaternary International, v113, pp. 111–132.

Williams, M. A. J. and Clarke, M. F. (1995) Quaternary geology and prehistoric environments in the Son and Belan valleys, North Central India, Geological Society of India, pp. 282-307.

Williams, M. A. J. and Clarke, M. F. (1984) Late Quaternary environments in North-Central India, Nature, v308, pp. 633-35.

Williams, M. A. J. and Faure, H. (Eds.) (1980) The Sahara and The Nile, Quaternary Environments and Prehistoric Occupation in Northern Africa.

Williams, J. W., Shuman, B. and Bartlein, J. B. (2009) Rapid responses of the prairie-forest

ecotone to early Holocene aridity in mid-continental North America Global and Planetary Change, v66, pp. 195-207

Willard, D.A. (1994) Palynological record from the North Atlantic region at 3 Ma: vegetational distribution during a period of global warmth Review of Palaeobotany and Palynology, v83, No. 4, pp. 275-297.

Willard, D. A., and Edwards, L. E. (2000) Palynomorph biostratigraphy and paleoecology of subsurface upper Neogene and Quaternary sediments in southern Jackson County, Mississippi, in Gohn, G.S., ed., Stratigraphic framework of the Neogene and Quaternary sediments of the Mississippi coastal zone, Jackson County, Mississippi, U.S. Geological Survey Bulletin.

Wilson, M. J. (2004) Weathering of the primary rock-forming minerals, processes, products and rates, Clay Minerals, v39, pp. 233–266.

Wintle, A. G. and Catt, J. A. (1985) Thermoluminescence dating of Dimlington stadial deposits in eastern England, Boreas, v14, pp. 231–234.

Wintle, A. G., Dijkmans, J. W. A. and van Mourik, J. M. (1992) Thermoluminescence dating of aeolian sands from polycyclic soil profiles in the southern Netherlands Quaternary Science Reviews, v11. No.1-2, pp. 85-92.

Wintle, A. G. and Murray, A. S. (2000) Quartz OSL, effects of thermal treatment and their relevance to laboratory dating procedures, Radiation Measurements, v32, pp. 387–400.

Wronkiewicz, D. J. and Condie, K. C. (1987) Geochemistry of Archean shales from the Witwatersrand Supergroup,South Africa, source-area weathering and provenance, Geochim. Cosmochim, Acta, v51, pp. 2401–2416.

Wronkiewicz, D. J. and Condie, K. C.(1989) Geochemistry and provenance of sediments from the Pongola Supergroup, South Africa, evidencefor a 3.0-Ga-old continental craton, Geochim. Cosmochim, v53, pp. 1537–1549.

Yang, B., Wang, J., Bräuning, A., Dong, Z. and Esper, J. (2009) Holocene Climate Variability in Arid Asia, Nature and Mechanisms, Selected Contributions from the 4th Rapid Climate Change in Central Asia's Drylands (RACHAD) Symposium, v194. No.1-2, pp. 68-78.

Zahn, R. (1994) Fast flickers in the tropics, Nature, v372, pp. 621-622.

APPENDIX 1 : Additive dose curves (OSL)

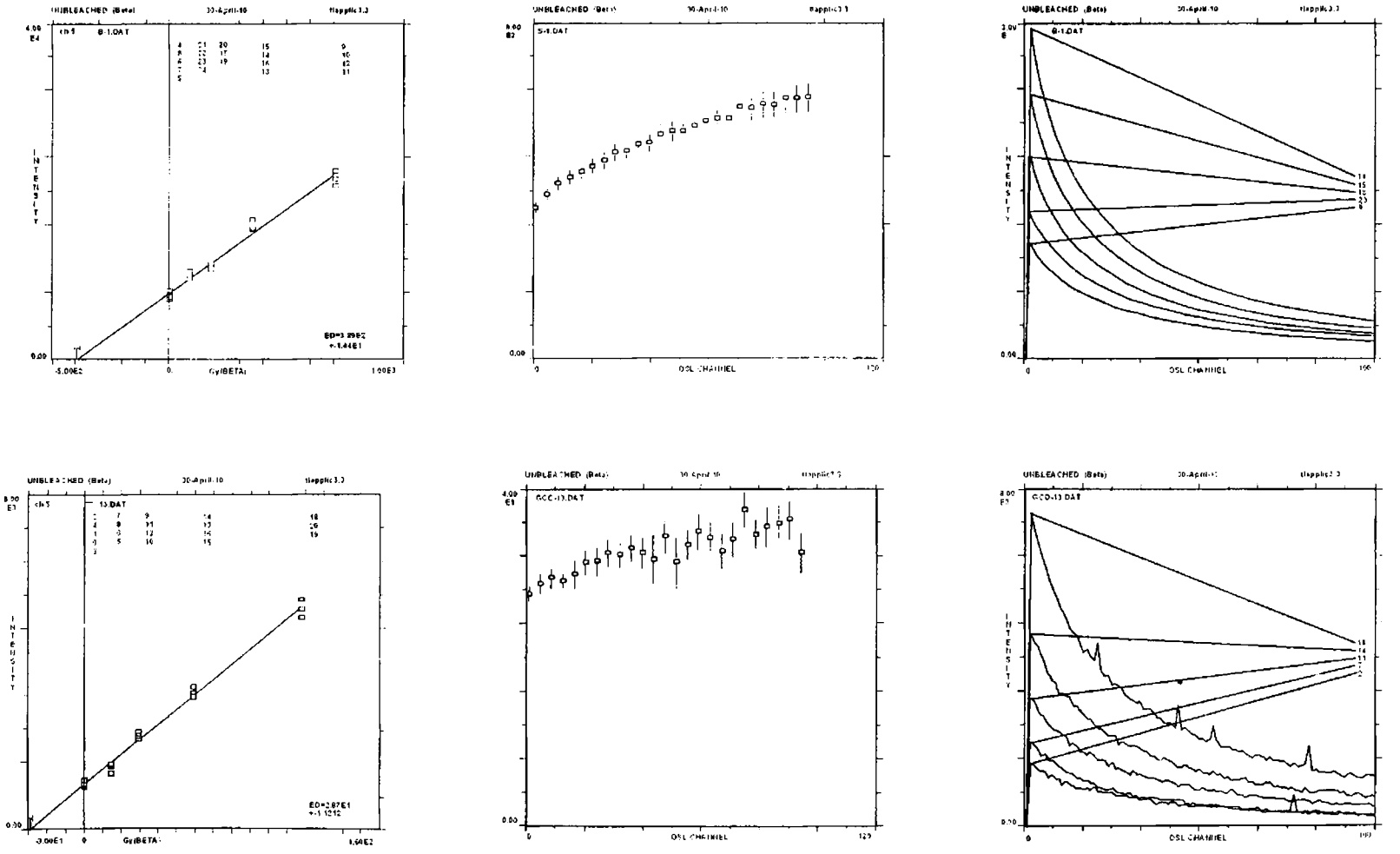

Appendix 1.1 Additive dose growth curve for samples processed from TRV10/26(top) and TRV1/5(bottom)

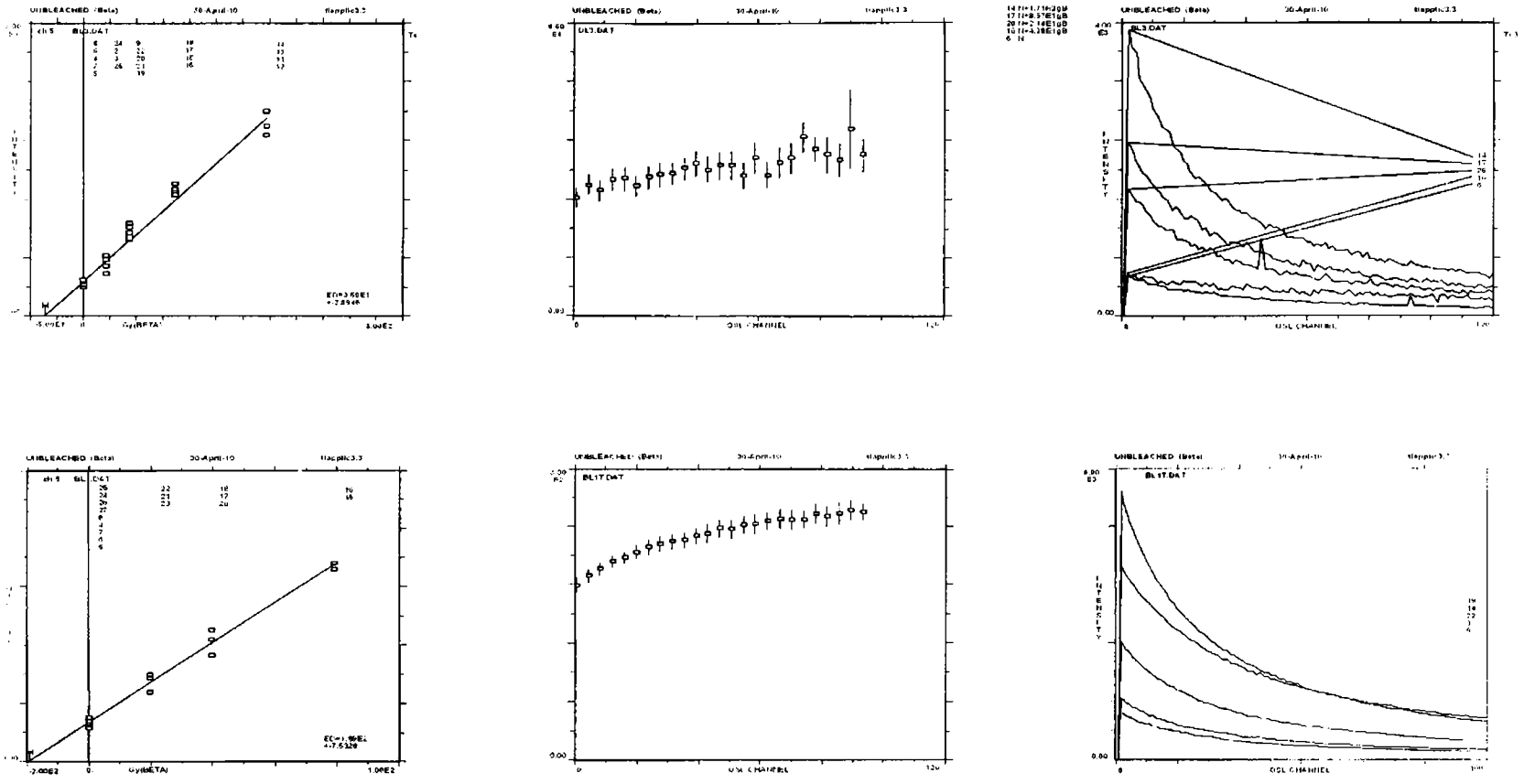

Appendix 1.1(contd.) Additive dose growth curve for samples processed from TRV1/10(top) and TRV10/27(bottom)

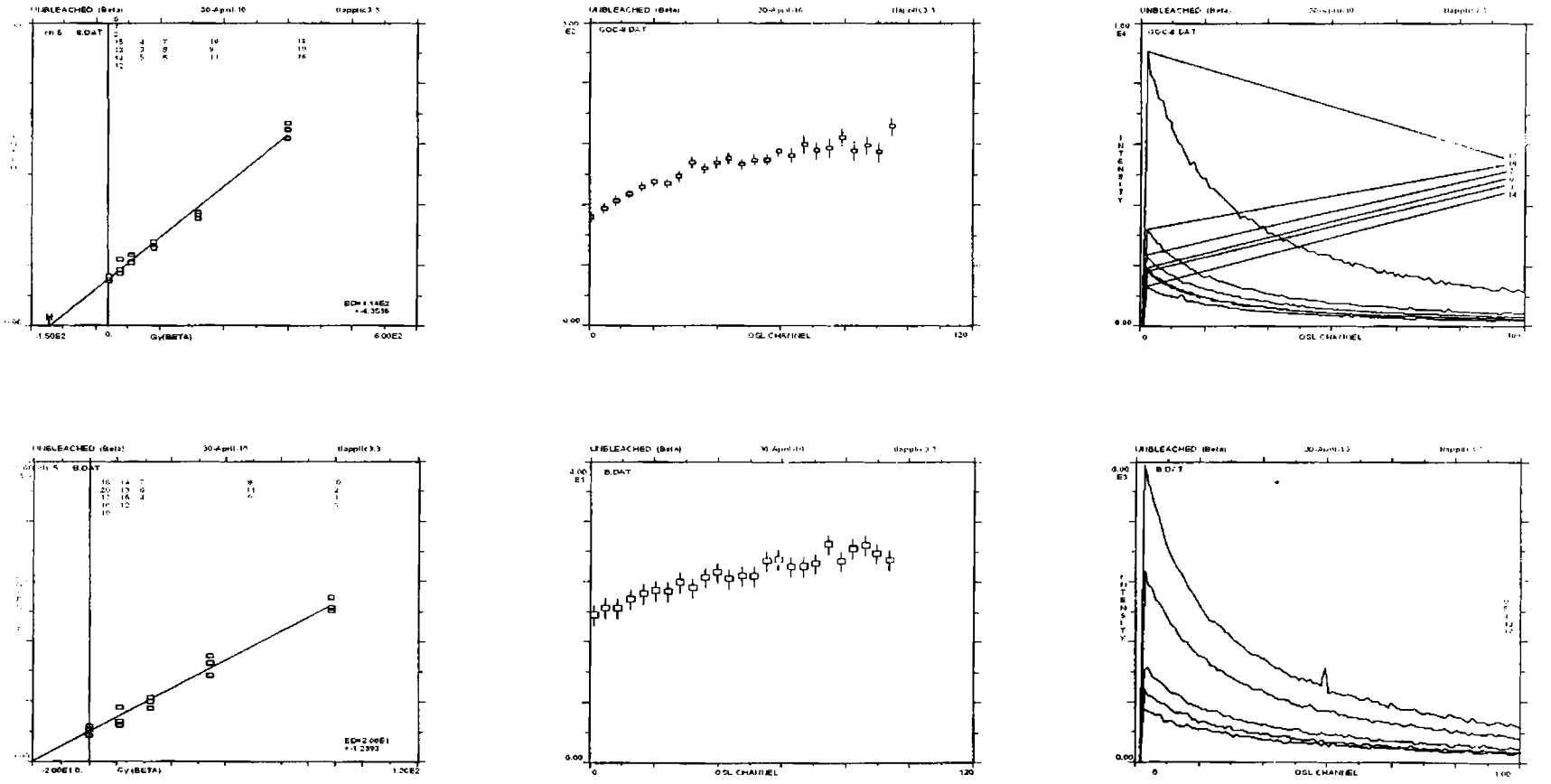

Appendix 1.1(contd.) Additive dose growth curve for samples processed from TRV1/22(top) and

TRV6/5(bottom)

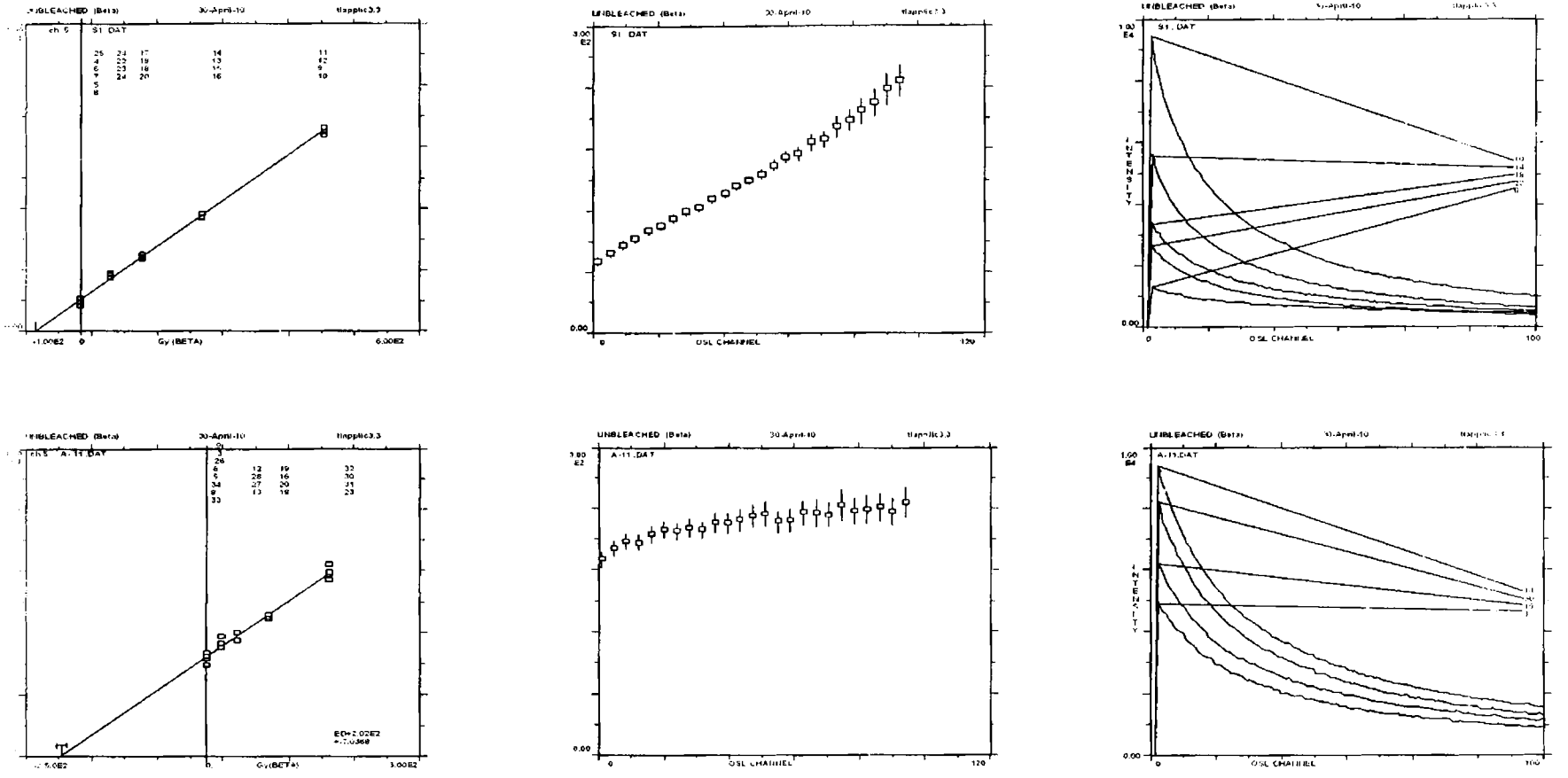

Appendix 1.1(Contd.) Additive dose growth curve for samples processed from TRV6/20(top) andTRV 10/19(bottom)

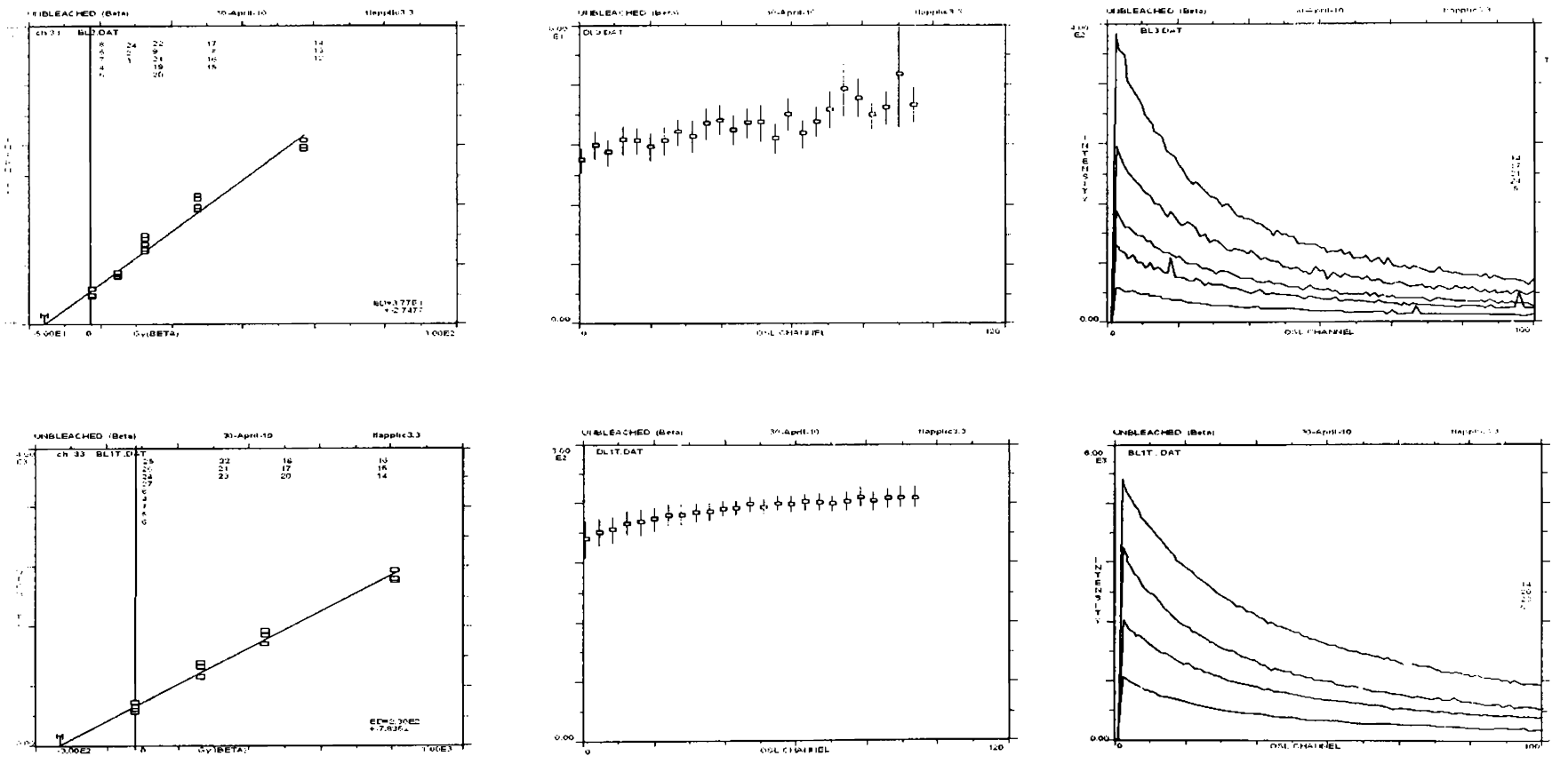

Appendix 1.1(contd.) Additive dose growth curve for samples processed from TRV6/5(top) and TRV7/13(bottom)

APPENDIX 2 (A): Sieve Data

Location	TRV 1						TRV 4			
Depth	11	19	22	24	25	27	12	14	16	19
SAMPLE TYPE:	Unimodal, Moderately Sorted	Bimodal, Moderately Sorted	Unimodal, Moderately Sorted	Bimodal, Poorly Sorted	Trimodal, Poorly Sorted	Trimodal, Poorly Sorted	Bimodal, Moderately Sorted	Unimodal, Moderately Sorted	Unimodal, Moderately Sorted	Unimodal, Moderately Sorted
TEXTURAL GROUP	Sand	Sand	Sand	Sand	Sand	Sand	Sand	Sand	Sand	Sand
SEDIMENT NAME:	Moderately Sorted Medium Sand	Moderately Sorted Medium Sand	Moderately Sorted Medium Sand	Poorly Sorted Medium Sand	Poorly Sorted Medium Sand	Poorly Sorted Medium Sand	Moderately Sorted Medium Sand	Moderately Sorted Medium Sand	Moderately Sorted Medium Sand	Moderately Sorted Medium Sand
MEAN	1.380	1.151	1.299	1.580	1.445	1.227	1.882	1.370	1.889	1.318
SORTING	0.727	0.761	0.857	0.960	1.142	1.124	0.700	0.761	0.741	0.860
SKEWNESS	0.192	0.594	0.451	0.226	0.525	0.335	0.133	0.311	-0.413	0.510
KURTOSIS	3.469	3.397	3.025	2.258	2.321	1.900	3.157	3.519	3.407	3.100
MEAN:	Medium Sand	Medium Sand	Medium Sand	Medium Sand	Medium Sand	Medium Sand	Medium Sand	Medium Sand	Medium Sand	Medium Sand
SORTING:	Moderately Sorted	Moderately Sorted	Moderately Sorted	Poorly Sorted	Poorly Sorted	Poorly Sorted	Moderately Sorted	Moderately Sorted	Moderately Sorted	Moderately Sorted
SKEWNESS:	Symmetrical	Symmetrical	Symmetrical	Fine Skewed	Fine Skewed	Fine Skewed	Fine Skewed	Symmetrical	Symmetrical	Symmetrical
KURTOSIS:	Leptokurtic	Mesokurtic	Leptokurtic	Mesokurtic	Mesokurtic	Platykurtic	Mesokurtic	Leptokurtic	Leptokurtic	Leptokurtic
% GRAVEL:	0.00%	0.00%	0.00%	0.00%	0.00%	0.00%	0.0%	0.0%	0.0%	0.0%
% SAND:	100.00%	100.00%	100.00%	100.00%	100.00%	100.00%	100.0%	100.0%	100.0%	100.0%
% MUD:	0.00%	0.00%	0.00%	0.00%	0.00%	0.00%	0.0%	0.0%	0.0%	0.0%
% V FINE GRAVEL:	0.0%	0.0%	0.0%	0.0%	0.0%	0.0%	0.0%	0.0%	0.0%	0.0%
% V COARSE SAND:	4.5%	4.4%	9.3%	5.1%	11.4%	21.5%	0.6%	4.7%	2.2%	8.3%
% COARSE SAND:	22.2%	39.2%	27.2%	24.6%	29.3%	26.5%	7.4%	24.1%	8.3%	27.5%
% MEDIUM SAND:	60.4%	46.0%	44.7%	38.2%	31.1%	26.6%	57.6%	57.6%	45.8%	45.3%
% FINE SAND:	10.6%	8.4%	15.1%	23.0%	14.9%	18.8%	28.6%	10.3%	38.6%	14.7%
% V FINE SAND:	2.3%	1.9%	3.7%	9.1%	13.3%	6.6%	5.8%	3.3%	5.0%	4.1%
% V COARSE SILT:	0.0%	0.0%	0.0%	0.0%	0.0%	0.0%	0.0%	0.0%	0.0%	0.0%

Appndix 2.1. Textural characteristics of sediments collected from Litho Unit 1 in the study area deducted from Gradistat v5

Location						TRV 2				
Depth	22	24	25	27	29	13	14	16	19	22
SAMPLE TYPE:	Bimodal, Poorly Sorted	Bimodal, Moderately Sorted	Bimodal, Poorly Sorted	Trimodal, Poorly Sorted	Trimodal, Poorly Sorted	Bimodal, Moderately Well Sorted	Unimodal, Moderately Sorted	Trimodal, Poorly Sorted	Unimodal, Moderately Sorted	Trimodal, Poorly Sorted
TEXTURAL GROUP:	Sand	Sand	Sand	Sand	Sand	Sand	Sand	Sand	Sand	Sand
SEDIMENT NAME:	Poorly Sorted Medium Sand	Moderately Sorted Medium Sand	Poorly Sorted Medium Sand	Poorly Sorted Medium Sand	Poorly Sorted Medium Sand	Moderately Well Sorted Medium Sand	Moderately Sorted Medium Sand	Poorly Sorted Medium Sand	Moderately Sorted Medium Sand	Poorly Sorted Medium Sand
MEAN	1.431	1.160	1.607	1.404	1.307	1.886	1.380	1.395	1.305	1.448
SORTING	1.136	0.744	0.967	1.090	1.151	0.678	0.727	1.083	0.842	1.143
SKEWNESS	0.526	0.523	0.169	0.185	0.303	0.172	0.192	0.183	0.485	0.519
KURTOSIS	2.367	3.406	2.206	1.929	1.914	3.144	3.469	1.927	3.108	2.313
MEAN:	Medium Sand	Medium Sand	Medium Sand	Medium Sand	Medium Sand	Medium Sand	Medium Sand	Medium Sand	Medium Sand	Medium Sand
SORTING:	Poorly Sorted	Moderately Sorted	Poorly Sorted	Poorly Sorted	Poorly Sorted	Moderately Well Sorted	Moderately Sorted	Poorly Sorted	Moderately Sorted	Poorly Sorted
SKEWNESS:	Fine Skewed	Symmetrical	Fine Skewed	Symmetrical	Symmetrical	Fine Skewed	Symmetrical	Symmetrical	Symmetrical	Fine Skewed
KURTOSIS:	Mesokurtic	Mesokurtic	Mesokurtic	Platykurtic	Platykurtic	Mesokurtic	Leptokurtic	Platykurtic	Leptokurtic	Mesokurtic
% GRAVEL:	0.0%	0.0%	0.0%	0.0%	0.0%	0.0%	0.0%	0.0%	0.0%	0.0%
% SAND:	100.0%	100.0%	100.0%	100.0%	100.0%	100.0%	100.0%	100.0%	100.0%	100.0%
% MUD:	0.0%	0.0%	0.0%	0.0%	0.0%	0.0%	0.0%	0.0%	0.0%	0.0%
% V FINE GRAVEL:	0.0%	0.0%	0.0%	0.0%	0.0%	0.0%	0.0%	0.0%	0.0%	0.0%
% V COARSE SAND:	11.8%	4.5%	5.3%	13.4%	20.3%	0.3%	4.5%	13.4%	8.4%	11.3%
% COARSE SAND:	28.7%	37.3%	23.3%	26.0%	25.3%	6.9%	22.2%	26.3%	27.6%	29.1%
% MEDIUM SAND:	31.9%	48.6%	37.5%	29.4%	26.5%	58.8%	60.4%	29.4%	45.8%	31.2%
% FINE SAND:	14.7%	8.1%	24.4%	22.8%	19.1%	28.7%	10.6%	22.9%	14.6%	15.0%
% V FINE SAND:	12.9%	1.5%	9.5%	8.4%	8.8%	5.4%	2.3%	8.0%	3.6%	13.3%
% V COARSE SILT:	0.0%	0.0%	0.0%	0.0%	0.0%	0.0%	0.0%	0.0%%	0.0%	0.0%

Appndix 2.1. (Contd.)

Location				TRV 3						
Depth	25	26	27	12	13	14	16	20	22	24
SAMPLE TYPE:	Bimodal, Moderately Sorted	Bimodal, Poorly Sorted	Trimodal, Poorly Sorted	Bimodal, Moderately Sorted	Unimodal, Moderately Sorted	Unimodal, Moderately Sorted	Trimodal, Poorly Sorted	Unimodal, Moderately Sorted	Bimodal, Moderately Sorted	Bimodal, Poorly Sorted
TEXTURAL GROUP:	Sand	Sand	Sand	Sand	Sand	Sand	Sand	Sand	Sand	Sand
SEDIMENT NAME:	Moderately Sorted Medium Sand	Poorly Sorted Medium Sand	Poorly Sorted Coarse Sand	Moderately Sorted Medium Sand	Moderately Sorted Medium Sand	Moderately Sorted Medium Sand	Poorly Sorted Medium Sand	Moderately Sorted Medium Sand	Moderately Sorted Medium Sand	Poorly Sorted Medium Sand
MEAN	1.170	1.592	1.226	1.886	1.904	1.410	1.396	1.312	1.171	1.585
SORTING	0.755	0.959	1.123	0.689	0.736	0.775	1.088	0.852	0.757	0.964
SKEWNESS	0.537	0.179	0.341	0.158	-0.452	0.332	0.187	0.495	0.543	0.179
KURTOSIS	3.364	2.235	1.905	3.165	3.401	3.461	1.927	3.098	3.381	2.217
MEAN:	Medium Sand	Medium Sand	Medium Sand	Medium Sand	Medium Sand	Medium Sand	Medium Sand	Medium Sand	Medium Sand	Medium Sand
SORTING:	Moderately Sorted	Poorly Sorted	Poorly Sorted	Moderately Sorted	Moderately Sorted	Moderately Sorted	Poorly Sorted	Moderately Sorted	Moderately Sorted	Poorly Sorted
SKEWNESS:	Symmetrical	Fine Skewed	Fine Skewed	Fine Skewed	Symmetrical	Symmetrical	Symmetrical	Symmetrical	Symmetrical	Fine Skewed
KURTOSIS:	Mesokurtic	Mesokurtic	Platykurtic	Mesokurtic	Leptokurtic	Leptokurtic	Platykurtic	Leptokurtic	Mesokurtic	Mesokurtic
% GRAVEL:	0.0%	0.0%	0.0%	0.0%	0.0%	0.0%	0.0%	0.0%	0.0%	0.0%
% SAND:	100.0%	100.0%	100.0%	100.0%	100.0%	100.0%	100.0%	100.0%	100.0%	100.0%
% MUD:	0.0%	0.0%	0.0%	0.0%	0.0%	0.0%	0.0%	0.0%	0.0%	0.0%
% V FINE GRAVEL:	0.0%	0.0%	0.0%	0.0%	0.0%	0.0%	0.0%	0.0%	0.0%	0.0%
% V COARSE SAND:	4.3%	5.2%	21.5%	0.4%	2.0%	4.5%	13.6%	8.5%	4.4%	5.6%
% COARSE SAND:	37.7%	23.3%	26.7%	7.0%	8.4%	22.2%	26.2%	27.5%	37.5%	23.7%
% MEDIUM SAND:	47.8%	38.2%	26.5%	58.4%	44.5%	58.3%	29.2%	45.4%	47.8%	37.7%
% FINE SAND:	8.5%	24.1%	18.6%	28.6%	40.1%	11.1%	22.9%	14.8%	8.6%	23.9%
% V FINE SAND:	1.8%	9.0%	6.6%	5.6%	5.0%	3.9%	8.2%	3.8%	1.8%	9.0%
% V COARSE SILT:	0.0%	0.0%	0.00%	0.0%	0.0%	0.0%	0.0%	0.0%	0.0%	0.0%

Appndix 2.1. (Contd.)

Location			TRV 5							TRV 6
Depth	25	27	14	15	19	22	24	25	27	14
SAMPLE TYPE:	Trimodal, Poorly Sorted	Trimodal, Poorly Sorted	Unimodal, Moderately Sorted	Trimodal, Poorly Sorted	Unimodal, Moderately Sorted	Bimodal, Moderately Sorted	Bimodal, Poorly Sorted	Trimodal, Poorly Sorted	Trimodal, Poorly Sorted	Unimodal, Moderately Sorted
TEXTURAL GROUP:	Sand	Sand	Sand	Sand	Sand	Sand	Sand	Sand	Sand	Sand
SEDIMENT NAME:	Poorly Sorted Coarse Sand	Poorly Sorted Medium Sand	Moderately Sorted Medium Sand	Poorly Sorted Medium Sand	Moderately Sorted Medium Sand	Moderately Sorted Medium Sand	Poorly Sorted Medium Sand	Poorly Sorted Medium Sand	Poorly Sorted Medium Sand	Moderately Sorted Medium Sand
MEAN	1.258	1.443	1.412	1.396	1.312	1.168	1.588	1.271	1.465	1.375
SORTING	1.134	1.148	0.800	1.086	0.849	0.758	0.968	1.149	1.158	0.805
SKEWNESS	0.327	0.514	0.598	0.189	0.500	0.556	0.182	0.324	0.493	0.462
KURTOSIS	1.902	2.299	3.868	1.927	3.113	3.421	2.213	1.900	2.250	3.461
MEAN:	Medium Sand	Medium Sand	Medium Sand	Medium Sand	Medium Sand	Medium Sand	Medium Sand	Medium Sand	Medium Sand	Medium Sand
SORTING:	Poorly Sorted	Poorly Sorted	Moderately Sorted	Poorly Sorted	Moderately Sorted	Moderately Sorted	Poorly Sorted	Poorly Sorted	Poorly Sorted	Moderately Sorted
SKEWNESS:	Symmetrical	Fine Skewed	Symmetrical	Symmetrical	Symmetrical	Symmetrical	Fine Skewed	Symmetrical	Fine Skewed	Symmetrical
KURTOSIS:	Platykurtic	Mesokurtic	Leptokurtic	Platykurtic	Leptokurtic	Mesokurtic	Mesokurtic	Platykurtic	Mesokurtic	Leptokurtic
% GRAVEL:	0.0%	0.0%	0.0%	0.0%	0.0%	0.0%	0.0%	0.0%	0.0%	0.0%
% SAND:	100.0%	100.0%	100.0%	100.0%	100.0%	100.0%	100.0%	100.0%	100.0%	100.0%
% MUD:	0.0%	0.0%	0.0%	0.0%	0.0%	0.0%	0.0%	0.0%	0.0%	0.0%
% V FINE GRAVEL:	0.0%	0.0%	0.0%	0.0%	0.0%	0.0%	0.0%	0.0%	0.0%	0.0%
% V COARSE SAND:	20.7%	11.8%	3.7%	13.4%	8.3%	4.3%	5.6%	21.0%	11.5%	4.4%
% COARSE SAND:	26.5%	29.1%	24.1%	26.4%	27.5%	37.7%	23.8%	26.0%	28.6%	25.8%
% MEDIUM SAND:	26.4%	30.7%	58.1%	29.1%	45.7%	47.8%	37.6%	26.2%	31.0%	55.4%
% FINE SAND:	18.9%	14.9%	9.4%	22.8%	14.7%	8.4%	23.6%	18.7%	14.5%	9.6%
% V FINE SAND:	7.5%	13.4%	4.8%	8.2%	3.7%	1.8%	9.4%	8.1%	14.4%	4.8%
% V COARSE SILT:	0.0%	0.0%	0.0%	0.0%	0.0%	0.0%	0.0%	0.0%	0.0%	0.0%

Appndix 2.1. (Contd.)

Location							TRV 7			
Depth	16	18	20	24	25	29	13	15	19	21
SAMPLE TYPE:	Trimodal, Poorly Sorted	Unimodal, Moderately Sorted	Unimodal, Moderately Sorted	Bimodal, Moderately Sorted	Bimodal, Poorly Sorted	Trimodal, Poorly Sorted	Unimodal, Moderately Sorted	Trimodal, Poorly Sorted	Unimodal, Moderately Sorted	Unimodal, Moderately Sorted
TEXTURAL GROUP:	Sand	Sand	Sand	Sand	Sand	Sand	Sand	Sand	Sand	Sand
SEDIMENT NAME:	Poorly Sorted Coarse Sand	Moderately Sorted Medium Sand	Moderately Sorted Medium Sand	Moderately Sorted Medium Sand	Poorly Sorted Medium Sand	Poorly Sorted Medium Sand	Moderately Sorted Medium Sand	Poorly Sorted Medium Sand	Moderately Sorted Medium Sand	Moderately Sorted Medium Sand
MEAN	1.245	1.303	1.369	1.173	1.602	1.440	1.365	1.278	1.302	1.352
SORTING	1.126	0.852	0.734	0.756	0.961	1.137	0.801	1.128	0.846	0.730
SKEWNESS	0.305	0.513	0.159	0.504	0.149	0.513	0.427	0.243	0.505	0.151
KURTOSIS	1.875	3.142	3.213	3.356	2.212	2.288	3.436	1.857	3.142	3.313
MEAN:	Medium Sand	Medium Sand	Medium Sand	Medium Sand	Medium Sand	Medium Sand	Medium Sand	Medium Sand	Medium Sand	Medium Sand
SORTING:	Poorly Sorted	Moderately Sorted	Moderately Sorted	Moderately Sorted	Poorly Sorted	Poorly Sorted	Moderately Sorted	Poorly Sorted	Moderately Sorted	Moderately Sorted
SKEWNESS:	Fine Skewed	Symmetrical	Symmetrical	Symmetrical	Fine Skewed	Fine Skewed	Symmetrical	Symmetrical	Symmetrical	Symmetrical
KURTOSIS:	Platykurtic	Leptokurtic	Leptokurtic	Mesokurtic	Mesokurtic	Mesokurtic	Leptokurtic	Platykurtic	Leptokurtic	Leptokurtic
% GRAVEL:	0.0%	0.0%	0.0%	0.0%	0.0%	0.0%	0.0%	0.0%	0.0%	0.0%
% SAND:	100.0%	100.0%	100.0%	100.0%	100.0%	100.0%	100.0%	100.0%	100.0%	100.0%
% MUD:	0.0%	0.0%	0.0%	0.0%	0.0%	0.0%	0.0%	0.0%	0.0%	0.0%
% V FINE GRAVEL:	0.0%	0.0%	0.0%	0.0%	0.0%	0.0%	0.0%	0.0%	0.0%	0.0%
% V COARSE SAND:	21.5%	8.5%	4.6%	4.8%	5.5%	11.1%	4.8%	22.1%	8.4%	5.1%
% COARSE SAND:	26.8%	27.9%	23.4%	36.6%	23.1%	30.0%	25.6%	24.3%	28.0%	21.5%
% MEDIUM SAND:	25.4%	45.4%	57.9%	48.2%	37.8%	30.5%	55.5%	26.4%	45.6%	59.3%
% FINE SAND:	20.0%	14.5%	12.4%	8.7%	24.4%	15.2%	9.7%	20.8%	14.5%	12.0%
% V FINE SAND:	6.3%	3.7%	1.8%	1.7%	9.1%	13.1%	4.4%	6.4%	3.6%	2.0%
% V COARSE SILT:	0.0%	0.0%	0.0%	0.0%	0.0%	0.0%	0.0%	0.0%	0.0%	0.0%

Appndix 2.1. (Contd.)

Location				TRV 9						
Depth	23	27	30	13	15	17	19	20	23	25
SAMPLE TYPE:	Bimodal, Poorly Sorted	Bimodal, Moderately Sorted	Trimodal, Poorly Sorted	Bimodal, Moderately Sorted	Unimodal, Moderately Sorted	Unimodal, Moderately Sorted	Unimodal, Moderately Sorted	Trimodal, Poorly Sorted	Bimodal, Moderately Sorted	Bimodal, Poorly Sorted
TEXTURAL GROUP:	Sand	Sand	Sand	Sand	Sand	Sand	Sand	Sand	Sand	Sand
SEDIMENT NAME:	Poorly Sorted Medium Sand	Moderately Sorted Medium Sand	Poorly Sorted Medium Sand	Moderately Sorted Medium Sand	Moderately Sorted Medium Sand	Moderately Sorted Medium Sand	Moderately Sorted Medium Sand	Poorly Sorted Medium Sand	Moderately Sorted Medium Sand	Poorly Sorted Medium Sand
MEAN	1.593	1.171	1.446	1.863	1.370	1.393	1.306	1.456	1.171	1.590
SORTING	0.963	0.752	1.137	0.688	0.809	0.760	0.853	1.141	0.759	0.970
SKEWNESS	0.150	0.506	0.504	0.157	0.434	0.180	0.508	0.495	0.525	0.143
KURTOSIS	2.219	3.354	2.265	3.147	3.487	3.507	3.109	2.237	3.406	2.213
MEAN:	Medium Sand	Medium Sand	Medium Sand	Medium Sand	Medium Sand	Medium Sand	Medium Sand	Medium Sand	Medium Sand	Medium Sand
SORTING:	Poorly Sorted	Moderately Sorted	Poorly Sorted	Moderately Sorted	Moderately Sorted	Moderately Sorted	Moderately Sorted	Poorly Sorted	Moderately Sorted	Poorly Sorted
SKEWNESS:	Fine Skewed	Symmetrical	Fine Skewed	Fine Skewed	Symmetrical	Coarse Skewed	Symmetrical	Fine Skewed	Symmetrical	Fine Skewed
KURTOSIS:	Mesokurtic	Mesokurtic	Mesokurtic	Mesokurtic	Leptokurtic	Leptokurtic	Leptokurtic	Mesokurtic	Mesokurtic	Mesokurtic
% GRAVEL:	0.0%	0.0%	0.0%	0.0%	0.0%	0.0%	0.0%	0.0%	0.0%	0.0%
% SAND:	100.0%	100.0%	100.0%	100.0%	100.0%	100.0%	100.0%	100.0%	100.0%	100.0%
% MUD:	0.0%	0.0%	0.0%	0.0%	0.0%	0.0%	0.0%	0.0%	0.0%	0.0%
% V FINE GRAVEL:	0.0%	0.0%	0.0%	0.0%	0.0%	0.0%	0.0%	0.0%	0.0%	0.0%
% V COARSE SAND:	5.7%	4.7%	11.1%	0.4%	5.0%	5.6%	8.4%	11.0%	4.8%	6.1%
% COARSE SAND:	23.2%	36.9%	30.0%	7.6%	25.4%	20.9%	28.1%	30.0%	36.9%	22.9%
% MEDIUM SAND:	37.8%	48.3%	30.3%	59.0%	55.1%	58.5%	45.2%	30.0%	48.0%	37.9%
% FINE SAND:	24.3%	8.4%	15.4%	27.7%	10.0%	13.3%	14.5%	15.5%	8.3%	24.0%
% V FINE SAND:	9.0%	1.7%	13.2%	5.3%	4.4%	1.7%	3.9%	13.5%	1.9%	9.2%
% V COARSE SILT:	0.0%	0.0%	0.0%	0.0%	0.0%	0.0%	0.0%	0.0%	0.0%	0.0%

Appndix 2.1. (Contd.)

Location		TRV 8				TkV 10				
Depth	27	15	17	20	24	19	20	21	24	26
SAMPLE TYPE:	Trimodal, Poorly Sorted	Trimodal, Poorly Sorted	Bimodal, Moderately Sorted	Unimodal, Moderately Sorted	Bimodal, Moderately Sorted	Unimodal, Moderately Sorted	Unimodal, Moderately Sorted	Unimodal, Moderately Sorted	Trimodal, Moderately Sorted	Bimodal, Poorly Sorted
TEXTURAL GROUP:	Sand	Sand	Sand	Sand	Sand	Sand	Sand	Sand	Sand	Sand
SEDIMENT NAME:	Poorly Sorted Medium Sand	Poorly Sorted Coarse Sand	Moderately Sorted Medium Sand	Moderately Sorted Medium Sand	Moderately Sorted Medium Sand	Moderately Sorted Medium Sand	Moderately Sorted Medium Sand	Moderately Sorted Medium Sand	Moderately Sorted Medium Sand	Poorly Sorted Medium Sand
MEAN	1.292	1.387	1.479	1.318	1.135	1.305	1.380	1.410	0.870	1.568
SORTING	1.139	1.105	0.803	0.867	0.785	0.842	0.727	0.775	0.896	0.979
SKEWNESS	0.243	0.142	0.357	0.540	0.503	0.485	0.192	0.332	0.482	0.181
KURTOSIS	1.858	1.893	3.199	3.165	3.234	3.108	3.469	3.461	2.708	2.196
MEAN:	Medium Sand	Medium Sand	Medium Sand	Medium Sand	Medium Sand	Medium Sand	Medium Sand	Medium Sand	Coarse Sand	Medium Sand
SORTING:	Poorly Sorted	Poorly Sorted	Moderately Sorted	Moderately Sorted	Moderately Sorted	Moderately Sorted	Moderately Sorted	Moderately Sorted	Moderately Sorted	Poorly Sorted
SKEWNESS:	Symmetrical	Symmetrical	Symmetrical	Symmetrical	Symmetrical	Symmetrical	Symmetrical	Symmetrical	Symmetrical	Fine Skewed
KURTOSIS:	Platykurtic	Platykurtic	Leptokurtic	Leptokurtic	Leptokurtic	Leptokurtic	Leptokurtic	Leptokurtic	Platykurtic	Mesokurtic
% GRAVEL:	0.0%	0.0%	0.0%	0.0%	0.0%	0.0%	0.0%	0.0%	0.0%	0.0%
% SAND:	100.0%	100.0%	100.0%	100.0%	100.0%	100.0%	100.0%	100.0%	100.0%	100.0%
% MUD:	0.0%	0.0%	0.0%	0.0%	0.0%	0.0%	0.0%	0.0%	0.0%	0.0%
% V FINE GRAVEL:	0.0%	0.0%	0.0%	0.0%	0.0%	0.0%	0.0%	0.0%	0.0%	0.0%
% V COARSE SAND:	22.0%	12.4%	3.7%	8.1%	8.4%	8.4%	4.5%	4.5%	25.0%	6.8%
% COARSE SAND:	24.2%	30.7%	21.2%	27.9%	35.1%	27.6%	22.2%	22.2%	29.3%	23.4%
% MEDIUM SAND:	25.7%	27.2%	56.7%	45.2%	46.1%	45.8%	60.4%	58.3%	37.2%	37.1%
% FINE SAND:	21.2%	22.7%	11.8%	14.5%	8.6%	14.6%	10.6%	11.1%	6.8%	23.3%
% V FINE SAND:	6.9%	7.0%	6.5%	4.4%	1.7%	3.6%	2.3%	3.9%	1.7%	9.3%
% V COARSE SILT:	0.0%	0.0%	0.0%	0.0%	0.0%	0.0%	0.0%	0.0%	0.0%	0.0%

Appndix 2.1. (Contd.)

Location	
Depth	27
SAMPLE TYPE:	Trimodal, Poorly Sorted
TEXTURAL GROUP:	Sand
SEDIMENT NAME:	Poorly Sorted Medium Sand
MEAN	1.443
SORTING	1.163
SKEWNESS	0.524
KURTOSIS	2.289
MEAN:	Medium Sand
SORTING:	Poorly Sorted
SKEWNESS:	Fine Skewed
KURTOSIS:	Mesokurtic
% GRAVEL:	0.0%
% SAND:	100.0%
% MUD:	0.0%
% V FINE GRAVEL:	0.0%
% V COARSE SAND:	12.1%
% COARSE SAND:	29.3%
% MEDIUM SAND:	30.3%
% FINE SAND:	14.5%
% V FINE SAND:	13.9%
% V COARSE SILT:	0.0%

Appndix 2.1. (Contd.)

Location	TRV 1			TRV 4			TRV 2		TRV 3	
Depth	8	9	10	8	9	10	9	11	9	10
SAMPLE TYPE:	Unimodal, Moderately Well Sorted	Unimodal, Moderately Sorted	Bimodal, Moderately Well Sorted	Unimodal, Moderately Sorted	Unimodal, Moderately Sorted	Bimodal, Moderately Well Sorted	Unimodal, Moderately Sorted	Unimodal, Moderately Sorted	Unimodal, Moderately Well Sorted	Unimodal, Moderately Sorted
TEXTURAL GROUP:	Sand	Sand	Sand	Sand	Sand	Sand	Sand	Sand	Sand	Sand
SEDIMENT NAME:	Moderately, Well Sorted Very Fine Sand	Moderately Sorted Fine Sand	Moderately Well Sorted Medium Sand	Moderately Sorted Very Fine Sand	Moderately Sorted Fine Sand	Moderately Well Sorted Medium Sand	Moderately Sorted Very Fine Sand	Moderately Sorted Medium Sand	Moderately, Well Sorted Very Fine Sand	Moderately Sorted Very Fine Sand
MEAN	2.855	2.596	1.886	2.575	2.594	1.886	2.603	1.898	2.855	2.596
SORTING	0.754	0.896	0.678	0.932	0.897	0.678	0.892	0.723	0.754	0.907
SKEWNESS	-2.099	-1.090	0.172	-1.087	-1.076	0.172	-1.091	-0.447	-2.099	-1.098
KURTOSIS	8.291	3.730	3.144	3.631	3.670	3.144	3.758	3.421	8.291	3.744
MEAN:	Fine Sand	Fine Sand	Medium Sand	Fine Sand	Fine Sand	Medium Sand	Fine Sand	Medium Sand	Fine Sand	Fine Sand
SORTING:	Moderately Well Sorted	Moderately Sorted	Moderately Well Sorted	Moderately Sorted	Moderately Sorted	Moderately Well Sorted	Moderately Sorted	Moderately Sorted	Moderately Well Sorted	Moderately Sorted
SKEWNESS:	Coarse Skewed	Very Coarse Skewed	Fine Skewed	Very Coarse Skewed	Very Coarse Skewed	Fine Skewed	Very Coarse Skewed	Symmetrical	Coarse Skewed	Very Coarse Skewed
KURTOSIS:	Very Leptokurtic	Leptokurtic	Mesokurtic	Leptokurtic	Leptokurtic	Mesokurtic	Leptokurtic	Leptokurtic	Very Leptokurtic	Leptokurtic
% GRAVEL:	0.00%	0.00%	0.00%	0.0%	0.0%	0.00%	0.0%	0.0%	0.00%	0.0%
% SAND:	100.00%	100.00%	100.00%	100.0%	100.0%	100.00%	100.0%	100.0%	100.00%	100.0%
% MUD:	0.00%	0.00%	0.00%	0.0%	0.0%	0.00%	0.0%	0.0%	0.00%	0.0%
% V FINE GRAVEL:	0.0%	0.0%	0.0%	0.0%	0.0%	0.0%	0.0%	0.0%	0.0%	0.0%
% V COARSE SAND:	1.8%	1.8%	0.3%	2.5%	2.0%	0.3%	2.0%	1.9%	1.8%	2.3%
% COARSE SAND:	3.1%	5.5%	6.9%	5.7%	5.6%	6.9%	5.1%	7.9%	3.1%	5.2%
% MEDIUM SAND:	3.4%	14.3%	58.8%	14.4%	13.9%	58.8%	14.5%	46.1%	3.4%	14.2%
% FINE SAND:	41.6%	39.4%	28.7%	38.3%	39.5%	28.7%	39.1%	39.6%	41.6%	39.0%
% V FINE SAND:	50.0%	39.0%	5.4%	39.1%	39.0%	5.4%	39.4%	4.5%	50.0%	39.3%
% V COARSE SILT:	0.0%	0.0%	0.0%	0.0%	0.0%	0.0%	0.0%	0.0%	0.0%	0.0%

Appendix 2.1. Textural characteristics of sediments collected from Litho Unit 2 in the study area deducted from Gradistat v5

Location		TRV 5		TRV 6		TRV 7		TRV 9		TRV 8
Depth	11	9	11	10	12	10	12	10	12	11
SAMPLE TYPE:	Bimodal, Moderately Well Sorted	Unimodal, Moderately Sorted	Unimodal, Moderately Well Sorted	Unimodal, Moderately Sorted	Unimodal, Moderately Sorted	Unimodal, Moderately Sorted	Unimodal, Moderately Sorted	Unimodal, Moderately Sorted	Unimodal, Moderately Sorted	Unimodal, Moderately Sorted
TEXTURAL GROUP:	Sand	Sand	Sand	Sand	Sand	Sand	Sand	Sand	Sand	Sand
SEDIMENT NAME:	Moderately Well Sorted Medium Sand	Moderately Sorted Very Fine Sand	Moderately Well Sorted Medium Sand	Moderately Sorted Fine Sand	Moderately Sorted Medium Sand	Moderately Sorted Fine Sand	Moderately Sorted Medium Sand	Moderately Sorted Fine Sand	Moderately Sorted Medium Sand	Mod. Sort. ... Fine Sand
MEAN	1.886	2.604	1.967	2.594	1.917	2.599	1.935	2.602	1.940	2.611
SORTING	0.678	0.899	0.690	0.897	0.744	0.893	0.741	0.889	0.745	0.887
SKEWNESS	0.172	-1.106	-0.572	-1.076	-0.499	-1.082	-0.451	-1.076	-0.453	-1.082
KURTOSIS	3.144	3.788	4.070	3.670	3.202	3.700	3.184	3.684	3.170	3.716
MEAN:	Medium Sand	Fine Sand	Fine Sand	Fine Sand	Medium Sand	Fine Sand	Medium Sand	Fine Sand	Medium Sand	Fine Sand
SORTING:	Moderately Well Sorted	Moderately Sorted	Moderately Well Sorted	Moderately Sorted	Moderately Sorted	Moderately Sorted	Moderately Sorted	Moderately Sorted	Moderately Sorted	Moderately Sorted
SKEWNESS:	Fine Skewed	Very Coarse Skewed	Symmetrical	Very Coarse Skewed	Symmetrical	Very Coarse Skewed	Symmetrical	Very Coarse Skewed	Symmetrical	Very Coarse Skewed
KURTOSIS:	Mesokurtic	Leptokurtic	Mesokurtic	Leptokurtic	Leptokurtic	Leptokurtic	Leptokurtic	Leptokurtic	Leptokurtic	Leptokurtic
% GRAVEL:	0.00%	0.0%	0.0%	0.0%	0.0%	0.0%	0.0%	0.0%	0.0%	0.0%
% SAND:	100.00%	100.0%	100.0%	100.0%	100.0%	100.0%	100.0%	100.0%	100.0%	100.0%
% MUD:	0.00%	0.0%	0.0%	0.0%	0.0%	0.0%	0.0%	0.0%	0.0%	0.0%
% V FINE GRAVEL:	0.0%	0.0%	0.0%	0.0%	0.0%	0.0%	0.0%	0.0%	0.0%	0.0%
% V COARSE SAND:	0.3%	2.2%	2.0%	2.0%	1.9%	2.0%	1.6%	1.8%	1.7%	1.8%
% COARSE SAND:	6.9%	5.1%	3.4%	5.6%	9.3%	5.5%	8.9%	5.6%	8.9%	5.2%
% MEDIUM SAND:	58.8%	14.0%	47.0%	13.9%	42.0%	13.8%	42.0%	13.7%	41.7%	14.1%
% FINE SAND:	28.7%	39.2%	42.7%	39.5%	41.5%	39.6%	41.5%	39.6%	41.6%	39.4%
% V FINE SAND:	5.4%	39.5%	4.9%	39.0%	5.4%	39.1%	5.9%	39.2%	6.1%	39.6%
% V COARSE SILT:	0.0%	0.0%	0.0%	0.0%	0.0%	0.0%	0.0%	0.0%	0.0%	0.0%

Appendix 2.1. (Contd.)

Location		TRV 10		
Depth	14	12	14	16
SAMPLE TYPE:	Unimodal, Moderately Sorted	Bimodal, Moderately Sorted	Unimodal, Moderately Sorted	Bimodal, Moderately Well Sorted
TEXTURAL GROUP:	Sand	Sand	Sand	Sand
SEDIMENT NAME:	Moderately Sorted Medium Sand	Moderately Sorted Medium Sand	Moderately Sorted Medium Sand	Moderately Well Sorted Medium Sand
MEAN	1.904	1.860	1.912	1.886
SORTING	0.729	0.692	0.721	0.678
SKEWNESS	-0.437	0.170	-0.442	0.172
KURTOSIS	3.423	3.202	3.365	3.144
MEAN:	Medium Sand	Medium Sand	Medium Sand	Medium Sand
SORTING:	Moderately Sorted	Moderately Sorted	Moderately Sorted	Moderately Well Sorted
SKEWNESS:	Symmetrical	Fine Skewed	Symmetrical	Fine Skewed
KURTOSIS:	Leptokurtic	Mesokurtic	Leptokurtic	Mesokurtic
% GRAVEL:	0.0%	0.0%	0.0%	0.0%
% SAND:	100.0%	100.0%	100.0%	100.0%
% MUD:	0.0%	0.0%	0.0%	0.0%
% V FINE GRAVEL:	0.0%	0.0%	0.0%	0.0%
% V COARSE SAND:	2.1%	0.5%	1.8%	0.3%
% COARSE SAND:	7.7%	7.6%	7.8%	6.9%
% MEDIUM SAND:	45.7%	59.3%	45.2%	58.8%
% FINE SAND:	39.7%	27.3%	40.7%	28.7%
% V FINE SAND:	4.8%	5.4%	4.6%	5.4%
% V COARSE SILT:	0.0%	0.0%	0.0%	0.0%

Appendix 2.1. (Contd.)

Location	TRV 1						TRV 4			TRV 2
Depth (m)	2	4	5	7	1	2	4	6	7	1
SAMPLE TYPE:	Unimodal Moderately Well Sorted	Unimodal Moderately WellSorted	Unimodal Moderately Sorted	Unimodal Moderately Sorted	Unimodal, Moderately Well Sorted	Unimodal, Moderately Well Sorted	Unimodal, Moderately Sorted	Unimodal, Moderately Sorted	Unimodal, Moderately Sorted	Unimodal, Moderately Well Sorted
TEXTURAL GROUP:	Sand	Sand	Sand	Sand	Sand	Sand	Sand	Sand	Sand	Sand
SEDIMENT NAME:	Moderately Well SortedMedium Sand	Moderately Well Sorted Medium Sand	ModeratelySorted Medium Sand	Moderately Sorted Medium Sand	Moderately Well Sorted Medium Sand	Moderately Well Sorted Medium Sand	Moderately Sorted Medium Sand	Moderately Sorted Medium Sand	Moderately Sorted Medium Sand	Moderately Well Sorted Medium Sand
MEAN	1.353	1.479	1.399	1.367	1.340	1.502	1.377	1.353	1.417	1.354
SORTING	0.621	0.650	0.727	0.700	0.627	0.664	0.731	0.711	0.740	0.622
SKEWNESS	-0.003	0.109	0.129	0.327	0.083	0.072	0.129	0.191	0.244	-0.003
KURTOSIS	3.346	3.371	3.542	3.641	3.638	3.425	3.356	3.380	3.543	3.329
MEAN:	Medium Sand	Medium Sand	Medium Sand	Medium Sand	Medium Sand	Medium Sand	Medium Sand	Medium Sand	Medium Sand	Medium Sand
SORTING:	Moderately Well Sorted	Moderately Well Sorted	Moderately Sorted	Moderately Sorted	Moderately Well Sorted	Moderately Well Sorted	Moderately Sorted	Moderately Sorted	Moderately Sorted	Moderately Well Sorted
SKEWNESS:	Coarse Skewed	Symmetrical	Coarse Skewed	Symmetrical	Coarse Skewed	Symmetrical	Symmetrical	Symmetrical	Symmetrical	Coarse Skewed
KURTOSIS:	Mesokurtic	Leptokurtic	Leptokurtic	Leptokurtic	Mesokurtic	Leptokurtic	Leptokurtic	Leptokurtic	Leptokurtic	Mesokurtic
% GRAVEL:	0.00%	0.00%	0.00%	0.00%	0.0%	0.0%	0.0%	0.0%	0.0%	0.0%
% SAND:	100.00%	100.00%	100.00%	100.00%	100.0%	100.0%	100.0%	100.0%	100.0%	100.0%
% MUD:	0.00%	0.00%	0.00%	0.00%	0.0%	0.0%	0.0%	0.0%	0.0%	0.0%
% V FINE GRAVEL:	0.0%	0.0%	0.0%	0.0%	0.0%	0.0%	0.0%	0.0%	0.0%	0.0%
% V COARSE SAND:	1.7%	2.4%	4.0%	3.3%	1.8%	2.7%	4.1%	4.3%	4.2%	1.7%
% COARSE SAND:	25.4%	17.0%	20.5%	23.1%	26.3%	15.5%	22.0%	22.8%	19.3%	25.5%
% MEDIUM SAND:	64.3%	62.3%	62.6%	58.7%	63.9%	62.5%	60.4%	58.2%	59.5%	64.1%
% FINE SAND:	8.0%	17.1%	10.6%	12.8%	6.9%	18.0%	11.3%	12.5%	14.1%	8.1%
% V FINE SAND:	0.7%	1.2%	2.3%	2.1%	1.1%	1.4%	2.2%	2.2%	2.9%	0.7%
% V COARSE SILT:	0.0%	0.0%	0.0%	0.0%	0.0%	0.0%	0.0%	0.0%	0.0%	0.0%

Appendix 2.1. Textural characteristics of sediments collected from Litho Unit 3 in the study area deducted from Gradistat v5

Location			TRV2		TRV 3				TRV3	TRV 5
Depth (m)	2	4	6	7	1	3	6	7	8	1
SAMPLE TYPE:	Unimodal, Moderately Well Sorted	Unimodal, Moderately Sorted	Unimodal, Moderately Well Sorted	Unimodal, Moderately Well Sorted	Unimodal, Moderately Well Sorted	Unimodal, Moderately Well Sorted	Unimodal, Moderately Sorted	Unimodal, Moderately Sorted	Unimodal, Moderately Sorted	Unimodal, Moderately Well Sorted
TEXTURAL GROUP:	Sand	Sand	Sand	Sand	Sand	Sand	Sand	Sand	Sand	Sand
SEDIMENT NAME:	Moderately Well Sorted Medium Sand	Moderately Sorted Medium Sand	Moderately Well Sorted Medium Sand	Moderately Well Sorted Medium Sand	Moderately Well Sorted Medium Sand	Moderately Well Sorted Medium Sand	Moderately Sorted Medium Sand	Moderately Sorted Medium Sand	Moderately Sorted Medium Sand	Moderately Well Sorted Medium Sand
MEAN	1.495	1.388	1.358	1.385	1.341	1.498	1.386	1.357	1.405	1.348
SORTING	0.646	0.722	0.674	0.689	0.622	0.663	0.727	0.703	0.718	0.627
SKEWNESS	0.057	0.108	0.177	0.133	0.034	0.086	0.124	0.145	0.244	0.036
KURTOSIS	3.340	3.471	3.426	3.428	3.526	3.391	3.404	3.322	3.579	3.290
MEAN:	Medium Sand	Medium Sand	Medium Sand	Medium Sand	Medium Sand	Medium Sand	Medium Sand	Medium Sand	Medium Sand	Medium Sand
SORTING:	Moderately Well Sorted	Moderately Sorted	Moderately Well Sorted	Moderately Well Sorted	Moderately Well Sorted	Moderately Well Sorted	Moderately Sorted	Moderately Sorted	Moderately Sorted	Moderately Well Sorted
SKEWNESS:	Symmetrical	Coarse Skewed	Symmetrical	Symmetrical	Coarse Skewed	Symmetrical	Symmetrical	Symmetrical	Symmetrical	Coarse Skewed
KURTOSIS:	Leptokurtic	Leptokurtic	Leptokurtic	Leptokurtic	Mesokurtic	Leptokurtic	Leptokurtic	Leptokurtic	Leptokurtic	Mesokurtic
% GRAVEL:	0.0%	0.0%	0.0%	0.0%	0.0%	0.0%	0.0%	0.0%	0.0%	0.0%
% SAND:	100.0%	100.0%	100.0%	100.0%	100.0%	100.0%	100.0%	100.0%	100.0%	100.0%
% MUD:	0.0%	0.0%	0.0%	0.0%	0.0%	0.0%	0.0%	0.0%	0.0%	0.0%
% V FINE GRAVEL:	0.0%	0.0%	0.0%	0.0%	0.0%	0.0%	0.0%	0.0%	0.0%	0.0%
% V COARSE SAND:	2.4%	4.0%	3.3%	3.5%	1.9%	2.7%	4.0%	4.2%	3.7%	1.6%
% COARSE SAND:	16.3%	21.2%	22.7%	19.7%	25.8%	16.0%	21.6%	22.4%	19.5%	26.3%
% MEDIUM SAND:	62.2%	62.1%	59.9%	61.4%	64.6%	61.9%	61.1%	58.5%	60.4%	63.4%
% FINE SAND:	18.1%	10.5%	12.6%	13.7%	6.9%	18.0%	11.2%	13.1%	14.0%	7.9%
% V FINE SAND:	1.1%	2.1%	1.5%	1.8%	0.8%	1.4%	2.1%	1.8%	2.5%	0.8%
% V COARSE SILT:	0.0%	0.0%	0.0%	0.0%	0.0%	0.0%	0.0%	0.0%	0.0%	0.0%

Appendix 2.1. (Contd.)

Location					TRV5	TRV 6				
Depth (m)	2	4	6	7	8	1	3	6	7	8
SAMPLE TYPE:	Unimodal, Moderately Well Sorted	Unimodal, Moderately Sorted	Unimodal, Moderately Sorted	Unimodal, Moderately Sorted	Bimodal, Moderately Well Sorted	Unimodal, Moderately Well Sorted	Unimodal, Moderately Well Sorted	Unimodal, Moderately Sorted	Unimodal, Moderately Sorted	Unimodal, Moderately Sorted
TEXTURAL GROUP:	Sand	Sand	Sand	Sand	Sand	Sand	Sand	Sand	Sand	Sand
SEDIMENT NAME:	Moderately Well Sorted Medium Sand	Moderately Sorted Medium Sand	Moderately Sorted Medium Sand	Moderately Sorted Medium Sand	Moderately Well Sorted Medium Sand	Moderately Well Sorted Medium Sand	Moderately Well Sorted Medium Sand	Moderately Sorted Medium Sand	Moderately Sorted Medium Sand	Moderately Sorted Medium Sand
MEAN	1.500	1.388	1.333	1.402	1.934	1.340	1.500	1.404	1.357	1.400
SORTING	0.662	0.738	0.695	0.721	0.650	0.626	0.672	0.749	0.733	0.745
SKEWNESS	0.104	0.131	0.060	0.243	0.165	0.051	0.091	0.208	0.138	0.263
KURTOSIS	3.453	3.357	3.393	3.730	3.514	3.452	3.479	3.356	3.252	3.646
MEAN:	Medium Sand	Medium Sand	Medium Sand	Medium Sand	Medium Sand	Medium Sand	Medium Sand	Medium Sand	Medium Sand	Medium Sand
SORTING:	Moderately Well Sorted	Moderately Sorted	Moderately Sorted	Moderately Sorted	Moderately Well Sorted	Moderately Well Sorted	Moderately Well Sorted	Moderately Sorted	Moderately Sorted	Moderately Sorted
SKEWNESS:	Symmetrical	Symmetrical	Symmetrical	Symmetrical	Fine Skewed	Coarse Skewed	Symmetrical	Symmetrical	Symmetrical	Symmetrical
KURTOSIS:	Leptokurtic	Leptokurtic	Leptokurtic	Leptokurtic	Mesokurtic	Mesokurtic	Leptokurtic	Leptokurtic	Leptokurtic	Leptokurtic
% GRAVEL:	0.0%	0.0%	0.0%	0.0%	0.0%	0.0%	0.0%	0.0%	0.0%	0.0%
% SAND:	100.0%	100.0%	100.0%	100.0%	100.0%	100.0%	100.0%	100.0%	100.0%	100.0%
% MUD:	0.0%	0.0%	0.0%	0.0%	0.0%	0.0%	0.0%	0.0%	0.0%	0.0%
% V FINE GRAVEL:	0.0%	0.0%	0.0%	0.0%	0.0%	0.0%	0.0%	0.0%	0.0%	0.0%
% V COARSE SAND:	2.6%	4.3%	5.0%	4.2%	0.5%	1.7%	3.1%	3.9%	5.0%	4.3%
% COARSE SAND:	15.9%	21.4%	21.8%	18.5%	2.3%	26.8%	15.6%	21.7%	21.4%	18.4%
% MEDIUM SAND:	62.2%	60.6%	60.0%	61.6%	61.8%	63.8%	61.8%	59.5%	59.2%	61.6%
% FINE SAND:	17.8%	11.5%	12.0%	13.3%	29.7%	7.0%	18.0%	12.3%	12.3%	12.8%
% V FINE SAND:	1.5%	2.2%	1.3%	2.5%	5.6%	0.8%	1.6%	2.6%	2.1%	2.8%
% V COARSE SILT:	0.0%	0.0%	0.0%	0.0%	0.0%	0.0%	0.0%	0.0%	0.0%	0.0%

Appendix 2.1. (Contd.)

Location	TRV 6	TRV 7					TRV 7	TRV 9		
Depth (m)	9	1	2	4	6	7	8	2	5	6
SAMPLE TYPE:	Bimodal, Moderately Sorted	Unimodal, Moderately Well Sorted	Unimodal, Moderately Well Sorted	Unimodal, Moderately Sorted	Unimodal, Moderately Sorted	Unimodal, Moderately Sorted	Bimodal, Moderately Well Sorted	Unimodal, Moderately Well Sorted	Unimodal, Moderately Well Sorted	Unimodal, Moderately Sorted
TEXTURAL GROUP:	Sand	Sand	Sand	Sand	Sand	Sand	Sand	Sand	Sand	Sand
SEDIMENT NAME:	Moderately Sorted Medium Sand	Moderately Well Sorted Medium Sand	Moderately Well Sorted Medium Sand	Moderately Sorted Medium Sand	Moderately Sorted Medium Sand	Moderately Sorted Medium Sand	Moderately Well Sorted Medium Sand	Moderately Well Sorted Medium Sand	Moderately Well Sorted Medium Sand	Moderately Sorted Medium Sand
MEAN	1.860	1.351	1.502	1.397	1.414	1.387	1.861	1.356	1.506	1.391
SORTING	0.692	0.647	0.676	0.751	0.744	0.718	0.679	0.650	0.682	0.748
SKEWNESS	0.170	0.150	0.115	0.237	0.328	0.177	0.164	0.192	0.135	0.219
KURTOSIS	3.202	3.535	3.512	3.430	3.691	3.392	3.163	3.601	3.515	3.406
MEAN:	Medium Sand	Medium Sand	Medium Sand	Medium Sand	Medium Sand	Medium Sand	Medium Sand	Medium Sand	Medium Sand	Medium Sand
SORTING:	Moderately Sorted	Moderately Well Sorted	Moderately Well Sorted	Moderately Sorted	Moderately Sorted	Moderately Sorted	Moderately Well Sorted	Moderately Well Sorted	Moderately Well Sorted	Moderately Sorted
SKEWNESS:	Fine Skewed	Coarse Skewed	Symmetrical	Symmetrical	Symmetrical	Symmetrical	Fine Skewed	Coarse Skewed	Symmetrical	Symmetrical
KURTOSIS:	Mesokurtic	Mesokurtic	Leptokurtic	Leptokurtic	Leptokurtic	Leptokurtic	Mesokurtic	Mesokurtic	Leptokurtic	Leptokurtic
% GRAVEL:	0.0%	0.0%	0.0%	0.0%	0.0%	0.0%	0.0%	0.0%	0.0%	0.0%
% SAND:	100.0%	100.0%	100.0%	100.0%	100.0%	100.0%	100.0%	100.0%	100.0%	100.0%
% MUD:	0.0%	0.0%	0.0%	0.0%	0.0%	0.0%	0.0%	0.0%	0.0%	0.0%
% V FINE GRAVEL:	0.0%	0.0%	0.0%	0.0%	0.0%	0.0%	0.0%	0.0%	0.0%	0.0%
% V COARSE SAND:	0.5%	1.7%	3.0%	4.1%	3.8%	4.0%	0.4%	1.6%	3.0%	4.2%
% COARSE SAND:	7.6%	26.8%	15.6%	21.8%	18.6%	22.5%	7.2%	26.8%	15.6%	22.0%
% MEDIUM SAND:	59.3%	63.0%	61.8%	59.6%	61.7%	59.5%	59.7%	63.0%	61.6%	59.4%
% FINE SAND:	27.3%	7.3%	17.9%	11.6%	12.8%	12.3%	27.7%	7.3%	17.9%	11.7%
% V FINE SAND:	5.4%	1.2%	1.6%	2.8%	3.1%	1.7%	5.1%	1.3%	1.9%	2.6%
% V COARSE SILT:	0.0%	0.0%	0.0%	0.0%	0.0%	0.0%	0.0%	0.0%	0.0%	0.0%

Appendix 2.1. (Contd.)

Location			TRV 8					TRV 10	TRV 10	
Depth (m)	8	9	2	3	5	7	9	1	4	5
SAMPLE TYPE:	Unimodal, Moderately Sorted	Unimodal, Moderately Sorted	Bimodal, Moderately Sorted	Unimodal, Moderately Well Sorted	Unimodal, Moderately Sorted	Bimodal, Moderately Sorted	Unimodal, Moderately Sorted	Unimodal, Moderately Well Sorted	Unimodal, Moderately Well Sorted	Unimodal, Moderately Sorted
TEXTURAL GROUP:	Sand	Sand	Sand	Sand	Sand	Sand	Sand	Sand	Sand	Sand
SEDIMENT NAME:	Moderately Sorted Medium Sand	Moderately Sorted Medium Sand	Moderately Sorted Medium Sand	Moderately Well Sorted Medium Sand	Moderately Sorted Medium Sand	Moderately Sorted Medium Sand	Moderately Sorted Medium Sand	Moderately Well Sorted Medium Sand	Moderately Well Sorted [illegible] Sand	Moderately Sorted [illegible] Sand
MEAN	1.347	1.436	1.384	1.503	1.398	1.382	1.400	1.364	1.521	1.361
SORTING	0.752	0.777	0.714	0.672	0.772	0.762	0.738	0.640	0.676	0.742
SKEWNESS	0.163	0.351	0.019	0.105	0.256	0.252	0.312	-0.048	0.148	0.153
KURTOSIS	3.319	3.599	2.967	3.563	3.292	2.920	3.552	3.233	3.365	3.462
MEAN:	Medium Sand	Medium Sand	Medium Sand	Medium Sand	Medium Sand	Medium Sand	Medium Sand	Medium Sand	Medium Sand	Medium Sand
SORTING:	Moderately Sorted	Moderately Sorted	Moderately Sorted	Moderately Well Sorted	Moderately Sorted	Moderately Sorted	Moderately Sorted	Moderately Well Sorted	Moderately Well Sorted	Moderately Sorted
SKEWNESS:	Symmetrical	Symmetrical	Very Coarse Skewed	Symmetrical	Symmetrical	Symmetrical	Symmetrical	Coarse Skewed	Symmetrical	Symmetrical
KURTOSIS:	Leptokurtic	Leptokurtic	Mesokurtic	Leptokurtic	Leptokurtic	Leptokurtic	Leptokurtic	Mesokurtic	Leptokurtic	Leptokurtic
% GRAVEL:	0.0%	0.0%	0.0%	0.0%	0.0%	0.0%	0.0%	0.0%	0.0%	0.0%
% SAND:	100.0%	100.0%	100.0%	100.0%	100.0%	100.0%	100.0%	100.0%	100.0%	100.0%
% MUD:	0.0%	0.0%	0.0%	0.0%	0.0%	0.0%	0.0%	0.0%	0.0%	0.0%
% V FINE GRAVEL:	0.0%	0.0%	0.0%	0.0%	0.0%	0.0%	0.0%	0.0%	0.0%	0.0%
% V COARSE SAND:	6.0%	4.2%	2.0%	3.0%	4.3%	4.6%	4.0%	1.9%	2.4%	4.9%
% COARSE SAND:	21.3%	18.5%	34.3%	15.3%	22.4%	24.1%	20.3%	25.0%	16.8%	21.8%
% MEDIUM SAND:	58.5%	59.6%	53.9%	62.3%	57.9%	54.4%	60.3%	63.4%	59.5%	60.9%
% FINE SAND:	11.8%	13.9%	8.2%	17.8%	12.3%	14.5%	12.6%	8.9%	19.5%	10.0%
% V FINE SAND:	2.4%	3.8%	1.6%	1.6%	3.1%	2.4%	2.8%	0.7%	1.8%	2.5%
% V COARSE SILT:	0.0%	0.0%	0.0%	0.0%	0.0%	0.0%	0.0%	0.0%	0.0%	0.0%

Appendix 2.1. (Contd.)

Location			
Depth (m)	7	9	10
SAMPLE TYPE:	Unimodal, Moderately Sorted	Bimodal, Moderately Sorted	Unimodal, Moderately Sorted
TEXTURAL GROUP:	Sand	Sand	Sand
SEDIMENT NAME:	Moderately Sorted Medium Sand	Moderately Sorted Medium Sand	Moderately Sorted Medium Sand
MEAN	1.383	1.294	1.387
SORTING	0.766	0.798	0.718
SKEWNESS	0.156	0.449	0.177
KURTOSIS	3.018	3.036	3.392
MEAN:	Medium Sand	Medium Sand	Medium Sand
SORTING:	Moderately Sorted	Moderately Sorted	Moderately Sorted
SKEWNESS:	Symmetrical	Fine Skewed	Symmetrical
KURTOSIS:	Leptokurtic	Very Leptokurtic	Leptokurtic
% GRAVEL:	0.0%	0.0%	0.0%
% SAND:	100.0%	100.0%	100.0%
% MUD:	0.0%	0.0%	0.0%
% V FINE GRAVEL:	0.0%	0.0%	0.0%
% V COARSE SAND:	5.3%	5.7%	4.0%
% COARSE SAND:	24.5%	24.7%	22.5%
% MEDIUM SAND:	52.8%	49.3%	59.5%
% FINE SAND:	15.0%	18.0%	12.3%
% V FINE SAND:	2.4%	2.3%	1.7%
% V COARSE SILT:	0.0%	0.0%	0.0%

Appendix 2.1. (Contd.)

APPENDIX 2(B): EDS results

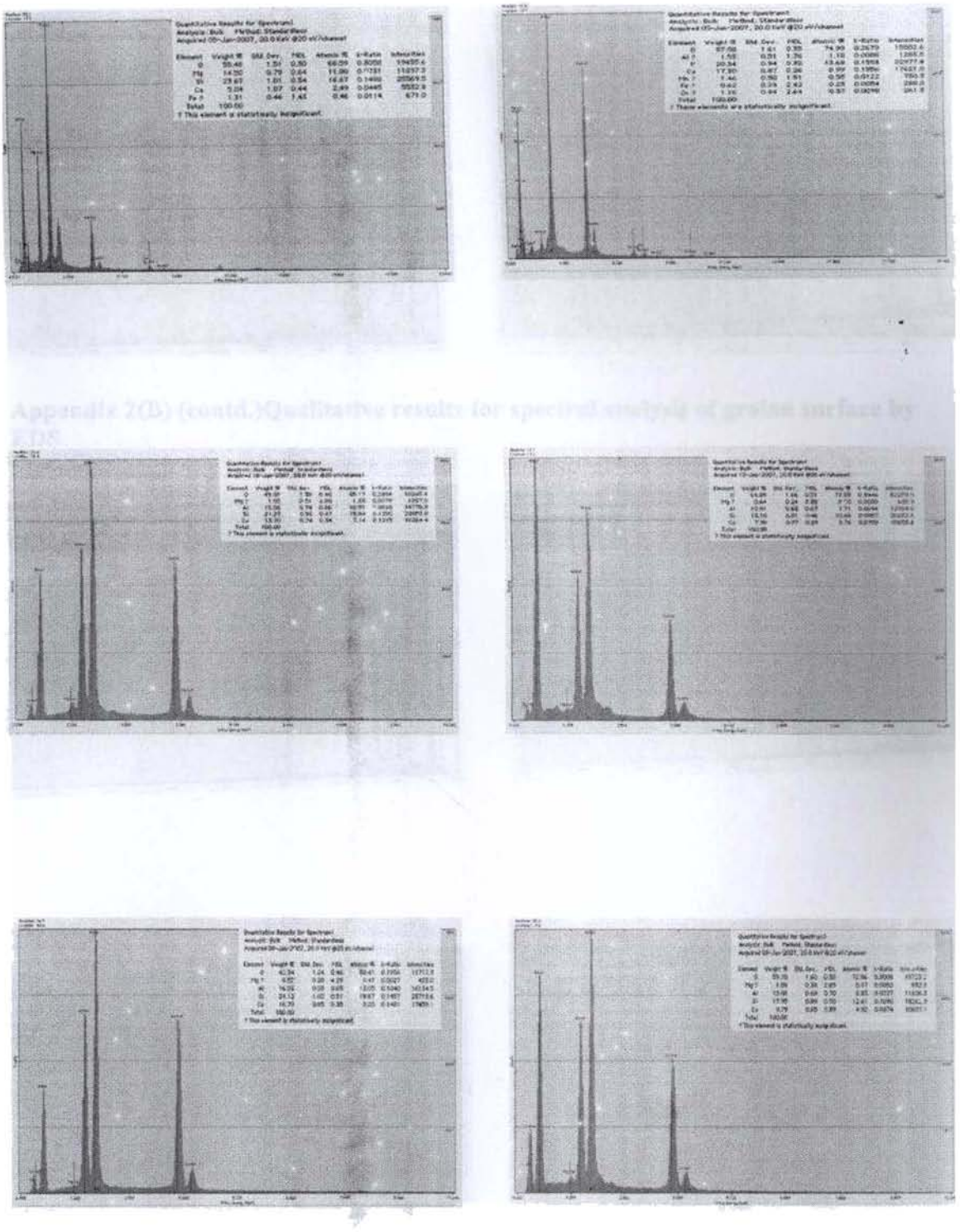

Appendix 2(B).Qualitative results for spectral analysis of grain surface by EDS

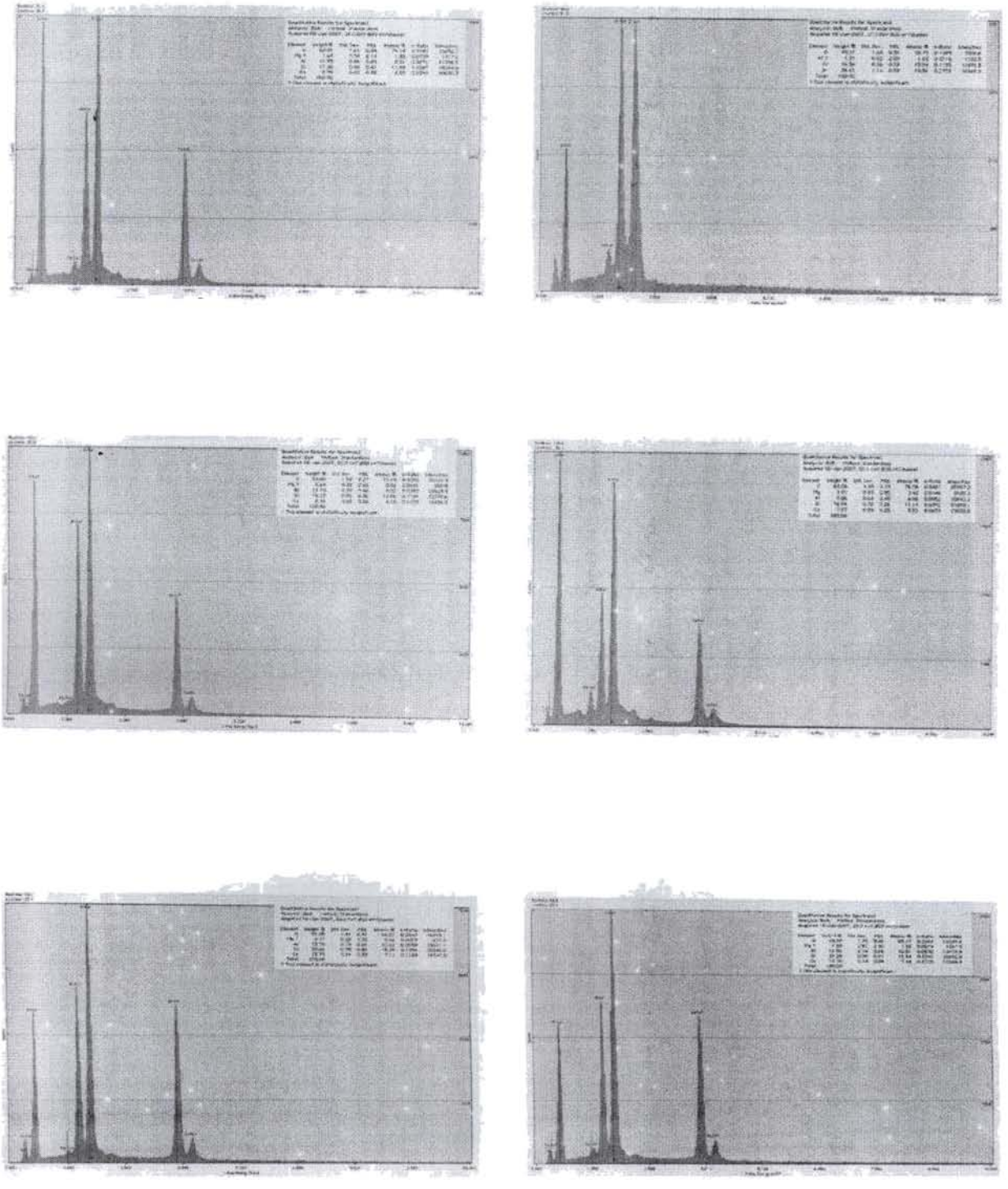

Appendix 2(B) (contd.) Qualitative results for spectral analysis of grain surface by EDS

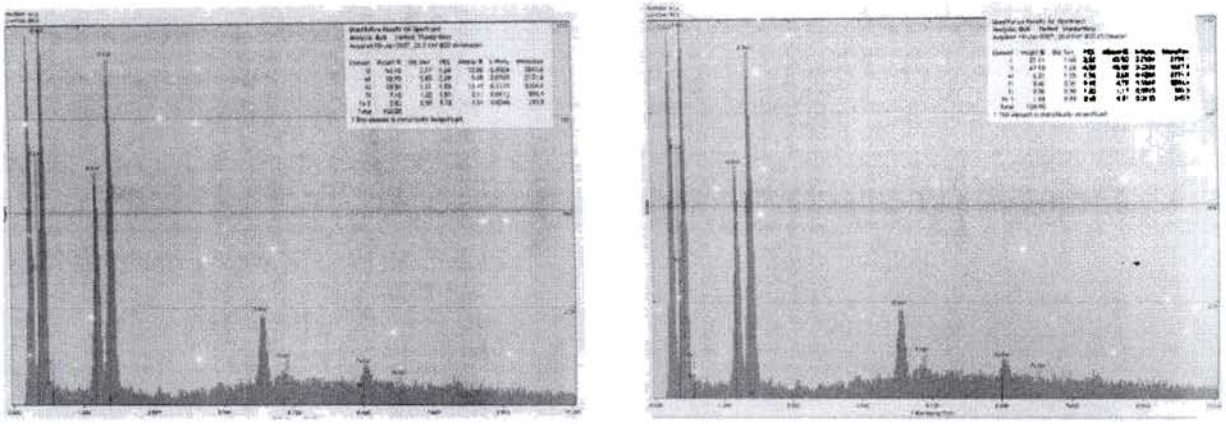

Appendix 2(B) (contd.)Qualitative results for spectral analysis of grainn surface by EDS

APPENDIX 3 : SEM Data

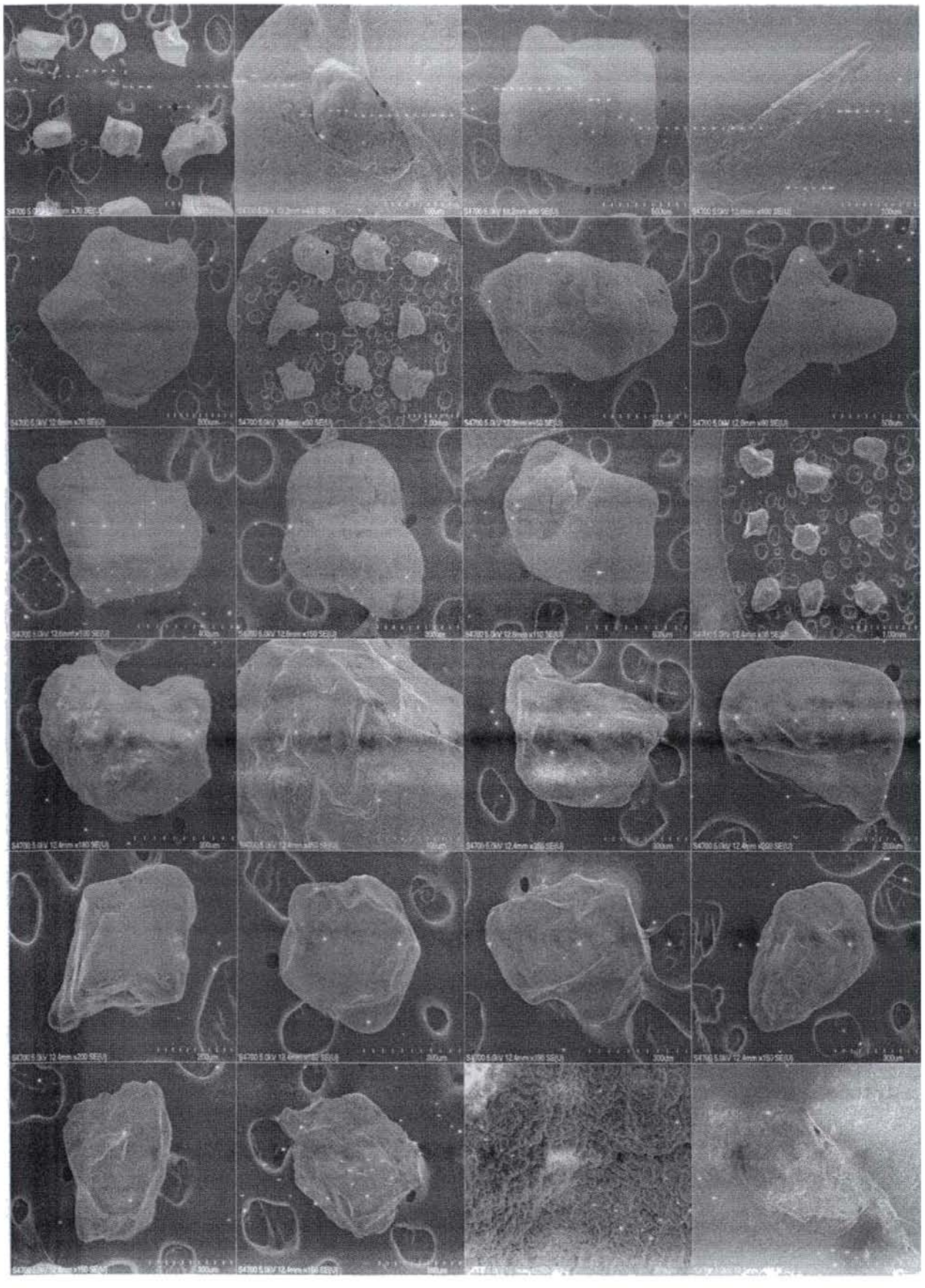

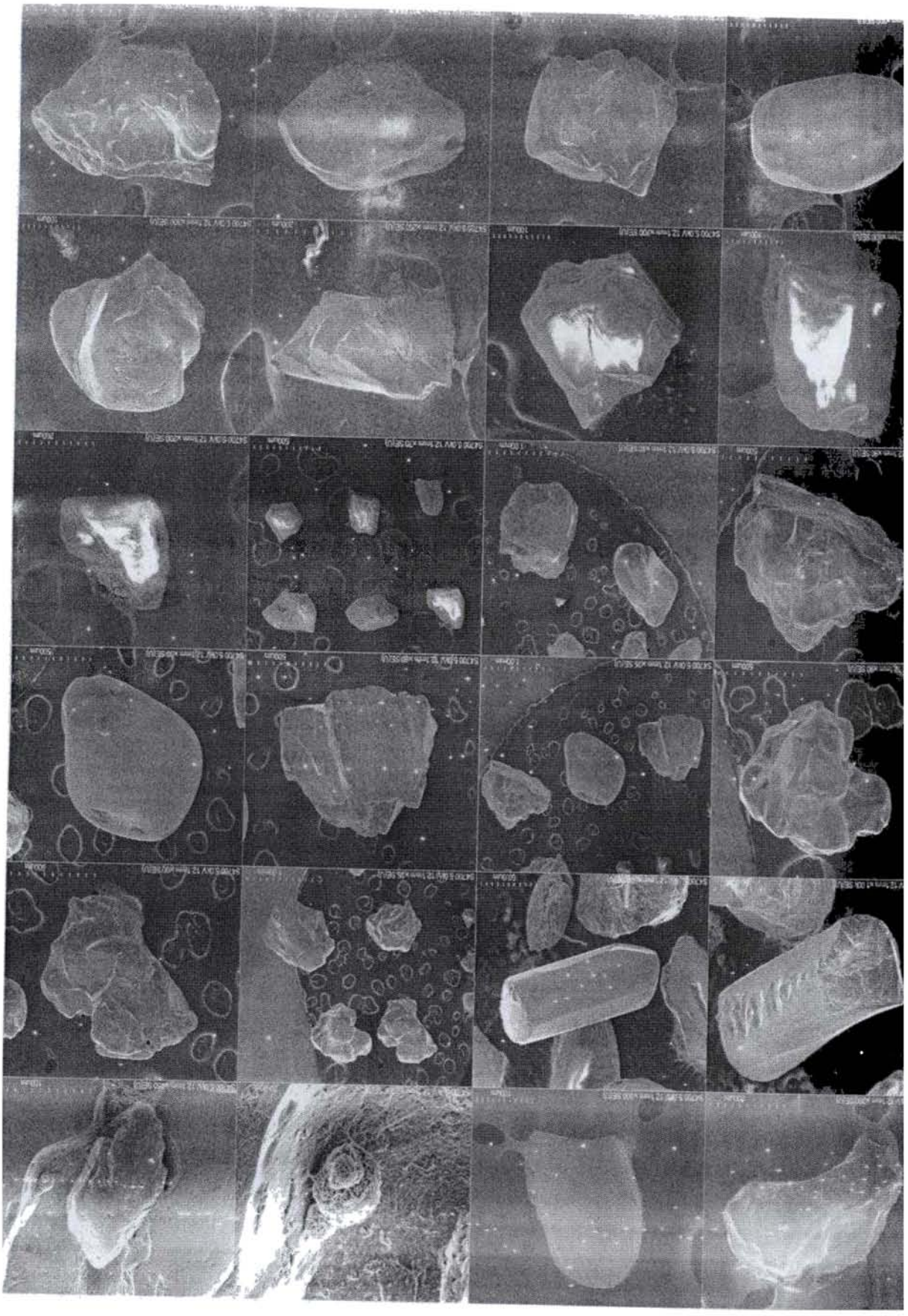

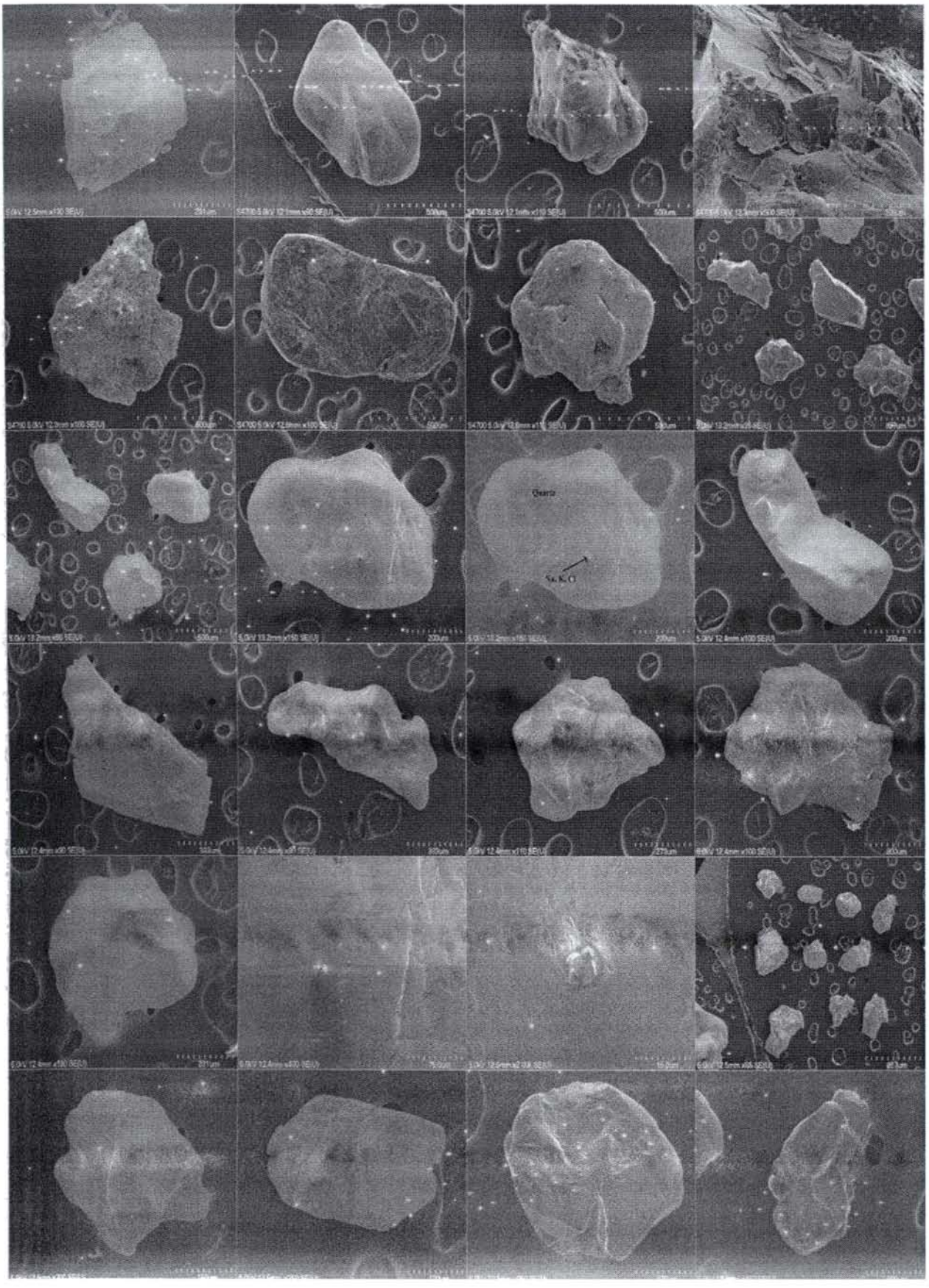
Quartz
Si, K, O

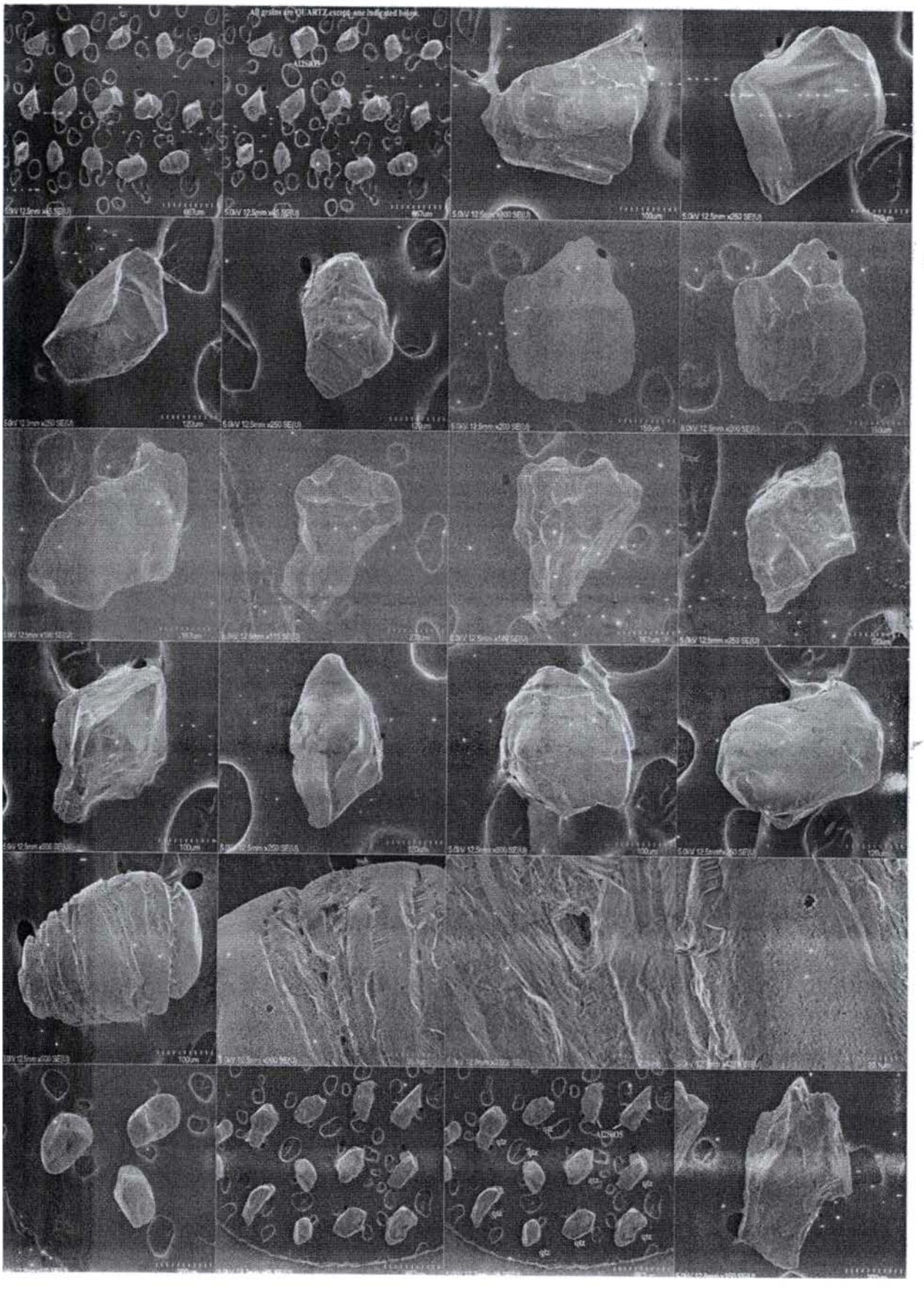
All grains are QUARTZ except one indicated below.
Al2SiO5
Al2SiO5
qtz
qtz
qtz
qtz

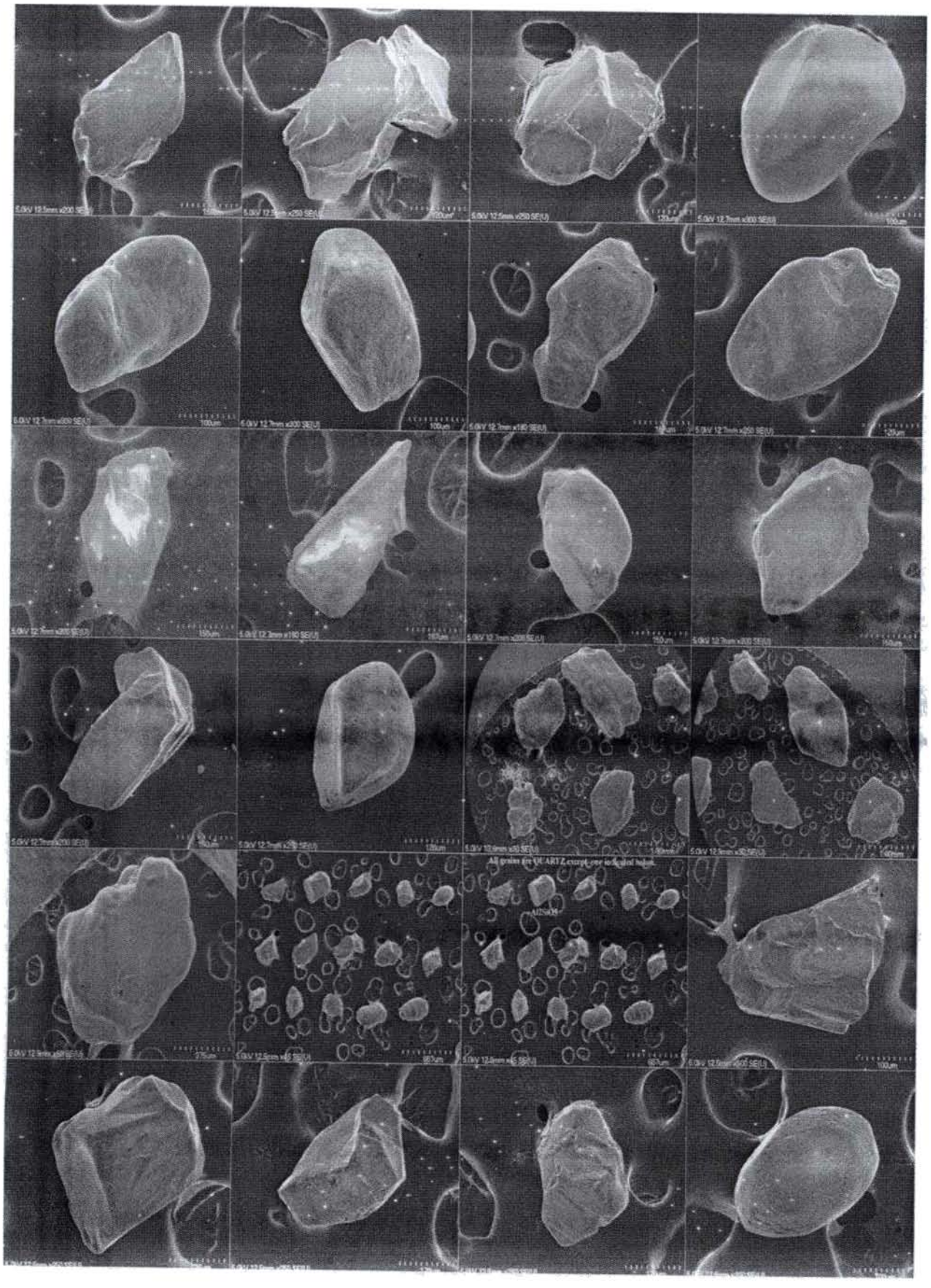
All grains are QUARTZ except one orthoclase below.

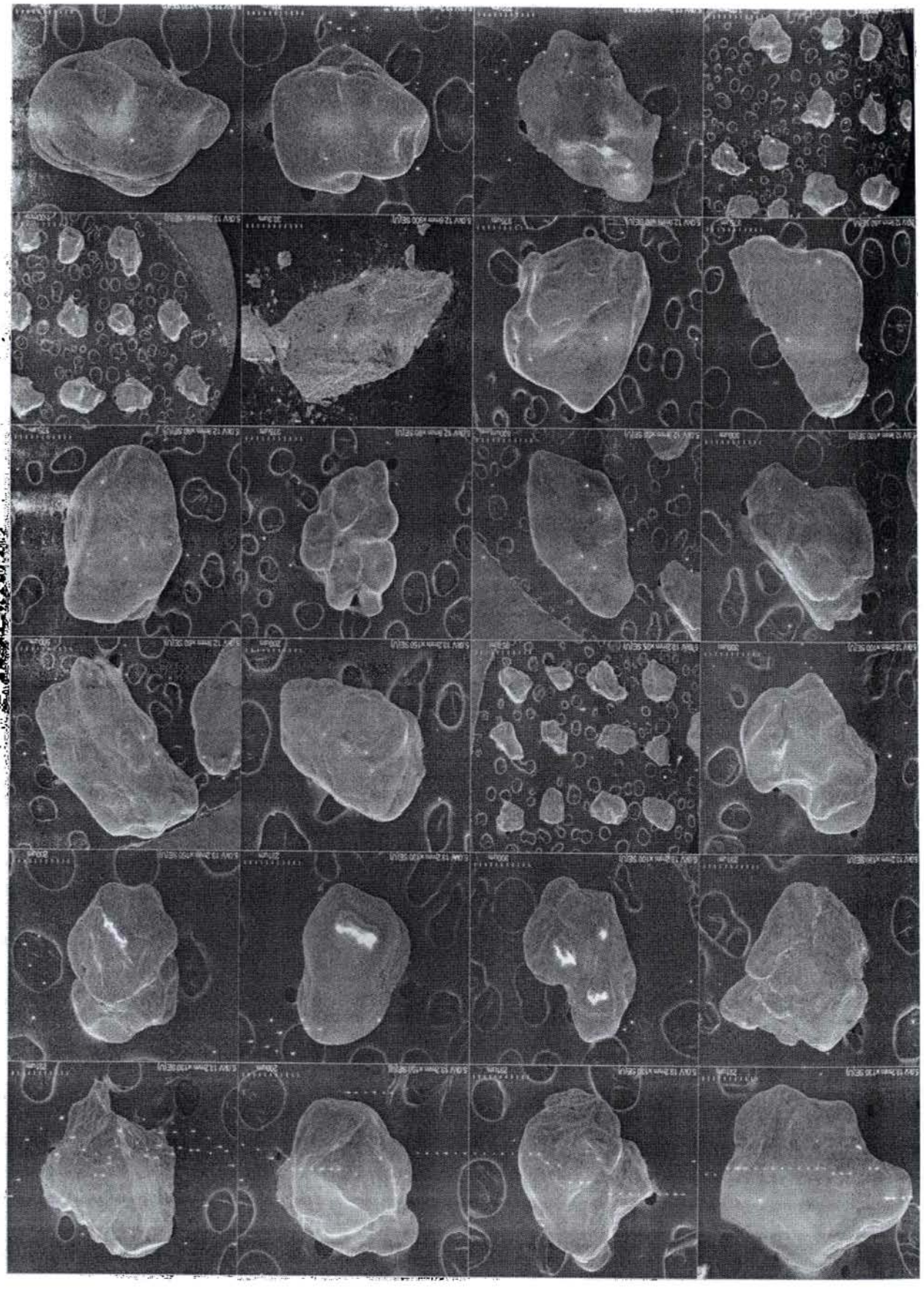

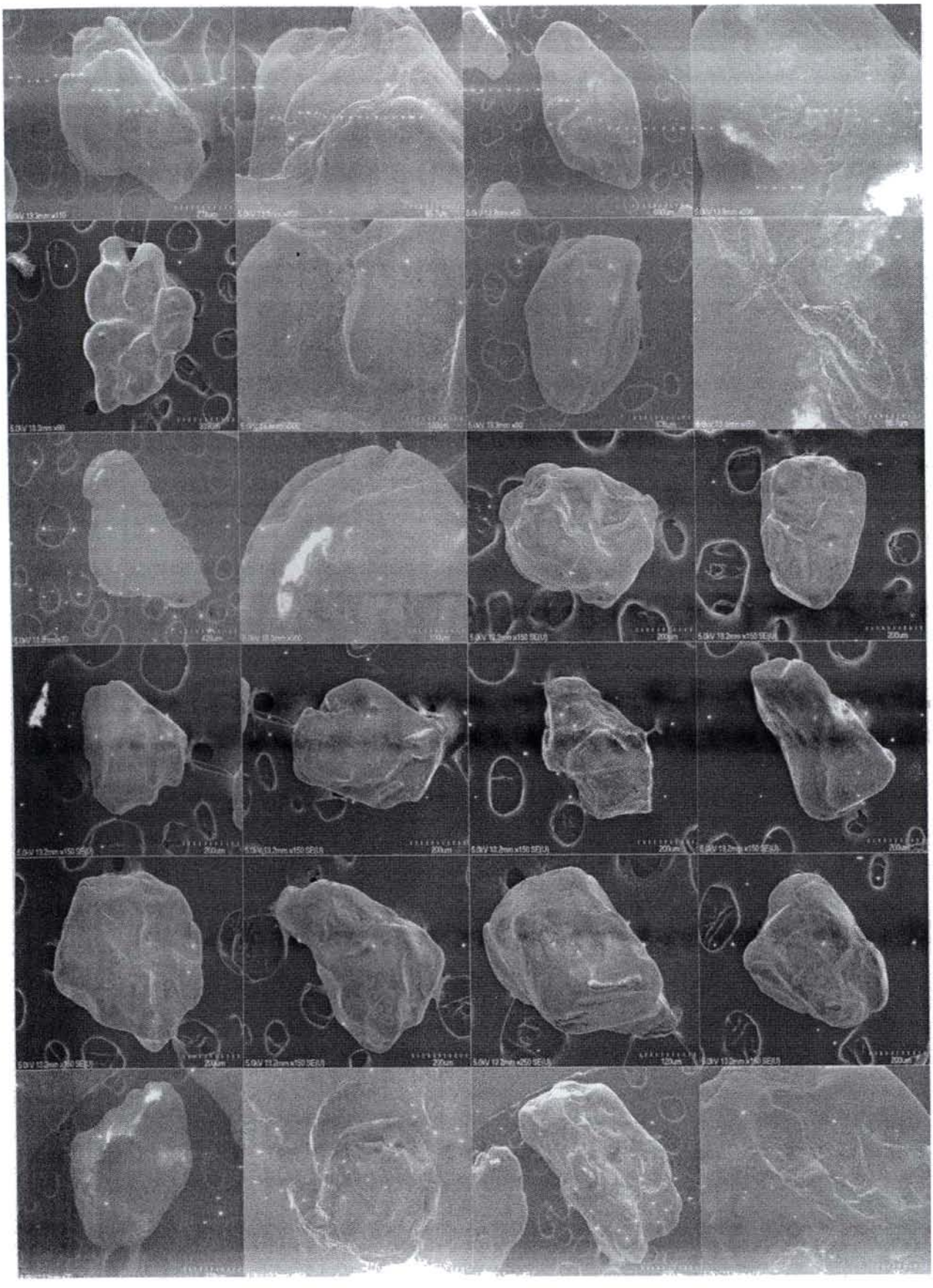

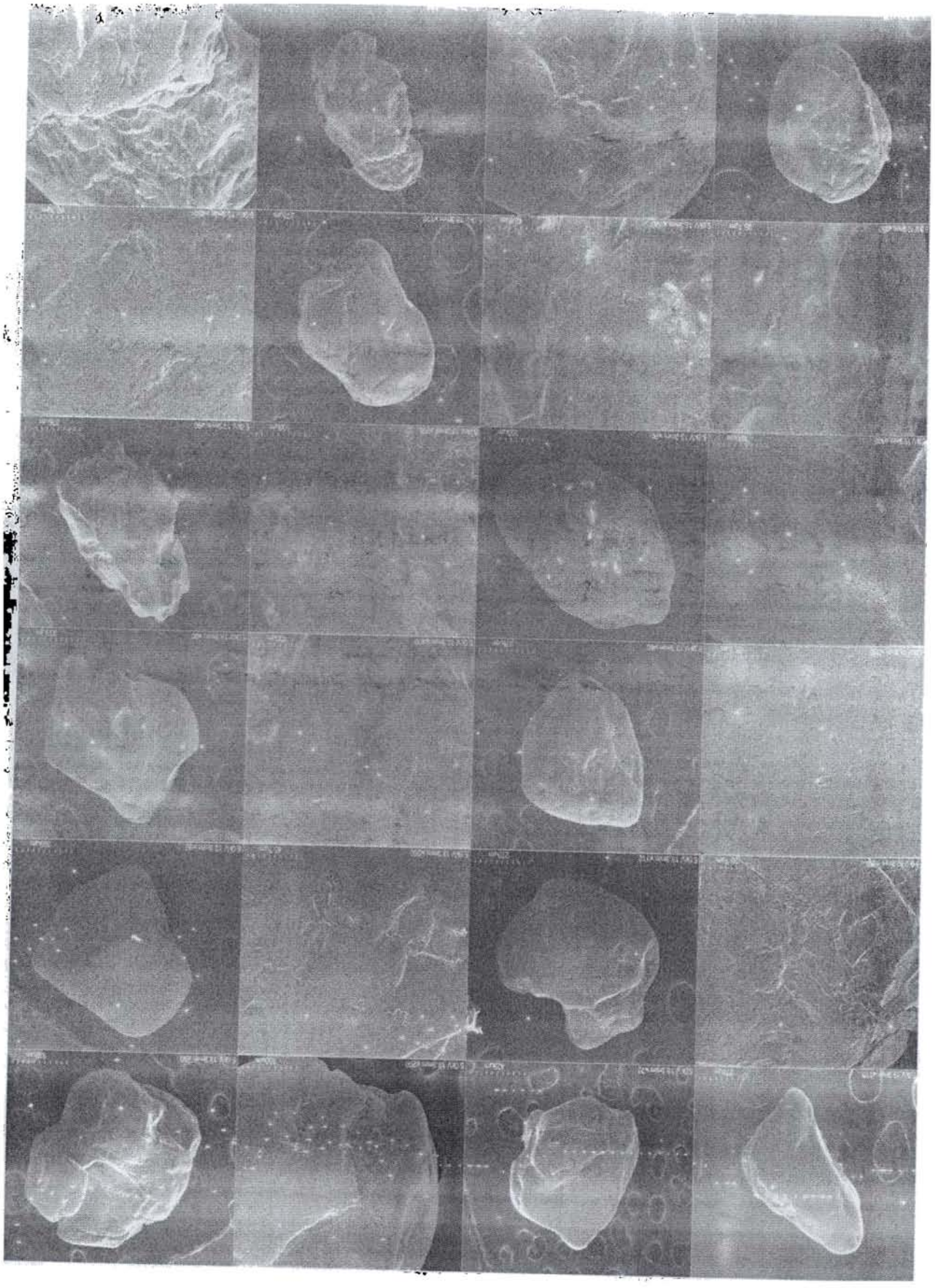

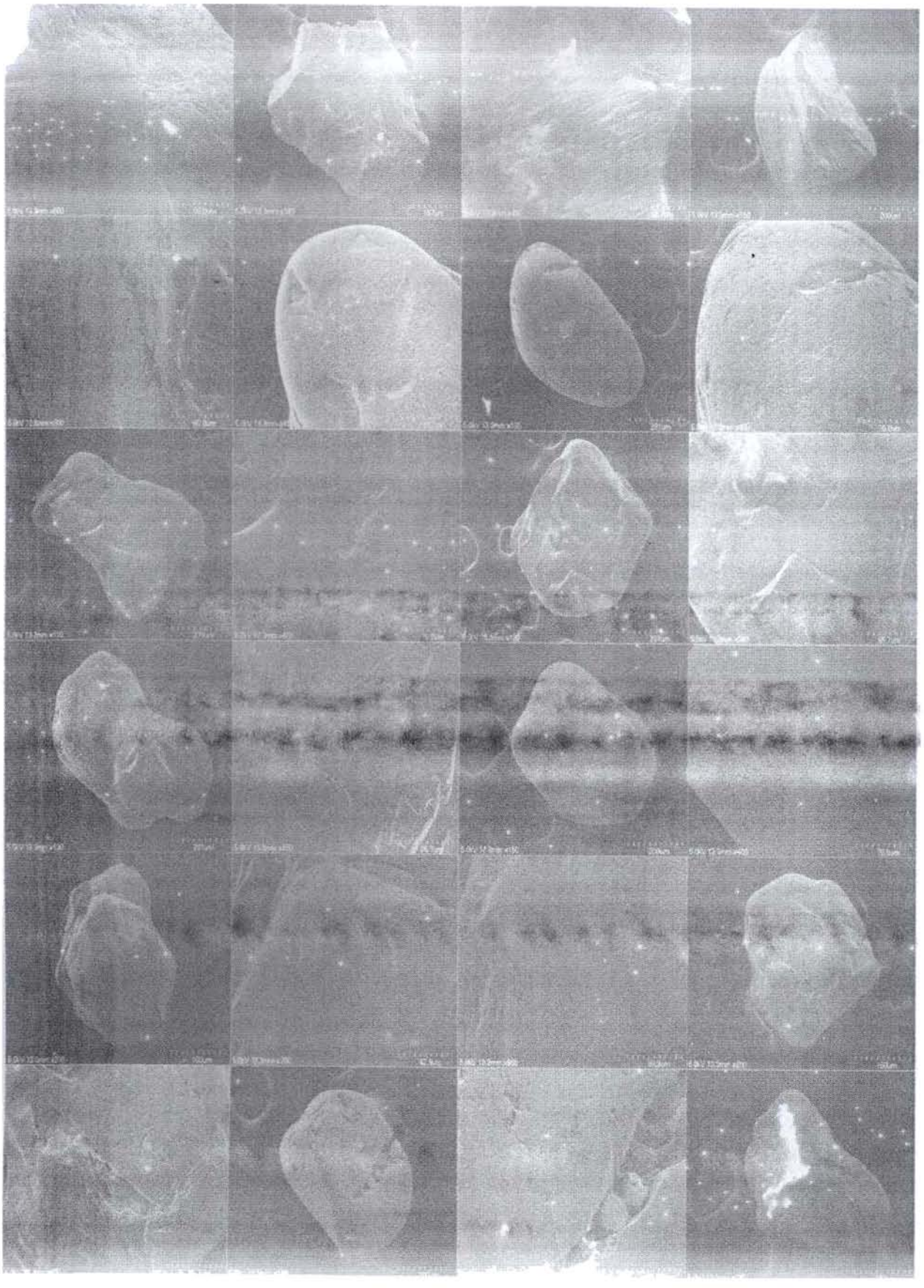

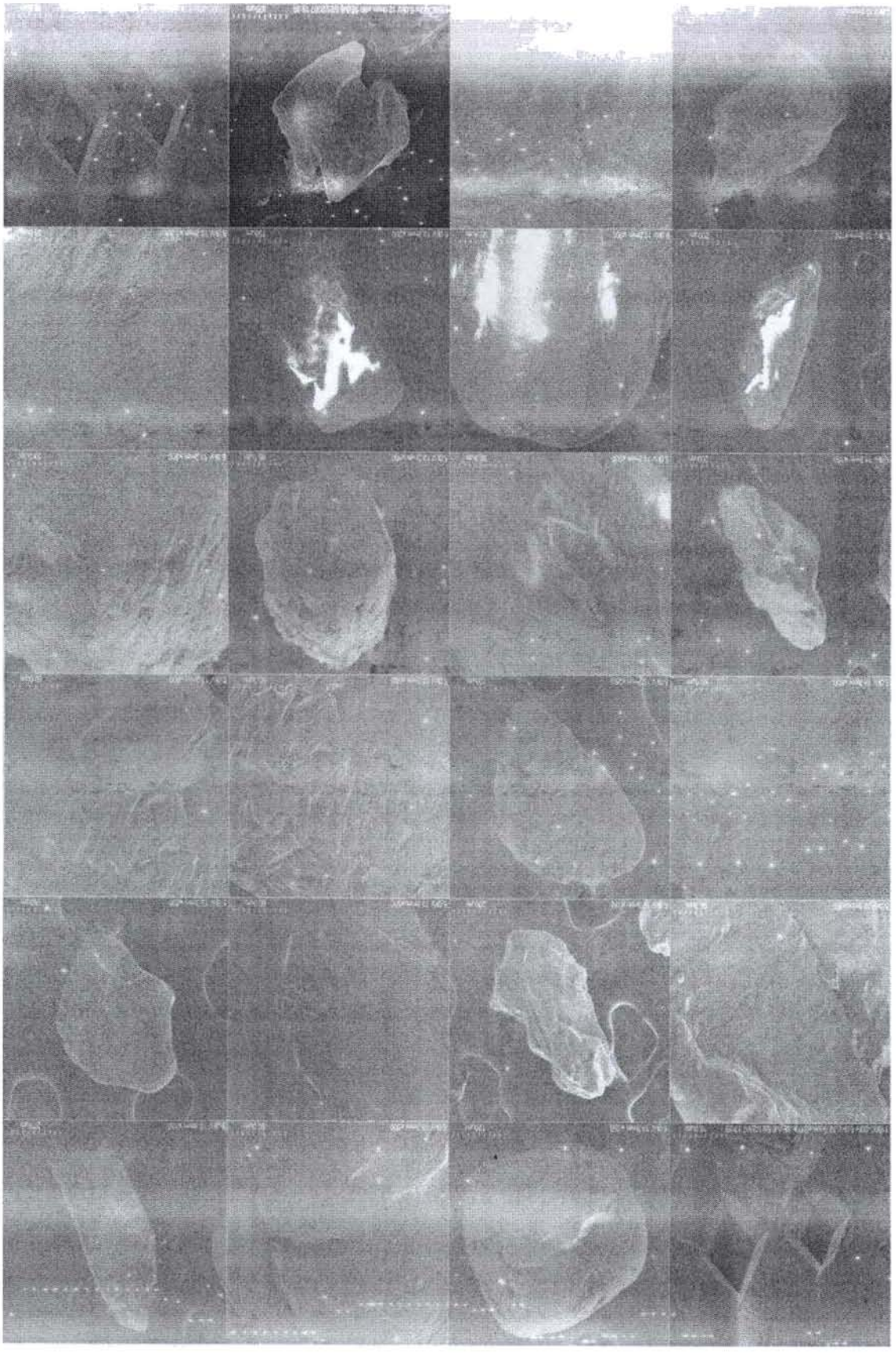

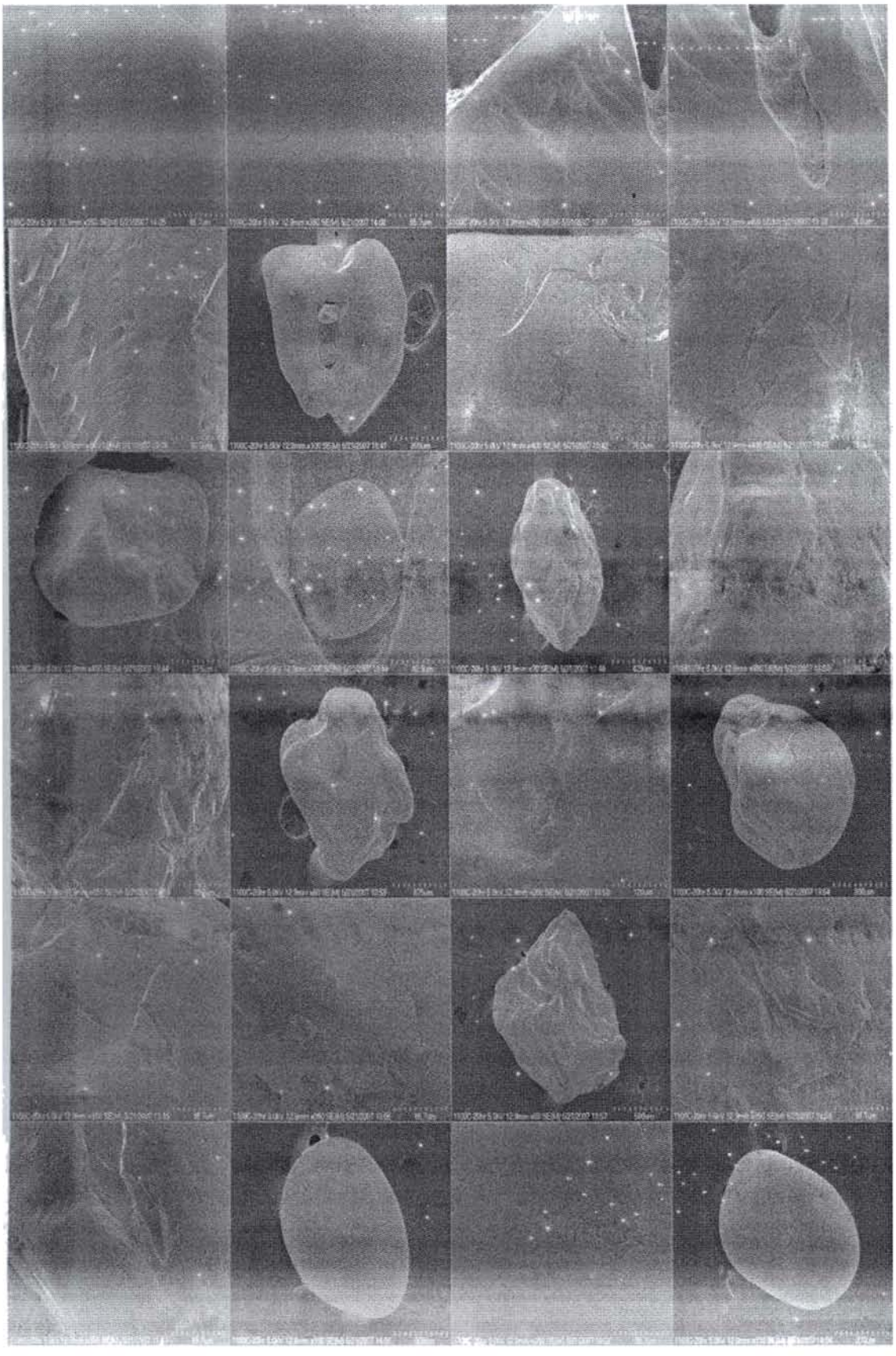

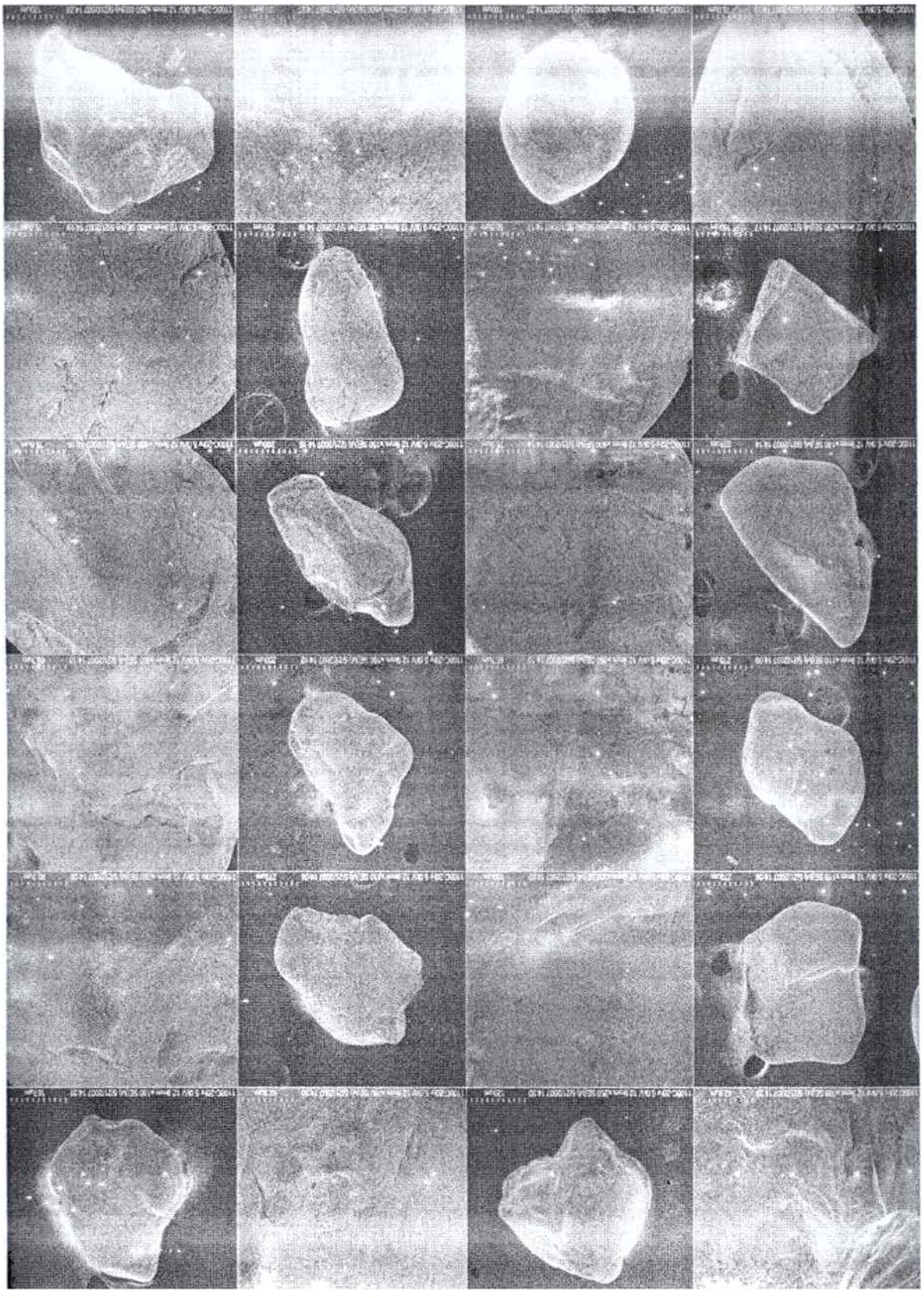

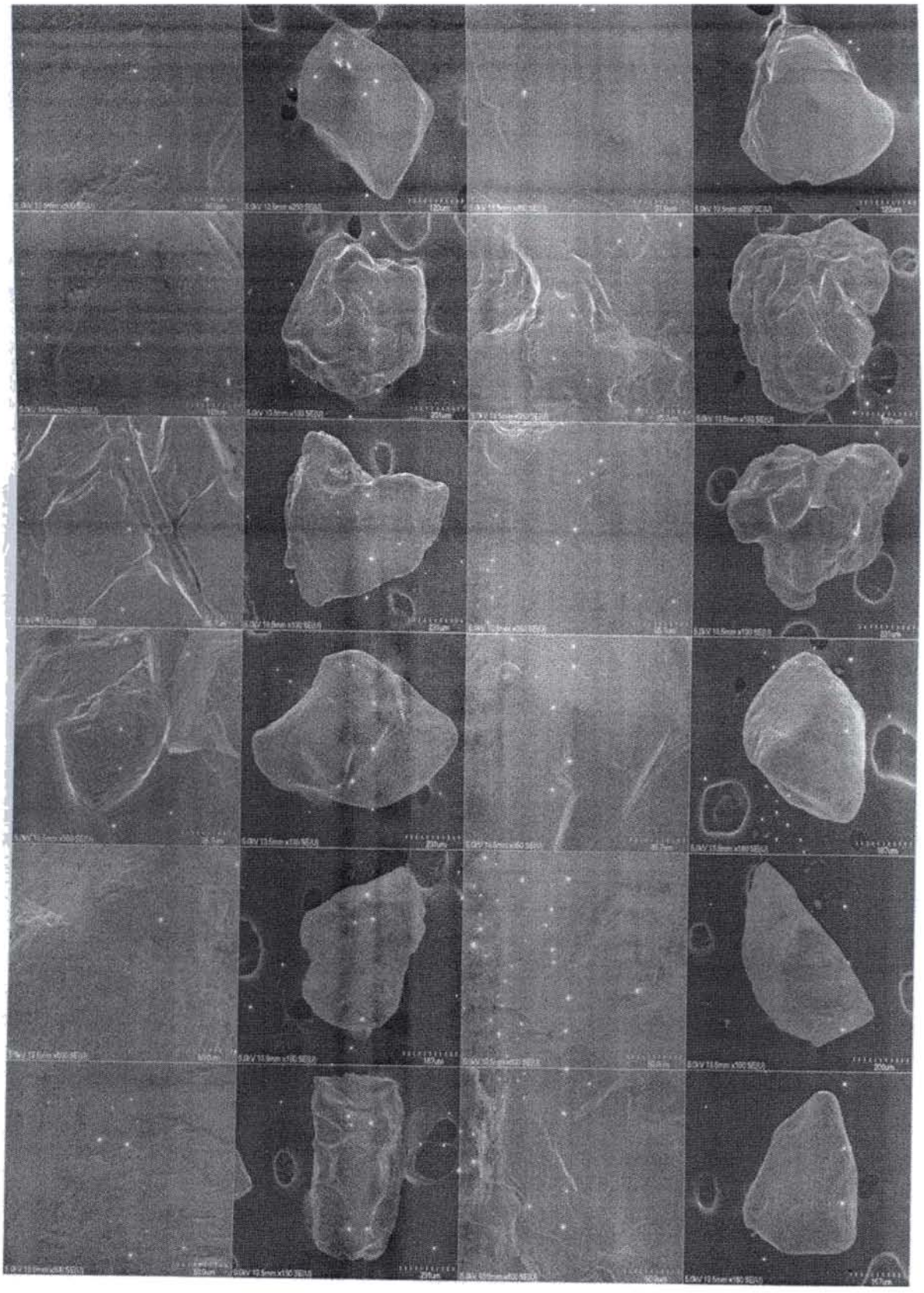

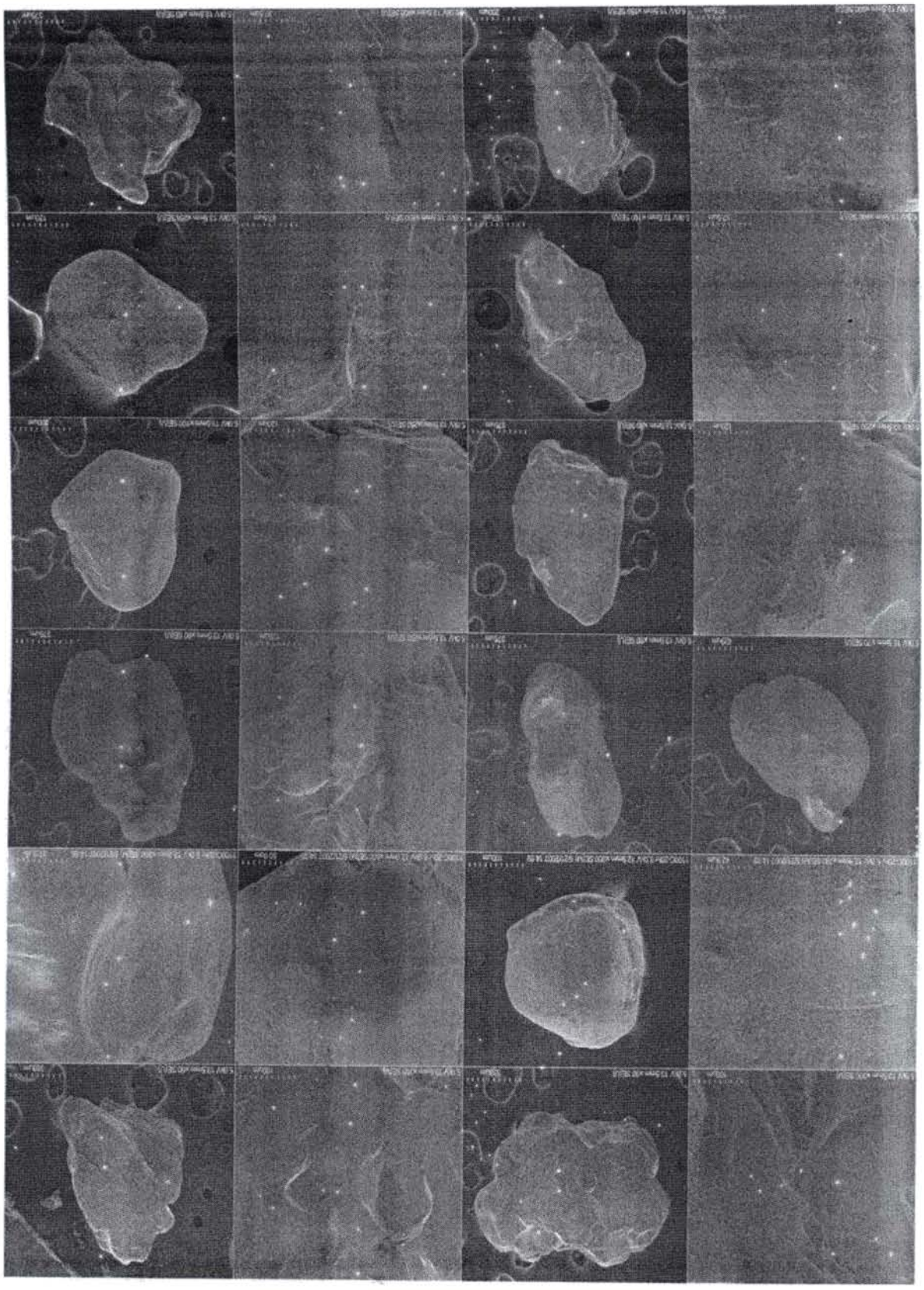

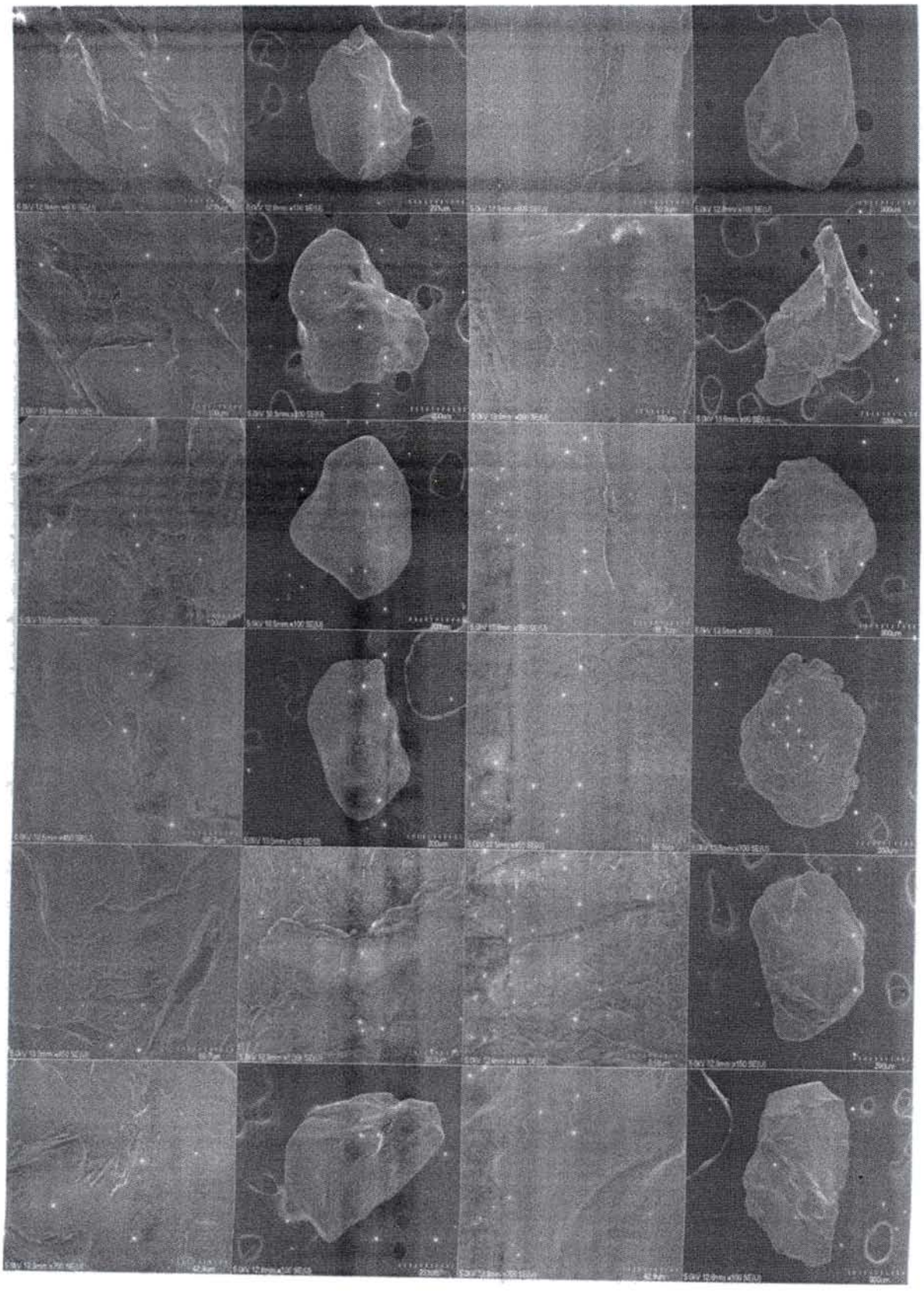

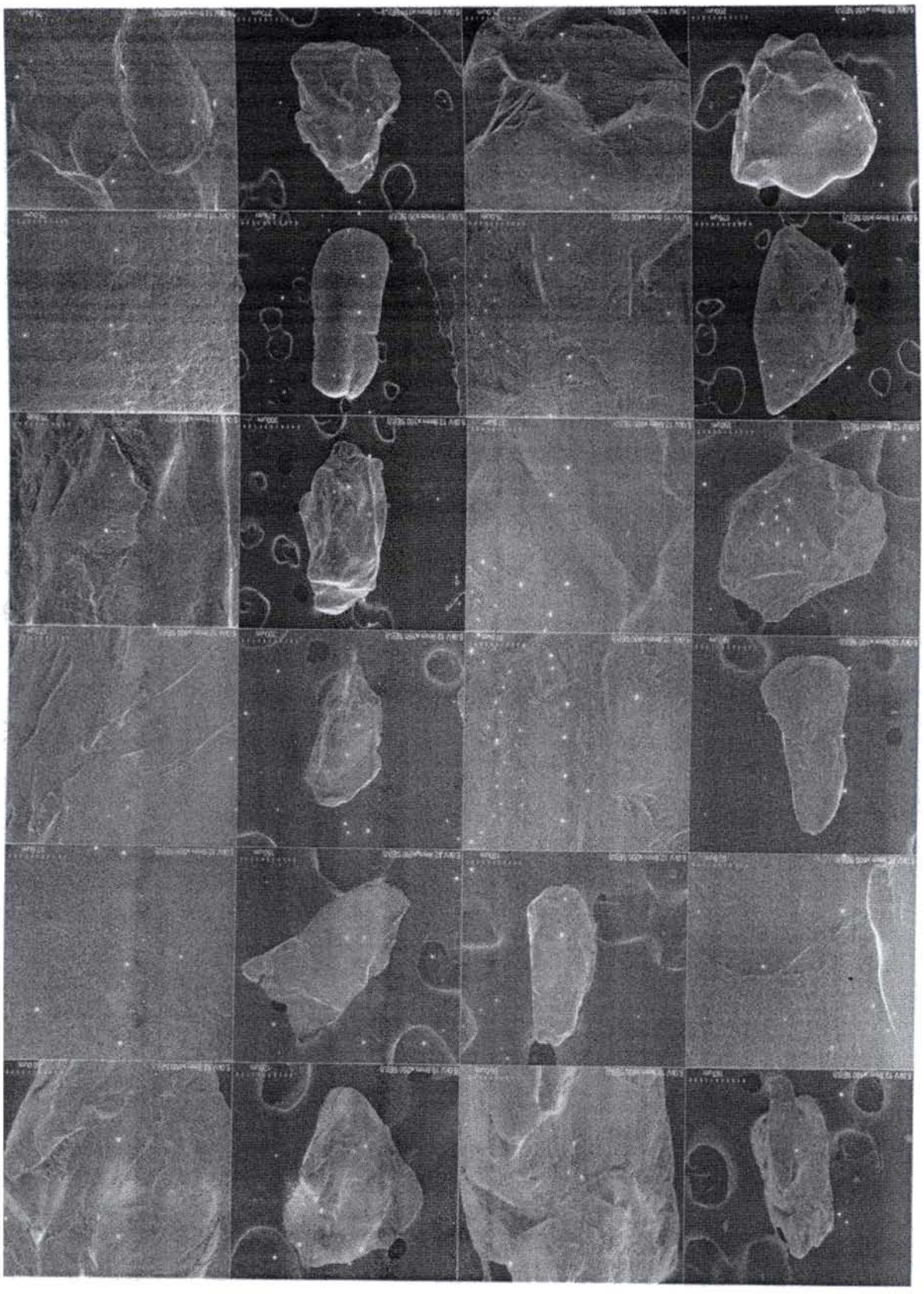

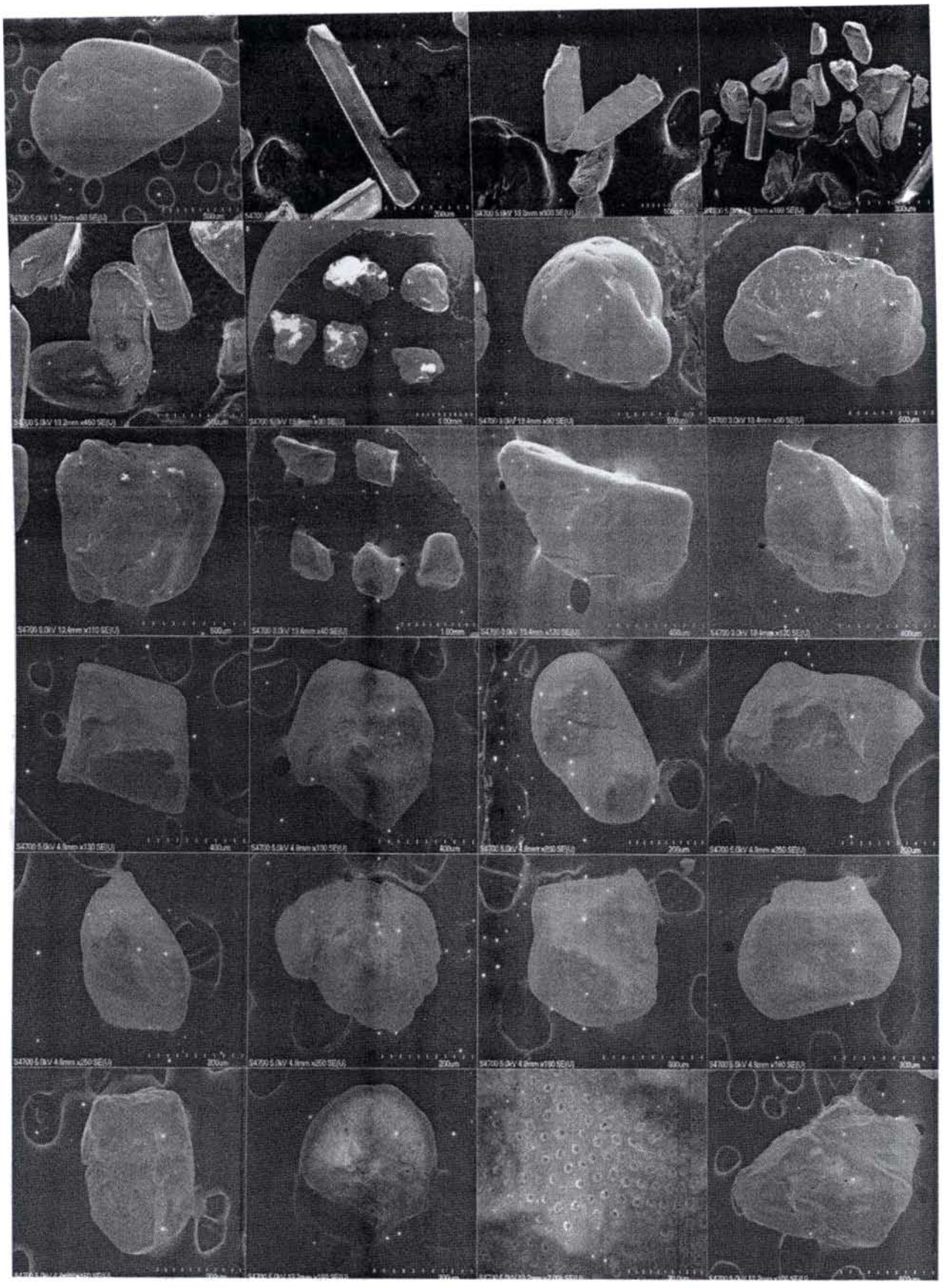

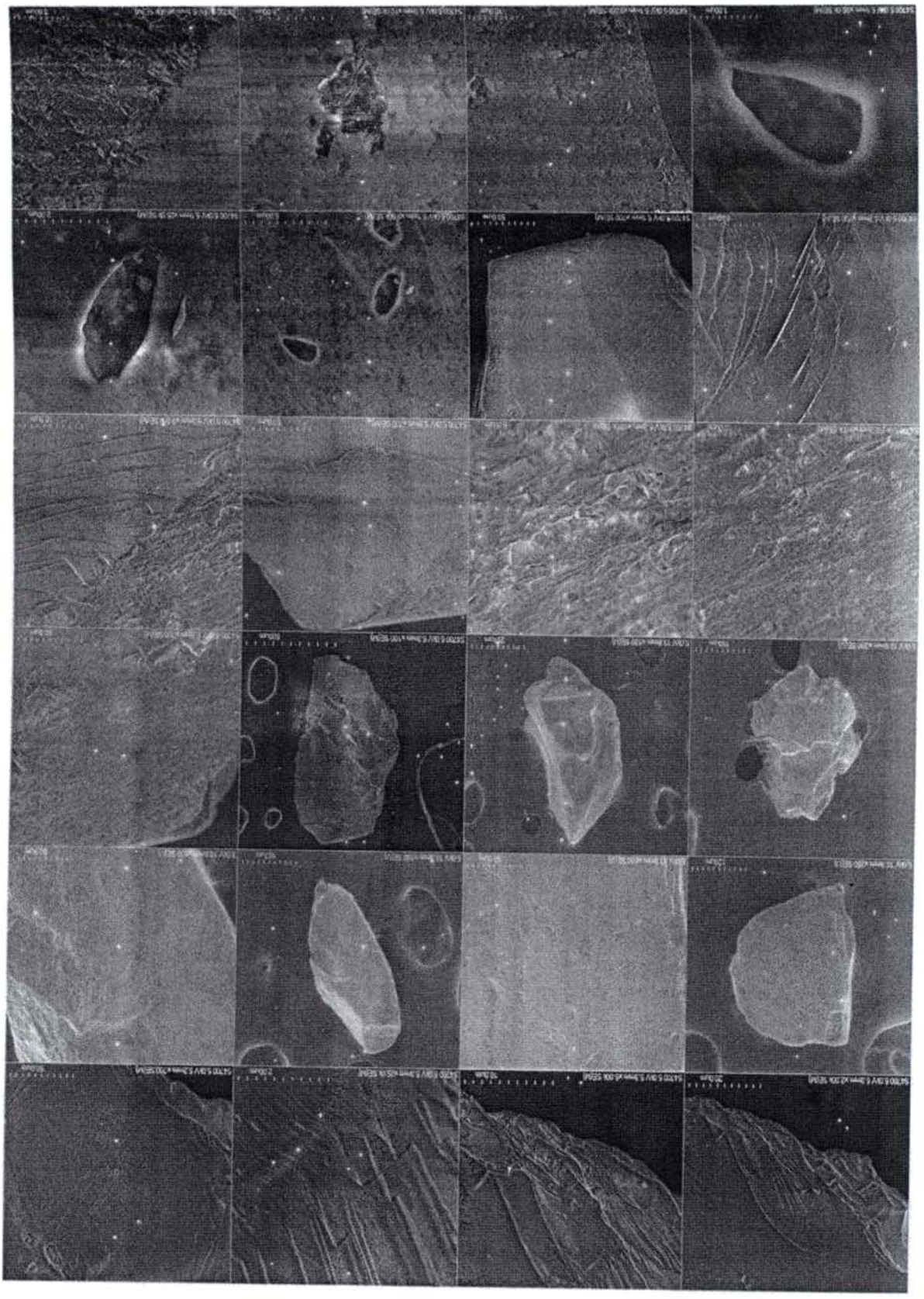

APPENDIX 4 : Geochemical Data

Depth(m)	TRV 01/ SiO2	TiO2	Al2O3	Fe2O3	MnO	CaO	MgO	Na2O	K2O	P2O5	OrganicLol	Total	
0	98.65	0.1	0.1	0.38	0	0	0	0.05	0.02	0.01	0.1	0.1	99.51
2	97.37	0.82	0.56	0.28	0	0.04	0.01	0.01	0.03	0.01	0	0.26	99.38
4	99.09	0.5	0.16	0.21	0	0.02	0	0	0	0	0	0	99.99
6	98.72	0.41	0.32	0.17	0	0.04	0	0.01	0	0	0	0	99.69
7	97.58	0.46	0.61	0.2	0	0.12	0.03	0.05	0.01	0	0	0.32	99.38
8	89.88	1.02	3	0	0.01	0.41	0.07	0.13	0.03	0.01	5.1	0.15	99.82
9	82.64	1.04	4.65	0	0.01	0.38	0.04	0.12	0.16	0.02	6.76	3.8	99.61
10	87.19	1.39	4.62	0.16	0.01	0.2	0	0.06	0.29	0.02	4.5	1.45	99.89
11	95.82	0.55	1.42	0	0	0.12	0.02	0.03	0	0.01	1.5	0.1	99.56
12	96.06	0.39	1.2	0.08	0	0.2	0.04	0.08	0.02	0.01	1.2	0.15	99.45
13	90.18	1.48	2.86	0.04	0.01	0.49	0.15	0.12	0.14	0.02	2.6	0.22	98.31
14	95.51	1	1.26	0.34	0.01	0.09	0.02	0.02	0.02	0.01	1.1	0.25	99.63
15	93.04	0.44	1.63	0	0	0.24	0	0.07	0.03	0.01	1.9	0.45	97.8
19	95.05	1.52	1.08	0.53	0.01	0.12	0.01	0.04	0.07	0.02	0	0.7	99.14
22	90.06	0.96	3.33	0.12	0	0.18	0.02	0.07	0.25	0.01	0	3.8	98.8
23	96.64	1.05	0.52	0.42	0	0.07	0	0.01	0	0.01	0	0.2	98.92
24	97.28	1.27	0.4	0.77	0.01	0.07	0.02	0.02	0	0.01	0	0	99.86
25	92.75	1.94	3.05	1.17	0.01	0.05	0.01	0	0.07	0.02	0	0	99.05
27	91.89	4.09	1.41	1.91	0.02	0.15	0.04	0.04	0.01	0.03	0	0	99.59
36	94.02	1.34	1.68	0.45	0.01	0.12	0.02	0.03	0.02	0.01	0	0	97.71
37	90.38	0.93	3.22	0.11	0	0.18	0.02	0.07	0.24	0.01	0	0	95.17
38	91.79	2.2	3.45	1.32	0.01	0.06	0.01	0	0.07	0.02	0	0	98.93

Appendix 4.1 Major element distribution

Depth(m)	TRV 02/ SiO2	TiO2	Al2O3	Fe2O3	MnO	CaO	MgO	Na2O	K2O	P2O5	OrganicLo!	Total	
												0.2	0.2
1	96.63	1.05	0.72	0.35	0	0.05	0.01	0.01	0.04	0.01	0	0.26	99.13
2	97.37	0.96	0.34	0.28	0	0.04	0.01	0.01	0.03	0.01	0	0.26	99.3
4	97.6	1.31	0.43	0.57	0.01	0.05	0.01	0.01	0	0.01	0	0	99.99
6	98.23	0.57	0.44	0.24	0	0.06	0.01	0.02	0	0.01	0	0	99.57
7	98.06	0.62	0.48	0.26	0	0.07	0.01	0.02	0	0.01	0	0	99.53
8	90.36	0.97	2.86	0	0.01	0.39	0.06	0.13	0.03	0.01	5.1	0.15	100.08
11	84.39	0.87	3.91	0	0.01	0.32	0.03	0.1	0.13	0.02	6.76	3.8	100.35
13	88.9	1.2	4	0.14	0	0.17	0	0.05	0.25	0.02	4.5	0.4	99.65
15	95.25	0.63	1.61	0	0	0.13	0.02	0.03	0	0.01	1.5	0.1	99.29
16	95.12	0.48	1.49	0.1	0.01	0.25	0.05	0.1	0.03	0.02	1.2	0.15	99
19	94.81	1.6	1.13	0.56	0.01	0.13	0.01	0.04	0.07	0.02	1.2	1.32	100.89
20	94.02	1.34	1.68	0.45	0.01	0.12	0.02	0.03	0.02	0.01	0	0	97.71
21	93.9	1.1	1.8	0.47	0.01	0.11	0.02	0.04	0.01	0.01	0	0	97.48
22	92.62	1.24	3.05	0.11	0.02	0.17	0.02	0.06	0.23	0.01	0	0.32	97.85
23	93.23	1.76	0.55	1.07	0.01	0.1	0.03	0.03	0.01	0.02	0	3.8	100.61
25	89.12	2.92	4.57	1.75	0.01	0.08	0.01	0	0.1	0.03	0	0	98.58
26	92.12	3.97	1.37	1.85	0.02	0.15	0.04	0.04	0.01	0.03	0	0.2	99.8
27	90.99	4.3	1.57	1.99	0.02	0.17	0.04	0.05	0.01	0.04	0	0.2	99.38

Depth(m)	TRV 03/ SiO2	TiO2	Al2O3	Fe2O3	MnO	CaO	MgO	Na2O	K2O	P2O5	Organic	Lol	Total
0	98.35	0.2	0.45	0.2	0	0	0	0.09	0.03	0.01	0.1	0.2	99.63
1	97.08	0.91	0.63	0.31	0	0.04	0.01	0.01	0.03	0.01	0	0.26	99.28
3	99.01	0.54	0.18	0.23	0	0.02	0	0	0	0	0	0	99.99
6	98.51	0.48	0.37	0.2	0	0.05	0.01	0.01	0	0	0	0	99.64
7	98.51	0.48	0.37	0.2	0	0.05	0.01	0.01	0	0	0	0	99.64
8	97.48	0.48	0.64	0.21	0.01	0.12	0.03	0.05	0.01	0.01	0	0.32	99.35
9	88.99	1.11	3.26	0	0.01	0.45	0.07	0.15	0.04	0.01	5.1	0.15	99.35
10	82.04	1.07	4.81	0	0.01	0.39	0.04	0.12	0.16	0.02	6.45	3.8	98.92
11	86.66	1.45	4.81	0.17	0.01	0.2	0	0.06	0.3	0.02	4.5	1.5	99.68
13	96.06	0.39	1.2	0.08	0	0.2	0.04	0.08	0.02	0.01	1.2	0.15	99.45
14	92.43	0.47	1.77	0	0	0.26	0	0.08	0.03	0.01	2.1	2.35	99.51
16	94.94	1.56	1.11	0.54	0.01	0.12	0.01	0.04	0.07	0.02	0	1.45	99.86
19	96.7	1.03	0.51	0.41	0	0.07	0	0.01	0	0.01	0	0.7	99.45
20	95.19	1.08	1.35	0.36	0.01	0.1	0.02	0.02	0.02	0.01	0	0	98.16
22	92.06	0.96	3.33	0.12	0	0.18	0.02	0.07	0.25	0.01	1.2	0.65	98.85
24	96.7	1.03	0.51	0.41	0	0.07	0	0.01	0	0.01	0	0.7	99.45
25	92.5	3.2	3.15	1.21	0.01	0.05	0.01	0	0.07	0.02	0	0	100.21
27	90.99	4.54	1.57	2.12	0.02	0.17	0.04	0.05	0.01	0.04	0	0.2	99.75

Appendix 4.1(cont.) Major element distribution

Depth(m)	TRV 04/ SiO2	TiO2	Al2O3	Fe2O3	MnO	CaO	MgO	Na2O	K2O	P2O5	Organic	LoI	Total
0.5	98.5	0.1	0.7	0.4	0	0	0	0.09	0.03	0.01	0.1	0.2	100.63
1	96.63	1.05	0.72	0.35	0	0.05	0.01	0.01	0.04	0.01	0	0.26	99.13
2	97.37	0.96	0.34	0.28	0	0.04	0.01	0.01	0.03	0.01	0	0.26	99.3
4	97.6	1.31	0.43	0.57	0.01	0.05	0.01	0.01	0	0.01	0	0	99.99
6	98.23	0.57	0.44	0.24	0	0.06	0.01	0.02	0	0.01	0	0	99.57
7	98.06	0.62	0.48	0.26	0	0.07	0.01	0.02	0	0.01	0	0	99.53
9	90.36	0.97	2.86	0	0.01	0.39	0.06	0.13	0.03	0.01	5.1	0.15	100.08
10	84.39	0.87	3.91	0	0.01	0.32	0.03	0.1	0.13	0.02	6.76	3.8	100.35
14	88.9	1.2	4	0.14	0	0.17	0	0.05	0.25	0.02	4.5	0.4	99.65
15	95.25	0.63	1.61	0	0	0.13	0.02	0.03	0	0.01	1.5	0.1	99.29
16	95.12	0.48	1.49	0.1	0.01	0.25	0.05	0.1	0.03	0.02	1.2	0.15	99
19	94.81	1.6	1.13	0.56	0.01	0.13	0.01	0.04	0.07	0.02	1.2	1.32	100.89
20	94.02	1.34	1.68	0.45	0.01	0.12	0.02	0.03	0.02	0.01	0	0	97.71
21	93.9	1.1	1.8	0.47	0.01	0.11	0.02	0.04	0.01	0.01	0	0	97.48
22	92.62	1.24	3.05	0.11	0.02	0.17	0.02	0.06	0.23	0.01	0	0.32	97.85
24	93.23	1.76	0.55	1.07	0.01	0.1	0.03	0.03	0.01	0.02	0	3.8	100.61
25	89.12	2.92	4.57	1.75	0.01	0.08	0.01	0	0.1	0.03	0	0	98.58
27	92.12	3.97	1.37	1.85	0.02	0.15	0.04	0.04	0.01	0.03	0	0.2	99.8
29	90.99	4.3	1.57	1.99	0.02	0.17	0.04	0.05	0.01	0.04	0	0.2	99.38

Depth(m)	TRV 05/ SiO2	TiO2	Al2O3	Fe2O3	MnO	CaO	MgO	Na2O	K2O	P2O5	Organic	LoI	Total
1	98.65	0.1	0.1	0.38	0	0	0	0.05	0.02	0.01	0.1	0.1	100.51
2	97.37	0.82	0.56	0.28	0	0.04	0.01	0.01	0.03	0.01	0	0.26	99.38
4	99.09	0.5	0.16	0.21	0	0.02	0	0	0	0	0	0	99.99
6	98.72	0.41	0.32	0.17	0	0.04	0	0.01	0	0	0	0	99.69
7	97.58	0.46	0.61	0.2	0	0.12	0.03	0.05	0.01	0	0	0.32	99.38
8	89.88	1.02	3	0	0.01	0.41	0.07	0.13	0.03	0.01	5.1	0.15	99.82
9	82.64	1.04	4.65	0	0.01	0.38	0.04	0.12	0.16	0.02	6.76	3.8	99.61
10	87.19	1.39	4.62	0.16	0.01	0.2	0	0.06	0.29	0.02	4.5	1.45	99.89
11	95.82	0.55	1.42	0	0	0.12	0.02	0.03	0	0.01	1.5	0.1	99.56
12	96.06	0.39	1.2	0.08	0	0.2	0.04	0.08	0.02	0.01	1.2	0.15	99.45
13	90.18	1.48	2.86	0.04	0.01	0.49	0.15	0.12	0.14	0.02	2.6	0.22	98.31
14	95.51	1	1.26	0.34	0.01	0.09	0.02	0.02	0.02	0.01	1.1	0.25	99.63
15	93.04	0.44	1.63	0	0	0.24	0	0.07	0.03	0.01	1.9	0.45	97.8
19	95.05	1.52	1.08	0.53	0.01	0.12	0.01	0.04	0.07	0.02	0	0.7	99.14
22	90.06	0.96	3.33	0.12	0	0.18	0.02	0.07	0.25	0.01	0	3.8	98.8
23	96.64	1.05	0.52	0.42	0	0.07	0	0.01	0	0.01	0	0.2	98.92
24	97.28	1.27	0.4	0.77	0.01	0.07	0.02	0.02	0	0.01	0	0	99.86
25	92.75	1.94	3.05	1.17	0.01	0.05	0.01	0	0.07	0.02	0	0	99.05
27	91.89	4.09	1.41	1.91	0.02	0.15	0.04	0.04	0.01	0.03	0	0	99.59
36	94.02	1.34	1.68	0.45	0.01	0.12	0.02	0.03	0.02	0.01	0	0	97.71
37	90.38	0.93	3.22	0.11	0	0.18	0.02	0.07	0.24	0.01	0	0	95.17
38	91.79	2.2	3.45	1.32	0.01	0.06	0.01	0	0.07	0.02	0	0	98.93

Appendix 4.1(cont.) Major element distribution

Depth(m)	TRV 06/ SiO2	TiO2	Al2O3	Fe2O3	MnO	CaO	MgO	Na2O	K2O	P2O5	OrganicLoI		Total
0	98.35	0.2	0.45	0.2	0	0	0	0.09	0.03	0.01	0.1	0.2	99.63
1	97.08	0.91	0.63	0.31	0	0.04	0.01	0.01	0.03	0.01	0	0.26	99.28
3	99.01	0.54	0.18	0.23	0	0.02	0	0	0	0	0	0	99.99
6	98.51	0.48	0.37	0.2	0	0.05	0.01	0.01	0	0	0	0	99.64
7	98.51	0.48	0.37	0.2	0	0.05	0.01	0.01	0	0	0	0	99.64
8	97.48	0.48	0.64	0.21	0.01	0.12	0.03	0.05	0.01	0.01	0	0.32	99.35
9	88.99	1.11	3.26	0	0.01	0.45	0.07	0.15	0.04	0.01	5.1	0.15	99.35
10	82.04	1.07	4.81	0	0.01	0.39	0.04	0.12	0.16	0.02	6.45	3.8	98.92
12	86.66	1.45	4.81	0.17	0.01	0.2	0	0.06	0.3	0.02	4.5	1.5	99.68
14	96.06	0.39	1.2	0.08	0	0.2	0.04	0.08	0.02	0.01	1.2	0.15	99.45
15	92.43	0.47	1.77	0	0	0.26	0	0.08	0.03	0.01	2.1	2.35	99.51
16	94.94	1.56	1.11	0.54	0.01	0.12	0.01	0.04	0.07	0.02	0	1.45	99.86
18	96.7	1.03	0.51	0.41	0	0.07	0	0.01	0	0.01	0	0.7	99.45
20	95.19	1.08	1.35	0.36	0.01	0.1	0.02	0.02	0.02	0.01	0	0	98.16
22	92.06	0.96	3.33	0.12	0	0.18	0.02	0.07	0.25	0.01	1.2	0.65	98.85
24	96.7	1.03	0.51	0.41	0	0.07	0	0.01	0	0.01	0	0.7	99.45
25	92.5	3.2	3.15	1.21	0.01	0.05	0.01	0	0.07	0.02	0	0	100.21
29	90.99	4.54	1.57	2.12	0.02	0.17	0.04	0.05	0.01	0.04	0	0.2	99.75

Depth(m)	TRV 07/ SiO2	TiO2	Al2O3	Fe2O3	MnO	CaO	MgO	Na2O	K2O	P2O5	OrganicLoI		Total
1	98.65	0.1	0.1	0.38	0	0	0	0.05	0.02	0.01	0.1	0.1	100.51
2	97.37	0.82	0.56	0.28	0	0.04	0.01	0.01	0.03	0.01	0	0.26	99.38
4	99.09	0.5	0.16	0.21	0	0.02	0	0	0	0	0	0	99.99
5	98.72	0.41	0.32	0.17	0	0.04	0	0.01	0	0	0	0	99.69
6	97.58	0.46	0.61	0.2	0	0.12	0.03	0.05	0.01	0	0	0.32	99.38
7	89.88	1.02	3	0	0.01	0.41	0.07	0.13	0.03	0.01	5.1	0.15	99.82
8	82.64	1.04	4.65	0	0.01	0.38	0.04	0.12	0.16	0.02	6.76	3.8	99.61
10	87.19	1.39	4.62	0.16	0.01	0.2	0	0.06	0.29	0.02	4.5	1.45	99.89
12	95.82	0.55	1.42	0	0	0.12	0.02	0.03	0	0.01	1.5	0.1	99.56
13	96.06	0.39	1.2	0.08	0	0.2	0.04	0.08	0.02	0.01	1.2	0.15	99.45
14	90.18	1.48	2.86	0.04	0.01	0.49	0.15	0.12	0.14	0.02	2.6	0.22	98.31
15	95.51	1	1.26	0.34	0.01	0.09	0.02	0.02	0.02	0.01	1.1	0.25	99.63
16	93.04	0.44	1.63	0	0	0.24	0	0.07	0.03	0.01	1.9	0.45	97.8
17	95.05	1.52	1.08	0.53	0.01	0.12	0.01	0.04	0.07	0.02	0	0.7	99.14
19	90.06	0.96	3.33	0.12	0	0.18	0.02	0.07	0.25	0.01	0	3.8	98.8
21	96.64	1.05	0.52	0.42	0	0.07	0	0.01	0	0.01	0	0.2	98.92
23	97.28	1.27	0.4	0.77	0.01	0.07	0.02	0.02	0	0.01	0	0	99.86
25	92.75	1.94	3.05	1.17	0.01	0.05	0.01	0	0.07	0.02	0	0	99.05
27	91.89	4.09	1.41	1.91	0.02	0.15	0.04	0.04	0.01	0.03	0	0	99.59
29	94.02	1.34	1.68	0.45	0.01	0.12	0.02	0.03	0.02	0.01	0	0	97.71
30	90.38	0.93	3.22	0.11	0	0.18	0.02	0.07	0.24	0.01	0	0	95.17
32	91.79	2.2	3.45	1.32	0.01	0.06	0.01	0	0.07	0.02	0	0	98.93

Appendix 4.1(cont.) Major element distribution

TRV 8/ Depth(m)	SiO2	TiO2	Al2O3	Fe2O3	MnO	CaO	MgO	Na2O	K2O	P2O5	Organic	LoI	Total
0	98.02	0.16	1.07	0.88	0	0	0	0.09	0.03	0.01	0.1	0.2	100.56
2	96.63	1.05	0.72	0.35	0	0.05	0.01	0.01	0.04	0.01	0	0.26	99.13
3	97.6	1.31	0.43	0.57	0.01	0.05	0.01	0.01	0	0.01	0	0	99.99
5	98.23	0.57	0.44	0.24	0	0.06	0.01	0.02	0	0.01	0	0	99.57
7	97.73	0.43	0.58	0.19	0	0.11	0.03	0.04	0.01	0	0	0.32	99.44
9	90.02	1.9	2.9	0.04	0.01	0.5	0.16	0.13	0.14	0.02	1.34	0.22	97.37
11	91.32	0.87	2.57	0	0.01	0.36	0.06	0.12	0.03	0.01	5.1	0.15	100.59
13	85.38	0.87	3.91	0	0.01	0.32	0.03	0.1	0.13	0.02	5.88	3.8	100.46
15	87.29	1.38	4.59	0.16	0.01	0.2	0	0.06	0.29	0.02	4.5	0.4	98.88
17	94.87	1.58	1.12	0.55	0.01	0.12	0.01	0.04	0.07	0.02	1.2	1.45	101.04
18	90.38	0.93	3.22	0.11	0	0.18	0.02	0.07	0.24	0.01	0	0	95.17
20	96.55	1.08	0.53	0.43	0	0.07	0	0.01	0	0.01	0	0.7	99.39
23	96.45	1.66	0.52	1.01	0.01	0.09	0.03	0.03	0.01	0.02	0	0.8	100.62
24	92.12	3.97	1.37	1.85	0.02	0.15	0.04	0.04	0.01	0.03	0	0.2	99.8

Appendix 4.1(cont.) Major element distribution

Depth(m)	TRV 09/ SiO2	TiO2	Al2O3	Fe2O3	MnO	CaO	MgO	Na2O	K2O	P2O5	OrganicLol	Total
0	98.35	0.2	0.45	0.2	0	0	0	0.09	0.03	0.01	0.1	0.2	99.63
1	97.08	0.91	0.63	0.31	0	0.04	0.01	0.01	0.03	0.01	0	0.26	99.28
2	99.01	0.54	0.18	0.23	0	0.02	0	0	0	0	0	0	99.99
5	98.51	0.48	0.37	0.2	0	0.05	0.01	0.01	0	0	0	0	99.64
6	98.51	0.48	0.37	0.2	0	0.05	0.01	0.01	0	0	0	0	99.64
8	97.48	0.48	0.64	0.21	0.01	0.12	0.03	0.05	0.01	0.01	0	0.32	99.35
9	88.99	1.11	3.26	0	0.01	0.45	0.07	0.15	0.04	0.01	5.1	0.15	99.35
10	82.04	1.07	4.81	0	0.01	0.39	0.04	0.12	0.16	0.02	6.45	3.8	98.92
12	86.66	1.45	4.81	0.17	0.01	0.2	0	0.06	0.3	0.02	4.5	1.5	99.68
13	96.06	0.39	1.2	0.08	0	0.2	0.04	0.08	0.02	0.01	1.2	0.15	99.45
15	92.43	0.47	1.77	0	0	0.26	0	0.08	0.03	0.01	2.1	2.35	99.51
16	94.94	1.56	1.11	0.54	0.01	0.12	0.01	0.04	0.07	0.02	0	1.45	99.86
19	96.7	1.03	0.51	0.41	0	0.07	0	0.01	0	0.01	0	0.7	99.45
20	95.19	1.08	1.35	0.36	0.01	0.1	0.02	0.02	0.02	0.01	0	0	98.16
22	92.06	0.96	3.33	0.12	0	0.18	0.02	0.07	0.25	0.01	1.2	0.65	98.85
23	96.7	1.03	0.51	0.41	0	0.07	0	0.01	0	0.01	0	0.7	99.45
25	92.5	3.2	3.15	1.21	0.01	0.05	0.01	0	0.07	0.02	0	0	100.21
27	90.99	4.54	1.57	2.12	0.02	0.17	0.04	0.05	0.01	0.04	0	0.2	99.75

Appendix 4.1(cont.) Major element distribution

Depth(m)	TRV 10/ SiO2	TiO2	Al2O3	Fe2O3	MnO	CaO	MgO	Na2O	K2O	P2O5	Organic	Loi
0	98.02	0.16	1.07	0.88	0	0	0	0.09	0.03	0.01		
	98.63		0.72	0.35	0	0.05	0.01	0.01	0.04	0.01		
4	97.6	1.31	0.43	0.57	0.01	0.05	0.01	0.01	0	0.01	0	0
5	98.23	0.57	0.44	0.24	0	0.06	0.01	0.02	0	0.01	0	0
7	97.73	0.43	0.58	0.19	0	0.11	0.03	0.04	0.01	0	0	0.32
9	90.02	1.9	2.9	0.04	0.01	0.5	0.16	0.13	0.14	0.02	1.34	0.22
10	91.32	0.87	2.57	0	0.01	0.36	0.06	0.12	0.03	0.01	5.1	0.15
12	85.38	0.87	3.91	0	0.01	0.32	0.03	0.1	0.13	0.02	5.88	3.8
16	87.29	1.38	4.59	0.16	0.01	0.2	0	0.06	0.29	0.02	4.5	0.4
19	94.87	1.58	1.12	0.55	0.01	0.12	0.01	0.04	0.07	0.02	1.2	1.45
20	90.38	0.93	3.22	0.11	0	0.18	0.02	0.07	0.24	0.01	0	0
21	96.55	1.08	0.53	0.43	0	0.07	0	0.01	0	0.01	0	0.7
24	96.45	1.66	0.52	1.01	0.01	0.09	0.03	0.03	0.01	0.02	0	0.8
27	92.12	3.97	1.37	1.85	0.02	0.15	0.04	0.04	0.01	0.03	0	0.2

Appendix 4.1(cont.) Major element distribution

TRV 1

Depth(m)	v	Cr	Co	Ni	Cu	Zn	Ga	Rb	Sr	Y	Zr	Nb	Ba	La	Pb	Ce	Nd
1	135	170	30	93	60	138	21	134	326	0	151	12	904	53	0	107	36
2	164	290	4	10	5	84	15	81	47	128	2225	258	0	187	32	730	271
4	199	256	12	9	3	111	12	76	27	372	3214	412	0	207	22	787	282
6	157	173	5	9	13	67	13	80	32	620	1544	212	0	93	32	340	124
7	145	154	6	12	15	62	15	82	46	643	935	134	0	77	29	244	78
8	138	210	5	13	22	53	15	82	58	636	350	71	0	41	29	97	39
9	136	235	5	14	19	50	14	85	47	0	337	44	0	41	0	80	29
10	136	255	14	86	37	143	17	107	203	0	180	14	528	53	0	121	55
11	141	289	5	16	11	66	18	86	75	538	727	92	0	61	32	213	72
12	141	181	7	16	18	56	17	79	33	635	484	97	0	54	32	154	52
13	137	158	8	10	16	81	15	84	49	0	391	191	0	46	34	120	53
14	143	230	3	12	15	58	17	84	87	676	516	113	0	52	34	161	50
15	135	135	0	10	18	40	13	83	38	0	287	44	0	35	32	53	29
19	161	257	4	8	7	77	15	82	54	341	1676	222	0	152	34	586	211
22	158	253	4	9	7	71	12	79	26	405	1666	229	0	144	32	516	213
23	191	178	10	11	4	107	10	78	38	320	2442	319	0	272	32	957	366
25	192	185	9	10	4	110	10	77	40	300	2580	321	0	281	31	980	383
27	202	265	9	9	<1	107	11	77	28	236	2869	356	0	298	31	1085	404
36	152	155	4	14	17	92	16	83	54	458	1192	183	0	113	29	392	152
37	140	236	0	16	12	52	15	89	94	504	692	96	136	56	33	169	61
38	179	376	5	25	7	104	16	84	33	293	2079	255	0	175	26	682	245

Appendix 4.2 Trace element distribution

TRV 2

Depth(m)	v	Cr	Co	Ni	Cu	Zn	Ga	Rb	Sr	Y	Zr	Nb	Ba	La	Pb	Ce	Nd
0.5	135	170	30	93	60	138	21	134	326	0	151	12	904	53	0	107	36
1	164	290	4	10	5	84	15	81	47	128	2225	258	0	187	32	730	271
2	199	256	12	9	3	111	12	76	27	372	3214	412	0	207	22	787	282
4	157	173	5	9	13	67	13	80	32	620	1544	212	0	93	32	340	124
6	145	154	6	12	15	62	15	82	46	643	935	134	0	77	29	244	78
7	138	210	5	13	22	53	15	82	58	636	350	71	0	41	29	97	39
8	136	235	5	14	19	50	14	85	47	0	337	44	30	41	0	80	29
11	136	255	14	86	37	143	17	107	203	0	180	14	423	53	0	121	55
13	141	289	5	16	11	66	18	86	75	538	727	92	0	61	32	213	72
15	141	181	7	16	18	56	17	79	33	635	484	97	0	54	32	154	52
16	137	158	8	10	16	81	15	84	49	0	391	191	0	46	34	120	53
19	143	230	3	12	15	58	17	84	87	676	516	113	0	52	34	161	50
20	135	135	0	10	18	40	13	83	38	0	287	44	0	35	32	53	29
21	161	257	4	8	7	77	15	82	54	341	1676	222	0	152	34	586	211
22	158	253	4	9	7	71	12	79	26	405	1666	229	0	144	32	516	213
23	191	178	10	11	4	107	10	78	38	320	2442	319	0	272	32	957	366
25	192	185	9	10	4	110	10	77	40	300	2580	321	0	281	31	980	383
26	202	265	9	9	<1	107	11	77	28	236	2869	356	0	298	31	1085	404
27	201	240	9	8	<1	105	10	72	27	235	2859	358	0	300	30	1083	402

TRV 3

Depth(m)	v	Cr	Co	Ni	Cu	Zn	Ga	Rb	Sr	Y	Zr	Nb	Ba	La	Pb	Ce	Nd
0.5	135	170	30	93	60	138	21	134	326	0	151	12	904	53	0	107	36
1	160	270	3	10	5	90	12	81	42	120	2180	248	0	190	30	703	262
3	173	260	11	9	4	98	13	79	30	289	2850	272	0	194	28	780	278
6	150	170	5	9	12	65	14	81	31	632	1567	210	0	106	31	340	120
7	145	154	6	12	15	62	15	82	46	643	935	134	0	77	29	244	78
8	140	167	6	12	16	59	15	81	50	468	730	114	0	50	25	178	50
9	136	211	5	13	17	53	14	82	58	O	250	50	0	32	19	84	16
10	134	236	4	30	19	50	14	85	47	0	200	44	10	34	1	80	24
11	136	255	14	70	37	120	26	110	220	0	180	18	300	45	3	121	50
13	146	288	6	16	10	66	18	86	75	538	727	92	0	61	32	210	72
14	148	180	7	18	20	56	17	80	33	635	484	97	0	54	32	154	52
16	148	158	7	10	16	81	15	84	49	0	391	191	0	46	34	119	53
19	143	210	4	12	15	60	17	84	87	676	516	113	0	52	34	161	50
20	150	139	1	10	18	40	13	83	38	0	287	44	0	35	32	50	30
22	158	253	4	9	7	70	12	79	26	405	1666	229	0	144	32	516	220
24	199	178	10	11	4	107	11	78	38	320	2442	319	0	272	32	1001	366
25	205	188	9	10	3	115	11	77	40	300	2580	321	0	281	31	960	383
27	210	260	10	9	<1	107	11	77	28	236	2869	356	0	298	31	1085	410

Appendix 4.2(cont.) Trace element distribution

TRV 4

Depth(m)	v	Cr	Co	Ni	Cu	Zn	Ga	Rb	Sr	Y	Zr	Nb	Ba	La	Pb	Ce	Nd
0.25	135	170	30	93	60	138	21	134	326	0	151	12	904	53	0	107	36
0.5	138	210	5	13	22	53	15	82	58	636	350	71	0	41	29	97	39
1	164	290	4	10	5	84	15	81	47	128	2225	258	0	187	32	730	271
2	199	256	12	9	3	111	12	76	27	372	3214	412	0	207	22	787	282
4	157	173	5	9	13	67	13	80	32	620	1544	212	0	93	32	340	124
6	145	154	6	12	15	62	15	82	46	643	935	134	0	77	29	244	78
7	138	210	5	13	22	53	15	82	58	636	350	71	0	41	29	97	39
9	136	235	5	14	19	50	14	85	47	0	337	44	30	41	0	80	29
10	136	255	14	86	37	143	17	107	203	0	180	14	423	53	0	121	55
14	141	289	5	16	11	66	18	86	75	538	727	92	0	61	32	213	72
15	141	181	7	16	18	56	17	79	33	635	484	97	0	54	32	154	52
16	137	158	8	10	16	81	15	84	49	0	391	191	0	46	34	120	53
19	143	230	3	12	15	58	17	84	87	676	516	113	0	52	34	161	50
20	135	135	0	10	18	40	13	83	38	0	287	44	0	35	32	53	29
21	161	257	4	8	7	77	15	82	54	341	1676	222	0	152	34	586	211
22	158	253	4	9	7	71	12	79	26	405	1666	229	0	144	32	516	213
24	191	178	10	11	4	107	10	78	38	320	2442	319	0	272	32	957	366
25	192	185	9	10	4	110	10	77	40	300	2580	321	0	281	31	980	383
27	202	265	9	9	<1	107	11	77	28	236	2869	356	0	298	31	1085	404
29	201	240	9	8	<1	105	10	72	27	235	2859	358	0	300	30	1083	402

Appendix 4.2(cont.) Trace element distribution

Depth(m)	TRV5 v	Cr	Co	Ni	Cu	Zn	Ga	Rb	Sr	Y	Zr	Nb	Ba	La	Pb	Ce	Nd
0.5	135	170	30	93	60	138	21	134	326	0	151	12	904	53	0	107	36
1	157	173	5	9	13	67	13	80	32	620	1544	212	0	93	32	340	124
3	164	290	4	10	5	84	15	81	47	128	2225	258	0	187	32	730	271
4	199	256	12	9	3	111	12	76	27	372	3214	412	0	207	22	787	282
6	157	173	5	9	13	67	13	80	32	620	1544	212	0	93	32	340	124
7	145	154	6	12	15	62	15	82	46	643	935	134	0	77	29	244	78
8	138	210	5	13	22	53	15	82	58	636	350	71	0	41	29	97	39
9	136	235	5	14	19	50	14	85	47	0	337	44	0	41	0	80	29
11	136	255	14	86	37	143	17	107	203	0	180	14	528	53	0	121	55
12	141	289	5	16	11	66	18	86	75	538	727	92	0	61	32	213	72
13	141	181	7	16	18	56	17	79	33	635	484	97	0	54	32	154	52
14	137	158	8	10	16	81	15	84	49	0	391	191	0	46	34	120	53
15	143	230	3	12	15	58	17	84	87	676	516	113	0	52	34	161	50
17	135	135	0	10	18	40	13	83	38	0	287	44	0	35	32	53	29
19	161	257	4	8	7	77	15	82	54	341	1676	222	0	152	34	586	211
22	158	253	4	9	7	71	12	79	26	405	1666	229	0	144	32	516	213
23	191	178	10	11	4	107	10	78	38	320	2442	319	0	272	32	957	366
25	192	185	9	10	4	110	10	77	40	300	2580	321	0	281	31	980	383
27	202	265	9	9	<1	107	11	77	28	236	2869	356	0	298	31	1085	404
36	152	155	4	14	17	92	16	83	54	458	1192	183	0	113	29	392	152
37	140	236	0	16	12	52	15	89	94	504	692	96	136	56	33	169	61
38	179	376	5	25	7	104	16	84	33	293	2079	255	0	175	26	682	245
38	179	376	5	25	7	104	16	84	33	293	2079	255	0	175	26	682	245

Appendix 4.2(cont.) Trace element distribution

TRV 6

Depth(m)	v	Cr	Co	Ni	Cu	Zn	Ga	Rb	Sr	Y	Zr	Nb	Ba	La	Pb	Ce	Nd
0.5	135	170	30	93	60	138	21	134	326	0	151	12	904	53	0	107	36
1	160	270	3	10	5	90	12	81	42	120	2180	248	0	190	30	709	262
3	173	260	11	9	4	98	13	79	30	289	2850	272	0	194	28	780	278
6	150	170	5	9	12	65	14	81	31	632	1567	210	0	106	31	340	120
7	145	154	6	12	15	62	15	82	46	643	935	134	0	77	29	244	78
8	140	167	6	12	16	59	15	81	50	468	730	114	0	50	25	178	50
9	136	211	5	13	17	53	14	82	58 O		250	50	0	32	19	84	16
10	134	236	4	30	19	50	14	85	47	0	200	44	10	34	1	80	24
12	136	255	14	70	37	120	26	110	220	0	180	18	300	45	3	121	50
14	146	288	6	16	10	66	18	86	75	538	727	92	0	61	32	210	72
15	148	180	7	18	20	56	17	80	33	635	484	97	0	54	32	154	52
16	148	158	7	10	16	81	15	84	49	0	391	191	0	46	34	119	53
18	143	210	4	12	15	60	17	84	87	676	516	113	0	52	34	161	50
20	150	139	1	10	18	40	13	83	38	0	287	44	0	35	32	50	30
22	158	253	4	9	7	70	12	79	26	405	1666	229	0	144	32	516	220
24	199	178	10	11	4	107	11	78	38	320	2442	319	0	272	32	1001	366
25	205	188	9	10	3	115	11	77	40	300	2580	321	0	281	31	960	383
29	210	260	10	9	<1	107	11	77	28	236	2869	356	0	298	31	1085	410

Appendix 4.2(cont.) Trace element distribution

TRV 7

Depth(m)	v	Cr	Co	Ni	Cu	Zn	Ga	Rb	Sr	Y	Zr	Nb	Ba	La	Pb	Ce	Nd
1	135	170	30	93	60	138	21	134	326	0	151	12	904	53	0	107	36
2	157	173	5	9	13	67	13	80	32	620	1544	212	0	93	32	340	124
4	164	290	4	10	5	84	15	81	47	128	2225	258	0	187	32	730	271
5	199	256	12	9	3	111	12	76	27	372	3214	412	0	207	22	787	282
6	157	173	5	9	13	67	13	80	32	620	1544	212	0	93	32	340	124
7	145	154	6	12	15	62	15	82	46	643	935	134	0	77	29	244	78
8	138	210	5	13	22	53	15	82	58	636	350	71	0	41	29	97	39
10	136	235	5	14	19	50	14	85	47	0	337	44	0	41	0	80	29
12	136	255	14	86	37	143	17	107	203	0	180	14	528	53	0	121	55
13	141	289	5	16	11	66	18	86	75	538	727	92	0	61	32	213	72
14	141	181	7	16	18	56	17	79	33	635	484	97	0	54	32	154	52
15	137	158	8	10	16	81	15	84	49	0	391	191	0	46	34	120	53
16	143	230	3	12	15	58	17	84	87	676	516	113	0	52	34	161	50
17	135	135	0	10	18	40	13	83	38	0	287	44	0	35	32	53	29
19	161	257	4	8	7	77	15	82	54	341	1676	222	0	152	34	586	211
21	158	253	4	9	7	71	12	79	26	405	1666	229	0	144	32	516	213
23	191	178	10	11	4	107	10	78	38	320	2442	319	0	272	32	957	366
25	192	185	9	10	4	110	10	77	40	300	2580	321	0	281	31	980	383
27	202	265	9	9	<1	107	11	77	28	236	2869	356	0	298	31	1085	404
29	152	155	4	14	17	92	16	83	54	458	1192	183	0	113	29	392	152
30	140	236	0	16	12	52	15	89	94	504	692	96	136	56	33	169	61
32	179	376	5	25	7	104	16	84	33	293	2079	255	0	175	26	682	245

Appendix 4.2(cont.) Trace element distribution

TRV 8																		
Depth(m)	v	Cr	Co	Ni	Cu	Zn	Ga	Rb	Sr	Y	Zr	Nb	Ba	La	Pb	Ce	Nd	
1	135	170	30	93	60	138	21	134	326	0	151	12	904	53	0	107	36	
2	158	265	4	10	4	89	13	80	41	121	2198	248	0	189	31	700	264	
3	199	256	12	9	3	111	12	76	27	372	3214	412	0	207	22	787	282	
5	157	173	5	9	13	67	13	80	32	620	1544	212	0	93	32	340	124	
7	145	154	6	12	15	62	15	82	46	643	935	134	0	77	29	244	78	
9	140	167	6	12	16	59	15	81	50	468	730	114	0	50	25	178	50	
11	140	210	5	13	22	53	15	82	58	636	350	71	0	41	29	97	39	
13	138	210	6	23	24	83	15	99	118	63	220	71	20	41	29	97	39	
15	132	255	14	86	38	143	17	107	203	4	160	14	434	55	0	124	50	
17	161	257	4	8	7	77	15	82	54	341	1676	222	0	152	34	586	211	
18	143	230	3	12	15	58	17	84	87	676	516	113	0	52	34	161	50	
20	135	135	0	10	18	40	13	83	38	0	287	44	0	35	32	53	29	
23	192	185	9	10	4	110	10	77	40	300	2580	321	0	281	31	980	383	
24	202	265	9	9	<1	107	11	77	28	236	2869	356	0	298	31	1085	404	

Appendix 4.2(cont.) Trace element distribution

TRV 9

Depth(m)	v	Cr	Co	Ni	Cu	Zn	Ga	Rb	Sr	Y	Zr	Nb	Ba	La	Pb	Ce	Nd
0.5	135	170	30	93	60	138	21	134	326	0	151	12	904	53	0	107	36
1	160	270	3	10	5	90	12	81	42	120	2180	248	0	190	30	703	262
2	173	260	11	9	4	98	13	79	30	289	2850	272	0	194	28	780	278
5	150	170	5	9	12	65	14	81	31	632	1567	210	0	106	31	340	120
6	145	154	6	12	15	62	15	82	46	643	935	134	0	77	29	244	78
8	140	167	6	12	16	59	15	81	50	468	730	114	0	50	25	178	50
9	136	211	5	13	17	53	14	82	58	O	250	50	0	32	19	84	16
10	134	236	4	30	19	50	14	85	47	0	200	44	10	34	1	80	24
12	136	255	14	70	37	120	26	110	220	0	180	18	300	45	3	121	50
13	146	288	6	16	10	66	18	86	75	538	727	92	0	61	32	210	72
15	148	180	7	18	20	56	17	80	33	635	484	97	0	54	32	154	52
16	148	158	7	10	16	81	15	84	49	0	391	191	0	46	34	119	53
19	143	210	4	12	15	60	17	84	87	676	516	113	0	52	34	161	50
20	150	139	1	10	18	40	13	83	38	0	287	44	0	35	32	50	30
22	158	253	4	9	7	70	12	79	26	405	1666	229	0	144	32	516	220
23	199	178	10	11	4	107	11	78	38	320	2442	319	0	272	32	1001	366
25	205	188	9	10	3	115	11	77	40	300	2580	321	0	281	31	960	383
27	210	260	10	9	<1	107	11	77	28	236	2869	356	0	298	31	1085	410

Appendix 4.2(cont.) Trace element distribution

TRV 10

Depth(m)	v	Cr	Co	Ni	Cu	Zn	Ga	Rb	Sr	Y	Zr	Nb	Ba	La	Pb	Ce	Nd
0.5	135	170	30	93	60	138	21	134	326	0	151	12	904	53	0	107	36
1	160	270	3	10	5	90	12	81	42	120	2180	248	0	190	30	703	262
4	199	256	12	9	3	111	12	76	27	372	3214	412	0	207	22	787	282
5	157	173	5	9	13	67	13	80	32	620	1544	212	0	93	32	340	124
7	145	154	6	12	15	62	15	82	46	643	935	134	0	77	29	244	78
9	140	167	6	12	16	59	15	81	50	468	730	114	0	50	25	178	50
10	140	210	5	13	22	53	15	82	58	636	350	71	0	41	29	97	39
12	138	210	6	23	24	83	15	99	118	63	220	71	20	41	29	97	39
16	132	255	14	86	38	143	17	107	203	4	160	14	434	55	0	124	50
19	161	257	4	8	7	77	15	82	54	341	1676	222	0	152	34	586	211
20	143	230	3	12	15	58	17	84	87	676	516	113	0	52	34	161	50
21	135	135	0	10	18	40	13	83	38	0	287	44	0	35	32	53	29
24	192	185	9	10	4	110	10	77	40	300	2580	321	0	281	31	980	383
27	202	265	9	9	<1	107	11	77	28	236	2869	356	0	298	31	1085	404

Appendix 4.2(cont.) Trace element distribution

	K2O	Na2O	K	Na	K/Na	Rb/Sr	CIA
	0.0107692	0.0237076	0.00022866	0.00076502	0.29889146	0.29889	73.2288198
	0.01585174	0.03148383	0.00033657	0.00101595	0.33128904	0.33129	76.748947
	0.01119625	0.0296413	0.00023773	0.00095649	0.24853812	0.24854	75.00783
	0.01787292	0.03984328	0.00037949	0.00128570	0.29516039	0.29516	77.0608072
	0.01457433	0.04215633	0.00030945	0.00136034	0.22748016	0.22748	74.2147337
Litho Unit 3	0.01119625	0.0296413	0.00023773	0.00095649	0.24853812	0.24854	75.00783
	0.0107692	0.0237076	0.00022866	0.00076502	0.29889146	0.29889	73.2288198
	0.03478467	0.05846537	0.00073857	0.00188662	0.39147761	0.39148	74.6199257
	0.01119625	0.0296413	0.00023773	0.00095649	0.24853812	0.24854	75.00783
	0.03478467	0.05846536	0.00073857	0.00188662	0.39147762	0.39148	74.6199258

	K2O	Na2O	K	Na	K/Na	Rb/Sr	CIA
	0.16134044	0.10452733	0.0034257	0.00337299	1.0156195	1.01562	81.193671
	0.19314546	0.07613182	0.0041010	0.0024567	1.66930594	1.66931	83.5348306
	0.16819106	0.11062726	0.0035711	0.00356983	1.00036479	1.00036	81.1198734
	0.19314546	0.07613182	0.0041010	0.0024567	1.66930594	1.66931	83.5348306
	0.15014044	0.06968733	0.0031879	0.00224874	1.41762546	1.41763	83.6408422
Litho Unit 2	0.23402572	0.09289741	0.0049690	0.00299771	1.65759191	1.65759	83.5110491
	0.16134044	0.10452733	0.0034257	0.00337299	1.0156195	1.01562	81.193671
	0.21166667	0.08	0.0044942	0.00258152	1.7409253	1.74093	83.676819
	0.23402572	0.09289741	0.0049690	0.00299771	1.65759192	1.65759	83.5110491
	0.21166667	0.08	0.0044942	0.00258152	1.74092532	1.74093	83.6768189

	K2O	Na2O	K	Na	K/Na	Rb/Sr	CIA
	0.06718072	0.04333393	0.00142642	0.00139834	1.02007998	1.02008	81.7631721
	0.04834995	0.04290817	0.00102659	0.0013846	0.74143595	0.74144	83.26396
	0.05199946	0.03940972	0.00110408	0.00127171	0.86818671	0.86819	81.4133349
	0.04834995	0.04290817	0.00102659	0.0013846	0.74143595	0.74144	83.26396
	0.07234847	0.04436885	0.00153615	0.00143174	1.07292369	1.07292	81.6112238
Litho Unit 1	0.05199946	0.03940972	0.00110408	0.00127171	0.86818671	0.86819	81.4133349
	0.07234847	0.04436885	0.00153615	0.00143174	1.07292369	1.07292	81.6112238
	0.06461094	0.03741135	0.00137186	0.00120723	1.13637164	1.13637	79.235311
	0.05700078	0.03834149	0.00121027	0.00123724	0.97820408	0.97820	81.6392054
	0.06461094	0.03741135	0.00137186	0.00120723	1.13637159	1.13637	79.235311

Appendix 4.3 Details of calculation of CIA

	Al2O3	Al	Na	Al/Na	CIA
	0.3522956	0.00691027	0.00076502	9.03279302	73.2288198
	0.88009641	0.01726307	0.00101595	16.9920253	76.748947
	0.43976069	0.0086259	0.00095649	9.01823628	75.00783
	0.85436835	0.01675842	0.0012857	13.0344432	77.0608072
	0.79384633	0.01557128	0.00136034	11.4465878	74.2147337
Litho Unit 3	0.43976069	0.0086259	0.00095649	9.01823628	75.00783
	0.3522956	0.00691027	0.00076502	9.03279302	73.2288198
	1.24588264	0.02443796	0.00188662	12.953314	74.6199257
	0.43976069	0.0086259	0.00095649	9.01823622	75.00783
	1.24588264	0.02443796	0.00188662	12.9533143	74.6199258

	Al2O3	Al	Na	Al/Na	CIA
	4.08889844	0.08020366	0.00337299	23.778195	81.193671
	3.95543728	0.07758582	0.0024567	31.5813522	83.5348306
	4.29345515	0.08421604	0.00356983	23.5910461	81.1198734
	3.95543728	0.07758582	0.0024567	31.5813522	83.5348306
Litho Unit 2	3.56113311	0.06985155	0.00224874	31.0625276	83.6408422
	4.80887838	0.09432605	0.00299771	31.4660769	83.5110491
	4.08889844	0.08020366	0.00337299	23.778195	81.193671
	4.24916667	0.08334732	0.00258152	32.2861462	83.676819
	4.80887838	0.09432605	0.00299771	31.4660769	83.5110491
	4.24916667	0.08334732	0.00258152	32.2861462	83.6768189

	Al2O3	Al	Na	Al/Na	CIA
	1.89315881	0.03713427	0.00139834	26.5559211	81.7631721
	1.88227651	0.03692082	0.0013846	26.6652616	83.26396
	1.61060683	0.03159202	0.00127171	24.8421188	81.4133349
	1.88227651	0.03692082	0.0013846	26.6652616	83.26396
Litho Unit 1	1.9296861	0.03785075	0.00143174	26.4369238	81.6112238
	1.61060683	0.03159202	0.00127171	24.8421188	81.4133349
	1.9296861	0.03785075	0.00143174	26.4369238	81.6112238
	1.35273879	0.02653394	0.00120723	21.9792575	79.235311
	1.61621408	0.03170201	0.00123724	25.6231396	81.6392054
	1.35273879	0.02653394	0.00120723	21.9792568	79.235311

Appendix 4.3 (cont.) Details of calculation of CIA

	Co	K	Cu	Ga	La
Crust	17.3	2.8	28	17.5	31
soil	10	1.97	25	17	35
Water	0.3	2.3	7	0.1	0.05
stream sediments	8	2.01	17	12	32.5
Flood plain sediments	7	2	17	11	24.9

	Ca	Ce	Mg	Na	Nb
Crust	3.59	63	2.48	3.27	12
soil	1.96	65	1.49	1.3	12
Water	12	0.79	2.9	5	0.001
stream sediments	2.33	66.6	1.2	0.9	13
Flood plain sediments	2.07	50.2	1.2	0.8	10

	Ni	P	Pb	Rb	Sr
Crust	47	0.15	17	84	320
soil	20	0.17	17	65	240
Water	2.5		0.03	2	0.5
stream sediments	21	0.14	20.5	70	126
Flood plain sediments	22	0.11	22	71	131

	Si	Ti	V	Y	Zn
Crust	66.6	0.64	97	21	67
soil	59.8	0.7	90	20	70
Water	6	3	1	0.7	20
stream sediments	61.3	0.625	62	25.7	71
Flood plain sediments	64.6	0.48	56	20.1	65

	Zr	Al	Ba	Nd
Crust	193	15.4	628	27
soil	230	11.2	500	28
Water	2.6		30	0.38
stream sediments	391	10.3	386	28.2
Flood plain sediments	215	10.4	379	21.3

Appendix 4.4 World Geochem data compiled from various sources